Studies of Brain Function, Vol. 9

Studies of Brain Function

Volumes already published in the series:

1 *W. Heiligenberg*
Principles of Electrolocation and Jamming Avoidance in Electric Fish
A Neuroethological Approach

2 *W. Precht*
Neuronal Operations in the Vestibular System

3 *J. T. Enright*
The Timing of Sleep and Wakefulness
On the Substructure and Dynamics of the Circadian Pacemakers Underlying the Wake-Sleep Cycle

4 *H. Braak*
Architectonics of the Human Telencephalic Cortex

5 *H. Collewijn*
The Oculomotor System of the Rabbit and Its Plasticity

6 *M. Abeles*
Local Cortical Circuits
An Electrophysiological Study

7 *G. Palm*
Neural Assemblies
An Alternative Approach to Artificial Intelligence

8 *J. Hyvärinen*
The Parietal Cortex of Monkey and Man

Eberhart Zrenner

Neurophysiological Aspects of Color Vision in Primates

Comparative Studies on Simian Retinal Ganglion Cells and the Human Visual System

With 71 Figures

Springer-Verlag
Berlin Heidelberg New York 1983

Priv.-Doz. Dr. med. habil. EBERHART ZRENNER
Max-Planck-Institut für Physiologische und Klinische Forschung,
W. G. Kerckhoff-Institut
Parkstraße 1, 6350 Bad Nauheim/FRG

ISBN 978-3-642-87608-0 ISBN 978-3-642-87606-6 (eBook)
DOI 10.1007/978-3-642-87606-6

Library of Congress Cataloging in Publication Data. Zrenner, Eberhart, 1945 – Neurophysiological aspects of color vision in primates. (Studies of brain function ; v. 9) Bibliography: p. Includes index. 1. Color vision. 2. Neurophysiology. 3. Physiology, Comparative. 4. Primates—Physiology.
I. Title. II. Series. [DNLM: 1. Color perception—Physiology. 2. Neurons—Physiology. 3. Primates. 4. Retina—Cytology. W1 ST937KF v.9 / WW 150 Z91n] QP483.Z74 1983 599.8'041823 82-16922

2131/3130-543210

To my wife Claudia,
*to Christoph Daniel Frederik * 5.2.1981,*
and his grandparents

Preface

"To explain all nature is too difficult a task for any one man or even for any one age. 'T is much better to do a little with certainty, and leave the rest for others that come after you, than to explain all things . . ."
Sir Isaac Newton (1642–1727)

This book describes and discusses some new aspects of color vision in primates which have emerged from a series of experiments conducted over the past 8 years both on single ganglion cells in monkey retina and on the visually evoked cortical potential in man: corresponding psychophysical mechanisms of human perception will be considered as well. An attempt will be made to better understand the basic mechanisms of color vision using a more comprehensive approach which takes into account new mechanisms found in single cells and relates them to those found valid for the entire visual system. The processing of color signals was followed up from the retina to the visual cortex and to the perceptual centers, as far as the available techniques permitted.

Since the neurophysiological link between the physiological function of neurons and visual perceptions is still missing, it cannot be my intention to speculate on the neuronal basis of certain perceptions. However, in several cases the reverse approach was taken, namely to detect in the perceptive phenomena the action of the neuronal mechanisms of single cells, which beyond any doubt contribute to building up such perceptions as simultaneous color contrast, flicker-induced colors, brightness enhancement, transient tritanopia, and many others. Attention is also given to review articles and publications which enable the reader to gain information about matters which at first sight are not directly related to color vision but are crucial to the understanding of some mechanisms described here.

Since the primary object of this book is color vision, mechanisms subserving spatial resolution as well as light and dark adaptation will only be discussed as far as they interrelate with color vision. The well-known psychophysical and electrophysiological data on trichromatic color vision are touched upon only briefly; the reader interested in gaining a broader view of the subject is therefore referred to the

following sample of comprehensive books, chapters, reviews and articles, which have appeared over the last 25 years: Judd (1943), Pitt (1944), Boynton (1960), Trendelenburg (1961), Linksz (1964), MacNichol (1964), Schober (1964), Graham (1965), Jung (1965, 1973, 1978), De Valois and Abramov (1966), Wyszecki and Stiles (1967), Baumann (1968), Le Grand (1968), Sheppard (1968), Creutzfeld and Sakmann (1969), Wright (1969), Ripps and Weale (1969), Brindley (1970), Cornsweet (1970), Motokawa (1970), Abramov (1972), Rushton (1972a), Walraven (1972), Daw (1973), MacNichol et al. (1973), Rodieck (1973), Davson and Graham (1974), De Valois and De Valois (1975), Davson (1976), Scheibner (1976a,b), Hurvich (1977, 1981a,b), Verriest and Frey (1977), Baumgartner et al. (1978), Stiles (1978), Wasserman (1978), Boynton (1979), Dodt (1979), Robinson (1980), Gouras and Zrenner (1981b), Mollon (1982).

Nevertheless, the attempt is made in the introduction (Chap. 1) to summarize the pertinent information contained in these publications, including some historical backgrounds.

The questions raised by the newly discovered (or less known) mechanisms in single simian ganglion cells and visually evoked cortical potentials will, however, be described in depth. It is to be hoped that they can provide the basis for a more comprehensive understanding of the processes involved in primate color vision.

For a survey of the data and concepts presented in the following, the reader is referred to the summary at the end of the book.

Bad Nauheim, October 1982 Eberhart Zrenner

Contents

Acknowledgments

The experiments described in this paper were performed in the last 8 years with the support of several institutions: the Max-Planck-Institute for Physiological and Clinical Research, W.G. Kerckhoff-Institute, Bad Nauheim, F.R.G. (Dir.: Prof. Dr. R. Thauer, Prof. Dr. E. Dodt, Prof. Dr. E. Simon, Prof. Dr. W. Schaper); the University Eye Clinic Frankfurt (Dir.: Prof. Dr. W. Doden); the National Institutes of Health, National Eye Institute Bethesda, U.S.A. (Dir.: Dr. C. Kupfer, Dr. J. Kinoshita) and the Columbia University New York (Prof. Dr. P. Gouras). The collaboration with the several institutions was made possible by a generous Fogarty fellowship award (No. F05TW 2429-01 and F05TW 2429-02) granted by the Public Health Service of the United States of America for the years 1977 and 1978 and by funds for travel made available by the Deutsche Forschungsgemeinschaft for continuing the collaboration in 1979, 1980, and1981.

I would like to express my deepest thanks to Prof. Dr. E. Dodt for his continuing support and wise advice; to Prof. P. Gouras, who first introduced me to the fascinating world of single cells in his laboratory in Bethesda (1977/1978), for most inspiring collaboration during the following years; to Prof. Dr. Ch. Baumann, who raised many crucial questions and who encouraged me to begin and to finish this work; to Prof. Dr. H. Scheibner, who provided the positive criticism which enabled me to improve some of my evaluations and interpretations; to Prof. O.-J. Grüsser for many valuable suggestions on the final version of the manuscript; to Prof. V. Braitenberg for supporting publication of the manuscript in *Studies of Brain Function;* to Dr. R. Nelson, who provided enlightening comments on Chapters 1 and 4, especially regarding the membrane model in Fig. 4.10, and who, together with Prof. Helga Kolb gave me the link to anatomy; to Dr. H. Krastel, who provided very valuable suggestions from a clinical viewpoint, as well as to all other scientists with whom I collaborated over the years, studying

another piece of the picture: Drs. H. Abe, V. Gavriysky, Marie-Luise Hoffmann, E. Jankov, R. Klingaman, M. Kojima, C.J. Krüger, H.-J. Langhof, R.P. Schuurmans, Ch. Teping, and Marion Wienrich. Special thanks are also due to Dr. O. Ludwig and to Mr. K. Rockenfeller for solving statistical problems; to Ing. grad. Monika Baier, Mrs. Brita Maschen, Dipl.-Ing. J. Abellan and Mrs. G. Eckl for their dedicated technical assistance, to Mr. W. Klein for developing most excellent electronic equipment, to Mr. M. Wasserhess and the workshop of the Kerckhoff-Institute for creating beautiful precision machinery, to Miss Hedwig Buschtöns for help in searching for literature, to Mrs. Marie-Luise Dolleck for art work; special thanks are due to Mrs. Marianne Granz for excellent performance on the many unusual tasks involved in our studies, to Mrs. Heide Breitenfelder for her expert and dedicated work of typing the manuscript.

Thanks are also due to all the other members of the above named institutions as well as to the Max-Planck-Institute for Biochemistry in Martinsried (Documentation Services Department) for their friendly cooperation in handling the countless problems involved in searching literature.

The deepest thanks I owe to my wife Claudia for making gray days colorful, for moral support and encouragement, making me know what I am working for.

1 Introduction

The ultimate purpose of the visual system is the detection of objects and their spatial relationship. These objects appear in a continuously changing environment concerning their brightness, their position, and distance to the observer. In this respect, the primate visual system performs with great precision a number of outstanding tasks, which to a large degree even conflict with each other. Visual perception of brightness contrasts has an enormous dynamic range from a bright sunny beach (about 10^4 cd/m^{-2}) to a moonless night (about 10^{-7} cd/m^{-2}) without considerably losing its time resolution, as happens with photographical material at low light levels. Moreover, small spatial details, down to a few seconds of arc, can be resolved, *without* sacrificing the large visual field of more than 120°.

Color vision plays an important role in carrying out these functions. Since the borders of objects often have the same luminance as their background, only the capability of discerning illuminated areas by the wavelengths of the light quanta reflected enables the visual system to detect these objects (see Cavonius and Schumacher 1966). Moreover, differences in the spectral reflection properties of objects and the background on which they are presented are often small, so that the ability to discriminate adjacent colors must be outstanding in order to permit orientation in a spectrally more or less homogeneous environment. For instance, primates living in trees, surrounded by myriads of green leaves with very similar spectral reflectance and brightness, would easily become disoriented if they had to rely on a visual system which signalled only some twenty shades of grey. Color vision expands the range of discernable light stimuli to about seven to ten million (Judd 1952) taking into consideration different degrees of brightness and saturation of the about 200 hues which we can differentiate in the sun's spectrum. To this end, nature has to make compromises; for instance, the visual system obviously does not need to analyze the entire spectrum of frequencies in a stimulus (as the auditory system can to a certain extent), but it only needs to differentiate between groups of frequencies.

How was knowledge about color vision gained in the past few centuries?

1.1 Color Vision Theories. Historical Aspects

Historically, modern research on color perception probably originates with Sir Isaac Newton's finding that light is not a homogeneous form of radiation, but that it can be dispersed by a glass prism into a spectrum of colors which in turn cannot be altered by subsequent manipulation:

> "I have refracted it with Prismes, and reflected with it Bodies which in Day-light were of other colours; I have intercepted it with the coloured film of Air interceding two compressed plates of glass; transmitted it through coloured Mediums, and through Mediums irradiated with other sorts of Rays, and diversly terminated it; and yet could never produce any new colour out of it. But the most surprising, and wonderful composition was that of Whiteness. There is no one sort of Rays which alone can exhibit this. 'Tis ever compounded, and to its composition are requisite all the aforesaid primary Colours, mixed in a due proportion.... I have often with Admiration beheld, that all the Colours of the Prisme being made to converge, and thereby to be again mixed, reproduced light, entirely and perfectly white. Hence therefore it comes to pass, that Whiteness is the usual colour of Light; for, Light is a confused aggregate of Rays indued with all sorts of Colours, as they are promiscuously darted from the various parts of luminous bodies".
>
> (Letter of Sir Isaac Newton to the Royal Society, London, 1672).

Thus, the link between the distribution of rays and the perception of the color of a light was firmly established. However, initially these physical phenomena seemed incompatible with early psychophysical observations, such as those of Goethe (see Matthaei 1971, Jaeger 1979) until the trichromatic theory, the detection of color-opponency, and the isolation of photopigments provided a clue to the link.

Trichromatic Vision. According to Brindley (1970), the first written statement about three primary kinds of color (red, blue, and yellow) is that of Lomonosov (1757). Based on a well founded study and presented as an exciting detective story, Walls (1956) attributes the first written correct statement about dichromacy and trichromacy to a mysterious G. Palmer, published in 1777. The primacy question is yet unresolved. However, it was Thomas Young (1802, 1807) who concluded – primarily from studies on the color blindness of his contemporary Dalton – that the fibers in the optic nerve respond maximally to three different regions of the spectrum, namely red, yellow/green and blue/violet. This trivariance of color-perception was strongly supported by von Helmholtz (1867) who wrote that "three types of photochemically decomposable substances are deposited in the end organs of the fibers of the optic nerves, which types have a different sensitivity for the different parts of the spectrum". Subsequent ingenious work of Grassmann (1853), Maxwell (1857), König and Dieterici (1893), von Kries (1897, 1904), Exner (1902), König (1903), Schrödinger (1920), Guild (1931), Hecht (1931), Stiles (1939)

and Wright (1946) confirmed this view and led to modern colorimetry, so that Newton's prophecy was finally fulfilled:

> "A naturalist would scarce accept to see ye sciences of those colours become mathematicall, and yet I dare affirm that there is as much certainty in it as in any other part of Opticks" (Newton 1672).

For further historical aspects of trichromacy see Balaraman (1962), Judd (1966), Pastore (1971) and Sherman (1981); of color blindness Judd (1943); of physiological psychology Robinson (1976).

Color-Opponency. An alternative to the three-channel hypothesis was proposed by Hering (1878) in his opponent-color theory. He supposed that there are six basic sensations occurring in opponent pairs: red/green, blue/yellow and black/white, one member of each pair driving a catabolic ("dissimilation"), the other an anabolic ("assimilation") process. His remarkable book on the "light sense" was recently translated into English and edited by Hurvich and Jameson (1964). Apparently Hering (1878, p 135) received some impulses from Mach's (1865) "four + two" colour theory (red, yellow, green, blue, black and white. Mach (first publ. 1885) discusses the relation of his, Aubert's and da Vinci's theories to Hering's; he admits that Hering's antagonistic theory has prominent advantages over the previous ones.

Hering's biological viewpoint stood in sharp conflict with von Helmholtz' theory on almost every issue they both approached. Even though both theories for a long time seemed incompatible, some researchers proposed – following suggestions of von Kries (1882) – that vision is trichromatic at the receptor level, but that opponent processes occur in the postreceptoral neural elements of the retina and visual pathway (e.g. Adams 1923, Müller 1930a,b; see review of Richter 1951, Müller-Limmroth 1956). Schrödinger (1925) was the first to quantitatively work out that the so-called three-component theory can be transformed into an opponent one; for recent colorimetric data on this interrelation see Richter (1979), Paulus and Scheibner (1980), Klauder and Scheibner (1980), Valberg (1981), Scheibner and Wolf (1982). Subsequent psychophysical support for the opponent-process theory could be established by Hurvich and Jameson (1955, 1957) recently critically surveyed by Werner and Wooten (1979). Many of the models derived from such experiments involved both the trichromatic and color-opponent stages (e.g. Hassenstein 1968). However, only studies of the retina itself – either on the electrical responses of single neurons, or on visual pigments – could provide further insights on the nature and circuitry of the trichromatic and color-opponent stages in the visual system.

Photopigments. After the early work on pigment bleaching of Boll (1877) and Kühne (1879), a number of investigators have succeeded in measuring the

spectral absorption of portions of the retina separating three photolabile pigments (for reviews see Bridges 1972, Baumann 1972, 1977, 1978, for a symposium see Langer 1973). The use of retinal reflectance densitometry permitted the study of photolabile pigments in the living human eye (Rushton 1958a, Ripps and Weale 1963, for review see Rushton 1972b). This led to the identification of one rod pigment and of two cone pigments (chlorolabe and erythrolabe) by the method of partial bleaching (see Dartnall 1972). Many questions about the distribution of these pigments were left open. Microspectrophotometric measurements of light-sensitive pigments in a few single receptors revealed three absorption maxima (λ_{max}) near 445, 535, and 570 nm (Brown and Wald 1964, Marks et al. 1964, Liebman 1972). The newest and most extensive measurements on a larger sample of photoreceptors of Bowmaker and Dartnall (1980) on human retina and Bowmaker et al. (1980) on the retina of *macaca fascicularis* give λ_{max}-values near 420, 535, and 565 nm for the three classes of cones (uncorrected for losses in the ocular media). However, spectroscopic measurements on only a total of a few hundred individual cones are available at present.

The structural basis of the different kinds of photolabile pigments seems to rely on only one chromophoric unit (11-cis-retinal) but on different kinds of proteins (opsines) which finally define the maximum absorption in a single cone (Dartnall and Lythgoe 1965, Fatt 1981). Different kinds of interactions between the chromophoric unit and the protein were proposed as "wavelength-regulators" by Honig et al. (1979).

1.2 Electrophysiological Studies Related to Color Vision

According to Polyak (1941), there are 110 to 125 million rods and 4 to 7 million cones in the human retina, but only about one million fibers in the optic nerve. Hence, there must be a high degree of convergence between receptors and ganglion cells. Even in the retina of many lower animals, there is a transition between the "dim light" (scotopic) and the "bright light" (photopic) function based on rods and cones respectively (Purkinje-shift). In primates, rods are located mainly in peripheral areas of the retina, while the center (fovea) is occupied almost exclusively by cones.

Recordings from Cell Populations

A convenient way of studying directly the processing of color in a neural system is by recording its electrical activities. Two basic techniques can be applied: gross recording of electrical potential differences across a cell population from the retina (electroretinogram) as well as from the visual cortex

(visually evoked cortical potential), or recordings from a single cell by positioning a microelectrode onto (or into) its cell body or nerve fiber. To a certain extent, the function of individual retinal cell types can be correlated to certain ERG-components; for a recent survey see Tomita (1978).

The human *electroretinogram (ERG)* is strongly dominated by rods (for surveys see, e.g., Müller-Limmroth 1959, Straub 1961, Armington 1974); therefore it is very difficult to extract information about an individual cone mechanism. In ERG recordings, the blue-sensitive cone mechanism could be clearly isolated by chromatic adaptation (see below) in rhesus monkey (Gouras 1970), in the local ERG (Baron et al. 1979), in man (van Norren and Padmos 1973) and in the even more rod-dominated cat (Zrenner and Gouras 1979a, Schuurmans and Zrenner 1981a); the exact separation of the red- and green-sensitive cone system in the primate ERG was either not obtained at all (Cavonius 1964 using flicker stimuli) or only in part (Padmos and van Norren 1971, Mehaffey and Berson 1974, Langhof 1977, Langhof and Zrenner 1977) when compared with absorption spectra of individual cone photopigments. In protanopic observers, however, the absence of the red-sensitive cone mechanism was clearly evidenced by the ERG (Dodt et al. 1958).

On the other hand, the foveal region is strongly represented in the visual cortex. It was therefore easier to isolate the fundamental cone mechanisms in the *visually evoked cortical potential (VECP)* of normal trichromats (Kellermann and Adachi-Usami 1973, Zrenner 1977a) and in color-blind observers (Zrenner and Kojima 1976, 1977). Clear evidence for *color-opponent* processes between cone mechanisms were described in the human VECP by Zrenner (1977a, b) and in the VECP off-effect by Jankov (1978). Opponency in the ERG b-wave is much weaker, though there is some evidence for it in recordings from cat (Zrenner and Gouras 1977, 1979a) and primate (van Norren and Baron 1977, Baron 1980).

Since Chapter 6 is devoted to VECP-recordings and psychophysical aspects of color vision, additional references and a more detailed treatment of these subjects can be found there. However, it seems difficult ot obtain further results from *gross* potentials, which could elucidate *specific* mechanisms of color vision.

Single Cell Studies, Anatomy and Electrophysiology

In the following, anatomical and physiological aspects of the various retinal neurons will be briefly touched upon. Since for reasons of space no complete survey can be given, the references were selected, so that just an introduction to the individual fields of interest can be provided in the following. This part of the introduction covers also the earlier developments, while

some of the most recent findings are discussed in the chapters devoted to single cell recordings (Chaps. 3, 4, and 5).

Receptors. It is very arduous to record from individual cones, since they are so tiny, yet Baumann (1965) devised a method of tapping cone signals in isolated frog retinas, kept in a modified Sickel (1966) chamber. Tomita (1965) and his co-workers (see Tomita 1970, 1972, 1973) have been able to record intracellularly from single cones in carp, Baylor and Fuortes (1970) in turtle; they clearly confirmed the existence of three spectrally distinct cones. In cat, intracellular recordings from cones (Nelson 1977) also revealed interconnections between rods and cones. However, in primates, no intracellular recordings from single cones have yet been obtained.

Photoreceptors of vertebrates respond to light exclusively by hyperpolarization (Bortoff 1964, Tomita 1965), which in cones results from a decrease of conductance (Toyoda et al. 1969), based on changes in the membrane's sodium permeability. This is probably caused by an internal transmitter (see Hubbel and Bownds 1979); most probably calcium ions are involved in the process (Hagins 1972, Yoshikami et al. 1980). Interestingly, in rods of the tiger salamander, there is no prominent light-induced change of resistance (Lasansky and Marchiafava 1974).

Horizontal Cells. In some species horizontal cells (*chromatic or C-type*), laterally connecting the receptors, can change their polarity, i.e., they are hyperpolarized by light from one part of the spectrum, but depolarized by light from another. This change in polarity was first shown in fish by Svaetichin[1] (1965) and Svaetichin and MacNichol (1958), giving the first electrophysiological evidence for the validity of Hering's opponent-process theory. C-type horizontal cells have not been recorded in primates. There is a second group of horizontal cells (*luminosity or L-type*) which uniformly respond to light of any wavelength; this type seems to be predominant in primates (see Gouras and Zrenner 1979b). The combined electrophysiological and morphological classification of horizontal cells has been worked out in fish retina by Stell (1976), after indentification had been achieved by Kaneko (1970, 1971); in cat horizontal cell axon terminals by Nelson et al. (1975), in A II type horizontal cells which receive input from rods and cones by Nelson et al. (1976) and in the A I type, which receives input only from cones by Nelson (1977). Anatomically, also in monkey, two types of horizontal cells are found (Kolb et al. 1980). The electrical interactions leading to the various types of horizontal cell responses were extensively studied in turtle by

1 In early papers Svaetichin believed he was recording from cones, later it turned out that unwittingly he had studied horizontal cells

Fuortes and Simon (1974), who developed a model of color vision based extensively on horizontal cell recordings; for recent studies on the validity of feedback models see Yazulla (1976), Hashimoto and Inokuchi (1981), Neyton et al. (1981a, b) as well as Chap. 4 of this book. The graded intracellular potentials recorded from these cells are now commonly referred to as S-potentials in honor of the discoverer Gunnar Svaetichin. The contribution of rods and cones to the generation of S-potentials in cat was studied by Steinberg (1969a, b, c), Niemeyer and Gouras (1973) and Nelson (1977). For further details about this very interesting group of cells see the reviews and articles by Gouras (1972), Stell (1972) and, especially for anatomical observations, those of Gallego (1971), Kolb (1970, 1974) and Boycott and Kolb (1973).

Bipolar Cells. Bipolar cells form a pathway for transmission from the photoreceptors to the ganglion cells (Cajal 1933). Slow, graded potentials were recorded from bipolar cells in goldfish (Kaneko 1971), mudpuppy (Dowling and Werblin 1971) and cat (Nelson et al. 1981); they show a clear, spatially antagonistic, center-surround structure in their receptive field. Based on Golgi preparations of the goldfish retina, Stell (1972) classified bipolar cells into two groups: large- and small-sized ones. The former received inputs mainly from rods, whereas the latter had inputs exclusively from cones.

Scholes (1975), using the Golgi electron microscopy and photomicrographic densitometry techniques, described mixed cone-bipolar cells which were smaller and received inputs from both green- and blue-sensitive cones or from green- and red-sensitive cones; another small type of cone-bipolars was connected exclusively to blue-sensitive cones.

In many vertebrate retinas (Werblin and Dowling 1969, Kaneko 1973), two electrophysiologically different types of bipolar cells have been found: "on"-center ones and "off"-center ones. Recently, Famiglietti et al. (1977) demonstrated in the carp retina with the procion dye method that both the "on" and "off" center bipolars are positioned in different layers and can be further subdivided into large and small bipolars, respectively; the large bipolar cells correspond to the rod-bipolars, while the small bipolars correspond to the cone-bipolars described above in accordance with the distinction introduced by Cajal (1933) in mammalian retina (see also Famiglietti 1981). Kato and Negishi (1979) demonstrated the different waveforms and V-log I relations of rod- and cone-bipolar cells in the carp retina.

A series of anatomical studies suggests special circuitries for bipolar cells. Polyak (1957) categorized the bipolar cells of primates as either *polysynaptic* rod and cone bipolar cells which consisted of "mop" (Cajal's rod), and "brush" and "flat-top" (Cajal's cone) bipolar cells, or *monosynaptic* "mid-

get" cone bipolar cells (similar to those described by Cajal in the fovea of diurnal birds). Polyak's (1957) description of primate bipolar cells was essentially confirmed by Boycott and Dowling (1969). Subsequently, Kolb et al. (1969) demonstrated that the monosynaptic or midget bipolars were of two varieties: invaginating, forming central elements at the ribbon synapse; and flat, forming basal junctions. It was later demonstrated that rod bipolars were, indeed, connected exclusively to rods, while flat-top bipolars were diffuse cone-contacting bipolars which formed basal junctions with many cone pedicles (Kolb 1970). Thus, the cone bipolar cell system of primates is thought to be composed of two varieties of single (midget) cone-contacting bipolar cells, flat and invaginating, a multiple (diffuse) cone-contacting bipolar cell pathway of the flat variety as well as an invaginating counterpart (Mariani 1981). Intracellular staining and recording in cat revealed that the on-pathways are characterized by sign-inverting invaginating synapses in the outer plexiform layer, combined with sign-conserving ones in the inner plexiform layer located in the inner two-thirds of this layer (Nelson et al. 1978); off-pathways are anatomically discernable by sign-conserving flat synapses in the outer plexiform layer and by dendritic branching in the outer third of the inner plexiform layer (Nelson et al. 1978, see also Kolb 1979, Nelson et al. 1981, Wässle et al. 1981a, Peichl and Wässle 1981) although deviations from this pattern are reported (Nelson 1981). Interestingly, in carp retina double-opponent bipolar cells were found, with hyperpolarizing and depolarizing responses in both center and surround (Kaneko and Tachibana 1981).

Extensive electrophysiological studies on primate bipolar cells are not yet available. Work on midget ganglion cells in primates (Gouras 1971) suggests that there must be such a bipolar cell providing a "private" line between a single foveal receptor and a single ganglion cell (Polyak 1941), with a small, color-antagonistic, inhibitory surround; this cell-type could play an important role in color vision (see also Mariani 1982).

Amacrine Cells. Amacrine cells receive input from bipolars and other amacrine cells; they have output not only to ganglion cells and other amacrines but also to bipolar cells via reciprocal synapses; they can obviously integrate information over a large area of the retina; most of the cells respond with a transient depolarization at the on- and offset of a stimulus (see Werblin and Copenhagen 1974). They are possibly involved to a greater degree in temporal contrast and motion detection (Werblin and Dowling 1969) since they build up complex receptive fields (Dubin 1970).

In cat, 22 different types of amacrine cells are discerned morphologically (Kolb et al. 1981); amacrine cells (type A II) were found to play a special role as interneuron in the rod pathway (Kolb et al. 1976) probably quick-

ening the time course of rod signals (Nelson 1982); they often have a pronounced sustained response pattern in addition to the transient ones at light on- and offset, making them a likely source of an input to ganglion cells under dark-adapted conditions. Amacrine cells are possibly also highly involved in the circuitry responsible for the shift-effect (Krüger and Fischer 1973; Krüger 1981). There are many data and models on the function of amacrine cells in the visual system (e.g., see Arden 1976, Kaneko et al. 1981, Marchiafava and Weiler 1980, Weiler and Marchiafava 1981, Vallerga 1981); their role in color vision, however, is still unclear, although they could indeed provide a second stage for generating strong opponency between cone mechanisms (Gouras and Zrenner 1981 b); Kaneko (1973) described one example of a color-opponent amacrine cell in goldfish retina.

Biplexiform Cells. The so-called interplexiform cells of the mammalian retina (Boycott et al. 1975) branch within the inner and outer plexiform layer and are usually classified within the amacrine cell system.

Interestingly there is a previously undescribed class of *ganglion* cells, the so-called biplexiform cells; these cells have an axon in the nerve fiber layer and dendrites in the inner plexiform layer; however, they also possess long dendritic processes, which extend to the outer plexiform layer and directly contact rod photoreceptor terminals. These cell types were first described anatomically in Golgi impregnations by Mariani (1982); intracellular recordings and stainings with horseradish peroxidase were obtained by Zrenner et al. (1982a) permitting classification of this new cell type as a depolarizing non-color-opponent ganglion cell with input from at least two cone mechanisms and rods.

Ganglion Cells (Early Data). The early ganglion cell recordings made by Hartline (1938) in the frog's optic nerve were classified as on, off and on-off responses, depending whether a cell showed an increase in spike frequency during, after or at both on- and offset of a stimulus. Hartline (1938, 1949) also showed that the receptors converging onto a ganglion cell are arranged in a distinct area, which he named receptive field; he also demonstrated that in limulus, illumination of adjacent areas provides inhibition onto the center-responses via a lateral nervous connection.

Granit and his co-workers first applied microelectrodes to the investigation of color vision (for review see Granit 1945, 1955, 1947); they found cells with broad action spectra (dominators) and several others with narrow action spectra (modulators). From these data Granit developed a theory in which the dominators, subserving luminosity, determined the spectral sensitivity of the species, while the modulators formed a chromatic channel. Granit's theory is generally thought to be incomplete, since it did not expli-

citly state that excitatory and inhibitory signals respectively constitute color-opponency in a single cell. However, he deserves strong credit for being the first to have recorded from color-opponent cells, since the narrowband modulator cells typically reflect *one* spectral band (either excitation or inhibition, see below) of a color-opponent cell. Granit did not preclude modulator curves resulting from interaction between spectrally different cones; however, he noticed that "red and green elements are always coupled" (Granit 1941) and that one of the mechanisms can suppress the other (Granit 1949). Granit and Tansley (1948) already described various types of on-, off- and on-off-ganglion cells which showed different degrees of sensitivity to blue and red light with varying discharge patterns, subsequently observed also in single retinal elements of rabbits by Dodt and Elenius (1956).

Kuffler (1953) and Kuffler et al. (1957) discovered that the receptive fields of ganglion cells in cat are divided into a central and a peripheral area which give on- and off-responses, respectively; this finding shed new light onto the meaning of on- and off-responses even though they could not find color-coded ganglion cells. Recording from the *lateral geniculate body (LGN)* in rhesus monkey, De Valois et al. (1958, 1966), De Valois (1965) and Wiesel and Hubel (1966) found cells which increased their spike frequency when stimulated by light from one spectral region, but decreased their discharge rate when stimulated by light from another spectral region; these two response types have been recorded from *retinal ganglion cells* in macaque monkey (Gouras 1968), from the *optic nerves* of the spider monkey (Hubel and Wiesel 1960) and the ground squirrel (Michael 1966) as well as in the retina of goldfish (Wagner et al. 1960a, 1963) and carp (Motokawa et al. 1960, Witkovsky 1965); thus, color-opponent processes, as predicted by Hering a century ago, were finally proven to take place in the central nervous system.

The relation of the spatial to the spectral properties of primate ganglion cells was studied in depth first by Wiesel and Hubel (1966) recording from the LGN: Their classification was mainly based on spatial and spectral properties of the various cell types. Wagner et al. (1960a, b, 1963) had obtained similar results from retinal recordings in goldfish where they had correlated color-opponency with the spatial structure of the receptive field. Spectrally different cones therefore selectively feed center and surround mechanisms of the receptive field in many cells. Using spots and annuli, Daw (1968, 1972) discovered that a large number of goldfish ganglion cells respond in an even more complex, double-opponent manner; such units yield on-responses to red, and off-responses to green stimuli in their center, while their surround responds to red stimuli with inhibition and to green stimuli with excitation. In fish, at least three chromatically different types

of horizontal cells are involved in building up the circuitry for retinal coding of color in double-opponent ganglion cells (Spekreijse and Norton 1970). These types are very rare in primates, probably since only a single type of horizontal cell with monophasic hyperpolarization has been found to date. In non-primates, such as ground squirrel, double-opponent units were found in the optic nerve by Michael (1966).

The functional role of the two systems, one of which signals light increments (on-system), and the other light decrements (off-system) was clarified by Jung (1965, 1973); he succeeded in determining the correlations of brightness and contrast vision with these dual neuronal pathways; thereby the functional role of antagonistic cellular mechanisms for visual perception was firmly established.

After a brief excursion into methods, the more recent studies will be extensively discussed; new facts, data and models primarily concerning color coding in retinal ganglion cells will be presented. The knowledge gained in the last decade, which was not touched here, will be directly correlated in Chapters 3, 4, and 5 with the new findings on color coding in retinal ganglion cells, outlined in this book.

2 Methods

In the following, a general description of the methods applied in these studies will be given. Preparation, recording and evaluation techniques were very similar from experiment to experiment, while the stimulus conditions most often varied; therefore, specific data on the stimuli used in individual experiments are contained either in the text or in the figure legend. The methods employed for the investigations in *human* observers are lined out in the first part of Chapter 6.

2.1 Methods of Single Cell Recording in Rhesus Monkeys

The methods described in the following are similar to those developed by Gouras and Link (1966), Gouras (1967), De Monasterio and Gouras (1975) and Gouras and Zrenner (1979a).

Preparation

The eyes of 19 adult monkeys (*Macaca mulatta*, 2.5-4.8 kg) were studied. The animals were anesthetized with sodium pentabarbitone (Nembutal, 20 mg/kg/4 h intraperitoneally (i.p.) or 5 mg/kg/h intravenously (i.v.), paralyzed with gallamine triethiodide (Flaxedil, 10 mg/kg/h, i.v.) and sustained by artificial respiration (20-25 strokes/min, 25-35 ml/stroke). Rectal temperature and the percentage of CO_2 in the expired air (kept between 4% and 5%) were monitored. Interruption of the gallamine infusion indicated a light level of anesthesia. Mydriasis and cycloplegia were obtained with cyclopentolate hydrochloride (Cyclogyl, 1%) and phenylephrine hydrochloride (Neosynephrine, 10%) instilled every 12 h. The head was held by supports in the external auditory canals and under the hard palate. The cornea was moistened with a few drops of methyl cellulose 1% and then covered with a plastic contact lens, fitted to the rhesus monkey cornea. The lenses were removed and the eyes flushed with isotonic saline solution and closed for 8 h after every 10 h of experimentation. Corneal transparency usually remained normal during the experiments which lasted 2-3 days. A hole, 2 mm

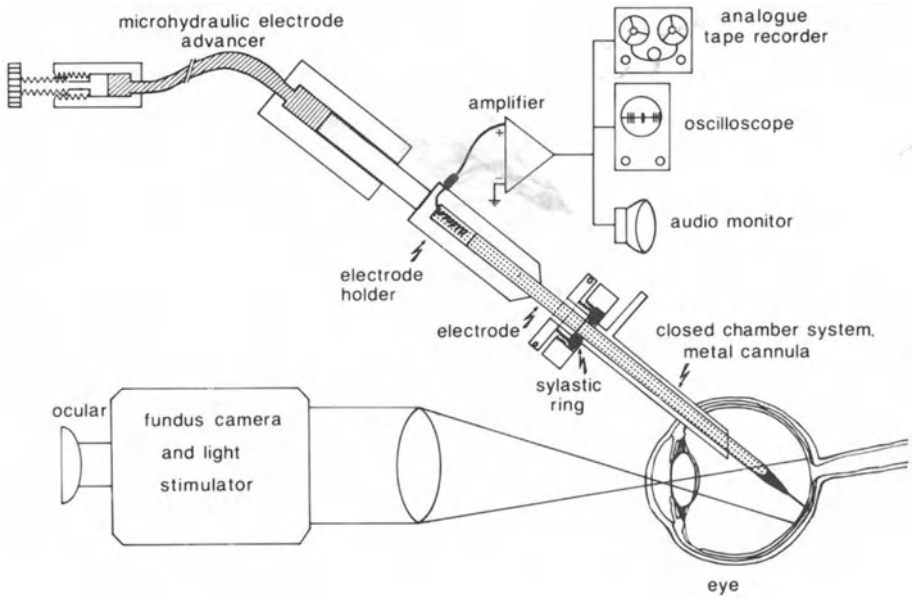

Fig. 2.1. Schematic description of the stimulation, recording and evaluation technique used for single cell recording in rhesus monkey retina

in diameter, was made about 5 mm temporal to the limbus using the tip of a scalpel blade or a trepan while observing the eye through a stereoscopic microscope. A metal cannula with 2 mm outer diameter, attached to a micromanipulator, was inserted into this hole and advanced about 5 mm into the vitreous body in order to serve as guide for the electrode (Fig. 2.1). Glass micropipette electrodes were pulled on a Narishigi two stage puller (with the electrode 1.2 mm in diameter and tightly fitting into the metal cannula); it then was introduced through the cannula and driven slowly onto the retina with a hydraulic microdrive. The distal end of the cannula contained an annular cuff made of sylastic, the inner diameter of which could be regulated by pressure to ensure an adequate fitting to the pipettes. Thus, a closed-chamber system was attained which avoids the loss of vitreous humor and thereby reduces the transmission of vascular pulsations.

The fundus was viewed through an ophtalmoscopic camera (Bausch and Lomb) so that the electrode's ultimate path could be estimated. The position of both eye and electrode could be altered in order to direct the electrode to a specific area of the retina.

Stimulation

The light source was a 1 kW, high pressure Xenon arc lamp (Osram XBO, color temperature ca. 5500 K) with the voltage being transformer-regulated with a ripple of approximately 5%.

Two independent light beams were projected into the eye in Maxwellian view[2] through the fundus camera. The area, timing, energy, wavelength and retinal position of the stimuli obtained from these beams could be independently controlled. One light path served as test-beam, the other as adapting beam. The energy and wavelength of the test-beam were varied by means of neutral density and narrow-band interference filters (399-666 nm) in steps of 0.15 to 0.3 log units and about 20 nm, respectively. Interference filters were checked for side-bands in a spectrophotometer. The irradiance E_Q (for simplicity called E) was determined on a quantal basis for each wavelength and calibrated in Quanta s^{-1} μm^{-2} with a reverse bias photodiode PIN 10 (United Detector Technology, Inc.). The transmission of the neutral density filters was measured for each wavelength used and corrected. Rectangular pulses of light, usually of 200 ms duration at 1 cycle per second (c/s) were obtained from a galvanometer-driven flag shutter placed at the first focal point in the test beam.

Circular or annular stops, concentrically mounted, were projected onto the retina through the fundus camera. Circular stimuli were available in the nominal range of 1/7°-32° in diameter in eight discrete steps. An annular stimulus was available in the nominal range of 3° in outer diameter and ca. 1° in inner diameter to test the cell's receptive field structure. These stimuli could be sharply focused upon and moved across the retina.

The retina was maintained in a light-adapted state; thresholds were always determined in presence of an adapting light completely covering the cell's receptive field and of sufficient energy to raise rod thresholds above those of cones. According to Aguilar and Stiles (1954) 2000-5000 scotopic troland (120-300 cd m^{-2}) are sufficient to saturate the rod mechanism. Under these conditions, in ganglion cells, most of which are fed by rods and cones (Gouras and Link 1966), only the cone signals are transmitted (Gouras 1967). Either a white (10 000-30 000 td) or one of three chromatic backgrounds (80 000-300 000 td) was used as adapting light (upper photopic range), obtained from Corning sharp cut glass filters, 2408 (red), 3482 (yellow), and 5543 (blue). The retinal illumination of these adapting lights was determined by matching them with the appropriate monochro-

2 For the problems of photometry, magnification and pupil size involved in using a "Maxwellian-view" system see Westheimer (1966)

matic light, previously standardized. Flickering stimuli with equal periods of light and darkness were produced by a two-sectored disk rotated at a focal point in one of these beams by a variable speed motor and continuously monitored by a photocell.

Recording and Evaluation Procedure

Fine glass micropipettes filled with 3M potassium chloride (resistance between 20 and 60 MΩ in situ) were advanced into the eye through the closed chamber system. The signals were recorded by a high impedance amplifier, displayed and superimposed on a storage oscilloscope; the signals were monitored on an audio amplifier and stored on electromagnetic tape. For extracellular recording of action potentials "spikes", and a.c.-coupled system was used with a frequency range from 8 c/s to 10 kc/s (3 db). For intracellular recordings, a d.c.-coupled system was used at lower gain with a high frequency attenuation at 2.5 kc/s (3 db). The reference electrode was a stainless-steel needle placed under the scalp. The responses were later photographed from the electromagnetic tape in order to evaluate the entire discharge pattern and to measure latencies.

Fusion and response latencies for increasing flicker frequencies were determined (± 1 ms) by superimposing 10 to 20 responses and stimuli on a double-beam storage oscilloscope which provided a continuous monitor of the phase relationship of the response to the stimulus cycle. Responses were also averaged with a signal averager CAT 400A (Mnemotron Corp.) and plotted as histograms with a conventional X-Y plotter. Some of the histograms were evaluated manually from the film by measuring the time intervals between spikes on a projection screen (average of at least four responses).

2.2 Identification of Cone Inputs in Retinal Ganglion Cells

In order to determine which type of cone has input to a retinal ganglion cell, in most cells the attempt was made to identify the spectrally different cones by their action spectra. For isolation of individual cone types, the so-called method of chromatic adaptation was used; according to Stiles (1949, 1959) and Wald (1964), the sensitivity of each cone can be selectively depressed by exposing the eye to visible radiation of appropriate wavelengths (the limitations of this method are discussed in Chap. 6.3). Figure 2.2 shows such data obtained in retinal ganglion cells of rhesus monkey (Wienrich and Zrenner 1981). For each monochromatic test light (abscissa)

the irradiance E (Quanta s^{-1} μm^{-2}) was determined which was necessary to produce a threshold-response in a ganglion cell, i.e., a small impulse frequency increment for excitatory responses or a decrement for inhibitory responses. The reciprocal of the irradiance renders the sensitivity S of the cell for each wavelength (ordinate; for additional information on this part of the method see comments and legend of Fig. 3.4). The action spectra of cells were determined for three different background lights (μ): Red-orange light (Schott RG 630, with a retinal illumination of $10^{6.2}$ td), suppresses the red- and green-sensitive cones, by heavily bleaching their pigment, so that only the blue cone – if present – determines the cell's action spectra below 560 nm. This is shown for three cells (*triangles* in Fig. 2.2, mean and standard deviation), the sensitivity of which closely follows the pigment absorption spectra of blue-sensitive cones (*solid lines*, λ_{max} = 440 nm) corrected for the absorption in the ocular media and in the macular pigment.

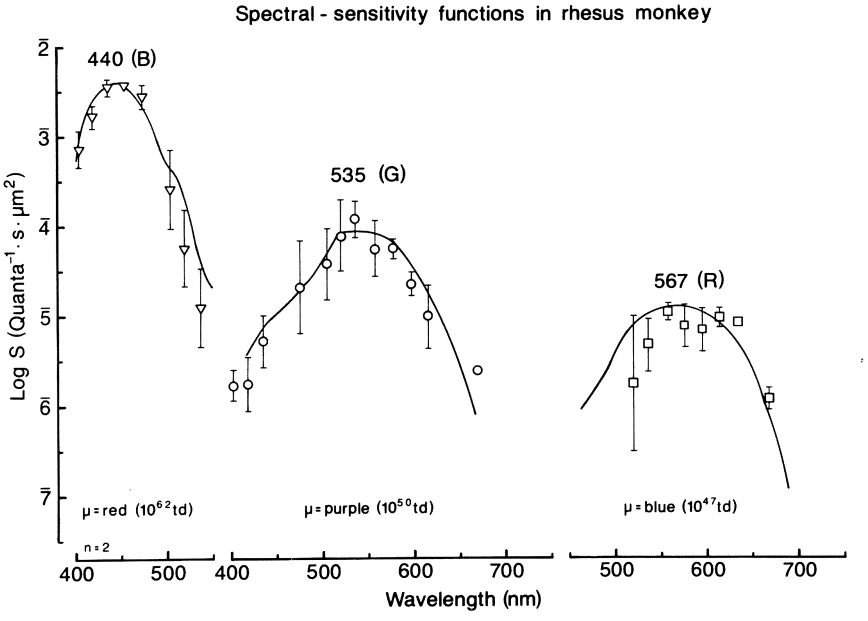

Fig. 2.2. Action spectra of three populations of retinal ganglion cells of rhesus monkey based on a constant threshold criterion, evoked by monochromatic wavelengths (stimulus size 15°, duration 200 ms). Isolated by the appropriate background illumination (μ), the blue-sensitive cone *(B)* determines the threshold in the population on the *left* (*triangles* n = 3, mean ± standard deviation, S.D.). The green-sensitive cone *(G)* is isolated in the cell population in the center, while the red-sensitive cone *(R)* is present in the population on the *right*. The functions are compared with the pigment absorption spectra (*solid lines*) of Bowmaker et al. (1980), obtained by microspectrophotometry in rhesus monkey photoreceptors, with λ_{max} values indicated on the top of each function. The R-function is completed with Stiles' (1959) π_5-function at the very long-wavelengths end of the spectrum (reported by Wienrich and Zrenner 1981)

Purple light (Schott interference filter with two bands at 422 and 630 nm) of 10^5 td suppresses the blue- and the red-sensitive cone, so that the green-sensitive cone – if present in the cell – determines the threshold. This is shown for another cell population in the center of Fig. 2.2 (*circles*). The function follows closely the pigment absorption curve of green-sensitive cones. Blue light (Schott BG 28) of $10^{4.7}$ td suppresses the blue and green cone's sensitivity, so that the red-sensitive cone – if present in the cell – determines the threshold. This was the case in the cell population on the right of Fig. 2.2 (*squares*), which throughout the long-wavelength part of the spectrum fits the pigment absorption curve of the red sensitive cone. At the short-wavelength branch the standard deviation increases, due to variations in color-opponency between the two long-wavelength-sensitive cones as described in Chap. 3.4.). The theoretical implications involved in measuring action spectra will be discussed in depth from various viewpoints in Chaps. 3.3, 3.4, 5.2, 5.6, 6.2, 6.3 and 6.4; Fig. 2.2 only serves to clarify the methodological approach to classify ganglion cells according to the spectral properties of their *cone* inputs, which were actually determined in the following experiments, in contrast to other classification schemes (e.g., Creutzfeldt et al. 1979), which are based on responsivity of cells to fixed test light irradiance of certain wavelengths.

Having gained knowledge about the spectral properties of these cells, an initial abbreviated classification procedure was developed (see Chap. 3.7), which serves to classify cells according to their cone input, even if they were held only shortly.

It should be emphasized that the terms "red-, green- and blue-sensitive cones" or "R-, G- and B-cones" do not at all relate these photoreceptors to certain sensations of color. In this book they exclusively denote the cones' ***pigment absorption spectra*** *according to the regions of the human visible spectrum in which these pigments are predominantly sensitive.*

3 Types of Retinal Ganglion Cells and Their Distribution

Only the common types of retinal ganglion cells which have an incidence of more than about 1% of electrophysiologically determined samples will be discussed here in depth. There are very rare cells, which deviate from the following description, e.g., showing indications of various trichromatic inputs (De Monasterio and Gouras 1975, De Monasterio et al. 1975a) which are still not well understood (Wooten and Werner 1979); it is questionable whether cells of such rarity can play a major functional role in the visual system. In Chap. 3.4 it will be demonstrated that cells showing rather striking variations in their spectral sensitivity can be easily assigned to one common group, taking into account retinal eccentricity and varying dominance of individual cone mechanisms. Blue-sensitive ganglion cells show a series of interesting properties, separately discussed in Chapter 4. For a comparison of the incidence of certain groups of color-opponent cells in several studies from different laboratories see Table 1 in the review article of Gouras and Zrenner (1981b).

3.1 Introductory Remarks

Two general classes can be distinguished in the sample of 385 ganglion cells described in this study, tonic cells and phasic cells.

Tonic Cells. Color-opponent tonic cells, which usually have a concentrically organized receptive field (RF) structure, generally involve at least two of the cone types (red-, green- or blue-sensitive), one in the center and another in the surround, as described, for example, by Wiesel and Hubel (1966), De Valois et al. (1966) and Gouras (1968). Since the center and the surround mechanisms act antagonistically through excitatory and inhibitory responses, different wavelengths can have opposite effects on such a cell; the strength of the chromatic antagonisms can vary considerably throughout the spectrum, depending on the degree to which the center and surround mechanism provide signals to a retinal ganglion cell (see Chap. 3.4). Moreover, color-opponent cells are more common near the foveolar region

of the retina (De Monasterio and Gouras 1975) and are characterized by tonic responses, i.e., the discharge rate of action potentials ("impulses" or "spikes") is approximately sustained during the whole period of stimulation with monochromatic light.

Phasic Cells. The second general class consists of spectrally non-opponent *phasic cells* as described by Gouras (1968) in monkey. Through the entire spectrum, such cells respond uniformly to the onset of light stimuli, either with excitation (increased impulse discharges, in about two thirds of the cells) or inhibition (decrease of impulse discharges, in one third of the cells). They have a concentrically organized receptive field structure, usually with the same spectral receptor types in their center *and* surround (red- or green-, but no blue-sensitive cones, as shown by Gouras 1968). They are more common in the retinal periphery and mostly respond in a phasic manner, i.e., with a transient discharge at the on- and/or the offset of the light stimulus. The average conduction velocity of their axon and their soma volume is higher than that of color-opponent tonic cells (Gouras 1969, Schiller and Malpeli 1977); this led to the hypothesis (see Gouras 1969, 1971) that phasic cell axons might project to the magnocellular layer, while tonic cell axons project to the parvocellular layer of the corpus geniculatum laterale, a suggestion that was experimentally proven by Dreher et al. (1976), Sherman et al. (1976), Schiller and Malpeli (1978) and Lee et al. (1979); some deviations from these projections were reported by Bunt et al. (1975). Although there is no functional reorganization, there is an anatomical segregation which suggests that magno- and parvocellular layers have special functions in coding color (Schiller and Malpeli 1977, Creutzfeldt and Lee 1978); this led Creutzfeldt et al. (1979) to an alternative classification of color-specific cells which, however, does not assign spectrally determined cone mechanisms to the several types of ganglion cells.

Phasic ganglion cells, on the other hand, may project to several different geniculate layers, as shown in cat ganglion cell projections by Bowling and Michael (1980). Since projections to the superior colliculus are made exclusively by phasic cells (Schiller and Malpeli 1977), they might carry out special tasks in the oculomotoric system.

X-Y Classification. For those who are used the thinking in terms of Enroth-Cugell and Robson's (1966) *X-Y classification*, applied to the cat's retina, it might be interesting to note that X-cells in many respects resemble tonic cells, while Y-cells resemble phasic ganglion cells in monkey (Dreher et al. 1976, De Monasterio 1978a, Perry and Cowey 1981, Leventhal et al. 1981); this also applies to the anatomical classification of Boycott and Wässle (1974) in terms of β- and α-cells (see also Peichl and Wässle 1979,

Wässle et al. 1979 and their subsequent papers discussed in Chap. 1) as well as to Cleland et al. (1971) distinction between sustained and transient ganglion cells, respectively (for review see Cleland et al. 1975, Wässle et al. 1975, Hughes 1979) and the distinction in terms of a slow- and fast-conducting fiber system (Gouras 1969, Hoffmann et al. 1972, Eysel and Grüsser 1974, Marrocco 1976).

A more extended review, concerning the projection of retinal neurons to the Corpus geniculatum laterale and the anatomical and electrophysiological experiments which substantiate the hypotheses of two parallel systems of ganglion cells is given by Gouras and Zrenner (1981b). However, it will be shown in Chapters 3,4 and 5 that the *functional* role of these two parallel systems might be rather different from the one assigned usually to them at present.

In the following chapter, a descriptive survey will first be given; the response pattern, spectral behavior, receptive field structure and retinal distribution of the individual cell types will be presented. A subgroup of spectrally *non*-opponent cells responding with *tonic* discharges will be introduced (Chap. 3.5), together with a small sample of cells which does not fit into this general description. Second, the role these cell groups might play in vision, and the extent to which variations in the strength of the chromatic antagonism might influence the visual system's performance will be discussed. Additional experiments performed on the cells described in this chapter will be presented and analyzed in Chapters 4 and 5.

3.2 The Concept of Color-Opponency

As outlined in Chapter 1, the concept of color-opponency was introduced into vision by Hering (1878), and first confirmed in modern neurophysiology by Svaetichin (1953, 1956). In the following a short introduction to this concept, as revealed by ganglion cell recordings will be given.

The responses of a typical red/green color-opponent ganglion cell to repetitive stimulation (1 c/s) and its simplified *functional* diagram are shown in Fig. 3.1. This diagram stresses the function rather than the circuitry; the action of interneurons (IN_2 and IN_3) can take place at two levels, that of horizontal cells as well as that of amacrine cells, that is, in the outer as well as in the inner plexiform layer. For the actual anatomical organization of the primate retina, the interested reader is referred to the extensive study of Polyak (1941), Boycott and Dowling (1969), Kolb et al. (1969), Dubin (1970), Kolb (1970), Dowling and Werblin (1971).

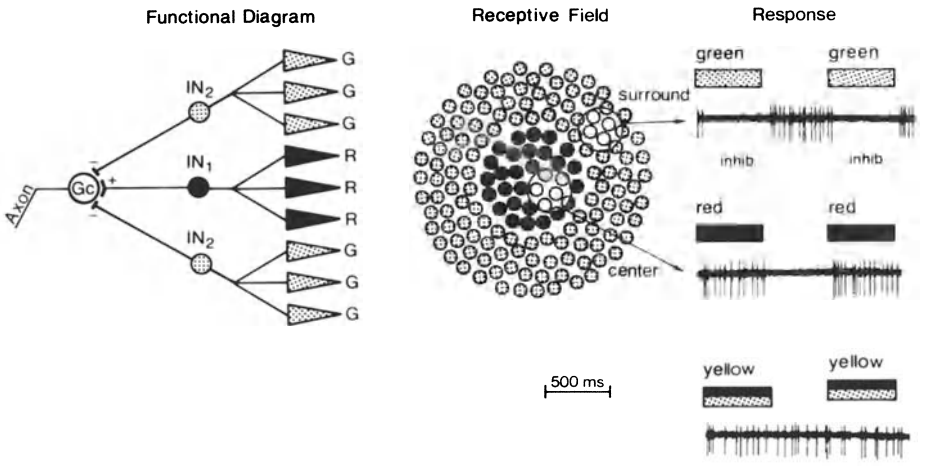

Fig. 3.1. Simplified functional diagram, receptive field structure and responses of a color-opponent ganglion cell. In this cell the red-sensitive cones in the center act excitatorily (+), the green sensitive cones in the surround act inhibitorily (−). Yellow light, which stimulates both red- and green-sensitive cones, produces no modulated response to light, since excitation and inhibition cancel each other out. The stimuli indicated by *bars on the right side* cover the entire receptive field. The number of receptors (*dotted* or *filled circles*) is arbitrary. The separation of the spectrally different receptors is not as strict as the border of center and surround as is depicted here for simplification

Color-Opponent Responses. Postponing the discussion of the link between receptor and ganglion cell responses until Chapter 4, the ganglion cell activity shown in Fig. 3.1 is generated as follows: When red light (*solid bars*) is projected onto the cell's receptive field (RF), i.e., the population of photoreceptors which converge onto this cell (Fig. 3.1, *center*) in this example red-sensitive cones (*black spots*) *excite* the cell through its center, so that it responds with an impulse discharge during the whole period of stimulation (tonic response); when the red light is turned off, the cell's discharge rate is low. Green light (*dotted bar*) produces the reverse phenomenon, *inhibiting* the cell through the green sensitive cones in the RF-surround. When the green light is turned off, the activity is high, due to an overshooting rebound depolarization of the ganglion cell, a phenomenon observed already in individual receptors after switching off a strong test light (e.g., Baylor and Fuortes 1970). Consequently, at the offset of a strong test light, a red-green opponent ganglion cell's membrane potential is driven transiently in the opposite direction, so that excitation is usually followed by inhibition and vice versa. Note that the responses of this cell to long and short wavelength lights are almost 180° out of phase. In this example the red-sensitive cones in the center of the RF cause excitation; impulse rate increases

in the ganglion cell in response to *in*crements of red light; cells with such structures are called on-center cells. If they caused excitation to *de*crements of red light, such cells would be called off-center cells.

"On" and "Off". The terms "on" and "off" deserve a short comment: Originally the term on- and off-responses in ganglion cells referred to spike discharges occurring at the beginning or the end of a light stimulus. Since discharges at the termination of a stimulus are almost exclusively accompanied by inhibition *during* the stimulation, in many papers this inhibition is called "inhibitory off-response". On the other hand, excitatory phases caused by the onset of light ("on-responses") are often accompanied by inhibitory phases after the offset of light. This also implies that off-neurons respond with excitation to light *de*crements, while on-neurons respond with inhibition; on-center neurons show excitatory responses in the center of their RF and inhibitory ones in the surround to light *in*crements; in off-center cells the situation is reversed. Cells which can *not* produce spikes are called off-neurons, if they respond with hyperpolarization to light increments, and on-neurons, if under the same conditions they respond with depolarization. For further details on the problems of terminology see Jung (1965, p. 74).

The Neutral Point. It should be emphasized that wavelengths in between the green and red part of the spectrum which stimulate both center and surround about equally do not produce modulated responses to light (for this cell: yellow; see *dotted/solid bar* in Fig. 3.1); in this case, phases of inhibition and excitation cancel each other mutually; the cell only shows a comparatively weak, continuous discharge. The spectral region in between the absorption maxima of the two cone types, in psychophysical terms, represents the so-called neutral point of a cell. This spectral antagonism, i.e., when a cell is excited in one part of the visible spectrum, but inhibited in another, is called color- or cone-opponency, chromatic or color-antagonism, or also color-opponent interaction (for the historical development of this term see Chap.1). Color-opponency implies that the mutual antagonism between two spectrally different cone mechanisms is strongest in intermediate spectral regions where the different cone types involved are both stimulated simultaneously.

Spatial Organization. Not only do excitation and inhibition act through separate, spectrally different cone mechanisms, but the receptive field of a color-opponent ganglion cell is also spatially organized as an antagonistic center-surround structure (Fig. 3.1). The spatial separation of red- and green-sensitive cones in ganglion cells with large receptive fields is most pro-

bably not as strict as shown in this diagram. The fields can overlap even though a general separation of the cone types was found in most ganglion cells by stimulation with small spots (1/12 of a degree) in several locations of the cells' receptive field. Consequently, the predominance of excitation or inhibition depends on the locus of stimulation as shown first by Hartline (1949) in limulus and by Kuffler (1953) in mammalian eyes for spectrally non-opponent neurons. The spatial properties of the various types of color-opponent ganglion cells were first studied by Wiesel and Hubel (1966) as summarized below.

The Cone Interaction. The general mechanism is indicated on the left side of Fig. 3.1. The three cone mechanisms which have their absorption maxima in the long-, middle- and short-wavelength part of the spectrum (cf. Chap. 2) are labeled R, G, and B, respectively; in this example, the red-sensitive cones (R) form the excitatory RF-center and via interneurons (IN_1) depolarize (+) the ganglion cell (Gc), so that its impulse frequency increases; the green-sensitive cones (G) form the inhibitory surround hyperpolarizing (−) the cell via other interneurons (IN_2 and IN_3), so that the impulse frequency decreases. With some limitations (Hochstein and Shapley 1976), in spectrally non-opponent cells the activity in the axon is thought to be the linear sum of excitation and inhibition (see Enroth-Cugell and Pinto 1972a); with large, homogeneous stimuli, this seems to apply to color-opponent cells only to a limited extent, the output being strongly dependent on the temporal properties of the stimulus (see Chap. 5). For the psychophysical correlations of lateral interactions between spectrally different cone mechanisms see McKee and Westheimer (1970).

Special features of the interaction betwen the center and surround mechanism, depending on spectral, spatial and temporal characteristics, are described in detail in Chapters 3.4, 4.4, and 5.3. An elaborate circuitry of center-surround interaction will be given in Chapter 4: It will be demonstrated that in color-opponent cells, inhibition of the cells' spontaneous activity by the surround can well be accompanied by a sensitization of the ganglion cell to signals arriving through the center pathway, if *two* spectrally different stimuli are involved.

3.3 The Various Types of Color-Opponent Cells

Incidence of the Main Types

Depending on the spectral properties of the mechanisms involved, several groups can be discerned among color-opponent ganglion cells: Fig. 3.2

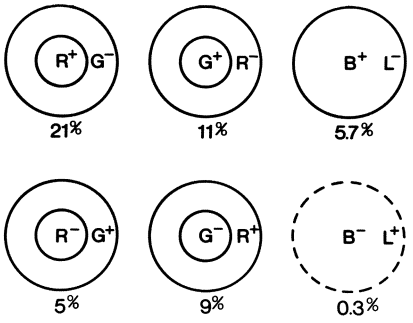

Fig. 3.2. The schematical structure and occurrence (in percent) of the six most common varieties of color-opponent ganglion cells. (Zrenner and Gouras 1981)

schematically presents the most common RF-structures (on-center neurons above, off-center neurons below) with their occurrence indicated in percent. There are several *rare* types of ganglion cells (e.g., De Monasterio and Gouras 1975), some of which are described later; considering the fine granulation of receptors necessary to detect small objects, the role of these odd cells in analyzing chromatic borders must be considered minor at higher spatial frequencies of stimulation. The most common type of ganglion cells (21%) has a RF structured so that the red-sensitive cones form an excitatory center with green-sensitive cones in the surround (R^+/G^-), as demonstrated by the scheme in Fig. 3.1. The index (+) or (−) denotes excitatory (on) and inhibitory (off) responses to light increments, as outlined p. 30. The second common type of cells (11%) is characterized by excitatory green-sensitive cones in the center and inhibitory red-sensitive cones in the surround (G^+/R^-). Cells with a blue-sensitive cone input are rare (only 6%) and show very typical responses in comparison to other cells (see below). Blue cones which *inhibit* a ganglion cell are extremely rare (0.3%) as also reported in the sample of Malpeli and Schiller (1978), Zrenner and Gouras (1978a, 1980, 1981), and Creutzfeldt et al. (1979); green or red cones, which inhibit a cell through the center of the RF are frequent (9% and 5%, respectively). It is difficult to judge which of the longer-wavelength-sensitive cones (L) forms the antagonistic mechanism of blue-sensitive ganglion cells. The data derived from spectral sensitivity measurements suggest that both long-wavelength-sensitive mechanisms act synergistically in these cells (De Monasterio et al. 1975a); often, however, chromatic adaptation does not reveal more than one antagonistc cone mechanism in blue-sensitive cells. Owing to this uncertainty, the antagonistic mechanism in blue-sensitive ganglion cells is referred to as long-wavelength (L). One has to be aware that deep violet lights (400-420 nm) can also stimulate the long-wavelength β-band of the *red*-sensitive mechanism (De Monasterio and Gouras 1977).

Just as the distribution of spectrally different cones in rhesus monkey varies (Marc and Sperling 1977), so does the spectral antagonism of the receptive field structure change with retinal eccentricity, favoring R-cones peripherally (see Chap. 3.6). Off-center neurons are generally less common than on-center neurons; their relation is about 2:3 in the sample described in this paper based on electrophysiological recordings. Statistical observations necessarily contain sample errors, due to the varying relation of electrode configuration to retinal cell size. Nevertheless, all these cell types can be found side by side in the retina; a single penetration very often hits two, three, or four different types of ganglion cells in sequence. However, their distribution across the retina changes *regularly* with eccentricity, as described in Chapter 3.6.

Comparison Between Spectrally Different Types

Receptive Field Structure. Excepting a small sample of cells described later, red/green-opponent ganglion cells usually show a concentrical field struc-

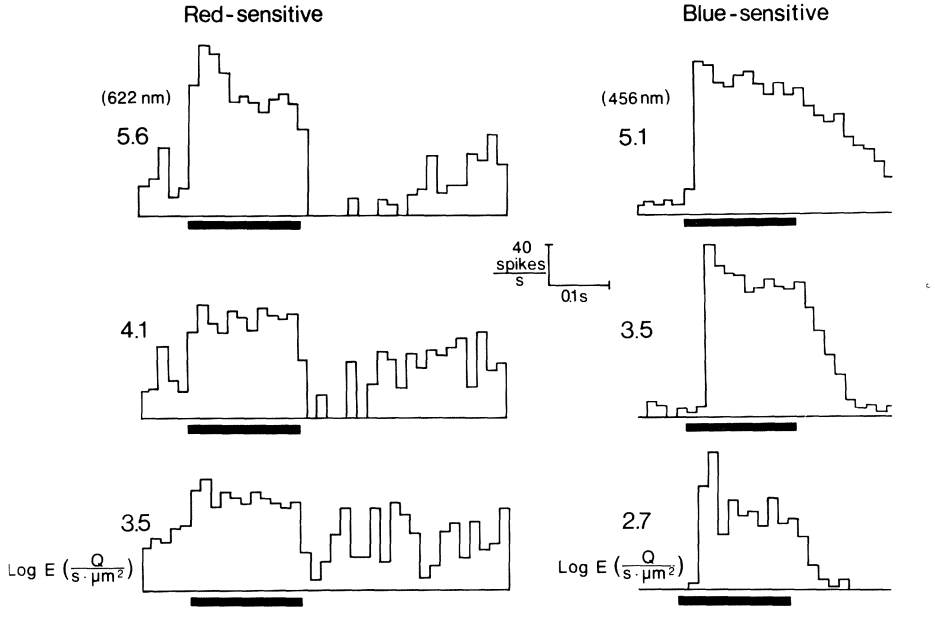

Fig. 3.3. Response profiles (histograms showing impulse/s vs. time) of cells with red-sensitive and blue-sensitive center mechanisms. In order to isolate the center mechanism, blue background was applied to the R/G-opponent cell (*left*) and yellow background was applied to the B/L-opponent cell (*right*, 300,000 td). The irradiance E of the test flash ($Q\ s^{-1}\ \mu m^{-2}$) is indicated beside each record. *Black bars* symbolize test flash duration. (Modified from Zrenner and Gouras 1981)

ture with center diameters between 0.1° and 0.3° angle; in contrast, blue-sensitive ganglion cells most often have a larger (0.5°-2°) coextensive field structure, where the excitatory and inhibitory parts of the receptive field cover about the same area (see Fig. 3.2). In the present study no attempt was made to determine precise sensitivity profiles of color-opponent ganglion cells beyond determining the *spectral* sensitivity of center and surround with small spots (see below). For the size of receptive fields and the sensitivity profiles of individual retinal ganglion cell types, see Gouras (1967, 1968), De Monasterio and Gouras (1975), and De Monasterio (1978b). These studies, as well as the present study, show that the spatial antagonism in *blue*-sensitive cells is obviously not developed to the same extent as the chromatic ones, indicating that spatial antagonism is not requisite for color-opponent ganglion cells. Two factors, coextensive large receptive fields and an obviously under-developed or slow-functioning off-mechanism (see Fig. 3.3) considerably reduce the spatial resolution; in addition to the scarcity of blue-sensitive cones in the fovea, these two factors decrease the visual acuity mediated by blue-sensitive ganglion cells. The larger receptive field size has its perceptual counterpart in the large field, in which van Tuijl's (1975) neon effect is maximal, as presented in a demonstration by Spillmann (1981).

Recent psychophysical investigations in man also strongly support the view that the red/green opponent tonic cells provide the trichromat's spatial resolution (e.g., Thoma and Scheibner 1980, 1982, Ingling and Martinez 1981, see also the comment of Ingling 1978).

Response Profiles. Furthermore, color-opponent ganglion cells, whose center mechanism is excited either by blue-sensitive or by red-sensitive cones, show striking differences in the *time course* of their responses. In Fig. 3.3, the impulse frequency obtained in a R/G- and a B/L-opponent cell is plotted against time in response to stimulation by the appropriate wavelength at three different levels of intensity; the wavelengths 456 nm and 622 nm were chosen so that threshold responses were evoked by each stimulus exclusively in *one* of the two cone mechanisms involved in a color-opponent cell. First, the response profiles of the two cell types show latency differences of more than 30 ms, when the onset of the stimulus and the rising phase of the response are compared; this is true for all levels of stimulation. Furthermore, as described by Zrenner and Gouras (1981) in blue-sensitive cells, the duration of the responses, especially ones evoked by strong test lights, is considerably longer than that of the test flash; after the offset of the test light, a blue-sensitive cell takes between 100 ms and 200 ms until its impulse frequency returns to the original level. Like the "after-effect" of rods (Steinberg 1969c) the response amplitude (in ganglion cells expressed

in terms of spike-frequency) only gradually returns to its prestimulus value after the stimulus is terminated; this return becomes accordingly slower as the strength of stimulation increases. Slow decay is seen to characterize blue-sensitive ganglion cells, while excitation in red/green-opponent cells ends abruptly with the termination of the test flash; in blue-sensitive ganglion cells, there is no inhibitory phase immediately after the offset of the test light as one observes in red-sensitive cells, where both the excitatory discharge and the degree of postexcitatory inhibition grow with strength of stimulation. These two features of blue ganglion cells, the long latency at the onset and the lack of immediate inhibition at the offset of lights which enables the cell to return rapidly to low impulse discharge frequencies (see also Chap. 4.2) apparently limit their time resolution; this observation is supported by experiments revealing a low maximal *flicker fusion frequency* of 35 c/s in blue-sensitive ganglion cells, while red- and green-sensitive cells reach a much higher flicker fusion frequency of 60-70 c/s (Zrenner and Gouras 1978a, 1981, Gouras and Zrenner 1979a, see also Chap. 5.1 for further discussion. The longer latency of the blue-sensitive system can be nicely demonstrated as a subjective perception by moving a slit, covered half by a blue and half by a red filter over a yellow area (see Mollon and Polden 1975 for further details); the blue part of the slit appears to move always behind the red part.

Spectral Sensitivity Functions. As outlined in Chap. 2.2 the action spectrum of a ganglion cell can be measured by determining the increment of irradiance E (Quanta s^{-1} μm^{-2}) necessary to produce a just-detectable response increment (in the range of +20 Imp/s) or decrement (-20 Imp/s) in impulse frequency as read off from the recordings for various wavelengths. Based on such a threshold response criterion, the action spectra of two groups of color-opponent cells are depicted in Fig. 3.4: cells which show opponency between green- and red-sensitive cones (*G* and *R*) and cells which show opponency between blue- and long-wavelength-sensitive cones (*B* and *L* in Fig. 3.4), respectively. Both sets of spectral sensitivity functions differ in several aspects: R/G-opponent cells show two peaks, near 500 nm and 600 nm, one for excitatory, the other for inhibitory responses, mediated by red- and green-sensitive cones, respectively. There is a neutral point between the two peaks (near 550 nm), where the cell's thresholds are relatively high. Both parts of the action spectrum are considerably narrower than the spectra of the isolated green- and red-sensitive cones (see Fig. 2.2); the narrowing is caused by the fact that color-opponent interactions between both mechanisms are particularly strong in that spectral region where both cone mechanisms are stimulated about equally (near the neutral point 550 nm). In this spectral region the mutual antagonism is

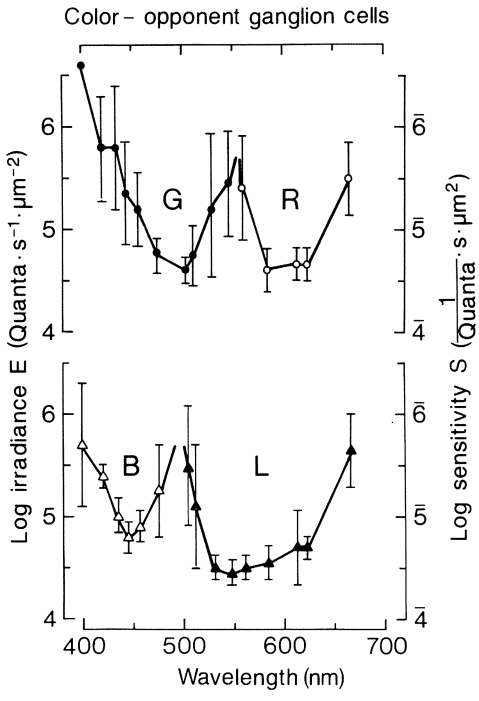

Fig. 3.4. Action spectra of 8 R/G-opponent (*circles, above*) and 3 B/L-opponent tonic ganglion cells (*triangles, below*), recorded in presence of white Ganzfeld background (20,000 td); mean ± S.D. *Open symbols* indicate thresholds of excitatory responses, i.e., just detectable spike frequency *in*crements in response to increments of the test flashes' (15° in diameter) irradiance. *Closed symbols* indicate thresholds of inhibitory responses, i.e., just detectable spike frequency *de*crements in response to increments of irradiance. Since the sensitivity *S* (*right ordinate*) is the reciprocal value of the threshold irradiance *E* of the monochromatic test flash (*left ordinate*), the logarithm of S is simply the negative logarithm of E. Since the neutral point varies among individual cells (see Chap. 3.4), the standard deviation increases in this neutral zone. Only cells with cone dominance values 2, 3, or 4 were taken (explanation in Chap. 3.4)

strongest, raising the threshold near the neutral point, so that the action spectra appear narrowed.

In B/L-opponent cells (*triangles* in Fig. 3.4), sensitivity peaks occur at 450 nm and 550 nm, with a neutral point at 500 nm. Color-opponent interactions occur again, this time between the B-cone and L-cone signal, so that both the inhibitory (*filled symbols*) and the excitatory (*open symbols*) parts of the cell's action spectra appear narrower than action spectra of individual cone mechanisms.

3.4 Variations in Color-Opponency

In early work on color-opponent cells of the monkey retina and LGN (e.g., De Valois et al. 1966) three general groups of cells seemed to be discernable: a red/green-opponent, a blue/yellow-opponent and a spectrally non-opponent one (i.e., a black and white one, according to De Valois 1972). The three groups appeared to be equally proportioned, with the two color-opponent ones having well-defined neutral points in the spectrum. Subsequent work has shown that the neutral point of a color-opponent cell is not fixed at one spectral region (even with identical background illumination), but can vary considerably, depending upon either the spatial (Wiesel and Hubel 1966, Gouras 1968, De Monasterio et al. 1975b, De Valois and De Valois 1975, Zrenner and Gouras 1979b, Gouras and Zrenner 1981a,b) or the temporal properties of the stimulus (Zrenner and Gouras 1978b, Gouras and Zrenner 1979a, Zrenner 1983, see also Chap. 5.2).

Dependence Upon Spatial Variables

An example of the dependence of a color-opponent cell's spectral sensitivity on the stimulus' spatial configuration is given in Fig. 3.5: The ganglion cell had a typical red/green opponent action spectrum as demonstrated in Fig. 3.4 (*top*). As shown here (Fig. 3.5, *upper row*), the cell is excited by 456 nm (via green-sensitive cones) and inhibited by 666 nm light (via red-sensitive cones), if the stimulus (subtending 5° in diameter) covers the cell's entire receptive field. The wavelength 456 nm was chosen

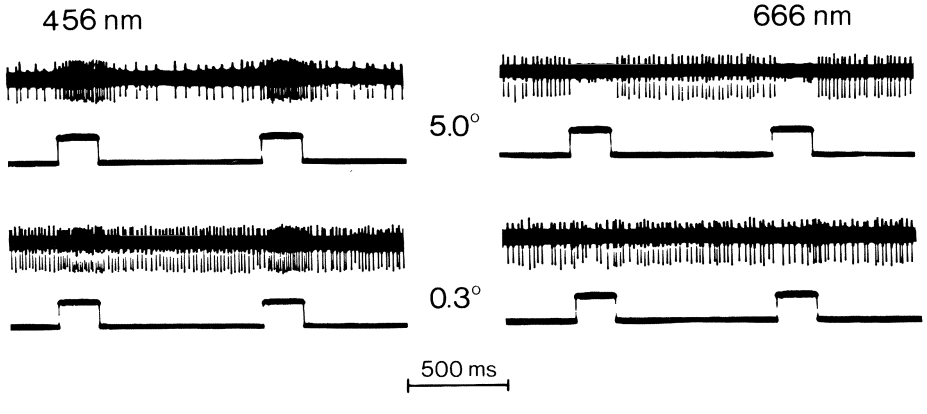

Fig. 3.5. Responses of a color-opponent cell obtained with large (5°) stimuli (*above*) and small (0.3°) stimuli (*below*). Test wavelength of 456 nm and 666 nm ($10^{5.2}$ Quanta s^{-1} μm^{-2}) were applied in presence of a white (neutral) background of 20,000 td

in order to stimulate the G-cone selectively at its short wavelength branch; longer wavelengths (such as 530 nm) would stimulate both G and R cones at supra-threshold light levels. When the stimulus diameter is gradually reduced to 0.3° and centered on the receptive field (*lower row*), the excitatory response to 456 nm light is still present, while the inhibitory response to 666 nm is practically lost. Stimulated by small, centered spots, the cell showed an action spectrum resembling only that of green sensitive cones. This test therefore reveals which mechanism (excitatory or inhibitory) forms the center of a cell. Since the action spectrum of the cones involved in these responses is known (cf. Fig. 3.4), it is proven that the cell shown in Fig. 3.5 has an excitatory, green-sensitive mechanism in the center and an inhibitory, red-sensitive mechanism in the surround of its receptive field. In the abbreviated description[3] used subsequently, the cell will be called G^+/R^-.

Fluctuations in the Neutral Point

Variations in color-opponent interactions can also occur independently of certain stimulus conditions. Red/green color-opponent cells do not form a spectrally homogeneous group, even when they belong to the same functional category (e.g., R^+/G^-). There is a considerable variation in the action spectra of these cells, even under identical spatial and temporal test conditions; the two cone mechanisms involved in antagonistic interactions do not have equal strength in each cell; one of them usually dominates. This is demonstrated by the action spectra of such cells (Fig. 3.6), based on threshold response criteria. Eight R-G color-opponent cells recorded in four different monkeys (under otherwise identical conditions) exhibit quite different spectral sensitivity functions. The green-sensitive cone mechanism (*filled symbols*) strongly dominates in the uppermost cell's action spectrum; the strength of the green- and the red- (*open symbols*) sensitive mechanism is about balanced in the cell's spectrum shown in the center of the figure; by contrast, in the lowermost spectrum, the red-sensitive cone mechanism strongly dominates. In cell M9 - C66 (lowermost in Fig. 3.6) as in many

3 In this abbreviation, the *slash* between the two digits indicates that a cell's receptive field was mapped with small spots; the mechanism indicated by the first digit is situated in the center (here G) and the one indicated by the second digit is situated in the surround (here R). In this paper, if the digits are separated by a hyphen (e.g., G^+-R^-) the cell's receptive field was not mapped, also called "uncentered cell" (UC); in this case the first digit only indicates the spectrally *dominating* mechanism (see Fig. 3.6). The signs + and - indicate excitatory or inhibitory responses mediated by the respective cone type

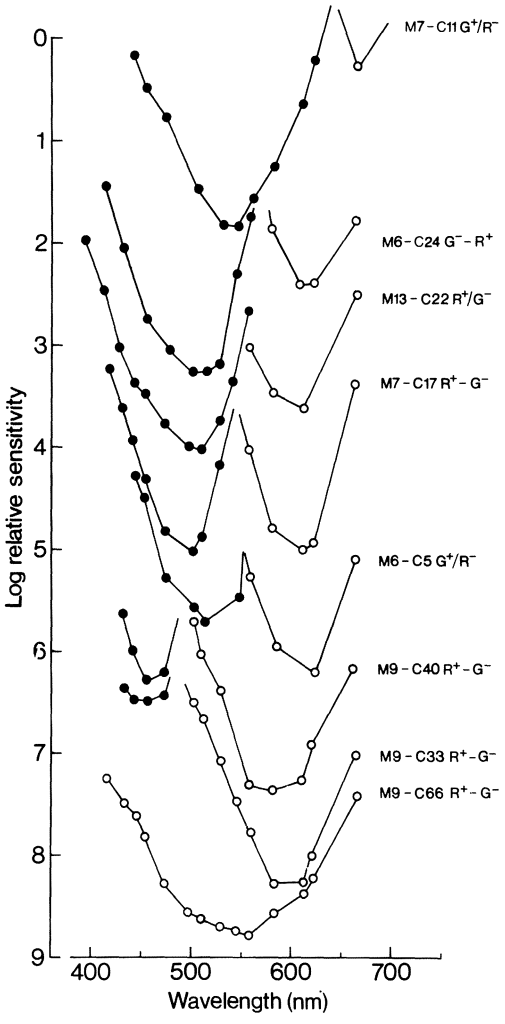

Fig. 3.6. Action spectra of 8 red/green color-opponent cells, recorded under identical conditions (white background, 20,000 td, Ganzfeld stimuli of 200 ms duration). Note the shift of the neutral point from 480 nm to 630 nm. In this figure, the action of R-cones is indicated by *open symbols*, that of G-cones by *closed symbols*. Action spectra are shifted arbitrarily along the X-axis (relative sensitivity) for comparison.

others, the antagonistic green-sensitive mechanism could only be detected when the cones of the dominating red-sensitive mechanism where bleached with strong chromatic (in this case long wavelength) adapting light as will be shown in Fig. 3.7 (*bottom right*). *This picture strikingly shows that there is an almost continuous gradation in color-opponency concerning the strength of the opponent mechanisms involved,* so that in R/G-opponent cells, under identical stimulus conditions, the neutral point can vary from 630 nm to 480 nm.

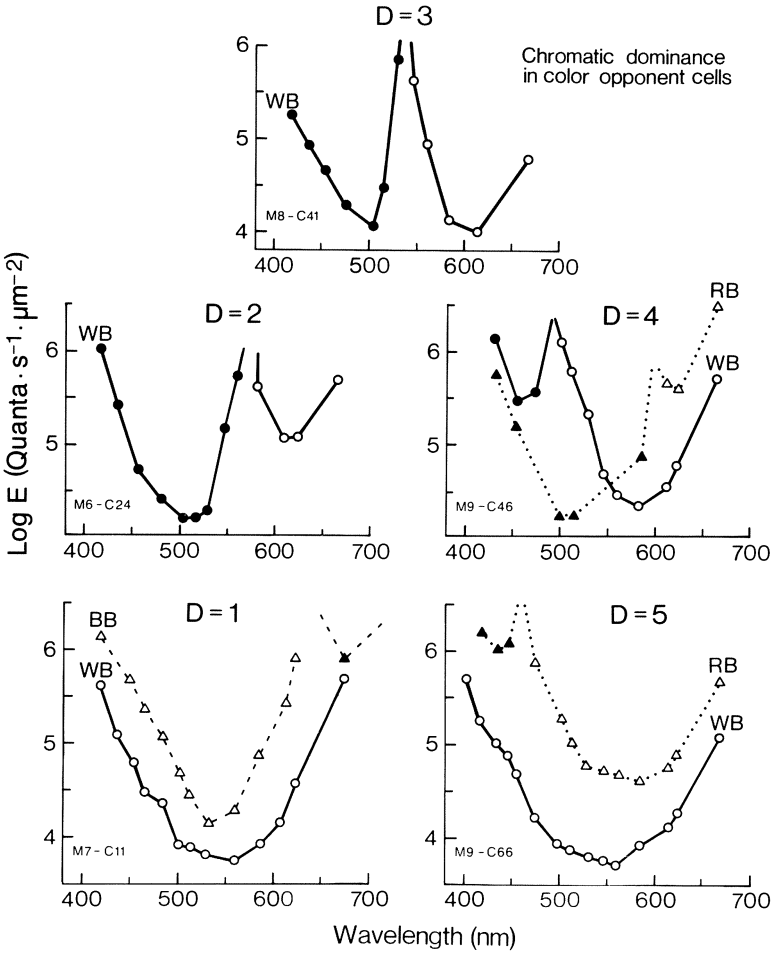

Fig. 3.7. Illustrations of the scale of cone dominance in red/green color-opponent cells. *D=3* indicates balance of both opposing mechanisms in presence of white background (WB, 5500 K, 20,000-30,000 td, *thick lines*). *D=2* and *D=4* indicate dominance of the green- and red-sensitive mechanism, respectively. *D=1* and *D=5* indicate extremely strong dominance of either the green or red mechanism. Application of chromatic backgrounds (300,000 td; red = RB and blue = BB, *dotted* and *broken lines*, respectively) in an individual cell clearly reveal the dominating mechanism. *Open symbols* indicate excitatory signals, *closed symbols* inhibitory ones. (Zrenner and Gouras, in prep.)

A Scale of Color-Opponency

In order to investigate these fluctuations systematically, a scale of cone dominance was introduced with values ranging from 1 to 5 (Zrenner and Gouras, in prep.). This classification will be clarified in Fig. 3.7: The upper-

most function in this figure shows the classical R/G color-opponent cell in presence of a neutral, white background of 30,000 td. For such cells, in which the maximum of the excitatory (*open symbols*) and of the inhibitory (*closed symbols*) responses occurs at about the same threshold, a dominance value (*D*) of 3 was chosen, indicating that the strength of mutual opponency is about balanced in the two cone mechanisms involved in ganglion cell responses.

Only 14% of the tonic ganglion cells investigated show such balanced opponency, where inhibition and excitation cover about half the spectrum and have similar minimal thresholds. The majority of the tonic ganglion cells (45%), when studied on white background (*thick solid lines* in Fig. 3.7), were dominated either by the red (D=4) or by the green (D=2) sensitive cone mechanism, with the neutral point shifted toward 500 nm or 575 nm, respectively. In such a cell (M9 - C46), a red background (RB) can suppress the activity of the dominant cones so that the inhibitory part of the spectrum becomes very pronounced, even though it was very insensitive in presence of a white background. A red background shifts the neutral point from 500 nm to 600 nm. One might have tentatively classified the very short-wave band of inhibition (*dots*, maximum near 440 nm), seen in presence of white backgrounds, as a mechanism mediated by blue-sensitive cones. However, the red background revealed that green-sensitive cones (*filled triangles*) were responsible for producing the short-wavelength part of the spectrum of cell M9 - C46, as described also by Zrenner and Gouras (1981). This indicates the necessity of testing cells against *various* chromatic backgrounds, in order to clearly identify the cone mechanisms operating in the RF of a color-opponent ganglion cell. Cells which showed clear color-opponency already in presence of white backgrounds and which exhibited clear dominance of one of the cone mechanisms were rated by a dominance value of 2 if green-sensitive cones were dominant, and by a dominance value of 4 if red-sensitive cones were dominant.

There is still a number of cells left (about 13%), which on a white background do not show color-opponency at all (*lowermost row* of Fig. 3.7). One might even have tentatively classified those cells as achromatic or non-color-opponent. Chromatic background lights, however, can reveal color-opponency in such cells as previously shown by Padmos and van Norren (1975a), named "concealed opponency" by De Monasterio et al. (1975b). In the cells shown in Fig. 3.7 (*bottom row*), such backgrounds (RB and BB) can weaken this extremely dominant mechanism, so that a very narrow spectral band of inhibition can be seen at the far end of the spectrum.

In the cell shown on the lower right, excitation is evoked by the green-cone mechanism; despite the sensitivity maximum at 440 nm, it is *not* the

B-cone mechanism which provides inhibition in this cell, as will be made clear in Chapter 4. The red-sensitive mechanism is so *extremely* dominant that even a strong red background cannot suppress it. Following the dominance scale mentioned above, such cells were given a value of 5, which expresses extreme dominance of red sensitive cones, even in presence of chromatic, long-wavelength backgrounds.

The extremely G-cone-dominated counterpart is shown on the *lowermost left side* of Fig. 3.7. G-cones which are considerably weakened by the blue background (BB), still dominate the cell to such a degree that opponency is only detectable at 666 nm; in this cell, the neutral point lies near 650 nm. The 666 nm test light even had to be dimmed to make inhibition visible, since with high test light intensities the excitatory G-cone would still have been hit. Therefore, with suprathreshold stimuli, opponency would not have been seen, even against chromatic backgrounds. Following the scale introduced above, a value of 1 expresses this *extreme* dominance of the green-sensitive cones, i.e., where opponency was seen only at the end of the visible spectrum, even in presence of chromatic backgrounds.

Since chromatic backgrounds act mainly on the receptoral adaptation, the circuitry of center and surround mechanisms in the first instance plays a minor role in these experiments; nevertheless, there is a neural control of sensitivity which can even increase the responsitivity of color-opponent cells, as discussed in Chapters 4.3 and 4.4.

Color-Opponency Varies with Retinal Eccentricity

When the incidence of each of these five groups (in terms of numbers of cells) is examined at different retinal eccentricities (Zrenner and Gouras, in prep.), an interesting picture of the distribution of color-opponent actions emerges; this is reflected in the histograms shown in Fig. 3.8 (*right hand ordinate*). In all retinal regions investigated, all varieties of dominance (1 to 5) can be seen (as indicated below each column) but their relation towards each other differs with respect to their retinal locus. In the foveal region (0°–1°) the largest fraction of cells has a dominance value of 3; as one moves away from the fovea, the fraction of cells which have a dominance value of 4 increases considerably; this indicates that a large number of peripherally located cells are dominated by the red-sensitive cone mechanism. When the average dominance value (*dots*) of the five groups is calculated for each individual area, it gradually shifts from 2.8 in the foveola to 3.4 in the periphery. The difference in the distribution of dominance values becomes highly significant toward the retinal periphery. The analysis of variance between the foveal and the peripheral group revealed a probability of error (P) less than 0.02.

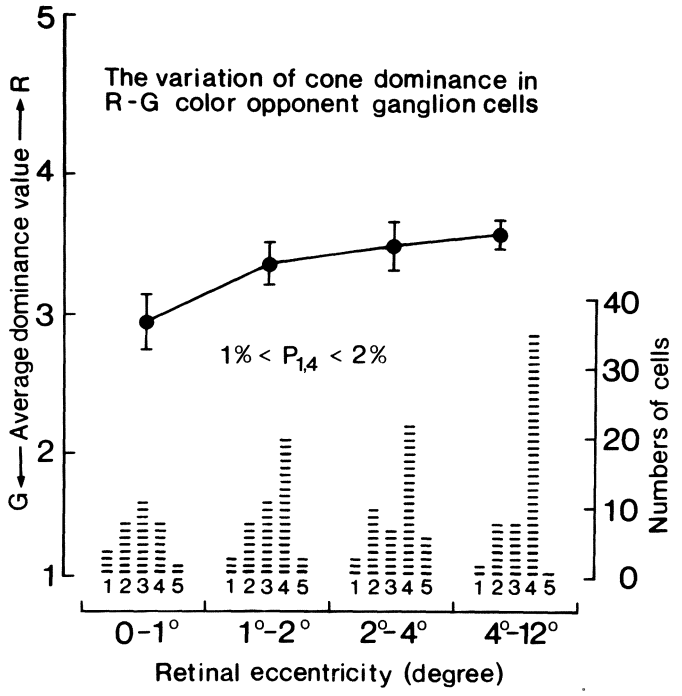

Fig. 3.8. The distribution of cone dominance (*1–5*, i.e., from extremely green to extremely red cone dominated cells) at different retinal eccentricities (*0–1°*, *1–2°*, *2–4°* and *4–12°*). The *right-hand ordinate* gives the incidence in terms of numbers of cells, as reflected in the histograms. The *left-hand ordinate* gives the average dominance value (*dots*) of each group; standard error of the mean (SEM) indicated by *vertical bars*

The three-dimensional graph in Fig. 3.9 relates retinal eccentricity, cone dominance and incidence (number of cells in percent) to each other. It becomes apparent by the gradual shift of cone dominance that the cell types shown in Fig. 3.6 do not represent various subgroups of color-opponent cells, but belong to the same system of red/green color-opponent tonic ganglion cells whose spectral behavior regularly changes.

In summary, the red/green-opponent tonic ganglion cells form a large, heterogeneous group; the entire range of heterogeneity is represented for each retinal area. Cone dominance changes systematically with retinal eccentricity; while the fovea is dominated by the G-cone mechanism (De Monasterio et al. 1975b), the R-cone mechanism becomes increasingly dominant toward the retinal periphery (Zrenner and Gouras 1979b, 1981). The psychophysical experiments of Abramov and Gordon (1977) support this view, since they describe a shift of hue category from blue to red at 580 nm, when the peripheral retina is stimulated. Connors and Kinney (1962) report that beyond 10° eccentricity the sensitivity to red light becomes much

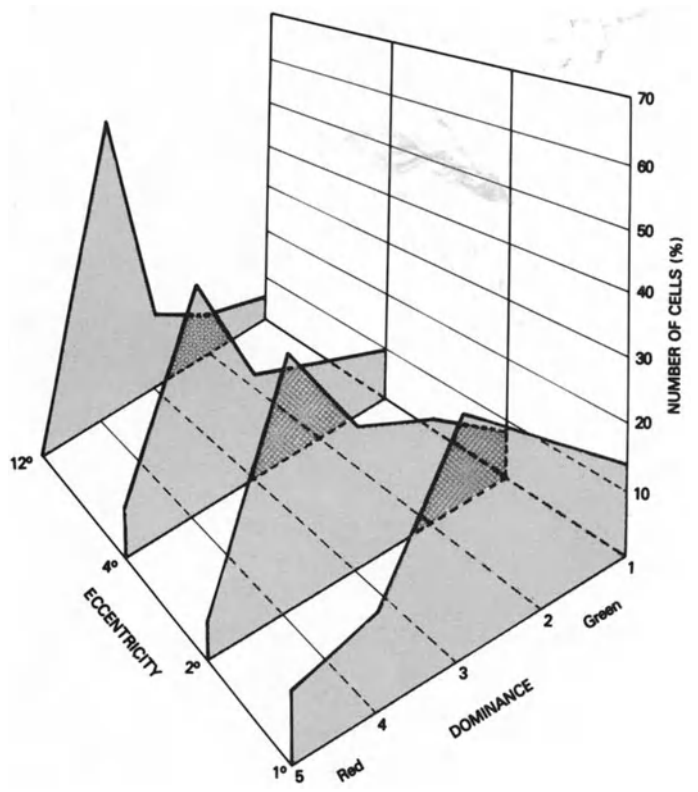

Fig. 3.9. The occurrence (number of cells in percent) of type and degree of color-opponency (green and red dominated, *1-5*) at different retinal eccentricities (1° to 12°)

higher than that to green; this is in agreement with the findings in ganglion cells described here, as well as with those of Krüger (1977).

Although G-cones dominate numerically throughout the entire retina (Marc and Sperling 1977), this does not necessarily imply that they dominate functionally; as seen quite often, they can form only a weak antagonistic surround of a single R-cone, which can strongly dominate the center of a midget bipolar cell, although being outnumbered by G-cones.

It is also noteworthy that with a few exceptions the spectrally dominating cone mechanism forms the *center* of the receptive field of a given cell. Almost exclusively the response of the center mechanism has shorter latencies (20 to 30 ms) than the surround (40 to 60 ms); thus, latency can serve as an additional indicator for defining the center or surround mechanism (see Chap. 5.3).

In cells which receive input from blue-sensitive cones, strength of color-opponency does not vary to the same extent. The spectral sensitivity func-

tions of all ganglion cells having input from blue-sensitive cones are strikingly similar in shape and absolute sensitivity, despite their different retinal locations. There are many more peculiarities about the blue-sensitive mechanism; these will be discussed in a separate chapter (4.1). The population of blue-sensitive cells studied is small (22 cells), because they are very rare; therefore, statistical correlations between retinal position and properties of blue-sensitive cells were not attempted.

3.5 Spectrally Non-Opponent Ganglion Cells

Thirty-nine percent of ganglion cells did not show color-opponency, even when selective chromatic adaptation was extensively applied. They can be subdivided in those which show tonic and those which show phasic responses (14% and 25%, respectively). Both types of cells have a relatively broad spectral sensitivity function (see Fig. 3.10 and 3.13); an individual cell shows only *one* type of response polarity, either spike frequency decrements or spike frequency increments in response to light increments at all possible wavelengths and background situations. It is still unclear whether only a single cone mechanism has input to all these cells, or whether two cone mechanisms act synergistically in these cells as Gouras (1968) and De Monasterio and Gouras (1975) have shown for phasic cells. However, there is also a group of tonic ganglion cells which are spectrally non-opponent. They are rarely mentioned in the literature on primate retina, even though they are relatively numerous (14%) in the sample described here; both cell types are discussed in the following.

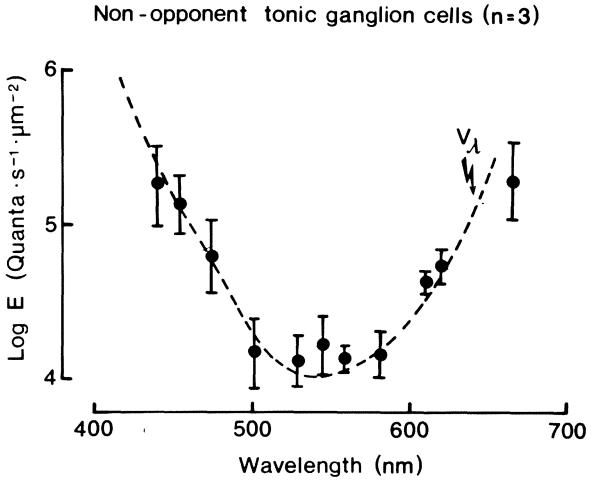

Fig. 3.10. Action spectra of 3 non-opponent tonic ganglion cells (mean and S.D.). Photopic relative luminous efficiency function (V_λ) indicated by *broken line*

Spectrally Non-Opponent Tonic Ganglion Cells

These cells did not show color-opponency at all, despite careful investigation with all available test lights and backgrounds. Due to the extensive spectral studies devoted to these cells, the spatial structure of their receptive field was examined only in few cells; thus, a survey of spatial data cannot be given. There was no change in the response properties accross the spectrum, nor did the action spectrum shift when chromatic backgrounds were applied. They responded with either tonic excitation or tonic inhibition throughout the whole spectrum. The average action spectrum, based on spike frequency threshold criteria in three cells, is shown in Fig. 3.10. The shape of the action spectrum did not change when different backgrounds were applied. Deprived of the opponent signal which provides a clear separation of spectral regions, it becomes very difficult to determine which cone mechanism this spectrum should be attributed to. The best fit can be obtained with the daylight spectral sensitivity function, indicated in Fig. 3.10 as V_λ, the photopic luminous efficiency function (CIE 1970).

It could well be that these cells represent extremes in the graded scale of dominance values introduced earlier. That is to say: in these cells, one of the cone mechanisms becomes so extremely dominant that a rudimentary antagonistic cone mechanism, usually present in tonic ganglion cells, can no longer be detected. It might well be that all or most tonic ganglion cells, which appear non-color-opponent in respect to their spectral sensitivity function are in fact color-opponent cells, in which color-opponency is so extremely weak that it cannot be detected at all at the adaptation levels employed in this study; thereby they would complete the scale of cone dominance presented in Fig. 3.7 by the values 6 (R-cone dominated, with no detectable G-cone input) and 0 (G-cone dominated with no detectable R-cone input).

Phasic Ganglion Cells

Phasic ganglion cells respond only transiently at the beginning and/or at the end of stimulation. The response to increments of light can be either a transient depolarization (on-cells, 15% of the total), associated with a generation of a few spikes of short latency (10-30 ms), or a transient hyperpolarization with a rapid, pronounced inhibition of spike activity (off-cells, 10% of the total); the hyperpolarizing phase is often followed by rebound depolarization, which expresses itself through some post-inhibitory spikes. An example of such intracellularly recorded cells (Fig. 3.11) shows monophasic spikes, excitatory postsynaptic potentials (EPSP's, see *arrows*) and transient hyperpolarization (*h*) at the onset and offset of the stimulus. This is to give an example of the dependence of the spike frequency on the

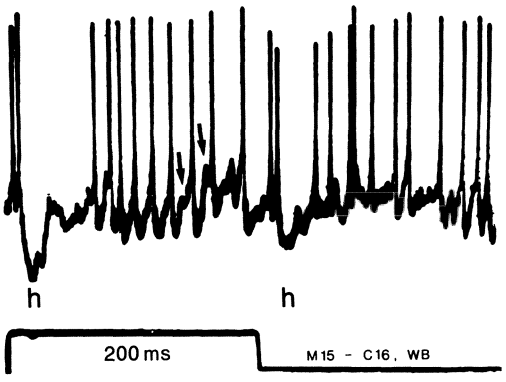

Fig. 3.11. Intracellular recording of a phasic ganglion cell. A transient hyperpolarization (*h*) accompanied by a spike frequency decrement occurs at on- and offset of light. Test light: 550 nm, $10^{4.8}$ Quanta s^{-1} μm^{-2}, Ganzfeld illumination, white background (30,000 td), stimulus frequency 1 Hz. The amplitude of the action potentials is 13 to 15 mV

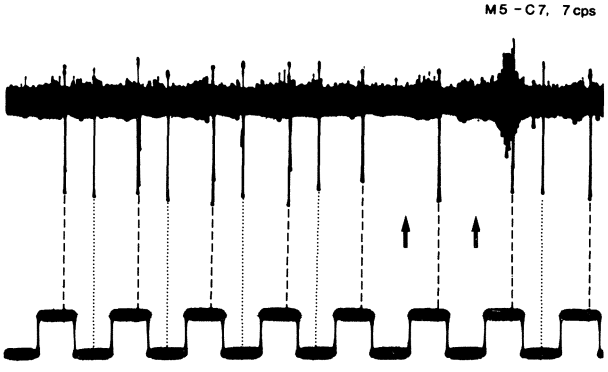

Fig. 3.12. Extracellular recording of a phasic ganglion cell responding with single spikes at the on- and offset of light, after a fixed delay. The off-spikes are often lacking (*arrows*), stimulus frequency 7 Hz, all other conditions as in Fig. 3.11

membrane potential. When the strength of stimulation is increased, the latency of the initial phase of hyperpolarization decreases. It was often seen that in phasic cells the response to the onset of light is more persistent than to the offset, which is sometimes lacking. This is shown in Fig. 3.12 for a phasic cell (recorded extracellularly with a stimulation frequency of 7 Hz) where the spike at light-off (*dotted lines*) is occasionally lacking (*arrows*). With increasing flicker frequency, the depolarizing phase becomes so short, that most often only one spike appears. The timing of the spikes, however, is surprisingly precise; it occurs after an almost fixed delay of 49 ± 1 ms after the light-onset (*dashed lines*). At low flicker frequencies phasic cells have shorter latencies of about 10 ms. The prolongation of latency at higher stimulation frequencies (10 ms in Fig. 3.11 versus 49 ms in Fig. 3.12) is

due to a phase shift between stimulation and response, which will be described in Chapter 5.

The action spectrum of phasic cells (Fig. 3.13) is broadband, single-peaked, with a maximum near 550 nm; it closely fits the V_λ photopic luminous efficiency function. The responses were found to be "univariant", i.e., they showed identical time courses at all wavelengths (for the concept of univariance, see Naka and Rushton 1966a, Scheibner and Schmidt 1969). Accordingly, there is no chromatic opponency in phasic cells. Nevertheless, *spatial* opponency could be seen through the application of differently sized spots. When the diameter of a spot centered on the cell's receptive field is increased stepwise, the cell responds with an increase of spike frequency up to about 1/2 degree of visual angle since the area and thereby the number

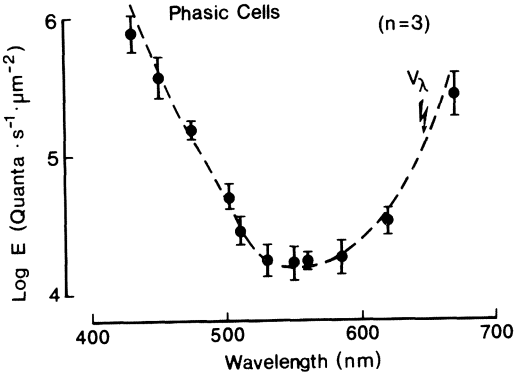

Fig. 3.13. Action spectra of 3 phasic ganglion cells; mean S.D. Photopic relative luminous efficiency function (V_λ) indicated by *broken line*

of stimulated receptors gradually increases. Larger spot sizes (up to 12° of visual angle), however, start to decrease the cell's activity; this is caused by the antagonistic action of the surround, which starts to be effective at a certain distance from the cell's RF center. Qualitatively the recordings yielded the same results for long and short wavelengths, indicating that center and surround are formed by the same cone mechanism(s), which show variations in the center-surround antagonism only in the spatial domain i.e., R^+/R^- or R^-/R^+ or G^+/G^- or G^-/G^+ or R^+G^+/R^-G^- etc. (see Gouras 1968).

Rare Cell Types

To a small percentage of cells (9%), the classification described above did not apply. In some cells, particularly in foveal ones, a regular, relatively slow spike discharge (25 to 35 spikes/s) was recorded, which could not be

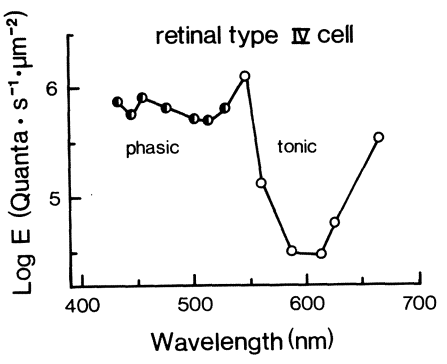

Fig. 3.14. Action spectrum of a retinal "type IV" cell. These cells show very sensitive tonic responses (*open symbols*) to long wavelengths but much less sensitive phasic responses (*half-filled symbols*) to shorter wavelengths. White background, $10^{4.2}$ td. Ganzfeld stimuli of 200 ms duration

influenced by light of any intensity or wavelength, nor by moving objects. These cells seemed to have either non-visual functions or to be deprived of receptoral connections. Such cells were classified as "undrivable" (UD).

There was another type of cells (2%) which was very sensitive to long-wavelength light, responding with a tonic discharge; it was very insensitive to short-wavelength light, showing only very weak phasic discharges. The action spectrum of such a cell is shown in Fig. 3.14, revealing a narrow-band spectral sensitivity function in the long-wavelength part (with its maximum near 600 nm) and an almost flat function in the short- and middle-wavelength part of the spectrum, about 30 times less sensitive. Cells with similar behavior were described by Wiesel and Hubel (1966) in the monkey's LGN, named "type-IV cells"; the same term was used in this study for cells of this type found in the retina. These cells are possibly color-opponent with relatively small center sizes. They must have a strong, spectrally different antagonistic mechanism which, however, appears to be strongly inhibited and therefore does not express itself in the spectral data. Apparently, apart from the red-sensitive cones, green-sensitive cones are acting through the excitatory center as well as through the inhibitory surround of this cell. Any middle- or short-wavelength light would excite as well as inhibit this cell and thereby produce phasic responses. Due to the change of response properties, correlated with the wavelength of the stimulus, these cells are *not* univariant.

3.6 Distribution of Classes of Ganglion Cells Across the Retina

All types of ganglion cells described in this part of Chapter 3 are grouped in Fig. 3.15 according to their retinal location, all the way from the fovea (0°-1°) to the periphery (up to 12°). The proportion of tonic to phasic

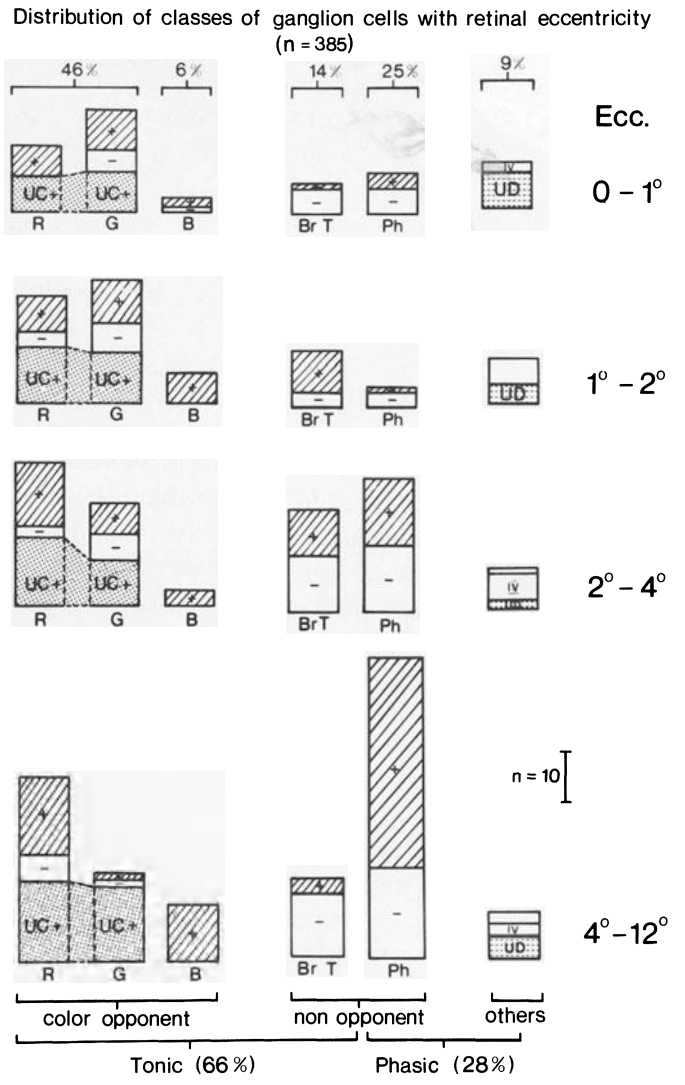

Fig. 3.15. Distribution of classes of ganglion cells with retinal eccentricity (*Ecc.*). On-center cells (+) are indicated by *hatched blocks*, off-center cells (−) by *white blocks*. Cells in which the center was not defined (uncentered cells) are called UC+ (*dotted blocks*). Color-opponent cells (*left columns*) are classified according to their center response (or excitatory response in case of uncentered cells) as red-, green- or blue-sensitive (*R*, *G*, *B*). Spectrally non-opponent cells (*center columns*) are grouped as spectrally broadband tonic (*Br T*) or phasic (*Ph*) cells. The rest of the cells (*right column*, *others*) were either unresponsive to light (undrivable, *UD*), "type IV" cells (see text), or unclassifiable. The percentage refers to the total number of 385 cells. The numbers of cells are not necessarily correlated with cone dominance (see Sect. 3.4)

cells is 66% to 28% in this sample (385 total). Interestingly, phasic cells (Ph) are relatively rare near the fovea (0°-1°, top of Fig. 3.15) but become more common near the retinal periphery (4°-12°, bottom of Fig. 3.15). However, this does not seem to be a common feature in visual systems, since in cat the density of phasic (alpha) cells is highest in the central area (Wässle et al. 1981b).

Of the investigated cells, 52% are color-opponent (concentric R and G or coextensive B centers with an antagonistic surround); 14% are non-color-opponent, spectrally broadband and tonic (Br T). In 46% of the cells, the center mechanism has inputs from R (26%) or G cones (20%), but in only 6% from B cones, which are more common in the extrafoveal region (for special properties of B cones, see Chap. 4). It is remarkable how the number of cells with R-cone driven RF-centers gradually increases toward retinal periphery, while those with G-cone-driven centers gradually become less frequent. This numerical dominance of R-cone-driven ganglion cells in the retinal periphery parallels the functional dominance of the R-mechanism in peripheral tonic ganglion cells described in Section 3.4. However, direct comparison between functional and numerical dominance is not possible in Fig. 3.15, since it indicates *numbers* of cell types, while Fig. 3.8 only considers *functional* dominance of cone mechanisms (see also summary of Chap. 3.4).

Generally, on-center cells (*hatched blocks* +) are more common than off-center cells (*white blocks* -). This is not a sample error, since the studies of Famiglietti and Kolb (1976) and of Nelson et al. (1978) have revealed that at least in cat, sublamina "a", containing the processes of off-center cells, forms one third of the inner plexiform layer of the retina, while sublamina "b", containing the processes of on-center cells, forms two thirds of this layer. Interestingly, depolarizing on- and hyperpolarizing off-bipolar cells can be differentiated also anatomically: As suggested by Gouras (1971), supported by the anatomical observations of Famiglietti and Kolb (1976), Stell et al. (1977), then actually proven in cat by Nelson et al. (1978) and in goldfish by Famiglietti et al. (1977) by intracellular recordings and dye injections, on-center bipolar cells are connected to cones by invaginating, sign-inverting synapses, while off-center bipolars contact cones by flat, sign-conserving synapses (for additional references see Chap. 1).

The predominance of on-center cells is particularly striking in cells with blue-sensitive cone inputs which are almost all excited by blue light (only one cell in the foveal region was inhibited). Obviously, the blue-sensitive cone mechanism plays a special role in color coding, since it works without a blue-sensitive off-system; this is in accordance with the electrophysiological data given in Fig. 3.3 and will be discussed in depth in Chapter 4.

In some of the red/green color-opponent cells, the center mechanism could not be defined, since experiments on color vision were given priority over those on spatial problems during the necessarily limited recording time. These uncentered (UC) cells were grouped according to their excitatory (+) mechanism as R^+ or G^+ cells, respectively. Since they could have been either R^+/G^- or G^-/R^+ and G^+/R^- or R^-/G^+ cells, they were grouped together in the dotted blocks in Fig. 3.15. The statistical error introduced into the histograms (in Fig. 3.15) by this procedure is very small, because cells, excited by red and green cones, are about equal in number.

Of the rare cell types, the "undrivable" ones (UD's) are most common near the fovea, whereas the "type-IV" cells obviously can occur anywhere. Ten of the 385 total cells were held only shortly and could not be classified precisely; they are indicated by open white blocks in the column "others" (*right side* of Fig. 3.15).

3.7 A Simplified Classification Procedure

This methodological part appears within Chapter 3 and not in the method section, since its understanding requires knowledge about the characteristics of the cell types presented in the previous sections of Chapter 3.

In single cell recording there is a high degree of variation as to the length of time a cell can be held; some recordings can last hours, others only minutes. It is therefore very expedient, at the beginning of each recording, to use a quick experimental procedure to at least classify a cell with a minimal number of tests; such tests should also serve as a control measure during a longer series of recordings from the same cell. The following decision-table (presented as a flow chart in Fig. 3.16) was found most effective and reliable in classifying a cell; it serves also to identify the dominant cone mechanism in color-opponent cells, without having to scan the entire spectrum. Superimposed on a white background (WB) capable of saturating rods (20,000-30,000 td), first the wavelength of the test stimulus was changed from 614 nm to 456 nm. When a change in polarity of the cell occurs (i.e., a transition from an excitatory depolarizing to an inhibitory hyperpolarizing response or vice versa, as indicated by "yes" in the first rhomb in Fig. 3.16, *left*) such cells (9,6%) are immediately classifiable as color-opponent (*long hatched horizontal box*). In presence of a white background, the test lights obviously stimulate both the excitatory and the inhibitory branches of the spectrum and thereby simultaneously the center and surround mechanism. Since the slightly suprathreshold test lights (456 nm and 614 nm) are of about equal strength (ca. $10^{4.0}$ Quanta s^{-1} μm^{-2}), the

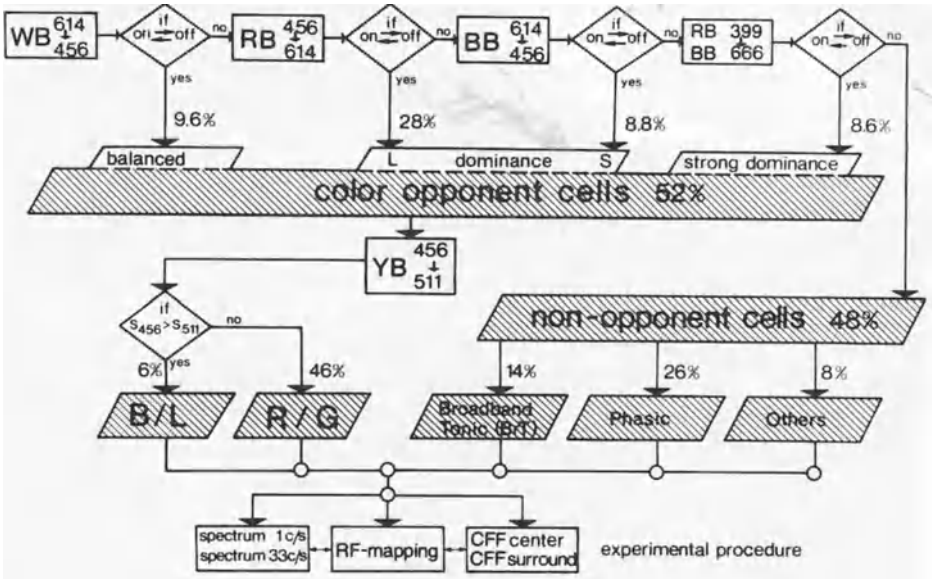

Fig. 3.16. Flow chart diagram of the tests performed to quickly classify a cell as color-opponent (B/L and R/G) or spectrally non-opponent (broadband tonic or phasic, respectively). Polarity change (see footnote on p. 64) in the cell's response is indicated by "yes" or "no". Depending on the background used (white *WB*; red *RB*; blue *BB*), the dominating cone mechanism (long or short wavelength, *L* or *S*, respectively) was revealed by the test lights 614 nm and 456 nm, respectively. Yellow background (*YB*) permitted the separation of *B/L* from *R/G*-opponent cells depending on their sensitivity (*s*) to 456 nm and 511 nm light as determined by a threshold response criterion. The experimental procedures performed after the classification are given below

responses of the antagonistic cone mechanisms involved in such a cell must be both present, when stimulated with the appropriate wavelength. Such a cell is assigned a dominance value of 3, according to the classification of cone dominance, given in Fig. 3.7.

The lack of a change in polarity does not necessarily indicate a lack of color-opponency. Since one of the cone mechanisms could dominate the cell, selective chromatic adaptation has to be used to reduce the activity of this mechanism and to reveal that of the weaker, antagonistic one. This is indicated in the second box of Fig. 3.16 (*top row, left to right*); a red background (*RB*) weakens a possibly present long-wavelength-sensitive mechanism and facilitates the action of a concealed, short-wavelength-sensitive cone mechanism, which does not otherwise emerge. If, in presence of a red background, a change of test light wavelength (456 nm → 614 nm) is accompanied by a polarity change, this cell would also have to be classified as color-opponent. Since a long-wavelength (red- or green-) sensitive mecha-

nism (L) is predominant, such cells (28%) have to be attributed a dominance value of 4; they would resemble the cell type shown in the middle row (*left*) of Fig. 3.7.

If a change in polarity does not occur, a blue background (*BB*, *third box*) has to be used, which suppresses a possibly dominant short-wavelength (blue- or green-sensitive) mechanism (*S*). If a change of the test light wavelength (614 → 456) produces a change in polarity, the dominance of a short-wavelength mechanism is confirmed. These cells (8.8%) have to be classified as color-opponent with a dominance value of 2, as they must resemble a cell with the spectral characteristics given in Fig. 3.7 middle row (*right*).

A considerable fraction of cells was still left, which, even on chromatic backgrounds, did not show color-opponency after stimulation with the test wavelengths mentioned above. It is evident from the spectral variations of the cells described in Fig. 3.7 that a strongly dominating cone mechanism can push the responsiveness of an opposing mechanism toward the far end of the spectrum. To discover even a very hidden opponent cone mechanism, an additional test has to be performed. Strong test wavelengths (of about 10^5 Quanta s^{-1} μm^{-2}) from both ends of the visible spectrum (399 nm and 666 nm) are applied successively in presence of a short- (BB) and a long-wavelength (RB) background (*fourth box* in Fig. 3.16). If the cell's polarity changes, it has to be classified as color-opponent, *however, strongly dominated* by one cone mechanism (*lowermost row* in Fig. 3.7). A dominance value of 1 (short-wavelength-dominated) and 5 (long-wavelength-dominated), respectively, is attributed to such cells (8.6% of the total). In this stage of the test, about half the cells (52%) turned out to be color-opponent, while the other half (48%) had to be classified as non-opponent. These two major groups were further subdivided as shown in the lower half of Fig. 3.16. For determining whether a color-opponent cell belongs to the R-G or to the B-L group, the following test was found to be very effective. The cell's threshold was determined in response to two monochromatic stimuli of 456 nm and 511 nm in presence of a strong yellow background (*YB*, 300,000 td), which suppresses any long-wavelength-sensitive cone's action (*center box* in Fig. 3.16) and enhances the action of a possibly present blue-sensitive cone (see Fig. 4.8). As shown in Fig. 4.2, the threshold of tonic ganglion cells with blue-sensitive cone inputs sharply increases when the wavelength of the test light is changed from 456 nm to 511 nm. Therefore, if this cell was more sensitive to short-wavelength light (s_{456}) than to long-wavelength stimuli (s_{511}), as indicated in the lower lefthand rhomb, the cell belonged to the B-L-group (6%). If the cell's sensitivity to the 511 nm stimulus was about equal to or higher than that of the 456 nm stimulus, it belonged to the R-G-group of color-opponent ganglion cells

(46%). The opposite difference in sensitivity between B-L and R-G cells in response to 456 nm and 511 nm stimuli is demonstrated in Fig. 3.6.

In the spectrally non-opponent group of cells (*hatched box, lower right*), a group of broadband tonic cells (*Br T*, 14%) could be distinguished from phasic cells (26%); they always responded with a tonic discharge without showing color-opponency under any of the test conditions, even when the entire action spectrum was defined on various backgrounds. The rest of the cells (8%, "others"), not directly classifiable under this procedure, are described in Chapter 3.5, last paragraph.

After this brief classification, the experimental procedure began. First, the whole action spectrum was determined at high and low temporal frequencies (1 c/s and 33 c/s). Then the spatial structure of the cell's receptive field (RF-mapping) was measured; this procedure (described in Chap. 3) is indicated in the lowermost row of boxes of Fig. 3.16. Finally, the critical flicker fusion frequency (*CFF*) was determined for center and surround, respectively. These data will be given in Chapters 4 and 5.

3.8 Résumé: Some Implications for the Understanding of the Visual System's Function

Red-Green Versus Blue-Yellow Opponency

Based on their action spectra, two main types of color-opponent cells can be discerned: one, in which the two long-wavelength cones act antagonistically (R-G-system) and a second one, in which the blue cones and the longer-wavelength-sensitive cones (B-L-system) oppose each other. It is not yet clear whether in all B-L-opponent cells the L-cones are of the red- or green-sensitive type or of both; the data of De Monasterio et al. (1975a) suggest that in many cells, both types of long-wavelength-sensitive cones are involved. Although an entire chapter (Chap.4) is devoted to ganglion cells with B-cone input, some differences between the R-G and the B-L group of color-opponent ganglion cells will be summarized here. Blue-sensitive ganglion cells are very rare (6%) and almost exclusively *excited* by short wavelength light (5.7%); they have coextensive receptive field structures (Fig. 3.2) lacking a noticeable spatial antagonism; their chromatic antagonism, however, is still present. This certainly limits their contribution to visual acuity, especially since they are rarely found in the foveolar region, but relatively common in the perifovea (Fig. 3.15). They can be clearly distinguished from red/green opponent cells by their long latency at the onset and their long after-discharge at the offset of a stimulus (Fig. 3.3); this characteristic also limits their temporal resolution, as will be shown in Chapter 5.1.

On the Neutral Point

The neutral point of the action spectra of *foveal* R-G opponent ganglion cells, i.e., the spectral zone where transition from excitation to inhibition occurs, lies mainly near 560-570 nm (Fig. 3.4). Note that the neutral point of R-G opponent cells is located in a similar spectral position as in a tritanopic human observer, i.e., one who lacks a blue-sensitive system (Walls 1964). The principles of complementary colors and the color-naming experiments on dichromats suggest that neutral points can be correlated with the sensation of white. The neutral point of B-L opponent ganglion cells lies near 490 nm -500 nm; this also applies to the relatively common human dichromats (Hecht and Shlaer 1936, Walls and Heath 1956, see also Chap. 6) who lack a red-sensitive (protanopes) or a green-sensitive system (deuteranopes). Since color-opponent ganglion cells have a neutral point which is unresponsive to light (Fig. 3.1, *below*), they cannot respond to certain hues; this weakness is compensated for by the fact that the B-L group has its sensitivity maximum near the neutral point of the R-G group and vice versa (see Fig. 3.4): in trichromatic systems, a higher-order neuron which has input from both groups can thereby easily overcome this weakness of color-opponent ganglion cells.

How Can Variations in Color-Opponency Improve Color Discrimination?

Color discrimination is remarkably well developed in the primate visual system. According to Judd (1952) several million of colors can be distinguished, taking into account the various degrees of hue, saturation, and brightness. Variations in color-opponency (as described in Chap. 3.4) could account for this capability, illustrated in the following. In contrast to the B-L opponent system, which forms a spectrally homogeneous group of tonic ganglion cells, the red/green opponent system shows considerably heterogeneous action spectra. Consequently, red/green-opponent ganglion cells form a continuum of spectrally different wavelength analyzers, ranging from strongly color-opponent to spectrally non-opponent tonic cells (Chap. 3.4). This is made clear in Fig. 3.17 where the whole range of red/green opponent cells from Fig. 3.6 is plotted again so that the (smoothed) action spectra of five of these cells are superimposed, with the excitatory parts of the spectra pointing upward (*solid lines*) and the inhibitory parts downward (*broken lines*). The spectra on the left represent R^+/G^- cells; those in the center G^+/R^- cells; on the right, the same procedure is performed for ganglion cells, which have excitatory input from blue-sensitive cones, and where the long-wavelength-sensitive cones act inhibitorily. The numbers beside each curve indicate the dominance of a certain mechanism, according to the scale given in Fig. 3.7.

Why would such an arrangement improve the visual system's abilities? Since the number of spectrally different wavelength analyzers is greatly enhanced by such a graded scale of color-opponent cells, the heterogeneity of red/green color-opponent cells provides a greater range of responsiveness to different chromatic borders within each area of the retina. If we call the boundary between two areas of different spectral composition a chromatic border, then many such borders can be imagined which, when moved through the receptive field of a specific color-opponent ganglion cell, would not produce a noticeable response gradient, since there are many colors which have quantitatively the same effect on such a cell, in either an excitatory *or* inhibitory manner. However, there is always a small fraction of cells, the neutral point of which lies *between* the spectral loci of the two colors forming a chromatic border. These cells and only these cells can respond maximally by changing from excitation to inhibition or vice versa, thus signalling optimally a chromatic border moved through the cell's receptive field. For instance, two colors with very close spectral loci (e.g., 530 nm and 540 nm) would have almost no effect on a cell of type *5* in Fig. 3.17 (*left*); another cell (type *3* in Fig. 3.17, *left*), however, has its neutral point in between the two spectral loci and would respond with a rever-

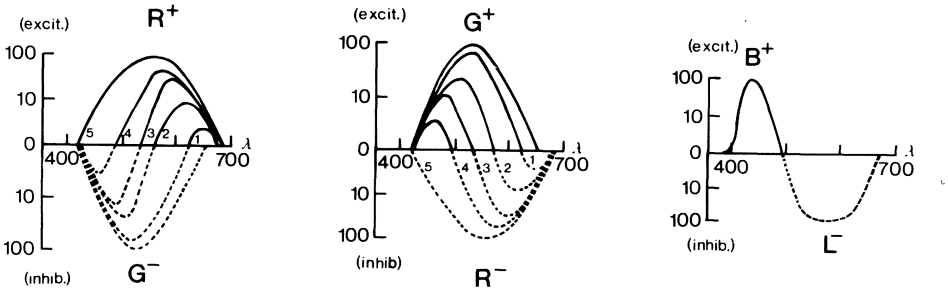

Fig. 3.17. Three sets of action spectra (smoothed and replotted in part from Fig. 3.6), indicating the spectral heterogeneity of R-G cells (*left side* and *center*) in comparison with the spectrally homogeneous group of B/L cells (*right side*). The threshold sensitivity (relative values in percent of the maximum) of excitatory responses (*solid line*, positive Y-axis) and inhibitory responses (*broken line*, negative Y-axis) is plotted against wavelength (X-axis). We can assume that this type of excitation is correlated with the sensation of chroma, mediated by red-, green- and blue-sensitive cones, forming the center of strongly color-opponent cells (see below). Excitatory and inhibitory parts of the red/green-opponent cells' action spectra can show various degrees of dominance (1-5, according to the scale given in Fig. 3.7), so that the neutral points (*crossing points at the zero line*) can vary gradually throughout a large range of the visible spectrum. Consequently, there is always an individual red/green-opponent cell which is reversed in polarity by two successively presented stimuli, even if their difference in spectral composition is small. On the other hand, all 21 blue-sensitive cells investigated show identical action spectra with neutral points at 490 nm (*right side*)

sal of polarity; if both wavelengths are presented successively to its receptive field, the cell would signal this small difference in wavelength very strongly. This applies not only to wavelengths but to chromaticity differences in general. Since the neutral points of the various types of R/G cells are spread continuously throughout the visible spectrum, there is always a cell which is reversed in polarity by successive color-contrast even if the differences in spectral composition are small.

Therefore, the heterogeneity of the red/green opponent tonic system can greatly enhance the visual system's capability of responding optimally to a large variety of chromatic borders within each part of the visual field, but particularly in the fovea, where cone dominance values are most evenly distributed (Fig. 3.8). It is not surprising that color discrimination in human observers improves as the stimulated area increases (Brown 1952), since a larger number of spectrally *different* ganglion cells becomes involved. It is also not surprising that the color discrimination (Δ_λ vs. λ) is best in the midspectral region, since *most* of the red/green color-opponent cells have their neutral point located there. Granit's (1945) observation of several spectrally different narrowband "modulator" cells in a single animal can be easily understood in terms of variations in the chromatic antagonism of color-opponent cells (cf. Fig. 3.6 and Chap. 1). This concept does not apply to the B-L-opponent group (see Fig. 3.17, *right*) which has special capabilities for signalling simultaneous color contrast, as discussed in Chapter 4.

Color Coding in the Retinal Periphery

The data also show that with retinal eccentricity, regular changes toward a more dichromatic processing of visual information take place. First, the proportion of red-, green- and blue-sensitive cells changes toward the retinal periphery from a trichromatic system to one which is excited mainly via red- and blue-sensitive cones (*hatched blocks* in Fig. 3.15, *lower left*); second, not only the number of cells with R-cone input, but also the dominance of the red-sensitive mechanism increases toward the periphery (Fig. 3.9). Thus, in all primates investigated so far, trichromatic vision with all its well-known psychophysical features seems to be restricted to the foveal region. In the retinal periphery, color vision apparently undergoes a transition from a trichromatic to a dichromatic[4] deuteranopic or possibly a deuteranomalous system. From psychological studies, Boynton et al. (1964b) similarly inferred the existence of a deutan-like structure in the peripheral

4 Dichromatic systems are marked by a deficiency in one of the three cone mechanisms. The terms protan, deutan and tritan indicates a defect in the red, green or blue-sensitive cone mechanism (see Chap. 6.3 for further details)

retina, and with small targets, the structure even appears tritan-like (Gordon and Abramov 1977); these effects depend on luminance levels (Weale 1951). The observation of Wooten and Wald (1973) that peripheral color blindness appears to involve mechanisms other than mere failure of receptors, receives its neurophysiological basis from the variation of color-antagonistic ganglion cells, shown in this chapter; to a certain degree it might also account for the variation of the Bezold-Brücke phenomenon in the extrafoveal retina (Stabell and Stabell 1979).

Spectrally non-opponent phasic cells have larger receptive fields and are most common in the retinal periphery (Fig. 3.15, *center row*). They resemble a differential detector in that they respond only transiently but quickly to sudden changes in the visual field; their main task, therefore, might consist in the simple detection of quickly moving objects in the retinal periphery so that the fovea, with all its capabilities (trichromatic vision, small receptive field, high acuity) can be directed toward this object for precise analysis. If phasic cells share the same R and G cones as tonic cells, there must be another separate set of bipolar and amacrine cells which produces this phasicity in parallel with neighboring tonic channels. The "background role" of Y-cells is discussed by Lennie (1980); the coverage of the entire retina by these cells (α-cells) is very nicely outlined in cat by Wässle et al. (1981c).

The Consequences for the Circuitry of the Retinocortical Pathway

Having presented this large variety of different retinal ganglion cells, some ideas will be outlined about their circuitry and the manner in which the visual system utilizes these individual capabilities in analyzing the various qualities of objects.

A Model. Figure 3.18 shows a diagram of the possible presynaptic circuitry which builds up these parallel systems of ganglion cells subserving the *same* R and G cones. Horizontal cells can mediate antagonistic interactions between R and G cones; since each horizontal cell is either completely or mostly postsynaptic to one class of cones, (R or G), a certain degree of color-opponency is conferred onto each R and G cone. Therefore all ganglion cells which share these R and G cones may have some underlying cone opponency. This may not be obvious in phasic ganglion cells because both R and G cones synergistically contribute to *both* center and surround.

In this model, as presented by Gouras and Zrenner (1981a,b), all ganglion cells subserving the mid-spectral cones share identical horizontal cell circuits; separate sets of bipolars and amacrine cells determine their unique behavior. The tonic R or G, on- or off-center ganglion cells showing *weak*

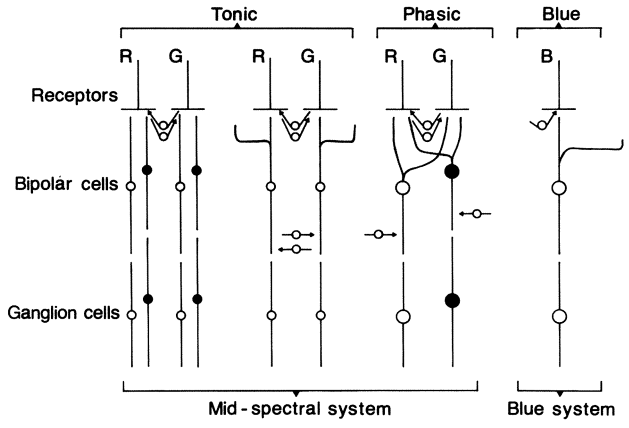

Fig. 3.18. Simplified schematical circuitry, modelled for the midspectral tonic and phasic, as well as for the blue-sensitive cone system in the retina. (Gouras and Zrenner 1981a,b)

color-opponency have a minimum of amacrine cell input and consequently mostly reflect the responses of the cones themselves. The tonic R or G on-center ganglion cells with *strong* color-opponency have a separate set of bipolars which receive an inhibitory input from a cone-specific amacrine cell system. This system is restricted to on-center cells for reasons given below. The phasic R an G on- and off-center ganglion cells also have separate sets of bipolars and inhibitory amacrine cells. The fact that both these bipolars and amacrines receive synergistic inputs from both R and G cones makes their responses phasic to all spectral stimuli. Note that in all cases, on-center bipolars interact with one set of amacrine cells, and off-center bipolars interact with another set, a good reason for their processes being segregated in separate lamina (Nelson et al. 1978).

The B-cones must use a separate bipolar and ganglion cell system since their responses cannot be detected in the pathway of the mid-spectral cone system, at least not overtly. Because B-cones invariably excite ganglion cells in macaque retina (see Chap. 4 for references), this system is also restricted to on-center bipolar cells and their corresponding ganglion cells.

Anatomical Considerations. This model is obviously an oversimplification: the rod system with its separate bipolar and amacrine cell channels (Kolb et al. 1976) is not included. No role is suggested for B-cone horizontal or amacrine cells. However, ganglion cells having input from B-cones are excited by white but inhibited by yellow light; some horizontal or amacrine cell systems fed by B-cones may facilitate this excitatory response to white light.

The midget ganglion cell system, so characteristic of the primate fovea (Gouras 1971), is most closely approached by tonic ganglion cells with *weak* color-opponency; Polyak (1941) already observed that midget bipolars terminate at two levels in the inner plexiform layer (see Gouras 1971) which correspond to the on- and off-center system (Nelson et al. 1978). These cells respond well to mid-spectral lights where spatial resolution is maximal, and because of their restricted synaptic contacts with ganglion cells might be expected to have minimal amacrine cell connections.

This model is consistent with the S-potentials we obtained in about 20 cells in the inner nuclear layer of primate retina, all of which showed tonic, hyperpolarizing responses without evidence of strong cone opponency (Gouras and Zrenner 1979b). These cells can mediate opponent signals without showing color-opponency themselves. Phasicity and strong cone opponency must be established beyond the photoreceptor cells in primate retina.

This information may provide the basis for a suggestion as to how color vision is organized in the primate geniculostriate system. There appears to be little functional reorganization of these systems in the LGN, only a segregation into different sublamina (see Sect. 3.1). In the striate cortex, on the other hand, there is a significant reorganization (see Hubel and Wiesel 1968). Some cells in striate cortex respond mainly to brightness, while others respond mainly to color contrast, even though all share the same cones (Gouras and Krüger 1979, Krüger and Gouras 1980).

Brightness, Whiteness, and Color-Contrast. In the model presented here, the mid-spectral tonic system contributes to *both* brightness and color-contrast-sensitive cortical cells. Evidence exists that mid-spectral cone opponency mostly affects brightness-sensitive cells in the foveal visual cortex (Krüger and Gouras 1980); it also seems indispensable for the construction of color-contrast-sensitive cells. In order to construct *color-constrast*-sensitive cells (Fig. 3.19, *right*), it would seem best to have R on-center cells with *strong* cone opponency on one side of a contour, and G on-center cells with strong cone opponency on the other side, exciting the same cortical cell. These cells would respond maximally when the ratio of R cone to G cone excitation on one side of a contour and the converse ratio on the other side of a contour is maximal (Gouras and Zrenner 1981a).

As pointed out by Baumgartner and Hakas (1962), reciprocal reactions of neurons which are excited (on-neurons), and of those which are inhibited (off-neurons) through the center of the RF form the basis for signalling simultaneous brightness contrasts. In order to construct *luminance-contrast*-sensitive cortical cells (Fig. 3.19, *left*) with the types of retinal ganglion cells described here, it would seem best to have both tonic R on-center and

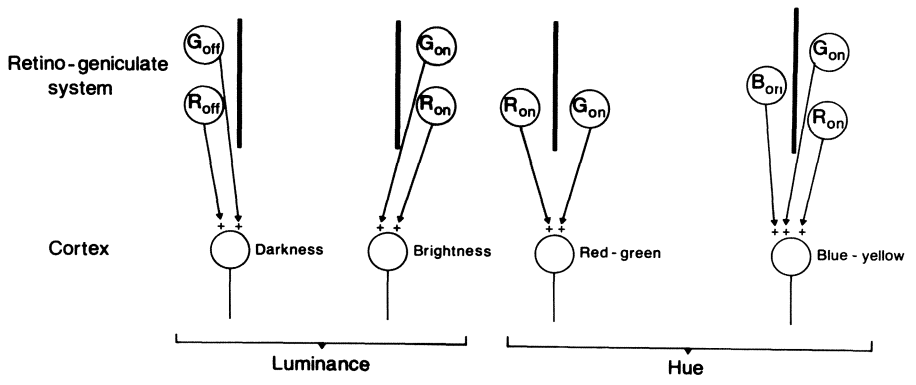

Fig. 3.19. Model of the reorganization of the retinogeniculate system for optimal cortical coding of darkness, brightness and hue (red/green and blue/yellow). *Vertical bars* indicate contours of different brightness and hue gradients. (Gouras and Zrenner 1981a)

G on-center cells with *weak* cone opponency on one side of a contour and tonic R off-center and G off-center cells on the other side of a contour excite the same cortical cell. These cells would respond maximally to effective luminance gradients across a contour.

The advantage of color-opponency in this system is to provide strong signals for the detection of spectrally different objects equiluminant for a single cone mechanism. The uniqueness of this cortical system lies in the fact that it uses only on-center cells to code for red/green color (hue) contrast. This may be the reason why the B-cone system, which contributes to color but not to brightness contrast, has only on-center cells. Blue/yellow contrast-sensitive cells would be formed in the visual cortex by having tonic B on-center ganglion cells on one side of a contour, and tonic R and G on-center ganglion cells with weak cone opponency on the other side of a contour exciting the same cortical cell (Fig. 3.19, *right*). The absence of B off-center cells combined with the relatively weak effect of blue light on the mid-spectral system may contribute to the darkness associated with blue colors.

The neurophysiological processing of the trichromatic sensation "white" – independent of luminance – requires involvement of signals originating in blue-sensitive cones. Since no B-cone signals were found in any other retinal ganglion cells, the 6% tonic blue-sensitive ganglion cells discussed here must signal to the brain information about the short-wavelength part of white light. White light indeed *excites* the blue channel (Fig. 4.1), while yellow and all other wavelengths longer than 500 nm do not. Consequently, the sensation of white, irrespective of luminance, cannot

depend on an – often hypothetized – separate retinogeniculate system that determines whiteness. Consequently, whiteness must depend upon the simultaneous excitation of retinal B, R, and G on-center cells on one side and off-center cells on the other side of a contour.

4 Special Properties of Blue-Sensitive Ganglion Cells

In Chapter 3.3 the temporal, spatial, and spectral differences between retinal ganglion cells, in which signals from blue-sensitive and from longer-wavelength-sensitive cones oppose each other, were compared with those in which the red- and green-sensitive cones oppose each other. The properties of the various ganglion cell types, including those with blue-sensitive inputs, and their retinal distribution were demonstrated in Chapter 3.6. In the following chapter, the blue-sensitive ganglion cells' unusual reaction to changes in adaptation and their curious interaction with spectrally different mechanisms will be discussed.

4.1 Some Recent Electrophysiological and Psychophysical Data on the Blue-Sensitive Cone System

The blue-sensitive cones, present also in many *non*-primate visual systems, differ in many ways from long-wavelength-sensitive cones, since they are much less numerous and particularly rare in the foveola (Willmer 1949a, Wald 1967, Marc and Sperling 1977); they probably contribute neither to enhance visual acuity nor to form detection (Brindley 1954, Van der Horst et al. 1967); they have a limited time resolution as compared with the L-cone system (Brindley et al. 1966, Gouras and Zrenner 1979b); their time course is slower and they lack an off-effect in monkey as well as in cat retina (Zrenner and Gouras 1979a, Schuurmans and Zrenner 1979). Apparently they are involved not in the coding of brightness but in that of hue only (see Smith and Pokorny 1975, Ingling et al. 1978, Walraven 1977, 1981a, King-Smith and Carden 1978, Boynton 1979, Eisner and MacLeod 1980). (A detailed discussion with additional references will be given in Section 4.5.)

Moreover, there must be an unusual interaction between the short- and long-wavelength-sensitive mechanisms (Cicerone et al. 1975) and probably a special retinal circuitry, since in psychophysical experiments the blue-sensitive cone system behaves curiously when adapted to long-wavelength light. When a yellow adapting light is switched off, the threshold for short-

wavelength light does not *de*crease as one expects in dark adaptation, but transiently *in*creases (see Stiles 1959, Das 1964, Mollon and Polden 1977b, Augenstein and Pugh 1977). Mollon and Polden (1977b) presented strong evidence that the blue cone mechanism's sensitivity is controlled by longer-wavelength-sensitive cones (transient tritanopia); this phenomenon was observed also in the primate ERG (Valeton and van Norren 1979a,b), in the optic nerve responses of cat (Schuurmans and Zrenner 1981b) and in ganglion cell recordings (Gouras 1968, Zrenner and Gouras 1979c, 1981); an extensive study is presented in Section 4.3. Recently Augenstein and Pugh (1977) and Pugh and Mollon (1979) offered a model to explain transient tritanopia; they propose two adaptation sites including a fast forward force in the receptors themselves and a slow restoring force proximal to the receptors (see Mollon and Polden 1979) for explaining the blue mechanism's paradoxical threshold elevation; their suggestions are mainly based on psychophysical findings such as failure of field additivity and, to a lesser extent, on data derived from single cell recordings. The absence of transient tritanopia after flicker adaptation, however, is apparently not accounted for by this model (Reeves 1980). To a lesser extent, a comparable phenomenon can be also observed in the interaction between red- and green-sensitive cone mechanisms (Reeves 1981b). Another reversed effect of adapting stimuli on visual sensitivity was described psychophysically by Polden and Mollon (1980) and – to a certain extent – previously by Stromeyer et al. (1978b), who found a range of conditions under which an added yellow field anomalously *increases* the human eye's sensitivity to blue or violet test light. This facilitation or sensitization was named combinative euchromatopsia by Polden and Mollon (1980); a comparable phenomenon was described in ganglion cell recordings of rhesus monkeys by Zrenner and Gouras (1979c, 1981) and in the optic nerve potentials of cat (Schuurmans and Zrenner 1979, 1982); it will be extensively discussed in the following sections.

This chapter will present some neurophysiological correlates of these phenomena as recorded from single blue-sensitive ganglion cells; based on these data, a model will be developed which explains the findings in terms of a retinal circuit.

4.2 Chromatic Adaptation and Spectral Sensitivity

Since color-opponent cells are inhibited by light of one wavelength and excited by light of another, spectrally different test and adapting lights might act very differently on the two cone mechanisms involved. Although in the ganglion cell layer the interaction between blue- and longer-wave-

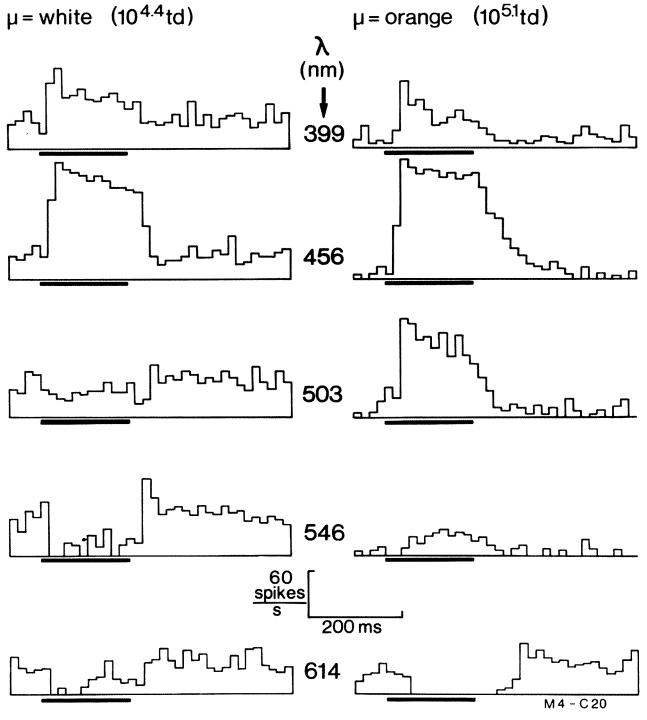

Fig. 4.1. Response profiles of a blue-sensitive ganglion cell in response to five different test wavelengths (λ) against two different backgrounds (μ). The spike frequency is plotted against time, flash duration is given by *black bars*. The irradiance of the Ganzfeld test flashes (*bars*) was $10^{4.3}$-$10^{4.5}$ Quanta s^{-1} μm^{-2}. Pre-excitatory inhibition is not as pronounced in responses near threshold as it is in supra-threshold responses (see Fig. 4.4). (Zrenner and Gouras 1981)

length-sensitive cones has already taken place, the contribution of individual cone mechanisms to the cell's action can still be identified by their characteristic response features (see Chap. 3.3).

Response Profiles. Figure 4.1 shows response profiles of a blue-sensitive ganglion cell, elicited by flashes of various wavelengths (λ) but fixed irradiance E (about $10^{4.4}$ Quanta s^{-1} μm^{-2}). In presence of even very dim neutral white backgrounds (μ = white, *left half* of the figure), blue-sensitive ganglion cells have a continuous high discharge rate (40-50 spikes/s) over a wide range of retinal illumination and respond to test lights only with a small frequency increment during stimulation (*black bar*). Having a response maximum near 456 nm, the responsiveness decreases toward longer wavelengths until a neutral zone is reached near 503 nm, where excitation and inhibition are about balanced. The cell's activity is only weakly modu-

lated by light in this neutral zone. Wavelengths beyond this point (546 nm and 614 nm) inhibit the cell. As seen on the right of Fig. 4.1, a long wavelength background eliminates or considerably decreases the "spontaneous" (continuous or maintained) discharge rate of such cells (best seen at the end of each trace), so that the response increment or decrement, elicited by test flashes, becomes more prominent. Furthermore, the cell's spectral characteristics are changed by the orange background. While the cell is still excited maximally by 456 nm light, inhibitory responses can only be produced by very long-wavelength stimuli (614 nm); all other wavelengths excite the cell. In this cell, an orange background shifts the neutral point by at least 50 nm toward longer wavelengths.

Action Spectra. Response thresholds (i.e., the number of quanta necessary to evoke a just-detectable spike frequency increment or decrement) are plotted against wavelengths in Fig. 4.2. In presence of a white background (*triangles*), a blue-sensitive ganglion cell shows the lowest threshold for excitation (*open symbols*) near 450 nm (as reported for the short-wavelength sensitive mechanism in monkey retina by Gouras 1968; van Norren and Padmos 1973, Jacobs 1974); the lowest threshold for inhibition occurs near 560 nm, mediated by long-wavelength-sensitive cones, similar to the cells described in Fig. 3.4; the neutral point is located near 500 nm. When the intensity of the white background is increased (*squares*), the sensitivity to short wavelength stimuli is decreased. In presence of an orange background,

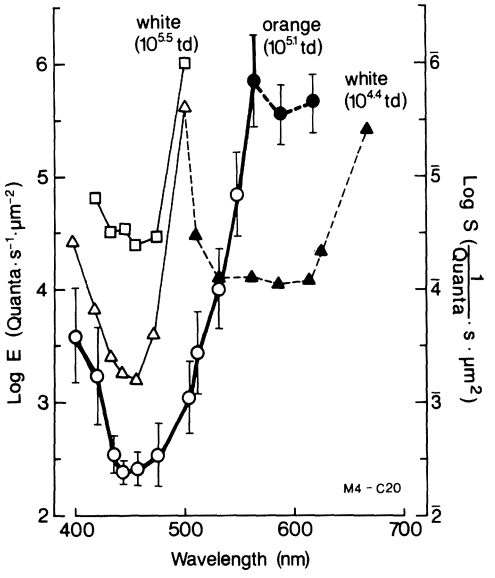

Fig. 4.2. Action spectra of a blue-sensitive ganglion cell based on response threshold criteria under three different adapting conditions (as indicated); Ganzfeld stimuli of 200 ms duration. For orange background ($10^{5.1}$ td, *thick line*) the cell's action spectrum is averaged with that of seven other blue-sensitive ganglion cells recorded under the same condition; mean values and ± S.D. as indicated. (Modified from Zrenner and Gouras, 1981)

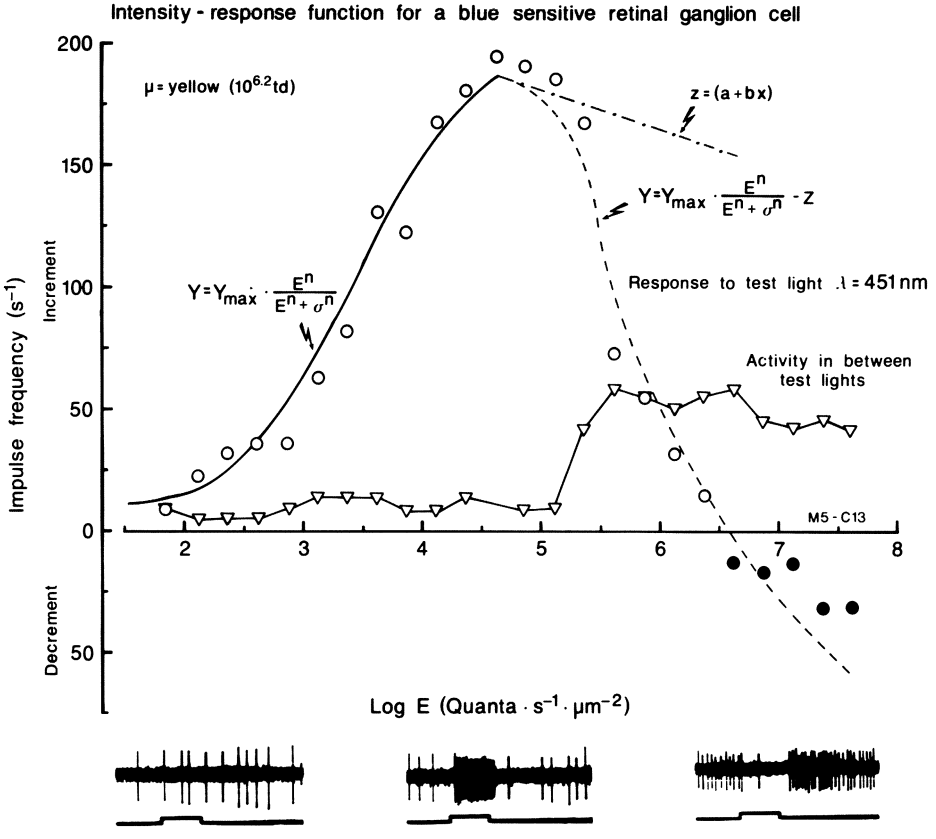

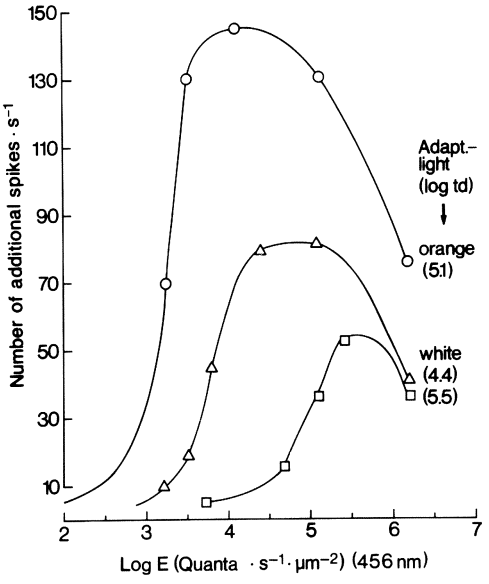

Fig. 4.3. *Left* Intensity-response function obtained with the three background conditions of Fig. 4.2. After several seconds of adaptation, the cells' responses had reached a steady state (cf. Fig. 4.4). The number of additional spikes/s elicited by 456 nm test flashes is plotted against the irradiance E applied. Data points are connected by *smoothed lines*, drawn by hand. *Above* The rising and falling phase of the I/R function obtained in another blue-sensitive ganglion cell in presence of yellow background light ($10^{6.2}$ td) is matched by combining two sigmoid functions. (Formula after Naka and Rushton 1966 b). The inhibitory L-cone response function (*broken line*) is subtracted from the excitatory (*solid line*) B-cone function. (Graph above reported by Wienrich and Zrenner 1981)

however, the action spectrum of this cell (as well as that of the seven other ganglion cells which had input from blue-sensitive cones) changes considerably as indicated by *circles connected with thick lines*; the maximum sensitivity increases by about 1 log unit and the action spectrum falls off sharply toward longer wavelengths; only beyond 560 nm do the test flashes produce inhibitory responses (*closed circles*). It should be noted that orange adapting light not only shifted the neutral point by about 50 nm, but simultaneously produced a threshold increase in the long-wavelength region combined with a threshold decrease in the short-wavelength region.

Intensity-Response Functions. Interestingly, the intensity-response functions (I/R-functions) of the excitatory mechanism obtained with the three backgrounds of Fig. 4.2 are very different. The spike frequency of tonic cells was measured during the second half of the stimulation period, since tonic ganglion cells then reach a steady discharge rate; as shown in Fig. 4.3 (*lower half*), the number of additional spikes (response increment) produced by the test light (as compared to the spontaneous activity) initially grows with increasing irradiance under all three conditions. However, while a strong white background ($10^{5 \cdot 5}$ td *squares*) causes saturation of spike frequency already at 50 spike/s, a dimmer white background ($10^{4 \cdot 4}$ td *triangles*) leads to saturation at much higher levels (80 spikes/s). With orange backgrounds (*circles*), spike frequencies almost as high as 150 spikes/s are obtained, before the I/R-function falls off. Blue-sensitive ganglion cells obviously can reach much higher maximal spike frequency increments on orange than on white backgrounds. This is due, first, to the low spontaneous activity present during orange adaptation and second, to a mechanism which increases the gain of the blue cones, as shown in the next paragraph. The decrease of the I/R-function's slope at higher test light intensities is apparently caused by another mechanism, which has a lower sensitivity to this wavelength and acts antagonistically (see also Naka and Rushton 1966b). As shown in Fig. 4.3 (*upper half*), the antagonism between two cone mechanisms can be inferred also from the subtraction of two intensity-response functions. At low intensities of the 451 nm test light, the steady increase in spike frequency with increasing intensities suggests that this blue-sensitive color-antagonistic ganglion cell is more responsive to excitatory than to inhibitory input. A growing influence of inhibitory input is indicated by the rapid decrease in impulse frequency with increasing test light intensity (*broken line*), finally resulting in a net decrement response (*filled symbols*). If the intensity-response function of the inhibitory mechanism is generally assumed to have a similar input-output function as the excitatory mechanism – here fitted with a Naka-Rushton function (Naka and Rush-

ton 1966b) for the rising phase – subtraction of the rapidly rising inhibitory function from the slowly falling excitatory function (*dotted line* z = 70 + 24.1) results in the curve (*broken line*) which closely fits the response of the ganglion cell to higher test light intensities. The values of σ, n, and Y_{max} were 4.2, 0.84 and 205 for the ascending part and 1.6, 0.84 and 205 for the descending part. The responses of the ganglion cell are shown underneath the I/R-function and strongly support this view, since the spike frequency increment observed at lower intensities of the test light changes into a response decrement at higher intensities. Simultaneously the maintained activity of the cell in between the test lights (*triangles*) increases, most possibly due to the rebound excitation following the offset of the inhibitory stimulus (reported by Wienrich and Zrenner 1981).

After having presented the spectral properties and the intensity response functions of blue-sensitive ganglion cells in relation to neutral and chromatic backgrounds, the interaction between the inhibitory long-wavelength and the excitatory short-wavelength cone mechanism in such cells will be discussed.

4.3 Paradoxical Phenomena Occurring During Light and Dark Adaptation in Blue-Sensitive Ganglion Cells

Figure 4.4 (*uppermost row*) shows the response of a blue-sensitive ganglion cell stimulated by 456 nm light flashes (irradiance $E = 10^{5.1}$ Quanta s^{-1} μm^{-2}), no background being present for the first three flashes shown. Each test flash produces a slight spike increment, preceded by a short phase of pre-excitatory inhibition; this indicates that the latency of the inhibitory response is shorter and that the short pause is mediated by the inhibitory long-wavelength-sensitive cones which respond to the strong blue light employed, a phenomenon observed especially in blue-sensitive ganglion cells. After the third test flash, a strong yellow background ($10^{3.6}$ td) is switched on for 7 s. The yellow adapting light immediately and completely suppresses all spontaneous activity. During the first few seconds, the activity evoked by the test stimulus is relatively weak but gradually increases from flash to flash. This *sensitization* of the cell seems paradoxical at first sight, since it is caused by light adaptation which normally desensitizes a visual receptor. When the yellow light is switched off, a strong, relatively short after-discharge occurs (best seen in the second row), during which the test stimulus does not produce a tonic spike frequency increment. This lack of responsiveness to the test light during the initial period of dark adaptation represents a *transient desensitization* as reported in ganglion cells by

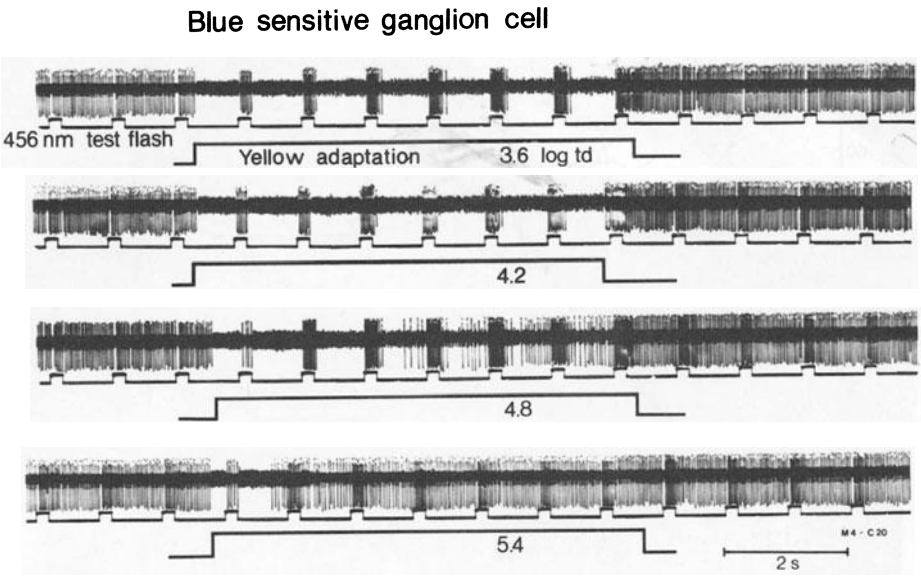

Fig. 4.4. Extracellular recording from a blue-sensitive ganglion cell. Test flashes (456 nm) are presented every second for 200 ms (*upper stimulus trace*). After 1 min of dark adaptation, a yellow adapting light (25° in diameter) is switched on for several seconds (*lower stimulus trace*, duration varied between 7 and 18 s). The strength of the yellow adapting light varies in the individual traces as indicated. The intervals between each presentation of adapting lights were in the range of 30 to 50 s. (Reported by Zrenner and Gouras 1979c, Gouras and Zrenner 1979b)

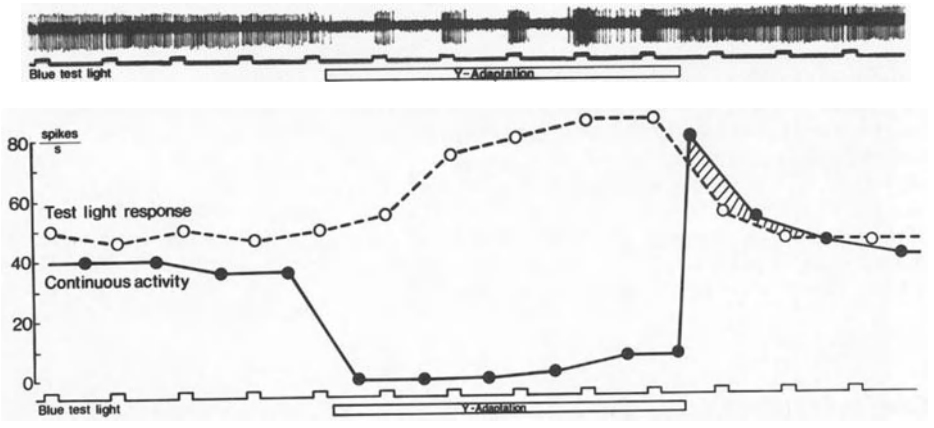

Fig. 4.5. Evaluation procedure. The response (spikes per second) *during* the presentation of the blue test light (*open circles*, evaluated for the second half of stimulus duration) is separated from the continuous activity (*filled symbols*) as measured in *between* the test light presentations. Both functions show characteristic behavior when yellow adapting light (*open bar*) is presented (retinal illumination of $10^{4.5}$ td). *Hatched area* indicates the period during which the continuous activity surpasses the test light response; this phase indicates relative response *de*crements. (Zrenner and Gouras 1981)

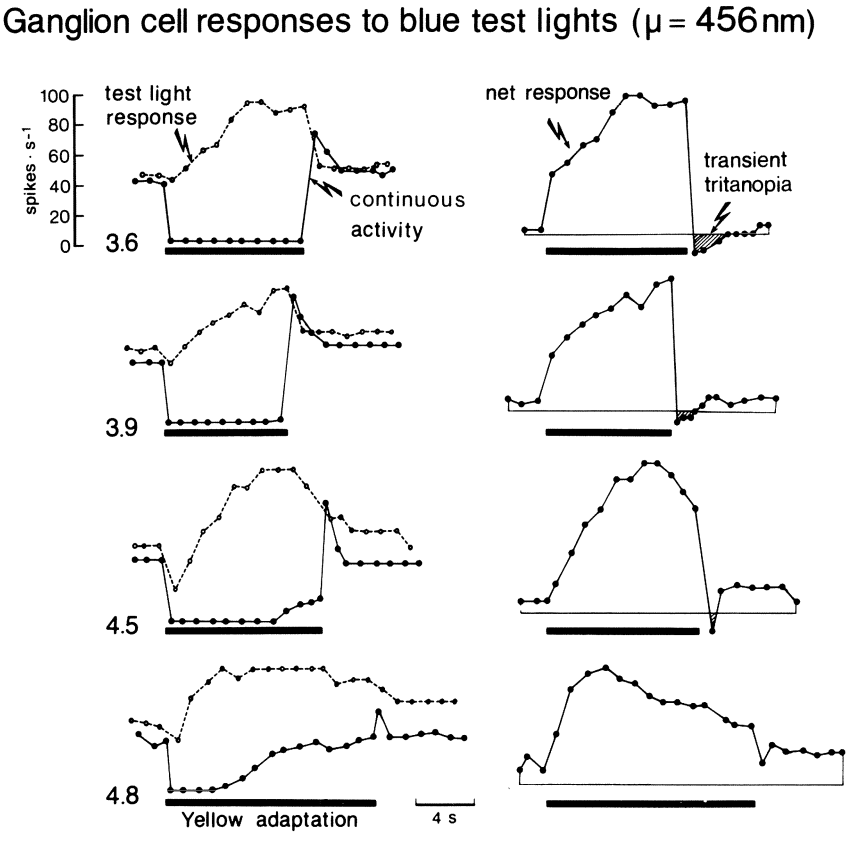

Fig. 4.6. *Left side.* Evaluations of the responses of a blue-sensitive ganglion cell (from recordings as those shown in Fig. 4.4 and 4.5). The spike frequency of the test light responses (*open circles, connected by broken lines*) and of the continuous activity (*closed circles, connected by solid lines*) is given before, during and after presentation of yellow adapting light (*black bar*) of different strength, as indicated on the left border in log (td). *Right side.* The net response of this ganglion cell (replotted from the left side) represents the difference between the continuous discharge rate and the test light response. The negative values (*below the thin zero line*) indicate a transient unresponsiveness to blue test lights after the offset of the yellow light (corresponding to the psychophysical phenomenon of transient tritanopia; see text)

Gouras (1968), Gouras and Zrenner (1979b) and Zrenner and Gouras (1981). If the retinal illumination of the yellow adaptation light is gradually increased to $10^{5.4}$ td (second, third and fourth row), both sensitization and desensitization grow at first, but decrease from about $10^{4.8}$ td on; finally, they even disappear, accompanied by a high spontaneous (or continuous) discharge rate which begins already in the presence of the yellow adapting light. At high intensities, no electrical event signals the offset of

the yellow adapting light in this cell. Interestingly, the first response – after switching on a very strong adapting light – *de*creases with respect to spike frequency.

In order to quantify these phenomena, spike frequency was plotted against time. As seen in Fig. 4.5, yellow adapting light decreases the continuous activity (*dots*) and, at the same time, sensitizes the cell for blue light (*circles*). After the offset of the yellow adapting light, the test light response decreases to the value it had before light adaptation took place. The continuous activity undergoes the greatest change, since it transiently surpasses the spike activity of the test light response, as indicated by the *hatched area*. This overlap of the two functions is very intriguing, since it indicates that the response to the test light must consist of a *transient decrease* of the cell's net response in relation to the continuous activity.

The net responses indicating the cell's effective output are shown for adapting lights of various strengths in Fig. 4.6 (*right column*), calculated from the difference between the test light response and the continuous activity as shown in the original evaluations (*left column*). Interestingly, at higher intensities of yellow adaptation, the cell's responsitivity decreases transiently, immediately after the *on*set of yellow adaptation; this phenomenon might correspond to recently published psychophysical observations of Mollon and Polden (1980) that in the initial phase of light adaptation, the threshold for short-wavelength light passes through a much lower level before reaching its saturated state. In the net response, the slowly rising sensitization *during*, as well as desensitization (*hatched area*) *after* the termination of the yellow light becomes very evident. Since it is well established that reduced response amplitudes are correlated with reduced sensitivity to homogeneous spectral lights, this sensitization could resemble the psychophysically determined "combinative euchromatopsia" (Polden and Mollon 1980), while the desensitization might be the cellular equivalent of the psychophysical phenomenon of transient tritanopia. As known from Mollon and Polden's (1977b) and Reeves' (1981a) work, this phenomenon disappears at very high intensities of adapting light, as also observed here (*lowermost row*) in blue-sensitive ganglion cells. Obviously, stronger yellow adapting lights (e.g., $10^{4.8}$ td) cause the continuous activity to resume during yellow adaptation; after 10 s the cell's spike frequency almost reaches the level it had before yellow adaptation took place (*lowermost graph on the left*). Therefore, sensitization and desensitization disappear at high levels of adaptation. In the following, some ideas on the nature of both phenomena will be outlined.

4.4 A Model Describing the Interaction Between Cone Mechanisms in Blue-Sensitive Color-Opponent Ganglion Cells

Existing ideas about the mechanism underlying the phenomena occurring in the blue-sensitive cone mechanism under light adaptation are relatively formal (see Pugh and Mollon 1979), even though the most plausible explanation that longer-wavelength-sensitive cones control the short-wavelength-sensitive cones' sensitivity becomes very clear in these models. In this paper, a neural circuitry will be discussed, which in a ganglion cell can cause the paradoxical sensitization to long-wavelength lights during light adaptation and the transient desensitization in the initial period of dark adaptation described above.

The basic observation is that the blue mechanism's responses are enhanced *in presence* of long-wavelength spectral lights, which strongly activate the antagonistic cone mechanism; i.e., stronger responses are elicited in a B^+-L^- cell via the blue-sensitive cones when the "inhibiting" long-wavelength lights are present; paradoxically weak responses, however, are obtained *after the termination* of long-wavelength light. In contrast to this latter desensitization, sensitization is not immediate, but builds up over several seconds.

Since two spectrally different stimuli are involved in the experiments described above, hypothetical models which explain these phenomena in blue sensitive ganglion cells have necessarily to include the short-wavelength-sensitive cone B, the long-wavelength cone L (either green- or red-sensitive or both), as well as a laterally connecting interneuron which allows the L-cone to modify the B-cone's signals.

4.4.1 Forward Versus Backward Inhibition: Two Models

General Circuitry. Consider the following two models, the simplified general circuit of which is given in Fig. 4.7 (from Zrenner and Gouras 1981): In both cases, blue test light predominantly stimulates the blue-sensitive cone B, while the yellow adaptation light predominantly stimulates the long-wavelength-sensitive cone L. In *model I* (forward inhibition model, as developed in lower vertebrates, Werblin 1974), the signal originating in the B-cone causes a discharge in the ganglion cell via an on-center bipolar cell; this signal is inhibited by the L-cone in the first stage through the horizontal cell H at its synapse with the corresponding bipolar cell in the blue sensitive cone's direct pathway. Feedback onto the receptors does not play a major role in such models. Models like this one would indeed explain the decrease in continuous activity when the L-cone is stimulated by the onset

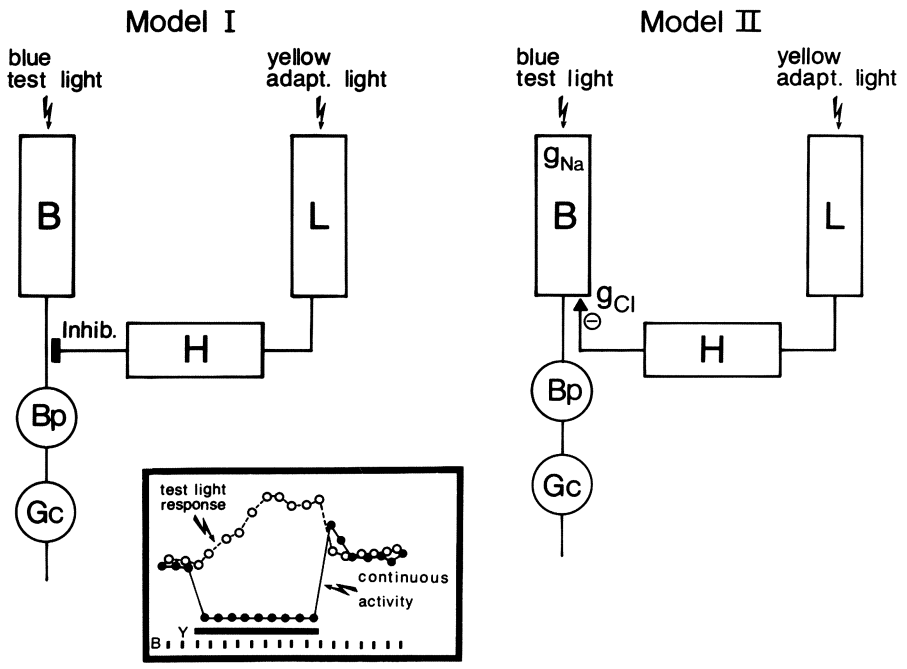

Fig. 4.7. Two models describing the possible interaction between blue-sensitive (*B*) and longer-wavelength sensitive (*L*) cones via the horizontal cell (*H*). In model I (forward inhibition) the signals originating in the B-cone, which influence the on-center bipolar cell (*Bp*) and the ganglion cell (*Gc*), are inhibited by the L-cone. In model II (backward inhibition), the signal transmission in the B-cone's pedicle *itself* is modulated, probably by a hyperpolarizing transmitter θ (see below) which acts on the K^+ (or Cl^-) conductance (g_{Cl^-}); this model can better explain the sensitization and desensitization occurring in blue-sensitive ganglion cells when yellow (*Y*) backgrounds are presented, as shown in the inset figure. (Modified from Zrenner and Gouras 1981)

of yellow light (*dots in the inset figure*, copied from Fig. 4.6). *Sensitization* (*open circles*), however, is not easily accounted for by model I, since under all conditions it entails an inhibition, rather than the enhancement of the test light response observed in blue-sensitive ganglion cells.

There are two further problems with this model: First, the desensitization of the B-cone signal after the *offset* of the yellow light cannot be easily explained, since the inhibitory effect of the L-cone, mediated via the H-cell, ought to decrease immediately; second, it was observed that in presence of stronger yellow adapting lights the steady inhibition of the continuous discharge wore off completely after several seconds (Fig. 4.4); in the circuitry of model I this ought to enhance the cell's response to blue test light; on the contrary, stronger yellow adapting lights *weakened* the response in ganglion cell recordings.

This drawback of model I has led to model II, which provides some major improvements (Zrenner and Gouras 1979c, 1981). In *model II*, the responsiveness of the blue cone to the blue test light is directly modulated by a horizontal cell feedback (backward inhibition; see Sperling 1970 for discussion on forward and backward inhibition). Such feedback loops between cones, mediated by horizontal cells, were observed in turtle retina, e.g., by Baylor and Fuortes (1970), Baylor et al. (1971), Gerschenfeld and Piccolino (1980). In fish, the model of Stell et al. (1975) assumed that horizontal cells feed back onto all three types of cones to produce chromatic signals, thus taking into account the special function of the cone pedicle's triad. Such a feedback loop is applied in model II for the circuitry between the blue-sensitive and longer-wavelength sensitive cones. The B-cone can be activated either by light (which causes hyperpolarization, by decreasing the sodium conductance, g_{Na^+}, see Chap. 1) or by the L-cone, which modulates the B-cone's sensitivity through the horizontal cell H. The simplest and most practical way of sensitizing the blue cone is to decrease its membrane's conductance (g) for ions such as Cl^-, or, in the opposite direction, K^+. It would probably be even sufficient to change the conductance of a patch of the blue cone's membrane inside the triad, so that this local effect would have its impact mainly on the release of transmitter-substances onto the postsynaptic neuron and less on the blue cone response itself. Whatever the details of this mechanism are, the decrease in membrane conductance can be easily accomplished through the horizontal cell H by stopping the hyperpolarizing transmitter Θ, which otherwise increases the conductance of the B-cone's membrane for Cl^- or K^+ ions.

The Anatomy of the Feedback. Although the triad in the cone pedicle is very well suited to mediate a feedback loop, anatomically there are no structures which point to a *chemical* feedback synapse from the horizontal cell back onto the receptors. However, Baylor et al. (1971) showed with double cell recordings that hyperpolarization of a horizontal cell causes depolarization in the postsynaptic cone; that is, polarity reversals can occur without the direct involvement of chemical synapses. The experiments of Lasansky and Vallerga (1975) support this finding. Morphological studies in goldfish also indicate (Stell 1976, 1978) that horizontal cells can act presynaptically on receptors. The objection that no vesicles are observed in these feedback synapses is weakened by the explanation of Marc et al. (1978), who have pointed out that reversal of the carrier-mediated diffusional transport system for GABA provides a plausible *non*-vesicular release system.

One can conceive of different models which would result in reducing or stopping this transmitter; it might well be that competition for the transmitter takes place in the region of the ribbon structure, so that the synap-

tic efficacy is controlled by a competition between the dendritic processes, forming an invaginating synapse for the same transmitter (proposed by Grüsser 1979); however, there appear to be no examples of such a mechanism in the literature on the outer plexiform layer of the retina.

4.4.2 Implications of the Backward-Inhibition Model in Terms of Membrane Properties, Ionic Action and Transmitters

In order to make model II more transparent, the action of its circuitry is redrawn in Fig. 4.8 (upper half) under three different conditions (**A**, **B**, **C**). The lower half represents the recorded data from Fig. 4.5 in order to clarify the processes involved in the model.

The Prerequisites. Model II is based on the following physiological observations:

a) Transmitter substances are released by depolarization and stopped by hyperpolarization (for references see Katz 1966, Hubbard et al. 1969, Fuortes 1972, Krnjević 1974).

b) In primates, all horizontal cells we observed so far (n = 19 recordings) are hyperpolarized when stimulated by light (see Gouras and Zrenner 1979b for a preliminary report); apparently the release of a depolarizing transmitter substance from photoreceptors onto horizontal cells continues in the dark and is reduced by light (Trifonov 1968, Trifonov et al. 1974). Depolarization of the cone therefore causes depolarization of the H-cell by releasing such a transmitter; hyperpolarization of the cone by light results in hyperpolarization of the H-cell; thus, in Fig. 4.8 the H-cell signal essentially reflects the L-cone signal, also in accordance with the experimental data of Brown and Murakami (1968).

c) A cone's sensitivity to test lights decreases the more it is hyperpolarized by physiological stimuli (background lights etc., however, *not* by extrinsic currents); see Baylor and Hodgkin 1974, cf. their Fig. 5.

d) The sensitivity of visual neurons can be modified by changes in conductance of Cl^- and/or K^+ channels by the action of their presynaptic neurons (see Miller and Dacheux 1976, Saito and Kondo 1978, Saito et al. 1979).

e) Horizontal cells can act directly onto receptor cells by a feedback mechanism (Baylor et al. 1971, O'Bryan 1973, Piccolino and Gerschenfeld 1978, Byzov 1979, Gerschenfeld and Piccolino 1980). In these experiments, hyperpolarization of the horizontal cell can be accompanied by depolarization in the postsynaptic receptor cell.

f) O'Bryan (1973) showed that the horizontal cell feedback is associated with a change in membrane conductance having two separate components, one of which is an increase in conductance, probably for Cl^-; this can occur in a sustained manner (Gerschenfeld and Piccolino 1980). Cl^- was proposed as the ion responsible for generating the horizontal cell response in rabbit and mudpuppy by Miller and Dacheux (1976). Lasansky's (1981) intracellular recordings from the tiger salamander cone membrane strongly support the involvement of this ion on the feedback mechanism; indirect evidence is given for the chloride conductance being *increased* by the surround illumination. For a consideration of the electrical current involved in such a feedback mechanism see Byzov et al. (1977); for a discussion of the chemical and electrical nature of the feedback mechanism see Gerschenfeld and Piccolino (1980).

g) Blue-sensitive cones are almost exclusively feeding on-center neurons (for references see Chap. 3). That is, a polarity reversal occurs between the blue cone and its postsynaptic bipolar cell (see below).

h) There are several types of horizontal cells, anatomically and/or electrophysiologically analyzed in cat. e.g., by Niemeyer and Gouras (1973), Kolb (1974), Nelson et al. (1975), Nelson et al. (1976), Foerster et al. (1977a,b) and van de Grind and Grüsser (1981); see also Chap. 1. Stell and Lightfoot (1975) and Witkovsky et al. (1979) observed corresponding anatomical structures in fish retina. Most probably individual types of horizontal cells are also responsible in primates for color-specific interactions between cones. Interestingly, in lower vertebrates there are two types of horizontal cells which build up a dual surround (Neyton et al. 1981a), which can produce a reversed polarity in the photoreceptor in response to surround illumination.

For further discussions on this model see Zrenner (1982a).

The Function in the Non-Adapted State. The model thereby describes the following actions: in the dark (Fig. 4.8A), the L-cone has a certain resting potential (hatched area) depending mainly on the prevailing Na^+ and Cl^- (or K^+)-conductance (represented by small openings at the right side of each cell's symbol). Since the L-cone is not strongly hyperpolarized, it releases a transmitter which has a *de*polarizing action ⊕ on the subsynaptic membrane of the H-cell (Trifonov 1968), probably by increasing its Na^+-conductance (Miller and Dacheux 1976). Depolarized by the action of these additional postive ions, the H-cell permanently releases a certain amount of *hyper*polarizing transmitter (⊖) onto the subsynaptic B-cone membrane. The hyperpolarizing transmitter (possibly GABA, see below)

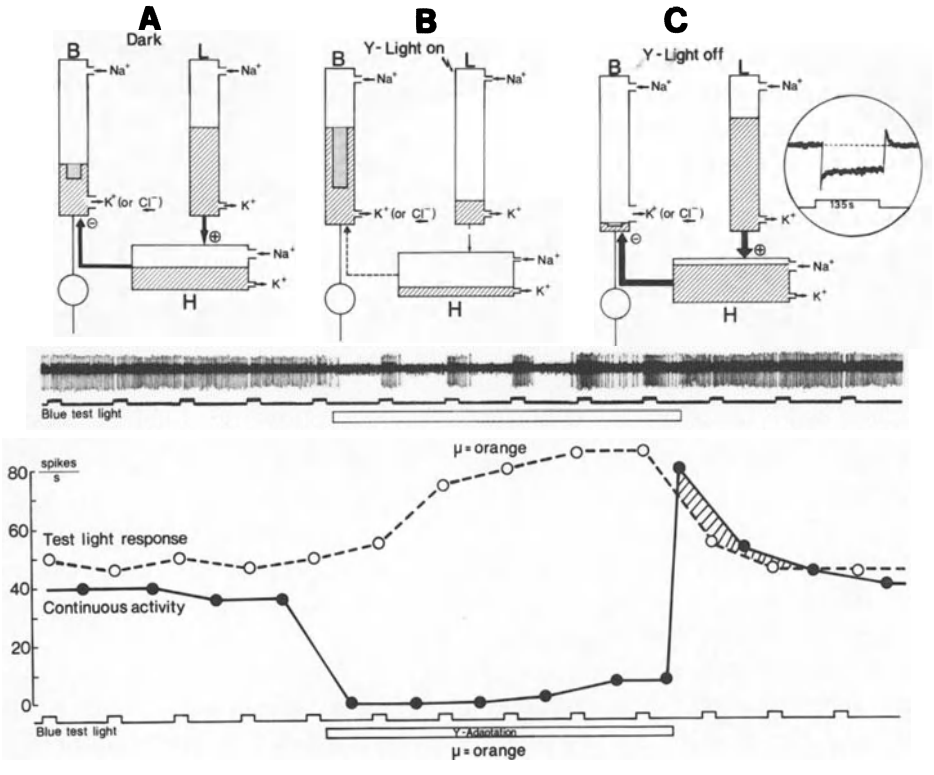

Fig. 4.8A-C. The action of the circuitry of the proposed model II in the dark **(A)**, during yellow adapting light **(B)** and immediately after the offset of the yellow light **(C)**. The L-cone modifies the B-cone membrane's response to blue test lights (*dotted inset bars*) via a horizontal cell (*H*) by means of a hyperpolarizing transmitter (Θ). The vertical boxes with levels of membrane potentials do not necessarily represent the entire outer segment of receptors, but can be imagined as potential changes of membrane patches inside the triad structure of the cone pedicle (see text and Fig. 4.9). The conductance of Cl^- (or possibly K^+ in the opposite direction) and Na^+ channels is indicated by the *width* of each ionic "channel". The *circled inset figure on the right* demonstrates the response of a red-sensitive cone (redrawn from Fig. 14 in Baylor and Hodgkin 1974). The data obtained in the three situations in the model refers to, are shown below in the original, as well as in the evaluated format, as described already in Fig. 4.5

shifts the B-cone's resting potential toward more negative values, because it increases the Cl^- (or K^+)-conductance. This steady hyperpolarization of a receptor causes a discharge in the corresponding (on-center) ganglion cell due to a polarity reversal (for recent review see Miller and Dacheux 1976 or Dowling 1979); thereby it becomes clear why the continuous discharge rate of the blue-sensitive ganglion cell is relatively high in the dark (*dots*). On the other hand, as known from Baylor and Hodgkin's (1974) recordings

from cones (Fig. 5 of their paper), sensitivity to test lights decreases when a cone is hyperpolarized by light. Therefore, blue test lights do not evoke a strong hyperpolarization in B-cones (Fig. 4.8, *dotted inset area*) in the dark, as indicated indeed by small response increments in the ganglion cell recordings below (*circles*).

The Function in the Light-Adapted State. When yellow light is switched on (Fig. 4.8B), the Na^+-conductance in the L-cone decreases; the L-cone and the H-cell hyperpolarize, so that the hyperpolarizing transmitter Θ is stopped (indicated by a *thin broken line*). This, in turn, depolarizes the B-cone by decreasing its Cl^-- or K^+-conductance, so that it can reach a new, more positive resting potential[5]. Consequently, the continuous activity of the ganglion cell is decreased (*dots in the lower trace*); however, the blue cone's responses (*circles*) to light are enhanced (sensitization); this is due to the fact that a less hyperpolarized receptor has a higher sensitivity (Baylor and Hodgkin 1974), at least in the middle range of its response function (Murakami et al. 1972). This facilitation observed in ganglion cells might be reflected in the psychophysical phenomenon of combinative euchromatopsia (Polden and Mollon 1980).

After a few seconds, a gradual change in the B-cone's equilibrium toward more negative values must take place, since, at least with stronger yellow light, the ganglion cell starts firing again; this can be observed in between the last two flashes during yellow adaptation in the center trace of Fig. 4.8. It becomes understandable since the L-cone's synaptic action onto the blue cone system slowly recovers after several seconds of light adaptation; Baylor and Hodgkin (1974) demonstrated this phenomenon in recordings from a red-sensitive cone during prolonged stimulation. The circled inset on the right side of Fig. 4.8 is redrawn from their paper (Fig. 14) for the sake of greater clarity.

The Function Immediately After the Termination of Yellow Adaptation. On the right side of Fig. 4.8C the situation after the offset of yellow light is outlined. It can also be observed that termination of the yellow adapting light causes a rebound depolarization in long-wavelength cones (*hatched area*). This transiently depolarizes the horizontal cell even more strongly (Normann and Perlman 1979), which in turn releases the hyperpolarizing transmitter onto the B-cone's subsynaptic membrane; due to the considerable increase in K^+- or Cl^--permeability, the B-cone is strongly hyperpolarized. The transient hyperpolarization of the B-cone produces a high-fre-

5 A similar mechanism was proposed for the connection between the receptors and on-center bipolars in fish retina by Kaneko and Shimazaki (1975), Toyoda and Tonosaki (1978) and Saito et al. (1979)

quency off-discharge in its on-center ganglion cell but makes the blue cone unresponsive to light; i.e., closing Na^+-channels by exposure to light in order to stimulate (hyperpolarize) the receptor has little or no effect on the B-cone, since it is already almost maximally hyperpolarized. This phenomenon would correspond to the phenomenon of transient tritanopia (Mollon and Polden 1977b) mentioned above, since a receptor which is maximally hyperpolarized can no longer respone to light. Thus, probably by controlling the ratio between Na^+- and K^+- or Na^+- and Cl^--permeability, the horizontal cell feedback-loop modulates the sensitivity of B-cones Zrenner and Gouras (1981); in many respects such a mechanism fits the neuromodulator concept (see Kupfermann 1979).

The Dynamics. If the adapting light is especially bright and is left on for some time, the horizontal cell's response returns close to its preadaptation level, a phenomenon observed in skate horizontal cells by Dowling and Ripps (1971). In this case, sensitization is slowly lost since the gradually depolarizing horizontal cell might release more and more transmitter, which has a hyperpolarizing action on the B-cone; correspondingly, the continuous activity in the ganglion cell increases and the sensitization is lost. As shown in Fig. 4.4, the stronger the adapting light, the faster this process occurs. Moreover, very bright lights do not produce a depolarizing rebound which surpasses the dark level in a horizontal cell (Baylor and Hodgkin 1974). Consequently, a transient desensitization of the B-cell to blue test light can no longer be observed. Analogously, transient tritanopia is also lost in human vision at high levels of adaptation (Mollon and Polden 1977b). A similar explanation can be given for the loss of sensitization at low light levels: The rebound depolarization becomes smaller al low light levels as well, so that from certain low yellow background intensity levels only very little or no hyperpolarizing transmitter is released onto the B-cone membrane.

The Transmitter. GABA would be a transmitter which could act in the way anticipated by this model. It is a hyperpolarizing transmitter and it increases the membrane conductance for chloride (see Krnjević 1974, Davidson 1976); pharmacological evidence in carp and catfish (Lam et al. 1978) suggests that GABA is tonically released in the dark onto cone photoreceptor terminals. Recent experiments of Schwartz (1982) in toad retina revealed GABA-release from isolated horizontal cells. The proposed circuit would thereby employ a kind of presynaptic inhibition where GABA is most often involved (see review of Nicoll and Alger 1979). GABA-antagonists, such as bicuculline, eliminate the phenomenon of transient tritanopia as detected in optic nerve of cat responses (Schuurmans and Zrenner 1981b, Schuurmans 1981), and can decrease the surround response substantially

while center driven responses are almost unaffected in certain types of cat ganglion cells (Kirby and Enroth-Cugell 1976); it is found in the horizontal cells of mammals and some other vertebrates (e.g. Voaden et al. 1974, Lam 1975, Voaden 1976, Marc et al. 1978, Bonaventure et al. 1980) even though in a series of animals GABA seems to be located mainly in the inner plexiform layer (Ehinger and Falck 1971, Pourcho 1980). In fish retina, Djamgoz and Ruddock (1980) provided evidence for a GABA-ergic feedback-loop in the outer plexiform layer. For recent data on this matter see Ehinger (1976), Dowling (1979), Gerschenfeld and Piccolino (1979, 1980), Nicoll and Alger (1979) and Yazulla (1981).

The discrepancy in the retinal localization of GABA is explained by Yazulla (1981) as follows. The tonic release of GABA in the dark could result in a relatively high extracellular GABA concentration implying a low-affinity receptor; if the on-rate of the GABA-receptor interaction had a typical value of 10^6 M $\cdot$ s^{-1}, then a low affinity such as 10^{-5} M to 10^{-6} M would indicate an off-rate of about 6 ms to 60 ms, which is far too fast to be detected by autoradiographic technique.

Nevertheless, such a feedback onto cones via such synapses could well be a feature of visual systems in general, since even in certain ocellar retinae GABA is proposed with good evidence as acting as feedback transmitter on photoreceptors (Stone and Chappell 1981).

Additional interactions between the two cone mechanisms at the amacrine cell level which can modify responses of ganglion cells (see Miller 1979) should also not be excluded. A subpopulation of amacrine cells could provide the second stage of such a circuitry (Gouras and Zrenner 1981, see also below), especially since GABA is also found in amacrine cells. It should be mentioned that experiments in lower vertebrates provide evidence for *direct* coupling between spectrally different cones (Baylor 1974), although the functional role of this coupling is not yet clear.

In summary: The advantage of model II lies in the fact that changes in K^+- or Cl^--permeability of the B-cone's membrane are controlled by the L-cone; i.e., the effect of short-wavelength light which changes the B-cone's Na^+-permeability is modulated by the long-wavelength light that stimulates the L-cone. Thereby the B-cone becomes depolarized in presence of a long-wavelength, adapting light; consequently, the continuous discharge in the blue-sensitive ganglion cell decreases but its response to blue test lights increases, i.e., inhibition of a ganglion cell's continuous activity by one cone mechanism does not necessarily inhibit an excitatory signal provided for the same ganglion cell by another cone mechanism.

4.4.3 The Limitations of the Model: Feedback onto the Receptor or onto the Bipolar Cell?

The model presented in Figs. 4.7 and 4.9 is used rather to outline the specific features common to all models of the backward-inhibition type than to pinpoint certain anatomical structures. In model II the on-center bipolar cell reflects the changes in the B-cone's sensitivity rather passively, however, with reversed polarity. Since the model is based on ganglion cell recordings, it is difficult to feel safe in determining to what extent the responsiveness of the blue cone itself is modulated by the feedback loop. It should be emphasized that the feedback loop would work as well if the horizontal cells' action on the B-cone's membrane rather locally changed the B-cone's transmitter release onto the bipolar cell, without greatly affecting the B-cone's outer segment.

Can the ERG Help to Solve the Problem? From ERG-measurements, Valeton and van Norren (1979a,b) concluded that transient tritanopia must take place at the bipolar cell level or earlier, since it is very pronoun-

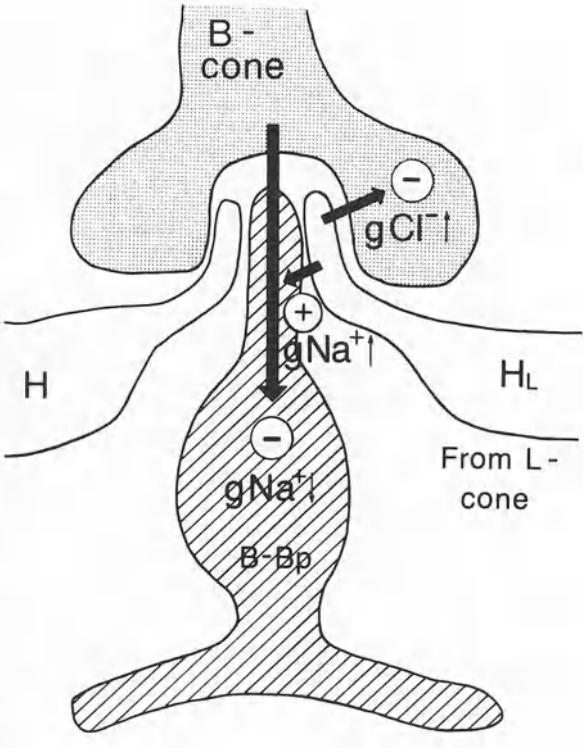

Fig. 4.9. Two possibilities of modulating the blue-sensitive (*B*) cone's signal (*thick vertical arrow*) via a horizontal cell (H_L), driven by long-wavelength sensitive cones (*L*): Either the B-cone's membrane is hyperpolarized (Θ), probably via chloride channels (g_{Cl^-}) or the blue cone's invaginating bipolar cell (*B-Bp*) is depolarized (Θ), probably via sodium channels (g_{Na^+}). Flat bipolar cells are left out in this scheme, since blue-sensitive cones apparently do not feed off-channels (see Sect. 3.3). For further details see text.

ced in the b-wave and much less in the a-wave of the electroretinogram; since the a-wave is thought to be generated in the receptor layer, this could indicate that the outer segments are only little affected by the horizontal cell feedback loop. However, Valeton and van Norren (1979b) could not determine the *amplitude* of the negative receptor potentials which generate the a-wave of the ERG; they used the slope of the very initial decay of the a-wave deflection to determine changes in sensitivity after the offset of yellow adaptation; it can be strongly assumed that the feedback loop does not affect the slope of the a-wave deflection which is mainly determined by the test lights' effect on Na^+-channels; however, the feedback loop proposed here does not act on Na^+-channels. Valeton and van Norren's (1979b) experiments therefore cannot exclude that the feedback loop acts on the *amplitude* of the receptor potential. Figure 1 of their (1979b) paper shows a local ERG (LERG) response with the amplitude of the plateau (after the b-wave) being unchanged during and after offset of yellow adapting light. According to the component analysis of the ERG (see e.g. Granit 1947) the plateau of Valeton and van Norren's LERG is the sum of the positive-going receptor potential[6] and the negative-going b-wave, together with a constant potential (PI); the b-wave "was virtually abolished" in their short-wavelength responses after the offset of yellow adapting light; keeping the amplitude of the plateau constant requires a *decrease* of the *amplitude* of the positive-going receptor potential after the offset of yellow light. Consequently, these ERG-recordings can even support a feedback effect of the L-cones on the B-cone receptors themselves, even though the time course of the potential has not changed. Moreover, the ERG – even locally recorded – sums the responses of many thousands of receptors. Due to the paucity of blue cones (see below) their responses can be greatly overlaid by the numerically dominant L-cone responses. This makes it very difficult to prove by ERG recordings to which extent the sensitivity of the B-cone's segment is affected by the feedback-loop. The comparison of a receptor potential's *slope* with a b-wave *amplitude* in Valeton and van Norren's (1979b) analysis raises an additional problem with respect to the L-cone mechanisms involved. Their spectral sensitivity functions obtained during yellow adaptation show the spectrum of a green cone in the b-wave and the spectrum of a red cone shoulder (in the V_λ-function) in the receptor potential; this could indicate that two *different* interaction pathways are involved in both potentials (B/L and R/G), which would render a direct comparison rather problematic. In any case, the interaction proposed here most probably takes place in the first stage rather locally in the blue cone's pedicle and thereby – strictly speaking – still in the receptor layer, without being ne-

6 The polarity of the ERG is reversed intraretinally

cessarily reflected extensively in the ERG a-wave. Therefore, on the basis of ERG recordings, the question regarding the exact site of the interaction of the long-wavelength horizontal cell with the B-cone channel cannot be solved easily. It should, however, be pointed out that the model presented here would work as well if the feedback interaction occurred directly between the horizontal cell and the on-center bipolar cell, fed by blue-sensitive cones; only a sign reversal would be necessary, since the bipolar cells' membrane potential would be simply a mirror image of the potentials attributed to the B-cone membrane in Figs. 4.7 and 4.8. The differences between both modes will be discussed in the following.

Hyperpolarizing Versus Depolarizing Transmitter in the Feedback-Loop. Figure 4.9 gives a closer look at the information processing in the cone pedicle. From the investigations of Nelson (1973), Toyoda and Tonosaki (1978) and Saito et al. (1979) it is known that illumination of cones in vertebrates increases the conductance of depolarizing on-center bipolar cells, most probably for sodium (see Section 1.2 for an extensive review on bipolar cells). Consequently, the cone-bipolar cell connection in Fig. 4.9 would rest on a hyperpolarizing transmitter, decreasing Na^+-conductance (Θ, $g_{Na}+ \downarrow$). When illuminated, the cone hyperpolarizes and stops the hyperpolarizing transmitter, so that the on-center bipolar cell depolarizes. As summarized by Grüsser (1979, 1981) in a model for cat retina, several ways are conceivable by which horizontal cells might interact with the signal transmission between receptors and bipolar cells: first, a feedback mechanism from horizontal cells to the receptor membrane within the triad (see Dowling 1979); second, synaptic interaction between horizontal cell dendrites and bipolar cell dendrites outside the triade via conventional chemical synapses or nonconventional synapses (Fisher and Boycott 1974, Kolb 1977). The biochemical mechanisms of these interactions are not yet known (see Grüsser 1979 for several "orthodox" and "unorthodox" possibilities). In Fig. 4.9 several modes of interaction are proposed which would be consistent with the above model's function. Since a powerful "off-pathway", fed by blue sensitive cones, is not present in the retina of primates, only an invaginating on-bipolar cell is considered in Fig. 4.9.

The reasoning is as follows: any action of the feedback loop described above which hyperpolarizes the blue cones' invaginating bipolar cell decreases its conductance; consequently the bipolar cell responds to the B-cone stimulation with a larger change in membrane potential then it did before the activation of the feedback loop, i.e., sensitization of the bipolar cell to B-cone signals is accomplished by its hyperpolarization via the horizontal cell feedback loop. Consequently, two ways of sensitization can be imagined in Fig. 4.9: the hyperpolarization of the horizontal cell produced

by illumination of the L-cone either stops a hyperpolarizing transmitter ($\ominus$) which acts on the Cl^- or K^+-conductivity of the subsynaptic B-cone membrane (see Section 4.4.2); or it stops a depolarizing transmitter ($\oplus$) which acts on the Na^+-conductance of the subsynaptic bipolar cell membrane. According to model II (Fig. 4.8) the transient desensitization at the offset of the yellow light is produced by transient depolarization in the L-cone and its horizontal cell. Moreover this penomenon can be produced in *both* pathways shown in Fig. 4.9, with respect to the polarity in just the opposite way described for sensitization. However, since GABA (acting at Cl^--channels) seems to be involved in the feedback loop (Schuurmans and Zrenner 1981b, 1982), the first solution ($\ominus$ transmitter) seems to be the more appropriate one (see above). It also became evident from the experiments of Lasansky (1981), that a change in the cone membrane's chloride conductance mediates surround responses. Details and further references were given in Section 4.4.2.

It should be noted that both solutions are very similar. In both cases a conductance decrease is necessary for the transient desensitization; it is achieved either at the receptor by a sign inverting synapse or at the bipolar cell by a sign conserving synapse. This differentiation is therefore minor, compared to the test of the general validity of such a feedback model.

4.4.4 Testing the Feedback Model

A Membrane Circuitry. To test this general model an *equivalent circuit* of the blue cone receptor's membrane was developed in accordance with Hodgkin's concept (1964); the model's function was simulated by means of a PDP MINC 11/23 computer. The blue-sensitive receptor in Fig. 4.10 is represented by several components:

1. The battery E_{Na}, representing the sodium ion concentration gradient, produces an inward current i_i.
2. A pair of resistors (R_{Na}) modulates the conductance g_{Na}. The conductance is high in the dark (smaller resistor $R_{Na\ dark}$) and low when the blue test light is switched on (larger resistor $R_{Na\ blue}$); i.e., switching from resistor $R_{Na\ dark}$ to $R_{Na\ blue}$ in this circuit represents stimulation by blue test lights.
3. The battery E_K represents the potassium ion concentration gradient which produces an outward current i_o.
4. A variable resistor $R_{K\ yellow}$ modulates the conductance g_K via the long-wavelength sensitive cone and its horizontal cell. The conductance g_K is high when the yellow light is off and decreases with the strength of the yellow adapting light.

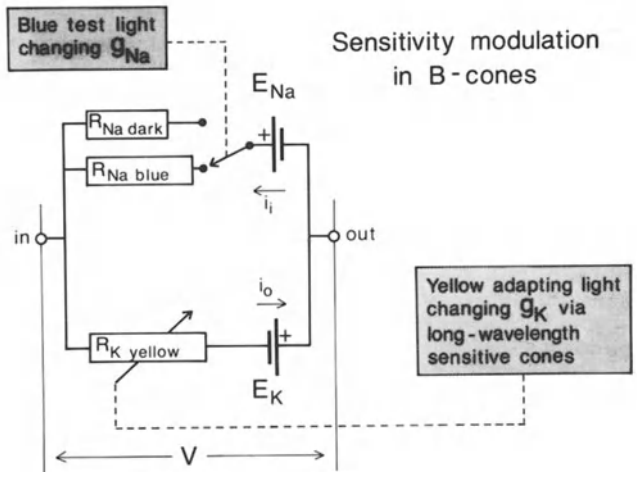

Fig. 4.10. General electrical circuit of a cell membrane (here: a blue-sensitive cone). The receptor's membrane potential (V) is modulated either by blue test lights, increasing the sodium resistance (R_{Na}), or by neighboring long-wavelength sensitive cones, changing the potassium (R_K) or chloride resistance via a horizontal cell (*lower hatched line*). The switch indicates the transition to a larger sodium resistance, when a blue test light of *fixed* irradiance is switched on. The switch represents two discrete positions of the potentiometer usually utilized in such circuits. (Zrenner 1982a)

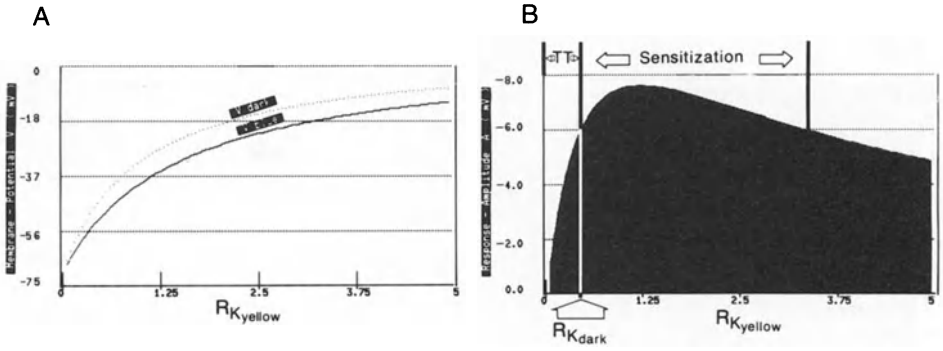

Fig. 4.11. A Membrane potential (V, *ordinate*) produced in the circuit (shown in Fig. 4.10) over a larger physiological range of changes in potassium resistance (R_K) caused by yellow adapting light. V is always less negative in the dark (V_{dark}, *dotted line*) than during illumination with blue test flashes (V_{blue}, *solid line*). **B** The difference between V_{dark} and V_{blue} is the response amplitude A (black). In the dark-adapted state ($R_{K\ dark} = 0.5$). the presentation of a weak blue test light which increases R_{Na} for 50% results in a change in membrane potential of -6 mV. Yellow light adaptation sensitizes the blue cone over a certain range (sensitization), while offset of the yellow light in this model causes a transient rebound of R_K towards zero, causing transient tritanopia (*TT*). For further explanation see text

The blue cone's response amplitude A produced by the blue test light under several conditions of yellow adaptation is the difference between the blue cone's membrane potential in the dark and during the onset of blue light:

$$A = V_{blue} - V_{dark} \tag{1}$$

Application of Ohm's law yields the following formula:

$$A = (E_{Na} + E_K)\left(\frac{R_{K\ yellow}}{R_{Na\ blue} + R_{K\ yellow}} - \frac{R_{K\ yellow}}{R_{Na\ dark} + R_{K\ yellow}}\right) \tag{2}$$

(for the deduction see Zrenner 1982a).

This formula show that the absolute value of A does not depend on the *absolute* values of $R_{K\ yellow}$, $R_{Na\ dark}$ and $R_{Na\ blue}$, but only on their relative proportion.

The values used in the model were therefore chosen as follows: E_{Na} = 5 mV; E_K = 70 mV (the polarity is respected by reversing the battery); $R_{Na\ dark}$ = 1; $R_{Na\ blue}$ = 1.5 (has to be larger than $R_{Na\ dark}$); $R_{K\ dark}$ = 0.5 (>0, due to the leakage); $R_{K\ yellow}$ = varying from 0.05 to 5. For a consideration of these values and their extremes, see Zrenner 1982a).

Computer Simulation of the Model. Increasing $R_{K\ yellow}$ in formula (2) from 0.05 to 5 by steps of 0.05 reveals the membrane potentials (V) shown in Fig. 4.11, left. As $R_{K\ yellow}$ increases, V becomes less negative, as it is well known in the course of light adaptation (see, e.g., Baylor et al. 1974). In the dark, -V is smaller than in the presence of blue light (i.e., $-V_{dark} < -V_{blue}$ in Fig. 4.11), since blue light hyperpolarizes the receptor. The difference between the two functions results in the light response A [see formula (2)], as represented in Fig. 4.11, right (*black area*). At a value of $R_{K\ yellow}$ = 1.3, i.e., in the lower range of yellow adaptation (*abscissa*), the response to blue light is larger than in the dark-adapted state ($R_{K\ yellow}$ = 0.5); this represents the sensitization, as described by Stromeyer and Madsen (1978) and Polden and Mollon (1980) in psychophysical measurements, by Zrenner and Gouras (1979c, 1981) in single retinal ganglion cells of rhesus monkey and by Schuurmans and Zrenner (1982) in retinal sum potentials. Only at higher ranges of adaptation ($R_{K\ yellow} > 3.5$) does the response amplitude decrease below its value in the dark, so that sensitization is lost. Switching off the yellow adapting light causes a transient overshoot (as described in Fig. 4.8) toward R_K = 0,

so that $R_{K\ yellow}$ can become smaller than 0.5. This produces a decrease of the response to blue light in Fig. 4.11B (TT-range), and a strong hyperpolarization in Fig. 4.11A (near 0), just as was seen in the recordings from cells where the transient desensitization was combined with high spontaneous activity. Therefore, the range of transient tritanopia (TT) is well accounted for in this model.

It should be kept in mind that the explicit modeling on the receptor site itself served only as an *example* of how such an ionic model could work. The general design of this model, as tested by computer simulation, will provide a rather simple and plausible explanation of several complex features of the blue cone's sensitivity modulation by longer-wavelength-sensitive cones on the basis of a single cellular connection, whatever polarity and transmitter substances or morphological substrates the interconnections are working with.

4.5 Résumé: What is Special About the Blue Cone Mechanism?

In order to explain this model's implications, some additional facts regarding the blue cone mechanism will be given. It certainly has some properties which differ greatly from those of the red- and green-sensitive cone mechanism; in some respects, blue cones have more properties in common with rods (Zrenner and Gouras 1979a, Gouras and Zrenner 1979b) than with other cones. A list of these properties is given in Fig. 4.12, taking into consideration additional aspects obtained in experiments with other mammals.

4.5.1 Properties of the B-Cone System: Summary

The data of Marc and Sperling (1977) give direct evidence that the B-cones, like rods, are located mainly in the perifovea, while R- and G-cones are most common in the fovea. De Monasterio et al. (1981) injected procion yellow into the vitreous body and found a population of stained cones, which they hypothetically consider to be blue cones on the basis of their retinal distribution; proof of this hypothesis is difficult. Psychophysical experiments, which were set up to stimulate individual blue cones, revealed that they are spaced roughly 10' of arc apart (Williams et al. 1981).

Considering the blue-sensitive system's circuitry, the data of Kolb and Famiglietti (1976) and Nelson et al. (1976) suggest that rods have only one type of bipolar cell with a peculiar amacrine cell (A II-type) acting as a

mediator, while the long-wavelength cones certainly have two types of bipolar cells, the invaginating and the flat type, providing on- and off-center pathways, respectively (see Chap. 3.6). It might well be that B-cones utilize a circuit more similar to that of rods than of cones (Zrenner and Gouras 1979a), as summarized in Fig. 4.12.

Psychophysical studies have well established the B-cone's low spatial and temporal resolution (Brindley et al. 1966, Green 1968, 1969, 1972; for further references see Chaps. 3.3, 4.1, 5, and 6.4), its larger Weber fraction (Stiles 1959, Mollon and Polden 1977a), its small field tritanopia (König 1903, Willmer 1949a,b, Wald 1967, Ingling et al. 1970), its tachistoscopic and neonatal tritanopia (see Mollon 1982) its slower course of dark adaptation (Auerbach and Wald 1954); in respect to transient tritanopia see Mollon and Polden (1977b) for psychophysical data, Valeton and van Norren (1979a,b) for ERG, Schuurmans and Zrenner (1979 and 1981b) for VECP and optic nerve recordings and Zrenner and Gouras (1981) for ganglion cell recordings. Also with respect to their spectral sensitivity do blue cones act in a region closer to rods than cones.

Electrophysiological studies in several mammals have shown that the B-system's response functions become saturated at low levels of light; the responses have only small amplitudes but longer latency and are lacking an off-effect (Ksinsik 1967, Gouras 1970, Boynton and Whitten 1972, van Norren and Padmos 1973, Schuurmans and Zrenner 1979, 1981b, Zrenner and Gouras 1979a, 1980, 1981; see also Chap. 3.3); they are almost exclusively excited by short-wavelength light (Malpeli and Schiller 1978, Zrenner and Gouras 1978a, 1980, 1981, De Monasterio 1979b, Creutzfeldt et al. 1979). They might even use a different type of transmitter (Schuurmans and Zrenner 1979, 1981b). Rods, as well as blue-sensitive cones, are arranged in large receptive field structures (De Monasterio 1978b), and both produce large afterpotentials (Steinberg 1969c, Zrenner and Gouras 1981).

From clinical studies (see Jaeger and Grützner 1963, Kalmus 1965, Marré 1970, Pokorny et al. 1979b, Zrenner 1982b), its high vulnerability to retinal diseases and its genetic determination, different from red and green cones, is well established. A drug which selectively affects the blue-sensitive cone mechanism will be presented in Section 6.4.3.2 (see also Zrenner 1982a and Zrenner et al. 1982b).

Blue cones also contribute to the perception of "violet". In this case too, the signal of longer wavelength sensitive cones must be combined with that of blue sensitive cones. Electrophysiological data from retinal ganglion cells (De Monasterio and Gouras 1977) also point to the R-cones' action through the β-band of their pigment absorption curve. Very short wavelength lights would therefore stimulate not only the B-cone, but also the R-cone through its β-band, leaving the G-cone untouched. However, it is un-

clear in what stages of the visual system the R- and B-cone signals are fed together to produce the sensation of "violet"; for models which attempt to account for the sensation "violet", see Ingling (1977), Ingling et al. (1978) and Paulus and Scheibner (1980).

On the other hand, the blue cone mechanism's sensitivity increases toward the extrafoveal region (Wooten et al. 1975, Stabell U. and Stabell B. 1980a), suggesting a variation of the strength of the above described feedback mechanism with retinal eccentricity up to a certain distance from the fovea (17°, according to Stabell and Stabell 1981), while changes in the far periphery seem to be minor (Stabell B. and Stabell U. 1980, 1981). The data of Buck and Makous (1981) on rod/cone interaction provide some clue that a similar feedback mechanism could be acting between rods and cones. Psychophysical studies indicated that rods and blue cones might act synergistically or antagonistically (Willmer 1961, Trezona 1970, 1976).

We are beginning to obtain considerable information about the blue-sensitive cone system in mammalian retina, its anatomy, its psychophysical data, its electrophysiology in the ERG, as well as at the level of single neurons; in genetics, many questions are still left open. The general picture which emerges is one of a relatively unique subsystem of photoreceptors, having many rod-like properties (see Fig. 4.12); nevertheless, it is made up of cones which probably are connected in a special way (Gouras and Zrenner 1981b) with only a small fraction of second- or higher-order retinal neurons. The seemingly paradox phenomena found in ganglion cells subserved by this mechanism have indicated unusual interactions between B-cones and L-cones. This particular point deserves some special comments in the following section.

4.5.2 The New Model of Cone-Interactions: Its Implications

Linearity. In the blue-sensitive ganglion cells shown here, an inhibitory signal, i.e., the decrease of the ganglion cell's spontaneous activity is provoked by stimulation of the L-cones. Since this inhibition is accompanied by an enhancement of the excitatory signal produced by the B-cones, the simple model (Fig. 3.1) of linear summation of inhibitory and excitatory signals in a ganglion cell, based on the work of Enroth-Cugell and Pinto (1972a) cannot easily account for the data obtained from B/L-opponent ganglion cells. By common consent (for recent review see Kaneko 1979), excitatory and inhibitory signals do not *directly* converge onto a ganglion cell (as schematically drawn in Fig. 3.1) but are combined and recombined in several stages in the outer and inner plexiform layer of the retina (see Gouras and Zrenner 1981b). While for spectrally homogeneous stimuli and

	R and G Mechanisms	B Mechanism	RODS
ANATOMY			
• Distribution	foveal	perifoveal	perifoveal
• Bipolar circuitry	two classes (on and off)	one class? (only on)	one class
PSYCHOPHYSICS			
• Spatial resolution	high	low	low
• Temporal resolution	high	low	low
• Weber fraction	low	high	high
• Wavelength sensitivity	medium	short	short
ELECTROPHYSIOLOGY			
• Response function	does not saturate	saturates	saturates
• Latencies	short	long	long
• ERG-off-effect	positive	negative	negative
• Ganglion cell response	no afterpotential	afterpotential	afterpotential
• Receptive field	small	large	large
• Vulnerability	low	high	high
GENETICS	sex-linked	autosomal?	autosomal

Fig. 4.12. Comparison of anatomical, psychophysical, electrophysiological and genetical findings in red- and green-sensitive cones, in blue-sensitive cones, and rods

spectrally equal receptors, models of linear summation of excitatory and inhibitory processes might be valid to a certain extent (see above), in color-opponent cells which are stimulated by a *pair* of colors this is obviously not the case; the two spectrally different cone mechanisms build up a circuitry which enhances the chromatic contrast of two spectrally different stimuli. That is, in B/L-cells, yellow light *increases* the gain of the excitatory B-cone's pathway for short-wavelength light via lateral long-wavelength-sensitive neurons. The inhibition of spike activity by long-wavelength light seen in these ganglion cells does not entail an active signal suppression; it is rather a side-effect of the gain-increasing shift of the resting potential in a presynaptic neuron. This side-effect is very desirable since it lowers the background noise or continuous spike activity in the B-cone channel (cf. Fig. 4.4) and thereby further sensitizes the postsynaptic neuron for any B-cone signal travelling along this channel.

This mechanism is not only present in B/L-opponent ganglion cells but also in R/G-opponent cells; in a certain range of adaptive illumination, the application of a chromatic background which inhibits a R/G-opponent cell makes the excitatory signal more prominent in R/G-opponent cells as well. Color-opponency therefore not only builds up the narrow spectral range of the various wavelength analyzers for spectrally homogeneous *singular* stimuli (see Chap. 3), but provides a direct enhancement mechanism for *two* spectrally different stimuli, especially for red/green and blue/yellow pairs, projected onto the receptive field of these cells. There is also psychophysi-

cal evidence (Reeves 1981b) for a feedback between the two long-wavelength-sensitive cones.

How is Color Contrast Enhanced by the Model? The mechanism described by the model can serve to enhance simultaneous color contrast. Since Leonardo da Vinci, and especially since Goethe (see Matthaei 1971), simultaneous color contrast has fascinated many scientists (see Oehler and Spillmann 1981). Schober (1964, p 328) nicely presents a well-known example of simultaneous color contrast: a grey field, when surrounded by a yellow ring, appears dark blue. The retinal mechanisms shown here can support this phenomenon: in a homogeneous grey field, red and/or green cones steadily inhibit the blue cones' signal (Fig. 4.8A). This inhibition weakens when the surrounding yellow field is projected onto the neighboring L-cones (Fig. 4.8.B). The increase in strength of the blue cone signal certainly also causes the *color* contrast to increase and the grey field to appear blue, especially at the borders. Note that the grey center field simultaneously appears *darker*, indicating that both color and luminance contrast are enhanced. The enhancement of luminance contrast in the very same field might be caused by the reciprocal action (see Jung 1973) of on- and off-center cells along the bright (yellow) and dark (grey) borders, as described by Baumgartner and Hakas (1962) and Eysel and Grüsser (1971). The fact that a field, which by the action of contrast mechanisms appears more bluish, simultaneously appears darker, points once more to a circuit in which the B-cones do not feed into a luminance channel (see Guth et al. 1969). This can be understood in light of the fact that the B-cone system obviously does not build up inhibitory fields (Chap. 3.3) necessary for such a mechanism of luminance contrast enhancement. Consequently, the lack of a powerful off-center cell system does not render the blue cone mechanism very well suited for detecting brightness borders. This is also in accordance with a series of psychophysical models (e.g., Ingling et al. 1977, Boynton 1978, see also Chap. 4.1). However, chromatic borders, i.e., the boundary between two areas, one of which reflects more short-wavelength, and the other more long-wavelength light, would be greatly enhanced by such a mechanism; it would enable the visual system to utilize also small differences in spectral composition for the detection of objects.

The Model's Possible Relation to Tritanopic Phenomena. The insensitivity of the B-cones produced by a permanent inhibition induced by L-cones in the dark-adapted state or in presence of large, neutral grey fields may explain the type of *small field tritanopia* which is not due to the scarcity of B-cones (Ingling et al. 1970). Moreover, in the model presented here, the phenomenon of *transient tritanopia* is due mainly to a rebound effect

caused by the termination of the L-cones' inhibitory action on the spontaneous activity. The postinhibitory excitation seen in blue-sensitive ganglion cells when a yellow adapting light has been switched off masks the B-cone's excitatory signal. Masking, however, cannot be the only explanation, since it is accompanied by a *real* decrease of the B-cone's signal as observed in the ganglion cells (see Figs. 4.5 and 4.6). In the model presented here, this is explained by the shift of the B-cone's equilibrium toward its potassium potential (Fig. 4.8C) simultaneously caused by the rebound depolarization of the L-cone.

Interestingly, in patients who possess only blue-sensitive cones (blue cone monochromats), the insensitivity to blue test lights after the offset of yellow adapting light is lacking, as observed psychophysically by Hansen et al. (1978); this finding provides strong evidence that the blue cone mechanism's sensitivity is controlled by longer-wavelength-sensitive cones.

The two-stage adaptation model of Pugh and Mollon (1979, see above) in many ways fits the electrophysiological model presented here: According to their hypothesis, the first site of adaptation is in the receptors themselves; in the model, this would most probably correspond to a modulation of Na^+ conductivity, as will be shown in Fig. 6.23. The second site is believed to be in the retina proximal to the receptors; it is thought to involve a yellow-blue opponent mechanism, as provided here by the horizontal cell feedback. They suggest that the sensitivity at the second site depends on the balance of the blue and yellow signals; in the model presented here, depolarization of the blue cone by the L-cone changes the B-cone's sensitivity accordingly. To account for transient tritanopia, Pugh and Mollon (1979) suggest a restoring force which counteracts this polarization, producing a transient polarization in the opposite direction. In the model presented here, this correlates to the transient strong hyperpolarization of the B-cone membrane after the offset of yellow light. The limitations of the model and alternative solutions were discussed in Chapter 4.4.3.

4.5.3 Comments on the Retino-Cortical Pathway of the B-Cone Mechanism

The "Yellow" Signal. It should be noted that the detection of *color* itself must depend on a comparison across color borders in higher-order neurons (see Gouras and Zrenner 1981b); as pointed out in Chapter 3.8, it seems reasonable to assume that only the excitatory signal carries the relevant information; since the L-cones act exclusively inhibitorily on B/L cells, there is no yellow excitatory signal originating from ganglion cells with input from blue-sensitive cones. The classical term "blue/yellow" opponent is there-

fore somewhat misleading for retinal ganglion cells; whatever excitatory signal is carrying the information for yellow, it is not antagonized by the blue-sensitive cones, at least not in the retina and probably not in the geniculate. The signal for yellow must be carried along the pathway of red/green opponent cells and probably be combined at later stages of the visual system to form a blue/yellow opponent channel.

Applying the Westheimer Paradigm. A preliminary model of the blue cone mechanism's retinocortical pathway is shown in Fig. 4.13, based on psychophysical investigations in man (Schuurmans et al. 1981) using Westheimer's (1965) paradigm. The Westheimer paradigm is marked by a threshold increase in response to a small centered test stimulus, when a background light of increasing diameter intrudes upon the surround of receptive or perceptive fields; this psychophysical method permits the estimation of perceptive field size in man (see Ransom-Hogg and Spillmann 1980). In the experiments of Schuurmans et al. (1981) it was ensured with Stile's increment threshold technique that in presence of a steady yellow surround light (μ_1 = 577 nm and 10^4 td; 5° in diameter at 7.5° ret. ecc.) the B-cone mechanism determines the threshold for a blue test light (λ = 454 nm; 0.15° in diameter), presented concentrically every 1.5 s for 40 ms, whereas the L-cone mechanism determined the threshold for a red test light (621 nm, 0.15° in diameter). In accordance with the Westheimer paradigm, the addition of a second steady red background light (μ_2 = 630 nm and 10^5 td) of variable diameter (0.18° to 5.0°) caused the L-cone mechanism's

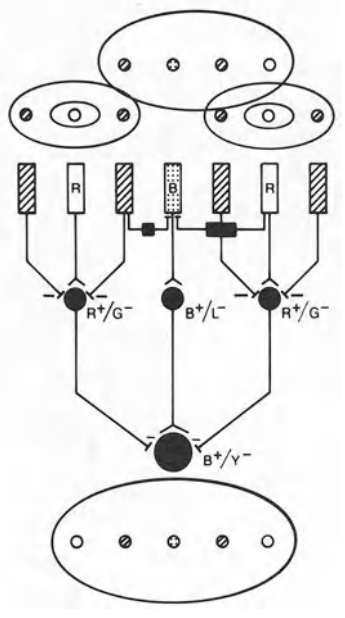

Receptive Field

Receptors
Horizontal cell
Ganglion cell
Retina

Visual cortex

Perceptive Field

Fig. 4.13. A preliminary model of the blue cone mechanism's retino-cortical pathway, based on experiments employing the Westheimer paradigm. For further explanation see text. (Schuurmans and Zrenner, 1983, in prep.)

threshold first to increase (over 2.0 log units, max. at 0.35°) and then to decrease. Paradoxically, the same background (μ_2) caused the B-cone mechanism also to follow Westheimer's paradigm (max. at 0.65°), although the B-cones could not have been directly stimulated by μ_2. This indicates that the spatial effect induced by the 630 nm background (μ_2) onto the B-cone mechanism could have acted only through the L-cone mechanism. The *increase* of the B-cones' threshold by long-wavelength light is not likely to result from a *retinal* interaction between the B- and L-cone mechanisms, since adaptation of the coextensive B-cone receptive field in primates by long-wavelength light will decrease the spontaneous activity and simultaneously *decrease* and not increase the threshold of the B-cone responses to a 454 nm test light (see Fig. 4.8).

The sensitivity increase observed with increasing background diameter can be explained by a mechanism which "inhibits the inhibition" of the long-wavelength-sensitive cones. The model in Fig. 4.13 shows one mode of projection of retinal neurons to the higher visual centers, building up a blue-sensitive perceptive field. The blue cone's output determines the excitatory input to the cortical neuron. This output is modulated already in the retina by longer-wavelength-sensitive cones via horizontal cells (see Fig. 4.8). On the other hand, increasing spatial stimulation of the receptive field (*large circle on top*) activates the R-cones which inhibit the cortical neuron via R^+/G^- ganglion cells. This explains the first part of the Westheimer paradigm, namely the initial sensitivity decrease observed with increasing field sizes. The subsequent sensitivity increase observed with field sizes larger than 0.65° can be explained if the inhibition provided by the R-cone on the cortical neuron is weakened, due to activation of the inhibiting surround of its own retinal receptive field structure (*concentric circles at top*), so that stimulation of the outermost G-cones disinhibits the R-cone. This disinhibition can provide the sensitivity increase of the Westheimer paradigm, observed with large background fields.

A series of control experiments with various wavelengths of μ_2 was performed in normal trichromats and dichromats which provided successful tests of this preliminary model (Schuurmans and Zrenner 1983); no incompatible objections were found, yet.

The psychophysical data obtained by applying the Westheimer paradigm also point to a control of the B-cone mechanism's threshold by the L-cone, occurring, however, only if the Westheimer paradigm has been completely realized in the red/green antagonistic mechanism, as shown in Fig. 4.13. Consequently, besides a mechanism which controls the blue cone's sensitivity at the retinal level (see Sect. 4.4), there must exist additional interactions between the B- and L-cone mechanism at a *higher* stage in the visual system, which generate the spatially induced Westheimer paradigm in the B-cone mechanism.

5 Temporal Properties of Color-Opponent Ganglion Cells

The data presented so far were obtained with flashes of relatively long duration (200 ms) and low frequency (~1 c/s) so that the cell's responses to each flash could be studied individually. Under physiological conditions, as for instance in a freely moving eye, a picture rapidly moves over the retina; consequently, a cell is usually stimulated by a series of different light stimuli of brief duration, occurring in rapid succession. In order to understand the action of retinal neurons under these physiological conditions, it is necessary to study the cell's responses to simple consecutive stimuli such as flicker, and to flashes of various duration. Since spectrally and thus functionally different receptors forming the center and surround of the receptive field are influencing the responses of opponent ganglion cells, one cannot exclude temporal interferences of the center and the surround mechanism, caused by repetitive stimulation; the stimulus duration, which determines the on- and offset of light is expected to influence the interaction between cone mechanisms, since excitation of center and surround occurs at light on- or offset, respectively. One can also imagine that cells respond quite differently to repetitive stimulation, depending whether center and surround are acting in a spectrally antagonistic or synergistic manner. The experiments outlined in Section 5.1 provide some answers to such questions.

Flicker Stimulation. There are psychophysical data which suggest various modes of flicker processing in the nervous system. Humans perceive flicker whenever there is a repetitive change of sufficient magnitude in either the luminance or the chromaticity of light. Pure chromatic flicker, which is a change in spectral composition but not in luminance, is more effective at *low* frequencies than pure luminous flicker, in which the luminance changes but not the hue. At *high* frequencies, however, the opposite is true, as it was well established by the psychophysical studies of De Lange (1958) and more recently by Kelly and van Norren (1977). The neurophysiological basis for these differences is still unknown, but is currently a subject of lively discussion (see Ingling 1978, King-Smith and Carden 1978, also Chap. 6.4). The psychophysical data obtained from human observers with luminous and chromatic flicker differ considerably in terms of spatial, tem-

poral, and spectral parameters; the psychophysical experiments of Cavonius and Estévez (1975) revealed that a cone mechanism's supersensitivity depends also on the level of adaptation. Because of these differences it is often suggested (e.g., by King-Smith 1975, King-Smith and Carden 1976, Kelly and van Norren 1977, Kranda and King-Smith 1979, Bowen and Nissen 1979, Hemminger and Mahler 1980), but not unequivocally accepted (Ingling and Drum 1973, Ingling 1978, Stromeyer et al. 1978, Foster 1981), that two functionally or anatomically different pathways (channels or classes of neurons) are responsible for the processing of chromatic and luminous flicker: one, receiving *antagonistic* signals from spectrally different cone mechanisms (i.e., the color-opponent *tonic* cells); the other, receiving apparently *synergistic* signals from spectrally different cone mechanisms (i.e., the achromatic, spectrally non-opponent *phasic* cells).

Testing the "Channel" Hypothesis. Electrophysiologically, the validity of such a hypothesis can be examined by determing how flickering stimuli are processed in *single* color-opponent as well as in the spectrally non-opponent cells of the primate retina. Therefore in each cell which could be held long enough, (following the procedure shown in Fig. 3.14) experiments with different flicker rates were performed, with the dark/light ratio of stimulation held constant. The results showed, however, that the same color-opponent cells which enhance chromatic more than luminous flicker at *low* frequencies enhance luminous more than chromatic flicker at *high* frequencies, changing their behavior from antagonistic to synergistic (Zrenner and Gouras 1978a,b, Gouras and Zrenner 1979a); thus, there is no need to invoke two separate neural systems to explain the differences between chromatic and luminous flicker. Indeed, color-opponent cells can process both types of stimulation in the way described also by psychophysical data, as will be shown in the following sections.

5.1 Critical Flicker Frequencies (CFF) in Tonic and Phasic Ganglion Cells

The critical flicker frequency (flicker fusion) is reached when repetitive stimuli can no longer be resolved in time, so that they essentially resemble a steady field. Fusion frequencies in ganglion cells were found by observing a cell's responses to flickering stimuli on a storage oscilloscope; fusion was defined as having occurred whenever discrete responses, time-locked to the frequency of the stimuli, could no longer be seen after responses had been superimposed 10-20 times.

Figure 5.1 shows the CFF as obtained with stimuli of different irradiance in retinal ganglion cells.

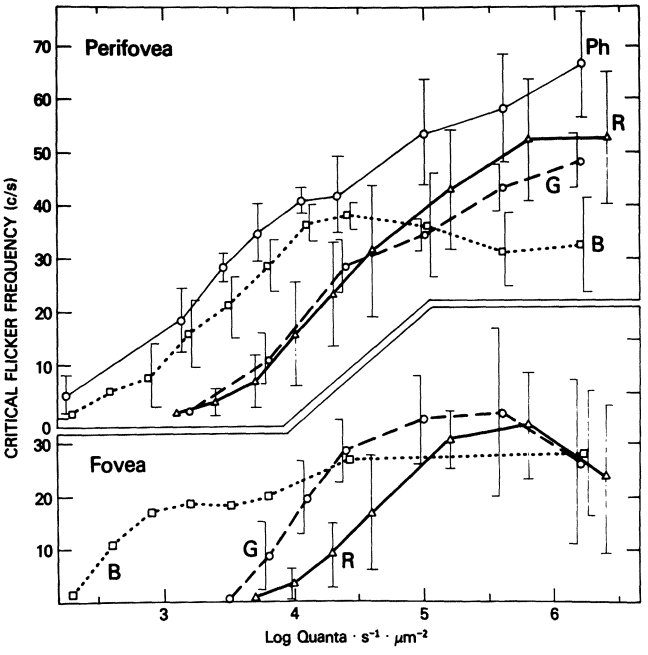

Fig. 5.1. The critical flicker frequency is plotted against the quantal energy necessary to produce fusion of the responses of retinal ganglion cells (mean values and S.D.). The center of tonic color-opponent cells (*R*, *G*, *B*) was stimulated with the adequate wavelength, 622 nm, 530 nm, and 456 nm, respectively. To avoid participation of other cone types, the wavelength of the test light was chosen so that color-opponent cells were stimulated at the margins of their spectral sensitivity function, if possible. The data for spectrally non-opponent phasic cells (*Ph*) are indicated by a *thin solid line* (test light λ = 560 nm). All data were obtained in presence of a white adapting light of 30,000 td, except for the blue-sensitive ganglion cells (*B*), which were adapted with yellow lights of 30,000 td to obtain maximal responses. Presented in part by Zrenner and Gouras (1981) (see Chap. 4)

The wavelengths used for stimulation of color-opponent cells were selected so that only the cell's receptive field center was stimulated; the spectral sensitivity of the center mechanism (R, G, B) was determined in each individual cell before repetitive stimuli were applied. Phasic cells were stimulated at the spectral point of the lowest threshold with 560 nm test lights, which explains the shift of these cells' CFF-function to the *left* in Figure 5.1.

All recordings except those from blue sensitive cells were performed in the photopic range in presence of a white adapting light. The appropriate adapting light for isolating the center of blue cone driven cells (*dotted line*), however, was yellow light as described in Chapter 4.2, i.e., light which avoids saturating responses of the blue-sensitive cone system and enhances the responsiveness. A yellow background shifts the dotted line in

Figure 5.1 to the left, so that under these conditions the functions cannot be compared in terms of absolute, but only of relative thresholds.

As seen in the *upper half* of Figure 5.1, the flicker fusion frequency of all cells generally increased with the intensity of light stimulation as shown by Enroth (1952), Dodt and Enroth (1954), and Dodt (1964) in retinal ganglion cells of cat, resembling the well-known Ferry-Porter relation. As outlined by Gouras and Zrenner (1979a) and Zrenner and Gouras (1978a,b, 1981) the average maximum CFF of phasic cells (N = 8) obtained at $10^{6.2}$ Quanta s^{-1} μm^{-2} was 62 ± 11 c/s (cycles per second); tonic cells with receptive field centers mediated by the red sensitive cone mechanism (R) had an average maximum flicker fusion frequency of 53 ± 13 c/s (N = 12); color-opponent cells with green-sensitive (G) receptive field center responses had slightly lower maximum fusion frequencies of 49 ± 4 c/s (N = 3); blue-sensitive cells (B) never attained fusion frequencies higher than 38 ± 2 c/s. Consequently, red- and green-sensitive color-opponent ganglion cells can follow flickering stimuli up to frequencies approaching and sometimes equalling those of cells which did not show color-opponency; in contrast, cells with input from blue-sensitive cones fuse at lower frequencies (near 30 c/s), as seen in the lower half of Figure 5.1. All these data are valid for parafoveal responses (2°-10° visual angle), since phasic cells are very rare in the foveal region.

Foveal cells (within 2° visual angle) generally reached lower maximal flicker fusion frequencies, near 30 c/s; those with red, green, and blue cone mechanisms subserving their receptive field centers attained 33 c/s (S.D. = 10; N = 5), 36 c/s (S.D. = 16; N = 6) and 29 c/s (S.D. = 9; N = 2), respectively. No flicker data could be obtained from the extremely rare foveal phasic cells.

These data indicate that flicker stimuli in foveal and parafoveal cells are processed in different ways. In the parafoveal cells, where phasic, spectrally non-opponent cells are common, color-opponent cells can similarly attain high values, an observation also made in the LGN by Kaiser et al. (1977). These findings are in accordance with psychophysical investigations describing such differences in CFF at various retinal eccentricities (Granit and Harper 1930, Hylkema 1942, Landis 1954, Lüddeke and Aulhorn 1974, Herbolzheimer 1976).

5.2 Influence of Stimulation Frequency on the Spectral Sensitivity Function: Loss of Color-Opponency at Higher Flicker Rates

With increasing flicker frequencies, color-opponent cells begin to lose their color-opponency and therefore their color selectivity (Zrenner and

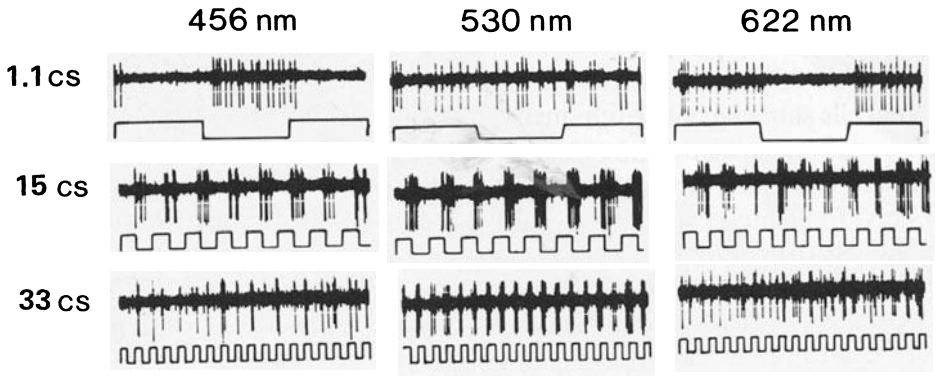

Fig. 5.2. Spectral responses of a red/green color-opponent cell (R^+/G^-). Extracellular recording from a parafoveal ganglion cell at 3 different flicker frequencies (1.1, 15, and 33 c/s), stimulated with $10^{4.8}$ Quanta s^{-1} μm^{-2} (Ganzfeld) at 3 wavelengths (456, 530, and 622 nm) on a white background of 30,000 td. At medium and high frequencies, three oscillographic records are superimposed. The response of a photocell to the light stimulus is shown below each response. Upward deflection indicates onset of light. (Gouras and Zrenner 1979a, as reported by Zrenner and Gouras 1978a,b)

Gouras 1978a,b, Gouras and Zrenner 1979a) as outlined in the following.

The General Response Pattern

Figure 5.2 illustrates the responses of a color-opponent ganglion cell with a red-sensitive on-center (R^+) and a green-sensitive off-surround (G^-) at three different wavelengths and three different flicker rates on a white background. At low frequencies (*upper row*), when the light stimulus goes on, the cell is *excited* by long wavelengths (622 nm) but inhibited by short wavelengths (456 nm). The opposite pattern emerges when the light goes off, i.e., inhibition occurs at 622 nm and excitation at 456 nm. Consequently, center and surround responses are almost 180° out of phase. Mid-spectral light (530 nm) is practically ineffective in producing light-modulated responses, since it stimulates the opposing cone mechanisms about equally, so that phases of inhibition and excitation cancel each other out at this neutral point (see Fig. 3.1). At medium flicker rates (*center row*) the effectiveness of 530 nm stimuli surprisingly begins to increase; at high flicker rates (*bottom row*), the cell is even more capable of following the flicker stimuli when stimulated with 530 nm than with 622 nm or 456 nm light; this phenomenon occurred in all color-opponent cells which were studied, including one color-opponent cell of the B/L-group. Evidently, flicker frequency strongly affects the spectral sensitivity function of such cells. What is the underlying mechanism?

The Transition of the Action Spectra

Figure 5.3 illustrates average action spectra (cf. Chap. 3.3) of nine ganglion cells showing color-opponency between the red and the green-sensitive cone mechanism. These action spectra are based on the irradiance E required to elicit a threshold flicker response at low (1 c/s) and at high (33 c/s) frequencies at different wavelengths. At low frequencies (*triangles*), the lowest thresholds for eliciting excitatory flicker responses (*open triangles*) occur in the orange/red part (~600 nm) of the spectrum; the lowest thresholds for inhibitory responses, (i.e., responses with opposite polarity, 180° out of phase, *closed triangles* in Fig. 5.3) are found in the blue/green part (~500 nm) of the visible spectrum. The threshold for midspectral wavelengths (~555 nm) at the peak of the luminous efficiency function is very low, due to the antagonistic action of color-opponency described above. The neutral point varies among red/green-opponent cells (see Chap. 3.4) but is found

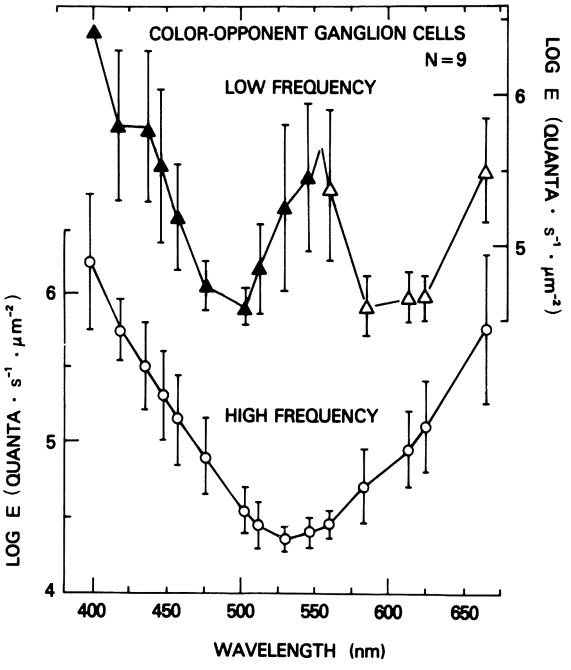

Fig. 5.3. Action spectra of nine red/green color-opponent ganglion cells (mean values ± S.D.), based on a flicker threshold criterion at low (1 c/s, *triangles*) and at high (33 c/s, *circles*) frequencies of stimulation using a white adapting light of 30,000 td. Only R/G-opponent cells with overt color-opponency were taken, i.e., cells with dominance values of 3 as described in Chap. 3.4. Curves were combined at their mean maximum sensitivity; vertical axes (absolute values) are split (*upper right*, *lower left*) to avoid overlap. (Gouras and Zrenner 1979a, as reported by Zrenner and Gouras 1978a,b)

most often within the range of 500-600 nm. At high flicker rates (*circles*), the thresholds of midspectral lights for producing flicker decrease; this spectral region becomes more effective than all others in producing a flicker response in color-opponent cells. The two-peaked action spectrum so typical of color-opponent cells (see Fig. 3.4) changed to a single-peaked, broadband spectrum, typical of spectrally non-opponent cells (Fig. 3.10 and 3.13); the cell loses its color-opponency and acts like an achromatic encoder, at least as far as its action spectrum is concerned.

The cell becomes most sensitive to mid-spectral light, as revealed by a comparison of *absolute values*; its sensitivity at the very short and at the very long wavelength branch of the spectrum decreases with higher flicker frequencies. Therefore, enhancement of the cell's responses must have occurred with higher flicker frequency exclusively in the middle range of the spectrum.

Obviously, the spectral response in a single color-opponent cell is not a constant, but a time dependent variable.

The Paradox in the Ferry-Porter Law and the Gradual Change in Spectral Sensitivity

Changes in a cell's action spectrum do not occur as a sudden jump but as a gradual transition, visible at stimulation frequencies between 1 and 33 c/s. This is shown in Figure 5.4.

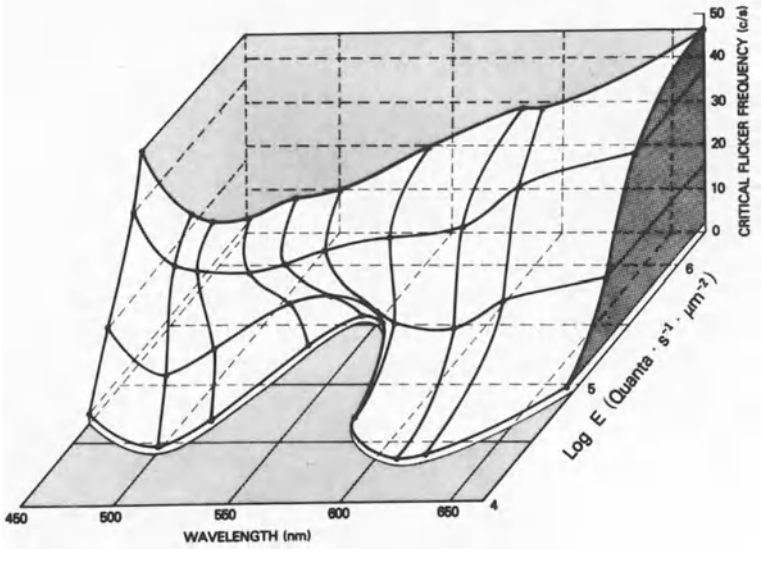

Fig. 5.4. Three-dimensional graph, relating wavelengths (nm), response thresholds (log E, Quanta s^{-1} μm^{-2}) and critical flicker frequencies (c/s) as obtained in a red/green color-opponent ganglion cell with stimuli of 20° visual angle, white adapting light of 30,000 td

In the horizontal plane of the three-dimensional graph, action spectra of a R^+/G^- color-opponent ganglion cell are shown at four different frequencies (vertical axis). At *low* flicker frequencies (2 c/s), such a color-opponent cell shows two sensitivity maxima in the blue/green and the red/orange part of its spectrum, one of which is excitatory, and the other inhibitory; in the mid-spectral region there is a broad neutral zone where the cell's sensitivity is very low. At *higher* frequencies, the spectral characteristics gradually change; the cell's sensitivity to wavelengths in the neutral zone (near 550 nm) slowly increases; at 37 c/s the action spectrum is broad and single-peaked, and color-opponency is lost. In the vertical planes, this graph also indicates that the Ferry-Porter law, according to which critical flicker fusion frequency (CFF) increases proportionally with the logarithm of stimulus intensity, does not hold near the neutral point of a color-opponent cell. Critical flicker frequency and intensity correlate as predicted only at long and short wavelengths. Near the neutral point, the threshold intensity necessary to obtain CFF first *de*creases with increasing frequencies and it is only in the higher frequency range that the expected behavior is seen.

The reason for this phenomenon appears to lie in the temporal interactions between the spectrally different center and surround mechanisms of a color-opponent cell as suggested by Figs. 5.2 and 5.3. What is the underlying mechanism which makes a color-opponent cell's two-peaked action spectrum become broadband and single-peaked?

5.3 The Basic Mechanism: Phase-Shift Between Center and Surround Responses

It can be demonstrated that the sensitivity increase in the mid-spectral region is based on a phase shift between center and surround responses of color-opponent cells. This is shown in Fig. 5.5, where the spike frequency of a color-opponent cell is represented by an analog signal. Center and surround responses of this cell (G^+/R^-) were studied separately by the use of adequate test lights in presence of a white adapting light. At lower frequencies (5.5 c/s), the excitatory and inhibitory responses generated by the center and those generated by the surround are almost 180° out of phase; the linear summation of center and surround responses, characteristic of ganglion cells (Enroth-Cugell and Pinto 1972a, Ikeda and Wright 1972, Enroth-Cugell et al. 1975) would approach zero[7] at low frequencies. The cell

7 For the limitations of this linear behavior see Rackensperger and Grüsser (1971). As already pointed out in Chapter 4.5, in color-opponent cells simple summation models hold only for spectrally homogeneous flashes as applied in these flicker experiments, not for *simultaneously* presented pairs of colors (see Chap. 4.5.2)

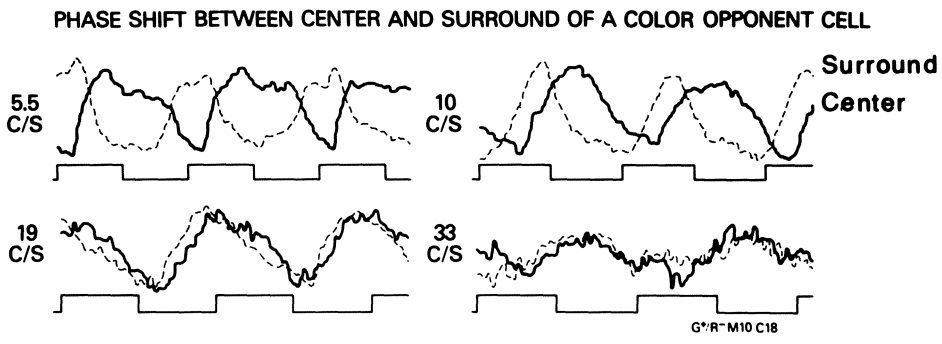

Fig. 5.5. Center (*solid line*) and surround (*broken line*) responses, isolated in a green/red-opponent ganglion cell (G^+/R^-) by the appropriate wavelength (456 and 622 nm, respectively. Irradiance E approx. $10^{5.5}$ Quanta s^{-1} μm^{-2}. White adapting light of 30,000 td). The spike frequency is converted to the analog signal. At low frequencies of stimulation (as indicated to the left of each trace), the responses of the center and surround mechanism act antagonistically, at higher frequencies they act synergistically

shows no modulated response to light when both the center and surround mechanisms are stimulated equally as seen in color-opponent cells at low frequencies when stimulated near their neutral point. At higher frequencies (10 c/s), a change of latency (or a phase shift) occurs, different for the center and surround mechanism, so that the phases of inhibition and excitation of both mechanisms begin to synchronize; near 19 c/s, this synchronization is almost perfect and the linear addition of the responses of the center and surround mechanism at the cell's output would result in a very strong flicker response. At frequencies beyond about 30 c/s, the amplitude of the response decreases, since fewer spikes are produced per stimulation period, thus weakening the flicker response.

5.4 Latency of Center and Surround Responses

In order to quantify the phase shift, the latency of the responses was measured in 21 red/green color-opponent cells at different flicker frequencies between 1 and 65 c/s (see Fig. 5.6A). This was done for the center and surround mechanism separately. In order to relate the excitatory phases of the ganglion cells to each other, the latency of the first spike occurring was measured from the onset of the stimulus, if there was an on-excitation, and from the offset of the stimulus, if there was an off-excitation (see inset Figure 5.6B and 5.6C). The latency criterion was very precise, since 6 to 20 responses were superimposed on a double beam storage oscilloscope, trig-

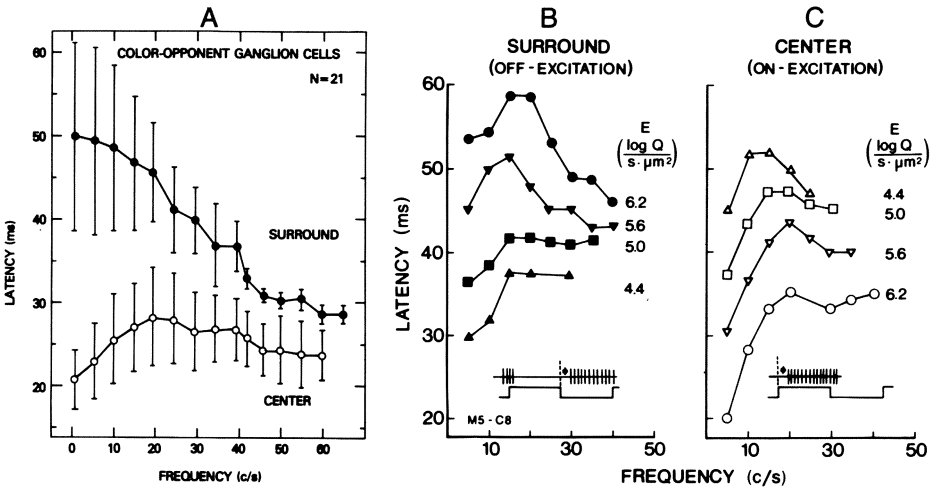

Fig. 5.6. A Averaged latencies of the excitatory response of 21 red/green color-opponent cells plotted against the frequency of stimulation for both center (*open circles*) and surround (*filled circles*) excitation. The stimulus was a 20° spot, illuminating each cell's entire receptive field; the center and surround responses were isolated by an appropriate choice of test wavelength (622 nm and 456 nm, respectively, $10^{6.2}$ Quanta s^{-1} μm^{-2}) in presence of a neutral white adapting field (30,000 td). *Vertical bars* indicate standard deviations[8]. (Gouras and Zrenner 1979a, as reported by Zrenner and Gouras 1978a,b). **B** and **C** Latencies of *surround* and *center*, respectively, recorded in a G^+/R^- cell at four different levels of irradiance E (as indicated beside each function) plotted against frequency of stimulation. The mode of latency measurements (*arrows*) is given below. Remaining conditions as in **A**

gered either by the positive or the negative flank of the test light, so that the beginning of an excitatory "block" could be measured with a precision of ± 1 ms. This provided a continuous monitor of the relationship between individual responses and the stimulus cycle. With stronger stimuli, excitation from the surround mechanism generally occurred later than from the center mechanism, regardless of whether they were on- or off-center cells. Latency differences between center and surround seem to be a common feature in the visual system, since they are observed also in non-color-opponent cells of the lateral geniculate body of the cat (Singer and Creutzfeldt 1970). Differences in latency of center and surround responses become smaller as background illumination increases, as reported in cat by Enroth-Cugell and Lennie (1975).

---

8 The standard deviation for the surround is large at low frequencies, since in some cells – depending on their action spectrum – the stimulus provided for the surround also slightly hit the center mechanism, and thereby produced some antagonistic action which bent the initial part of the curve downwards

As shown in Fig. 5.6A the latency of the center excitation in color-opponent cells is relatively short, about 20 ms at 1 c/s, and increases with frequency up to 30 ms. The latency of the surround excitation, however, is much longer, about 50 ms at 1 c/s, but decreases with frequency increase. Thus the time difference between center and surround excitation depends on the stimulus frequency, becoming progressively smaller as frequency increases. As shown in Fig. 5.6B and 5.6C, the latency values also depend on the strength of stimulation; with less intense stimuli, the functions of the surround shift downward, while those of the center shift upward. The relation given in Fig. 5.6 is therefore only valid for test stimuli of $10^{6.2}$ Quanta s^{-1} μm^{-2}. This implies that synchronization of center and surround responses strongly depends on the strength of stimulus irradiance occurring at different temporal frequencies, when the irradiance (E) is varied. At low E-values, surround *off*-excitation occurs even after shorter latencies than center *on*-excitation. However, the latency of the surround's on-*inhibition* was still longer than that of the center's on-*excitation*. Consequently there are always latency differences between center and surround responses of color-opponent cells. It is this difference in latency between center and surround responses which, at *high* frequencies, turns the cone *antagonism* (color-opponency), so characteristic of these cells at *low* frequencies, into *synergism*.

5.5 The Processing of Luminous and Chromatic Flicker

By measuring the values of the phase relation *between* the two spectrally different mechanisms of a color-opponent cell, it becomes possible to predict the interaction between its center and surround responses at any frequency for a given stimulus condition. This is exemplified in Figure 5.7 for the luminous and chromatic flicker responses of a R^+/G^- cell stimulated by a mixture of red and green light. When the red and green lights (*below and above each trace*) are completely in phase (*left side*), yellow *luminance flicker* is produced for a human observer; when they are 180° out of phase (*right side*), *chromatic flicker* is produced, i.e., the succession of a red and a green light of equal luminance. Red light excites the R^+/G^- cell of Figure 5.7 during the time of exposure, since the red cones produce excitation (ON) via the center mechanism. On the other hand, green light produces a spike frequency increment in the cell's response in between exposures (OFF), since the green-sensitive cones, when stimulated, produce inhibition via the surround mechanism, followed however, by post-inhibitory excitation. By applying the actual latencies measured in color-oppo-

nent cells to center and surround responses individually (noted below and above the *upper left-hand trace* in Fig. 5.7), it becomes evident that the excitation (*hatched blocks*) and the inhibition (*blank intervals* in between either on- or off-blocks) produced by the center and surround mechanisms cancel each other out completely. Consequently, at low frequencies, the cell generated small or no modulated responses to yellow or mid-spectral light. It becomes very obvious that this is due to the mutual cancellation of excitatory and inhibitory signals of the red-sensitive on-center and the green-sensitive off-surround in such color-opponent cells. A similar mechanism was suggested by Kelly (1973, 1975) for the low frequency attenuation found psychophysically in the temporal as well as in the spatial domain.

As flicker frequency increases (*lower left-hand trace*), the difference in latency between the responses of the center and surround mechanisms begins to turn antagonism into synergism; resonance between excitatory responses occurs, i.e., the excitatory as well as the post-inhibitory responses of both the center and surround mechanisms, respectively, are generated simultaneously. This resonance is most effective at precisely those wavelengths which produce *strong* responses from both the center and surround mechanism and consequently yield the weakest responses at low temporal frequencies. Therefore, action spectra based on flicker criteria for color-opponent cells gradually change with frequency (see Fig. 5.3); mid-spectral wavelengths, which are relatively ineffective at low flicker frequencies, become most effective at high frequencies and color-opponency is progressively lost. The broadband and single-peaked luminous efficiency function (V_λ) based on heterochromatic flicker photometry may be an inevitable result of this phenomenon, since all cells become single-peaked and broadband at higher flicker frequencies. This is also valid for the human visual system, as shown in Chapter 6.

Figure 5.7 (*right*) shows that the reverse occurs for chromatic flicker. In this case, the red and green stimuli are 180° out of phase and produce a flickering stimulus sequence that alternates only in chromatic composition but not in luminance. At *low* (1 c/s) frequencies (*upper right-hand trace*) the excitatory (ON) and the post-inhibitory (OFF) responses from the center and surround mechanism, respectively, synchronize and a strong response to flicker is generated; blocks of strong excitation follow each other in sequence, separated by pauses of strong inhibition. At *higher* frequencies (25 c/s, *lower right*), the latency differences between center and surround cause the blocks of excitation (ON) of the center mechanism and those produced by post-inhibitory excitation (OFF) of the surround to follow each other continuously. As a result, the modulated response to chromatic flicker is lost already at 25 c/s.

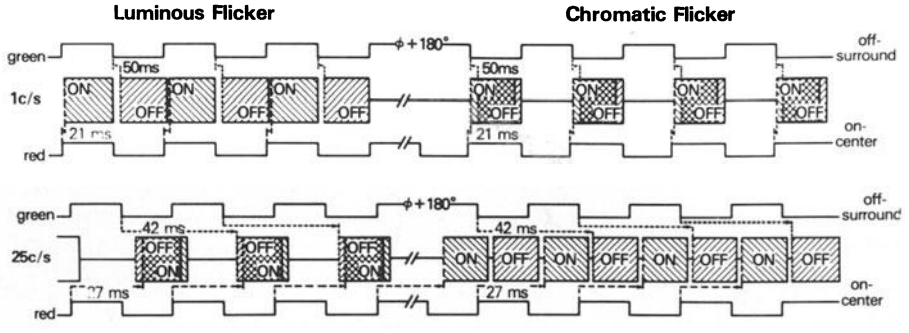

Fig. 5.7. Latencies applied for luminous (red and green light, in phase) and chromatic flicker (red and green light, 180° out of phase) for the excitatory phases (*hatched areas*) of a red ON-center, green OFF-surround cell at low (1 c/s) and high (25 c/s) rates of stimulation. The red mechanism excites the cell when the light goes on and inhibits it when the light goes off; the green mechanism acts conversely. Only the excitatory responses are illustrated. A resonance between center and surround responses occurs for chromatic flicker at low and for luminous flicker at high frequencies. (Gouras and Zrenner 1979a, as reported by Zrenner and Gouras 1978a,b)

Since the dynamics of luminous and chromatic flicker, as revealed by psychophysical investigations, can be found in an individual color-opponent ganglion cell, it is not necessary to postulate two anatomically different pathways in order to explain the differences between both ways of stimulation.

In addition, the phasic ganglion cell system may compensate for the unresponsiveness of the tonic or color-opponent system to low-frequency mid-spectral lights. Its role might be more that of an unspecific object-detection mechanism in the retinal periphery, and only to a lesser degree that of a luminance encoder (see Marr 1974); the tonic and phasic dichotomy might be nevertheless valid in the human visual system (for references see Legge 1978).

5.6 Stimulus Duration Changes the Action Spectrum

However, not only the increase in frequency of stimulation, but also the decrease of stimulus duration can cause a loss of color-opponent interactions in retinal ganglion cells. This is shown in Fig. 5.8 (*thick lines*) for a tonic ganglion cell of the R^+/G^- type. At low frequencies (1 c/s) and with a long stimulus duration (200 ms), this cell shows the typical two-peaked spectral sensitivity function with the maximum of the excitatory response near 610 nm, that of the inhibitory response near 510 nm, and with a neu-

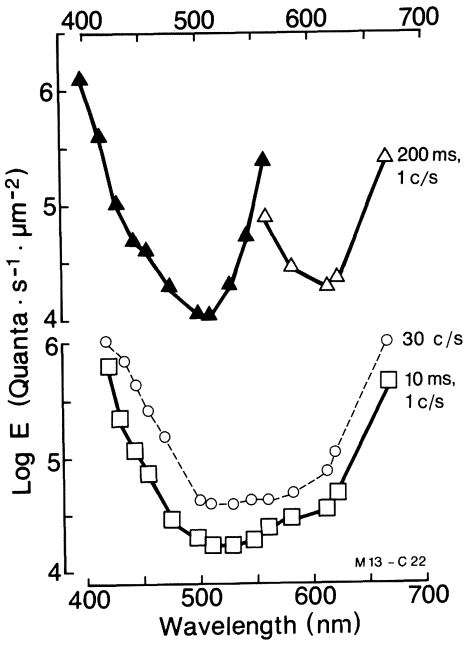

Fig. 5.8. Action spectra of a color-opponent ganglion cell (R^+/G^-), based on a spike frequency increment threshold criterion for stimuli of long (200 ms, *triangles*) and short duration (10 ms, *squares*) in presence of white adapting lights of 30,000 td. The action spectrum obtained with *flickering* stimuli in this cell (30 c/s, *broken line*) is presented for comparison

tral zone near 565 nm. As the stimulus duration is decreased (10 ms), spectral lights near the neutral point become more effective, so that the cell's action spectrum becomes broadband and approaches the CIE V_λ-function. In this respect, the data obtained by single flashes of short duration come very close to those obtained in the same cell during flicker stimulation with 30 c/s (*thin broken line* in Fig. 5.8). This experiment provides further support for the concept that it is not so much the frequency *dynamic* of the color-opponent channel acting as a *neural filter* (see Gielen 1980) which causes the loss of color-opponent interactions, but a mechanism of *synchronization*; when very short flashes are applied, the excitatory phase of the center mechanism occurs quasi-simultaneously with the post-inhibitory excitation of the surround mechanism, thereby increasing the spike frequency so that the sensitivity is enhanced especially near the neutral point. The dependence of latency on stimulus duration of single flashes is qualitatively the same for center and surround of (cat) ganglion cells (Enroth-Cugell and Pinto 1972 b).

In the human visual system, disinhibitory effects observed psychophysically in backward-masking experiments (Robinson 1966) might well be based on synchronization mechanisms of the kind described above, facilitating detection of flashes by appropriate combined sequences of stimuli. In psychophysical experiments, Stromeyer et al. (1979) noted that responses to on- and offsets of coarse spatial patterns are approximately sum-

mated; the synchronization mechanism described here in retinal ganglion cells can well account for these phenomena.

5.7 Résumé: Possible Implication of the Transition Between Antagonism and Synergism in Color-Opponent Ganglion Cells

5.7.1 Hue and Brightness Can Be Signalled via the Same Channel

As with flickering stimuli, the shortening of stimulus duration produces a transition from a double-peaked opponent spectrum into a single-peaked broadband one, usually observed in non-opponent cells. This phenomenon, described here in color-opponent ganglion cells, is found in psychophysical measurements as well (see Fig. 6.17). Its impact on the differences between hue substitution and increment measurements was pointed out by Breton (1977) and by Pokorny et al. (1979a). However, it should be emphasized again that the mechanisms observed in single color-opponent ganglion cells render it unnecessary to postulate functionally or anatomically different channels for hue and brightness as most present views try to explain these phenomena; the transition from a color-opponent hue-coder to a non-opponent brightness coder occurs in *individual* color-opponent cells, depending on the antagonistic or synergistic interaction between center and surround, which is controlled by the temporal and spatial variables of stimuli. Eisner and Mac Leod's (1981) idea that chromatic adaptation excessively suppresses signals originating in one class of cones when flicker photometry is used, but fails to do so, when increment threshold measurements are employed does not necessarily weaken the argument against channel theories. If two cone mechanisms act in an additive or synergistic manner, producing a single-peaked broadband curve, as observed in flicker studies, the suppression of one cone type's sensitivity by a weak chromatic background for a few tenths of logarithmic units is sufficient to make the other cone determine the threshold throughout the spectrum, since their sensitivity at the spectral ends is rather close; if the two cone mechanisms can act antagonistically (as in increment threshold measurements at low temporal frequencies), each cone suppresses the other's sensitivity very strongly; it is no wonder then, that the same weak background, which isolated a cone mechanism in a spectral sensitivity function determined by flicker criteria, fails to do so when an increment threshold criterion is employed which still permits a certain degree of cone antagonism.

5.7.2 Enhancement Occurs by Synergistic Action of Center and Surround

In primate color-opponent cells, chromatic flicker is the most effective stimulus at low frequencies; due to an enhancement effect at high frequencies (see Sect. 5.5), luminance flicker becomes the most effective stimulus in these cells, while pure chromatic flicker is ineffective; this was demonstrated in the retinal color-opponent neurons (Zrenner and Gouras 1978a,b, Gouras and Zrenner 1979a) as well as in those of the LGN (Gielen 1980). The enhancement of flicker by lateral inhibition may be a general property of all cells with a center surround organization, as suggested by von Békésy (1968) and supported by the psychophysical experiments of Robinson (1968, 1970), pointing to a retinal origin. Electrophysiologically, the amplification of flicker responses by facilitative interaction between center and surround mechanisms has been shown first in *limulus* by Ratliff et al. (1967). The possibility that it also exists in vertebrates was suggested by several flicker studies of cat retinal ganglion cells, none of which were color-opponent (Maffei et al. 1970, Büttner et al. 1971, van de Grind et al. 1973, Maffei 1968). It is impossible to achieve isolation and interaction of center and surround mechanisms in spectrally non-opponent cells without changing spatial variables; in color-opponent cells, however, this can be readily done by choosing the appropriate wavelength of stimulation. The potential relevance of flicker-enhancement by lateral inhibition for the action of color-opponent cells has been suggested by De Valois et al. (1977); however, several previous studies of flicker fusion properties of primate color-opponent and spectrally non-opponent cells had not indicated any change in spectral sensitivity or enhancement of luminance flicker caused by color-opponent interactions (Spekreijse et al. 1977, Kaiser et al. 1977). However, in contrast to the present study, these studies did not approach latency or phase-shift measurements separately for spectrally different center and surround mechanisms. In goldfish, where such studies were performed (Schellart and Spekreijse 1972, Schellart 1973), this type of interaction was not found, probably since the center-surround organization in goldfish (Schellart et al. 1979) is very different from that in primate (see also Section 1.2).

Conditions Which Can Modify or Suppress the Enhancement Effect. Since the enhancement occurs only when *both* mechanisms which form center and surround are stimulated simultaneously by flickering lights, chromatic backgrounds and the wavelength of test stimuli heavily influence the degree of enhancement. Depending on these factors, certain stimulation techniques might reveal supersensitivity (Kelly 1974), especially when the sensitization is produced by hue differences at higher background levels which

cause temporal interaction of the red and green mechanism (Sternheim et al. 1978). Studies performed at low background levels, where cone opponency is weak, might not reveal an enhancement effect (Cavonius and Estévez 1975, Estévez and Cavonius 1975); this is especially true when methods of silent substitution (Estévez and Spekreijse 1974) or of chromatic adaptation (Kelly and van Norren 1977, Sternheim et al. 1979) are employed which prevent interaction between spectrally different cone mechanisms. Synchronization also depends on wavelength; it is optimal near the spectral neutral point, while with other wavelengths it might occur only at higher intensity levels; one might miss it with a wavelength from the end of the spectrum. The same applies when chromatic adaptation is employed; all conditions which suppress one of the cone mechanisms usually prevent their interaction and consequently abolish the enhancement effect, since it is based upon a *synergistic* action of at least two cone mechanisms, as observed in color-opponent ganglion cells when flickering stimuli or flashes of short duration are employed. Moreover there seem to be rather pronounced individual differences in perception of brightness enhancement (Bowen and Markell 1980).

The V_λ-Function. The comparative studies of Spekreijse et al. (1971) have shown that flicker responses in monkey LGN resemble in many respects data on human flicker perception. On the other hand, action spectra change considerably with spatial or temporal variables as shown by Sperling and Harwerth (1971), King-Smith and Carden (1976), and Zrenner (1977c). The synchronizing mechanism shown in Section 5.3, causes the double-peaked action spectrum of color-opponent cells to become one-peaked and broadband at higher flicker frequencies; this might explain why heterochromatic flicker photometry reveals such a smooth, one-peaked V_λ-function for a trichromatic system (for further details see Section 6.5). It should be noted that the minimum distinct border (MDB)-technique reveals broadband functions similar to the V_λ-function (Wagner and Boynton 1972, for an extended bibliography see Serra 1981). The MDB-technique possibly also involves such a phenomenon: The detection of *spatial* patterns, if they are influenced by nystagmus, eye movements or drifts, could also involve *resonant* effects between center and surround of retinal ganglion cells, since the target hits center and surround with a certain delay; a synchronization of center and surround excitation thereby activated would eliminate or minimize color-opponent interactions and produce a V_λ-like funcion; this would depend upon the size of the center and surround mechanism of color-opponent cells and the velocity of eye movement (Kelly 1978). Indeed, with eye movements eliminated, chromatic gratings even of maxi-

mum contrast cannot be detected, as Kelly (1981) showed in experiments with stabilized images.

The Brücke-Bartley Effect, Brightness and Darkness Enhancement. Another related psychophysical phenomenon is the well-known Brücke (-Bartley) effect (1864); with flickering white light, a sensitivity maximum occurs at intermediate flicker frequencies. The neurophysiological basis of this effect was explained by Grüsser and Creutzfeldt (1957), Grüsser and Reidemeister (1959), Reidemeister and Grüsser (1959), as well as in the model of Varjú (1965), by superimposing excitatory and inhibitory responses in single retinal non color-opponent neurons of cat retina. As shown here, in color-opponent cells this has far-reaching consequences. Since two spectrally different cones are involved in such a mechanism, flickering light changes the color-opponent cells' action spectrum entirely, i.e., from double-peaked to broad-band. It is quite conceivable that the phase shift between center and surround responses is also responsible for the Brücke-Bartley effect of enhanced brightness produced by repetitive stimulation at certain frequencies, where the excitatory phases of both mechanisms synchronize and thereby cause a strong discharge; this corresponds to the psychophysically observed threshold decrease for the test light at certain intermediate frequencies. The synchronization of inhibitory responses could produce darkness enhancement as described by Magnussen et al. (1979).

5.7.3 The Fechner-Benham Top

Since the loss of color-opponency at high flicker frequencies is due to a phase-shift between antagonistic center and surround responses toward synergism, it is easily imaginable that the reverse phenomenon could produce chromatic sensations from white light. This can indeed easily be demonstrated by the well-known illusion named "Fechner-Benham top" after Fechner (1838) and Benham (1895). The unique temporal pattern of brightness contrast (see Fig. 5.8) projected onto a certain retinal area by the sequential motion of black and white stripes (5-10 c/s) produces the illusion of color. The neurophysiological explanation of this phenomenon is not yet available although several models have been developed; for a review see von Campenhausen (1968a,b). He also convincingly demonstrated that pattern-induced flicker colors in the visual system are produced rather by phase-dependent lateral interactions in the retina than by cortical mechanisms. The study conducted by Semm (1977) on retinal ganglion cells also has not yet yielded sufficient data to settle this issue.

Attempt at an Explanation. The temporal interaction of the center and surround in the RF of a color-opponent ganglion cell in this chapter invites the following attempt to explain the Fechner-Benham illusion. The half- or quarter-sectored black and white disk (shown in Fig. 5.9) produces flickering white light which causes the center and surround mechanisms in color-opponent ganglion cells to synchronize at certain frequencies (around 10 c/s, see Fig. 5.5); these cells consequently lose color-opponency (see Fig. 5.3), so that the response sequence of the on- (center) and the off- (surround) mechanism follows the pattern shown in Fig. 5.8 (*lower left*). Note that it is an indispensable condition, *first* to produce luminance flicker (e.g., by a sectored disk) and then to introduce *additional* patterns (e.g., stripes) to produce flicker-induced colors. The additional black and/or white stripes shown on the Fechner-Benham top, as well as their simplified analogs, when projected in succession (cf. Fig. 5.9, modified after von Campenhausen 1968a), introduce an additional phase shift between center and surround responses for two different conditions (*center* and *right-hand part* of Fig. 5.9). Depending on the length of the stripes, the synchronization of center and surround mechanism in certain types of cells is changed back into antagonism, caused by the stripe-induced delay between the stimulation of center and surround. Due to this *additional* phase-shift introduced by the black or white stripes (see Fig. 5.7), the sequence of spike-bursts of center and surround excitation again can become a non-flickering, steady signal; this is reflected in Fig. 5.7 by a transition from the situation shown in the *lower left* to that shown in the *lower right*. Thus, the signal at the output of such a cell is indistinguishable from that produced

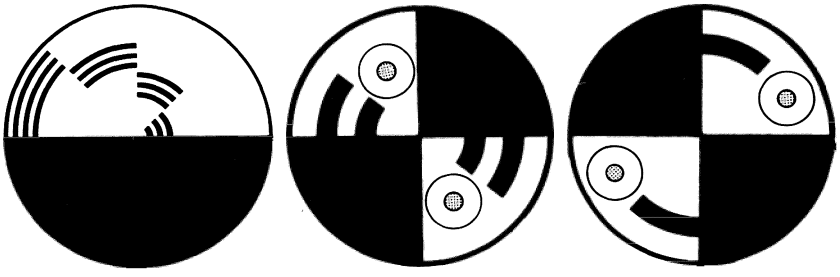

Fig. 5.9. *Left:* Fechner-Benham top in its original version. Rotation of the black and white disk at certain frequencies (5-15 c/s) produces the illusion of relatively desaturated colored rings. *Center* Simplified Fechner-Benham top after von Campenhausen (1968b); the additional *black stripes in the white field* introduce a phase-shift between the responses of the center and surround in the receptive field of a color-opponent cell (indicated by *concentric circles*). *Right* Situation for another type of simplified Fechner-Benham top, introducing phase shifts also between center and surround, however, in the opposite direction (From Zrenner, 1983)

by a *stationary* hue, and therefore produces a non-flickering sensation of color. Taking this explanation into account, it is not surprising that the visual system can be made to see colors when stimulated by unique temporal patterns of white light. It is consistent with the finding that deuteranopes and protanopes confuse flicker-induced colors in a similar manner as they do ordinary spectral colors (Rosenblum et al. 1981). Also the electrophysiological recordings of Adamczak (1981) in single cells of frog retina provide evidence that flicker-induced colors are produced by modifications in center-surround interactions of ganglion cells mediated by amacrine cells.

What Could Be the Reason for Different Colors in the Fechner-Benham Illusion? From the Fechner-Benham illusion it also follows that the timing of retinal signals is important for the perception of different colors. Piéron (1931) proposed that differences in the time constants of the basic cone responses are an important factor in producing different colors. This might be true for differences between the blue-sensitive system on the one hand and the red- and green-sensitive system on the other, as worked out in Chapter 4. However, the large variation of colors seen in Fechner-Benham illusions might rather be due to the large variations in the strength of possible interactions between the center and surround of color-opponent ganglion cells (see Sect. 3.4); this variation implies varations in the frequency dynamic of center-surround interaction. Consequently, there are always populations of cells which produce chromatic sensations, when stimulated by certain stripe-lengths as lined out by Zrenner (1983).

Since the strength of color-opponency varies with retinal eccentricity, it is no wonder that pattern-induced flicker colors also vary with retinal eccentricity (von Campenhausen 1968a). However, the fraction of retinal ganglion cells in which the stripes produce this additional phase-shift between center and surround is small (per unit retinal area); most of the cells would be not affected either, since the stripes do not hit their RF in the appropriate way, or since the length of the stripes does not produce a phase-shift of the right magnitude. These cells still would be able to signal luminance; it is not surprising then, that the colors of the Fechner-Benham illusion appear quite desaturated.

Colors Induced by "Stationary" Black and White Patterns. As shown by Festinger et al. (1971) and Müller et al. (1980), the *movement* of a stimulus across the retina is not necessary to produce pattern-induced flicker colors. However, stationary patterns such as stripes or checkerboard reversals also had to be employed in these studies to produce color sensations; this supports the explanation presented here which does not require movement or certain patterns, but only a phase-shifted stimulation of center and sur-

round, regardless of the means employed. Indeed, stepwise movements of bars or pattern reversals, even eye movements (occurring when a stationary pattern is viewed), necessarily introduce such phase shifts between center and surround responses; under certain spatial conditions, this can produce color illusions (see Spillmann and Redies 1980). There is only one indispensable requirement in this explanation: the center and surround excitations have to be synchronized *first* by "background" (luminance) flicker before additional phase shifts between center and surround of the RF are introduced by test patterns. The fact that in all experiments of the above kind, pattern-induced colors could not be produced without somehow introducing flicker even strengthens this explanation (preliminary report by Zrenner 1979). This explanation requires neither the interaction of rods and cones nor the involvement of phasic ganglion cells as proposed by Müller et al. (1980), nor even pulse coding mechanisms like the "Morse-code" (see Festinger et al. 1971).

5.7.4 The Loss of Color-Opponency

Is it Linked to a Loss of Visual Acuity? The loss of opponency between center and surround responses at higher flicker frequencies in color-opponent cells necessarily abolishes also the *spatial*, center-surround antagonism; the visual acuity should therefore considerably decrease, even though at low temporal frequencies the ganglion cells' receptive field structure provided a good spatial resolution, due to the maintained opponency in its center-surround mechanism. Based on psychophysical observations, Ingling and Martinez (1981) point out that tonic cells should lose color-opponency also at high spatial frequencies. The dependence of the spatial resolution of color-opponent cells on temporal frequency might resolve the controversy between Ingling (1978) and King-Smith and Carden (1978) in assigning visual acuity to a chromatic or a luminance channel. Visual acuity losses therefore do not necessarily point to a function breakdown of the tonic, color-opponent ganglion cells (King-Smith et al. 1980).

Models of the interrelation between spatial and temporal aspects of stimuli were recently proposed by Burbeck and Kelly (1980) and Green (1981). However, this chapter deals with the temporal aspects of color and brightness, so that spatial aspects can be only briefly touched upon. (For further references see the recent papers of Lennie 1980, Breitmeyer et al. 1981). It should be emphasized, however, that Barlow et al. (1957) already had observed a loss of spatial organization in cat retinal ganglion cells, when stimulus duration was shortened to 7 ms.

Can the Loss of Color-Opponency Provide an Advantage? The model given in Fig. 5.7 shows that the well known low-frequency attenuation for luminance flicker and the high-frequency attenuation for chromatic flicker does not require two cell systems or two pathways (as often suggested), but occurs in each individual cell. While at *low* frequencies, the functional dichotomy between a double-peaked color-opponent, tonic system on the one hand and a broadband-achromatic, phasic system on the other might still be valid, at *high* frequencies all cells become broadband and achromatic; both the phasic and the tonic systems are able to follow high rates of flicker (see Fig. 5.6). The nervous system's adaptability (see Granit 1975 for this term) provides a very advantageous mechanism: A static object, presented at low frequencies of stimulation, can be distinguished from a equiluminous background only by analyzing hue differences in color-opponent cells. At high frequencies of stimulation (e.g., in the case of quickly moving objects), the information concerning hue becomes secondary, since the object's brightness-contrast undergoes a permanent change in relation to the background, which is rather heterogeneous in a natural environment. In the above experiments, due to the high frequency of temporal changes (Fig. 5.3) or the short duration in which an object is presented (Fig. 5.8), color-opponent cells lose their ability to detect differences in wavelength. However, under these circumstances, they are much better equipped to follow the object's luminance changes up to much higher frequencies, since the excitatory phases of center and surround are synchronized and thereby enhance each other, which results in a better responsiveness at higher frequencies of stimulation at the expense of coding for color. Color-opponent retinal ganglion cells therefore show a surprising functional plasticity; in a way, they adapt to the tasks imposed by the physical characteristics of the objects to be analyzed (Zrenner 1979); they either detect an object by analyzing chromatic borders when it is static (e.g., a red bird sitting in a green tree) or, by analyzing its brightness contrasts when it is moving (e.g., a red bird *flying* over the trees). They waive the detection of chromatic differences for the sake of higher temporal resolution of these objects which can be detected by brightness differences anyhow. This might explain why quickly moving objects appear rather colorless (e.g., a flying bird). This adaptability to the task required is usually attributed to the function of higher neurons; it is rather surprising, though very economical, to find such mechanisms already built into retinal neurons.

5.7.5 Possible Consequences for Cortical Processing of Color

The well-established loss of color-opponency in ganglion cells at high flicker frequencies implies that their impulses alone cannot unambiguously code for color (Zrenner and Gouras 1978a,b, Gouras and Zrenner 1979a). The color signals which they transmit depend critically upon comparison between the phase relationship of different color-opponent cells subserving similar or neighboring areas of the retina. This is not to say that the so-called color-opponent retinal ganglion cells are, in themselves, color-detectors (see Gouras and Zrenner 1981a,b); they respond mainly to luminance within certain spectral windows narrowed by cone opponency. In the visual cortex, cells have been described which respond only to color-contrast (Michael 1978a,b, Krüger and Gouras 1980); they may be closer to true color detectors. The loss of color-opponent interactions in the retina must greatly interfere with the function of such cells as worked out in Fig. 3.19 where only cells with strong color-opponency can optimally detect chromatic borders. For example, the ability to differentiate alternating colors is already lost at a few cycles per second (van der Horst 1969); the ultimate detector, the visual cortex, probably only works optimally at low temporal frequencies of stimulation because color-opponent signals which carry the information (upon which this detector depends) are progressively lost at higher frequencies.

6 The Spectral Properties of the Human Visual System as Revealed by Visually Evoked Cortical Potentials (VECP) and Psychophysical Investigations

In order to correlate the performance of the primate visual system as a whole with some of the functions of single retinal cells (cf. Chaps. 2 to 5), in the following, experiments on human observers will be presented. There are two general methods of measuring[9] the human visual system's sensitivity to certain stimulus configurations. First, by determining psychophysically detection thresholds for individual stimulus variables; this involves cognitive higher-order cortical functions such as perception, recognition, and judgement; it is difficult to apply *suprathreshold* criteria by psychophysical methods. Secondly, by recording graded potentials generated by more or less numerous cell populations at various points of the *visual* system and by correlating the response magnitude with a variety of stimulus variables; the processing of signals up to the recording site does not extensively involve cortical functions higher than those of the primary visual cortex; furthermore, suprathreshold measurements can easily be performed electrophysiologically. In the following chapter, results obtained with *both* methods will be discussed and related to the functions obtained in single retinal ganglion cells.

Since this book is mainly concerned with aspects of color vision, it does not provide an exhaustive review of all additional questions such as spatial resolution and dark and light adaptation which might arise from the data described in this chapter. Beyond the references given in the preface, the interested reader is referred to the following more recent publications. On the anatomical organization of the visual system: e.g., Hassler (1965), Hubel and Wiesel (1977), van Essen (1979), and Rodieck (1979). On visual adaptation: MacLeod (1978). On visually evoked cortical potentials (VECP) in general: Riggs and Wooten (1972), Regan (1972), Regan and Spekreijse (1974), Desmedt (1977), Spekreijse et al. (1977), Lehmann and Callaway (1979) and Barber (1980). The electrophysiological basis of evoked potentials is discussed by Creutzfeldt and Kuhnt (1964), Mitzdorf and Singer (1978) and Stöhr et al. (1982).

---

9 Estimation methods (such as magnitude estimation) provide no measurements in the strict sense and are no matter of discussion here, though they yield valuable information

Color vision studies on the VECP with patterned stimuli (for a review see Regan 1972, 1977) could not be included in the discussion of this chapter, since only homogeneous test fields were applied.

Moreover, there are many questions regarding theories of cortical function which cannot be discussed here. For further details see Hajos (1968), Rauschecker et al. (1973), Barlow (1979a,b), Braitenberg (1979), Creutzfeldt (1979); on the organization of color-specific cortical cells see Gouras (1974), Gouras and Padmos (1974), Creutzfeldt and Nothdurft (1978), Michael (1978a,b), Gouras and Krüger (1979), Krüger and Gouras (1980), Zeki (1980) and Gouras and Zrenner (1981b).

6.1 Methods as Applied in Human Observers

The Observers; Determination of Color Vision. The experiments were performed in young, healthy students (age 18-23) with normal vision as checked by examination of the fundus, visus, dark adaptation curve, Nagel anomaloscope, Farnsworth's (1943, 1947) Panel D-15 and Farnsworth-Munsell 100-Hue test (computerized example in Fig. 6.1). For a brief survey of these procedures see Scheibner (1976b). In protanopic and deuteranopic observers who accepted the extreme settings on the Nagel anomaloscope (evaluation see Fig. 6.2), the neutral point (see below) and the color discrimination function ($\Delta \lambda/\lambda$) were also determined. Clinical cases are described in the text together with the recorded data. The subjects were asked to lie down in a dark, electrically shielded room, with their head in a specially moulded holder, and were required to monocularly observe a steady, small red fixation mark; the second eye was covered by a black plate. The pupil was usually dilated by instillation of a few drops of Mydriaticum "Roche". In experiments involving the rod system, the subject was dark-adapted for 45 min, otherwise light-adapted for at least 10 min.

Stimulation Technique. The four-beam stimulator shown in Fig. 6.3 permits independent variation of hue, brightness, saturation, stimulus-time and -interval, as well as of the field size presented.

The four beams originating in the Xenon arc lamps Xe 1 (Osram XBO, 450 W) and Xe 2 (Osram XBO, 150 W) are recombined by beam splitters and projected via an artificial pupil (*AP*) and a mirror (*Mi*) in Maxwellian view into the observer's eye, inside the Faraday cage F. The spectral composition is determined in beam 1 and 2 by grid-monochromators (M_1 and M_2, from Jobin Yvon, Type H.10, half band-width 12 nm) and in beam 3 and 4 by interference filters (Schott AL, half band-width 15-25 nm). The

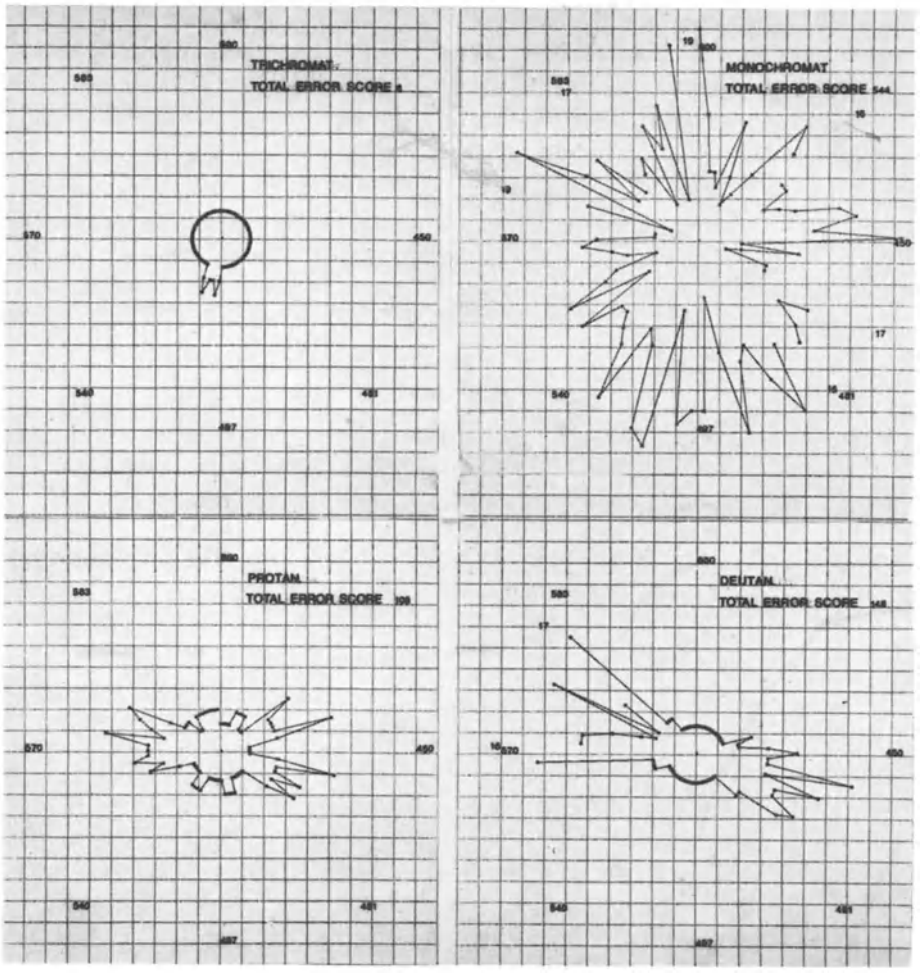

Fig. 6.1. Farnsworth-Munsell 100-Hue test. Examples of a normal trichromat, protanope, deuteranope and monochromat who participated in the experiments described in Chapter 6. After entering the sequence of the color cups used in the test, the computer (DECLAB 11/40) plots the error graph according to Farnsworth's (1957) procedure. Errors larger than the limits of the graphical area are indicated by *two digit numbers*. *Three digit numbers* arranged in a *circle* indicate the spectral loci of the individual cups. The total error score, partly represented by the inside area of each figure, is calculated and given on the *upper right* of each figure

brightness is varied either by steps of 0.3 log units by neutral absorption filters in boxes B_1 to B_4 or continuously by a neutral density wedge (GK). The retinal area which is adapted by a steady background light (12°-18° visual angle) is determined by the diaphragm D_2 (controlling beam 2 and 3); the stimulation beam is superimposed onto this area and controlled by

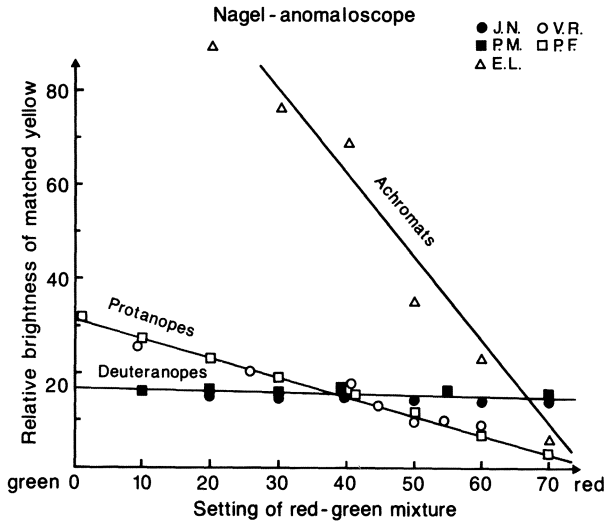

Fig. 6.2. The evaluation on the Nagel (1907) anomaloscope of the color-defective observers participating in these experiments

the diaphragm D_1 (affecting beams 1 and 4). Stimulus time (10-400 ms) and interval (0.1-40 c/s) are controlled by electromagnetic shutters (Sh_1-Sh_2); the wedge, monochromators, and shutters are controlled either by hand or via stepper motors by a digital computer (*DECLAB 11/40*) through the interfaces and the laboratory peripheral system (*LPS*).

The software utilized for stimulation and recording is described by Zrenner and Baier (1978). The essential task of this system is to randomly select stimulus conditions out of a given set, to record the electrical responses and to average them in separate memory-arrays in order to minimize long-term response variations. The processor calculates intensity-response functions from latencies as well as from maximum amplitudes and graphically displays spectral sensitivity functions based on threshold criteria. A simple code, consisting of the patient's personal data, serves for automatic filing. The spectral characteristics of the lamp, the monochromator, the neutral filters, the wedge setting and the interference filters are stored on a table in the computer's memory, so that for each stimulus condition the actual radiant intensity delivered by the stimulus flash is calculated individually. Flickering stimuli with equal periods of light and darkness were produced by a two-sectored disk rotated at a focal point in one beam by a variable-speed motor and continuously monitored by a photo-cell. The radiant intensity I_e (CIE 1970) of the test flash was determined at all wavelengths (400 nm to 650 nm) as follows: the irradiance E_e was measured with a "radiant flux meter" (Model 8330 A, Hewlett-Packard) at different distances (d) from the plane where the subject's pupil and the beam's focus would be. The value of $E_e\ d^2$ yields I_e, the radiant intensity expressed in

$nW\,sr^{-1}$. To indicate that the values thereby obtained refer to the pupillary level of the eye and do not include corrections for losses in the ocular media, I_e was renamed I_p. I_p then is a measure of radiant intensity on an *energy* basis at pupillary level, often used in psychophysical measurements in man. The irradiance values E_Q applied in monkey retina (Chaps. 2 to 5) were given on a *quantal* basis, more appropriate for direct comparisons with pigment absorption spectra (see Fig. 2.2). To compare both sets of data in terms of absolute values, the following calculation would have to be applied:

$$E_e\,[nW \cdot m^{-2}] = E_Q\,[\text{Quanta} \cdot s^{-1} \cdot \mu m^{-2}] \cdot \frac{h \cdot c}{\lambda} \cdot 10^{21}$$

$$I_e\,[nW \circ sr^{-1}] = E_e\,r^2 \quad (r = 16.683\ \text{mm, the effective length of the eye bulb})$$

$$I_p\,[nW \cdot sr^{-1}] = E_Q \cdot \frac{1.9861273 \cdot 10^{-25}}{\lambda} \cdot 10^{21} \cdot 2.7837 \cdot 10^{-4}$$

$$\boxed{I_p\,[nW \cdot sr^{-1}] = E_Q \cdot \frac{5.5287825}{\lambda} \cdot 10^{-8}} \quad [\lambda \text{ in m}]$$

Since λ is included as a variable, action spectra based on an energy basis are narrower in band-width and have their maximum slightly sifted to the left.

The retinal illumination of the adapting beam is given in troland and measured in a way similar to the one described above by means of a V_λ-corrected photometer (Gamma-scientific, Model 900, Head 820/6L).

For threshold measurements at various retinal eccentricities (Chap. 6.2), Maxwellian view could not be utilized due to its limited angle of vision. In this experiment, both beams illuminated a diffuse acrylic screen, 10 cm in diameter, positioned between 3 cm and 15 cm in front of the eye. The subject lay in a dark room and looked at a dim red lamp shining through a hole (1 mm in diameter) in the center of the screen. Size and retinal location of the test flash were controlled by appropriate diaphragms attached to the screen. To increase the strength of stimulation in these particular experiments, broadband absorption filters were used (Schott BG 28 absorption filter, maximum transmission at 440 nm, half-width 160 nm). For the photopic series of measurements, long-wavelength light (Schott OG 5, blocking 50% at 560 nm) was used for stimulation and short-wavelength light (Schott BG 28) for light adaptation.

Recording and Evaluation Techniques. The VECP was recorded by a gold disk electrode attached with collodion 4% (Merck) at Oz (according to the

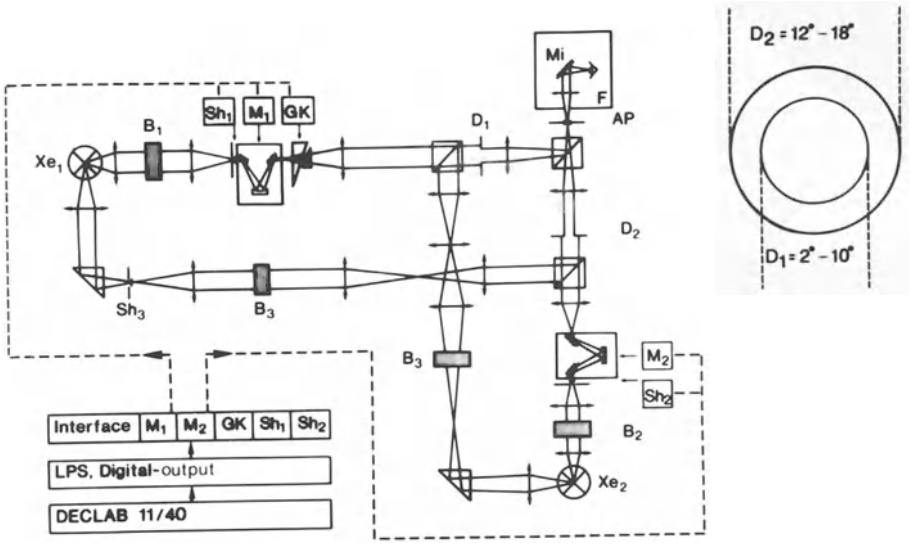

Fig. 6.3. Four beam stimulator, the individual components of which are controlled by the DECLAB 11/40 computer (Zrenner and Baier 1978) so that brightness, hue and saturation of the two superimposed fields, the area of which is controlled by the diaphragms D_1 and D_2, can be independently varied. For details see text

international 10-20 EEG system), placed about 3 cm above the inion; the indifferent electrode was attached to the earlobe. The signals were amplified (WP-Instruments, DAM 6A), led through a bandpass filter of 0.8-250 Hz, displayed on an oscilloscope (Tektronix 7000) and averaged (N = 32 to 256) by a Nicolet 1070 computer or a DECLAB 11/40 system (Digital Equipment). The software for the procedure is described by Zrenner and Baier (1978). The averaged data were digitally stored on a disk and plotted on an X-Y (HP 7035B) or on an electrostatic plotter (Gould). To avoid contamination with artifacts due to increased background activity, the light stimulus was, in many cases, triggered manually.

The amplitude of the VECP was determined from the first negative trough N_1 (about 70 ± 15 ms latency) or the second negative trough N_2 (about 140 ± 20 ms latency) to the first positive peak P_1 (110 ± 15 ms latency). The amplitude, as well as the latencies, were plotted against the radiant intensity in order to produce intensity-response (I/R) functions, also called V-log I functions. In the later stages of experimentation these curves were produced on-line on the computer terminal for optimally controlling the course of the experimental sessions. The reciprocal of the absolute pupillary radiant intensity I_p necessary for obtaining a criterion amplitude of 3 μV to 6 μV (kept constant from subject to subject), was plotted against the wavelength and interpolated from 4-5 VECP recordings as a

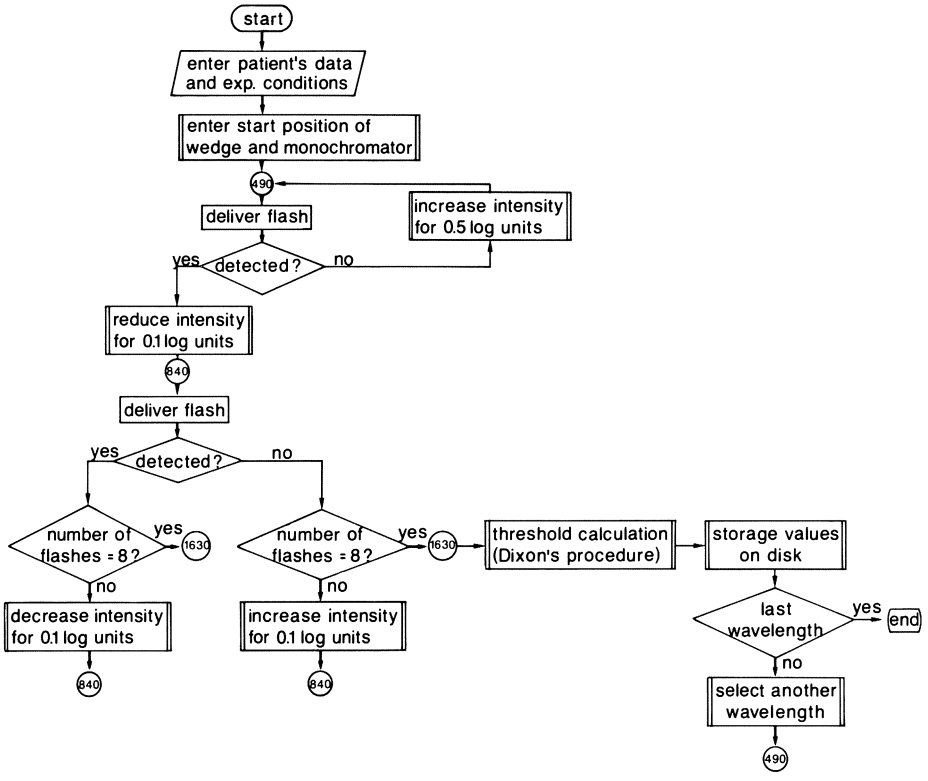

Fig. 6.4. Flow chart diagram of the BASIC program by means of which psychophysical thresholds are determined. The "up-and-down method with small samples" (Dixon 1965, modified after Little 1974) permits the determination of a 50% (frequency of seeing) threshold by 8 trials with steps of 0.1 log units, after the threshold was approached by 0.5 log units steps. *Encircled numbers* indicate jump addresses in the program. For details see text. (Modified from Baier and Zrenner in prep.)

measure of the observer's sensitivity. The psychophysical threshold data were obtained by a modified frequency-of-seeing procedure controlled by the DECLAB 11/40 system:

A click indicated that a flash would be delivered after a random delay (0.1-2 s); the observer had to press a button when he saw a flash in the center of the test field; depending on his response, the intensity of the test beam was automatically increased or decreased in a staircase-like manner by 0.1 log unit around the threshold, which had been initially approached by larger steps of 0.5 log units. The flow chart diagram of this program is shown in Fig. 6.4. According to Dixon's (1965) "up-and-down method for small samples", five or eight trials are sufficient for a remarkably precise determination of the 50% mark. This calculation (see Fig. 6.5, modified after Little 1974) was made immediately after each run, typed onto the

TABLE 1. VALUES OF k FOR ESTIMATING LD_{50} FROM UP-AND-DOWN SEQUENCE OF TRIALS OF NOMINAL LENGTH N. THE ESTIMATE OF LD_{50} IS $x_f + kd$ WHERE x_f IS THE FINAL TEST LEVEL AND d IS THE INTERVAL BETWEEN DOSE LEVELS. IF THE TABLE IS ENTERED FROM THE FOOT, THE SIGN OF k IS TO BE REVERSED

N	Second Part of Series	k for Test Series Whose First Part is					Standard Error of LD_{50}
		O	*OO*	*OOO*	*OOOO*		
2	*X*	−.500	−.388	−.378	−.377	*O*	.88σ
3	*XO*	.842	.890	.894	.894	*OX*	.76σ
	XX	−.178	.000	.026	.028	*OO*	
4	*XOO*	.299	.314	.315	.315	*OXX*	.67σ
	XOX	−.500	−.439	−.432	−.432	*OXO*	
	XXO	1.000	1.122	1.139	1.140	*OOX*	
	XXX	.194	.449	.500	.506	*OOO*	
5	*XOOO*	−.157	−.154	−.154	−.154	*OXXX*	.61σ
	XOOX	−.878	−.861	−.860	−.860	*OXXO*	
	XOXO	.701	.737	.741	.741	*OXOX*	
	XOXX	.084	.169	.181	.182	*OXOO*	
	XXOO	.305	.372	.380	.381	*OOXX*	
	XXOX	−.305	−.169	−.144	−.142	*OOXO*	
	XXXO	1.288	1.500	1.544	1.549	*OOOX*	
	XXXX	.555	.897	.985	1.000^{+1}	*OOOO*	
6	*XOOOO*	−.547	−.547	−.547	−.547	*OXXXX*	.56σ
	XOOOX	−1.250	−1.247	−1.246	−1.246	*OXXXO*	
	XOOXO	.372	.380	.381	.381	*OXXOX*	
	XOOXX	−.169	−.144	−.142	−.142	*OXXOO*	
	XOXOO	.022	.039	.040	.040	*OXOXX*	
	XOXOX	−.500	−.458	−.453	−.453	*OXOXO*	
	XOXXO	1.169	1.237	1.247	1.248	*OXOOX*	
	XOXXX	.611	.732	.756	.758	*OXOOO*	
	XXOOO	−.296	−.266	−.263	−.263	*OOXXX*	
	XXOOX	−.831	−.763	−.753	−.752	*OOXXO*	
	XXOXO	.831	.935	.952	.954	*OOXOX*	
	XXOXX	.296	.463	.500	$.504^{+1}$	*OOXOO*	
	XXXOO	.500	.648	.678	.681	*OOOXX*	
	XXXOX	−.043	.187	.244	$.252^{+1}$	*OOOXO*	
	XXXXO	1.603	1.917	2.000	2.014^{+1}	*OOOOX*	
	XXXXX	.893	1.329	1.465	1.496^{+1}	*OOOOO*	
		X	*XX*	*XXX*	*XXXX*	Second Part of Series	
		$-k$ for Series Whose First Part is					

Fig. 6.5. Tables of values for which the mean value has to be corrected if a small sample of stepwise increased or decreased stimuli around a threshold was applied. *Crosses* in the response sequences indicate that the person has detected the stimulus, *circles* indicate that he has not. The method was originally designed for pharmacological purposes. The term LD_{50} (lethal dosage in 50% of the cases) corresponds to the 50% threshold in terms of frequency of seeing. (Little 1974, his Table 1)

printer and graphically displayed on the terminal as well as stored on the disk. Thus, a quick and reliable method was utilized for precise psychophysical threshold determination.

In some cases, psychophysical thresholds were determined manually immediately before a VECP-recording; the flash-intensity was increased stepwise by 0.15 log units until detection was reported. This abbreviated procedure is necessarily less precise than the computerized one. It is indicated in the text which of the two methods was employed.

6.2 Rods and Cones

Studies on the sources of the human electroretinogram revealed that with diffuse light stimuli, rods dominate retinal responses at low frequencies of stimulation even under conditions which favor the activity of cones (for references see Armington 1974). It is therefore necessary to discuss the influence of rods and cones on the visually evoked critcal potential (VECP) before using such electrical signals for the isolation of cone-specific responses in higher visual centers.

Due to the overproportionally vast anatomical representation of the fovea and parafovea in the visual cortex in relation to the retinal periphery, the VECP mainly reflects cone activity (Cavonius 1965, Potts and Marriot 1965, De Voe et al. 1968, Wooten 1972). However, under appropriate con-

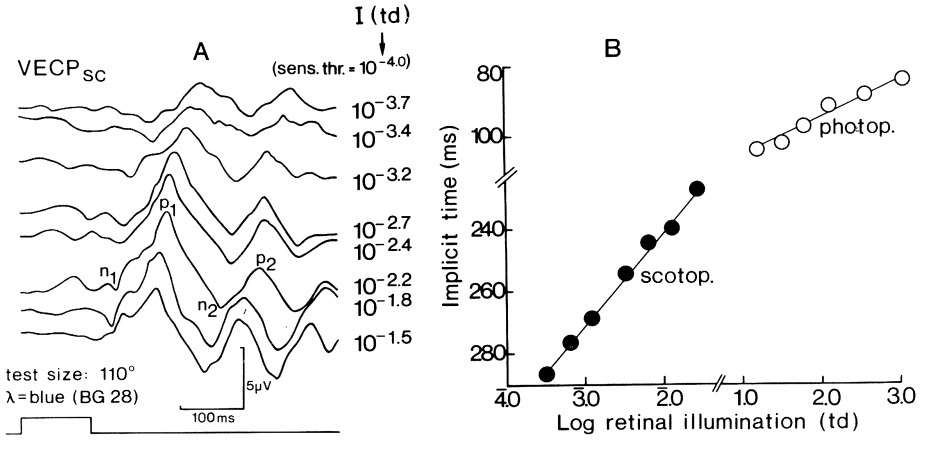

Fig. 6.6. A Scotopic VECPs (n=64) in response to a blue test light (λ), (BG 28, Schott) after 40 min of dark adaptation. Upward deflection indicates positivity of the scalp electrode (p_1, p_2). Size of test fields 110°, central fixation. Duration of test light: 110 ms (see lowermost record). *Numbers* beside records denote retinal illumination in photopic troland (td). **B** Implicit time of the first positive peak (p_1) versus log retinal illumination of test light for the scotopic (*filled symbols*) and the photopic VECP (*open symbols*); the latter was recorded in response to an orange light (OG 5, Schott) during adaptation to blue light (BG 28, Schott) of 50 td. (Modified from Kojima and Zrenner 1977)

ditions of stimulation, cortical signals of rod origin (scotopic VECP's) characterized by long-latency components can be recorded (Van Balen and Henkes 1960, Vaughan 1964, Adams et al. 1969, Kojima and Zrenner 1980).

Intensity-Amplitude Functions for the Rod and Cone System. Figure 6.6 shows VECP's of rod origin, described by Kojima and Zrenner (1977). After 40 min of dark adaptation, blue test light of 110° in diameter are presented (A). Retinal illumination (I, in troland), from 0.3 log units above the sensory threshold on, evokes a series of wavelets (peaks and troughs indicated by lower case letters) which culminate between 200 and 400 ms. The implicit time of these components (interval between stimulus onset and peak of an individual wave) decreases as retinal illumination increases. The implicit time of p_1 plotted against retinal illumination (*filled circles* in Fig. 6.6B) yields a constant slope value of 25 ms per log td under the scotopic conditions. Under photopic conditions (orange light stimuli, presented on a blue background of 50 td), the change of implicit time (latency of the culmination point of electric responses) of p_1 vs. retinal illumination was much smaller (*open circles* in Fig. 6.6B, about 10 ms per log td).

The origin of the components can be made apparent by measuring the spectral sensitivity function under both photopic and scotopic conditions. To this end, the procedure outlined in Fig. 6.6 was carried out with six monochromatic wavelengths between 425 and 651 nm. As shown in Fig. 6.7, the slope of these functions runs parallel between 501 and 601 nm for the

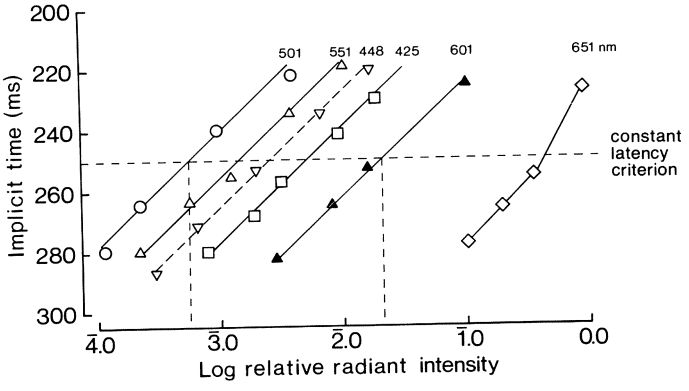

Fig. 6.7. Plottings of the implicit time versus log radiant intensitiy of the scotopic VECP after 40 min of dark adaptation for six stimulus wavelengths as indicated. Size of the test field 110°. Data were obtained by measurements of component p_1's implicit time. Values at 448 nm (*broken line*) are displaced to higher intensities by 0.25 log units to prevent overlap

dark-adapted eye; the break of the function at 651 nm probably indicates the transition to another long-wavelength mechanism (Kojima and Zrenner 1977).

Spectral Sensitivity of Rod and Cones. If the radiant intensity required to evoke a p_1-component of 250 ms is plotted against wavelength, spectral sensitivity functions based on a constant response criterion are obtained (*filled symbols* in Fig. 6.8).

For the dark-adapted eye, the data points agree well with the scotopic (V'_λ) CIE luminosity function (Huber and Adachi-Usami 1972, Kojima and Zrenner 1977). Under photopic conditions (steady exposure to white light of 100 td), the sensitivity obtained by VECP measurements in the short wavelength range of the spectrum is higher than the CIE photopic luminosity function (V_λ). It best matches Wald's (1945) curves of extrafo-

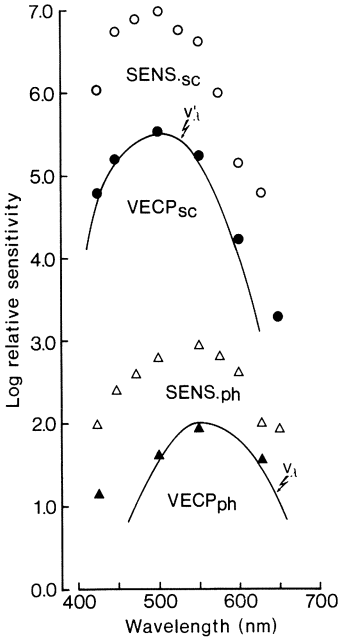

Fig. 6.8. Spectral sensitivity functions derived from sensory thresholds (*open symbols*) and from VECP measurements (*filled symbols*) under scotopic (*circles*) and photopic conditions (*triangles*). The photopic function was obtained in presence of white adapting light (100 td). The function based on the VECP was obtained by measuring the radiant intensity necessary to obtain an implicit time criterion of 250 ms in the dark-adapted eye ($VECP_{sc}$) and 180 ms in the light adapted eye ($VECP_{ph}$). The *solid lines* represent the CIE (= Commission Internationale de l'Eclairage) scotopic (*above*) and the CIE photopic luminosity function (*below*). Size of test field 110°. Stimulus duration 110 ms. Random stimulus frequency between 1.5 and 10 s. (Kojima and Zrenner 1977)

veal cones showing increased sensitivity in the blue part of the spectrum, probably caused by the lack of macular pigment and the higher proportion of blue cones in the retinal periphery; these conditions are induced by the large stimulus area used. (The relation between stimulus size and threshold in VECP measurements was studied by Kojima and Zrenner 1977).

The sensory threshold measurements performed simultaneously (*open symbols* in Fig. 6.8) generally agree with the electrophysiological determination (see also Siegfried, 1971); however, psychophysical thresholds appear at higher sensitivity levels since they are based on a lower criterion than the electrical threshold criterion. Since the V-log I functions are parallel, it is permitted to compare the shape of spectral sensitivity functions, although they were obtained with different criteria. Only the absolute values of sensitivity depend on the choice of the criterion.

Rod and Cone VECP Evoked by Eccentric Stimulation. How does the threshold for rod and cone vision in the VECP change with retinal eccentricity? For the determination of *local* scotopic VECP thresholds (Fig. 6.9), an implicit time of 340 ms (p_2) was chosen as criterion, since this is the typical latency of n_2-p_2 amplitudes which show relatively little interindividual variation (Kojima and Zrenner 1980). The retinal illumination at which this criterion was obtained is plotted against retinal eccentricity. This is shown for the temporal visual field in the upper part of Fig. 6.9 (*left-hand ordinate*) for four observers for VECP (*filled symbols*) as well as for sensory threshold measurements (*open symbols*). The *straight horizontal lines* drawn through the symbols indicate the size of the test field (5°). The measurements generally indicate that the scotopic threshold of the retina determined by the scotopic VECP is lowest at about 20° and increases more slowly and more gradually in the periphery than in the central parts of the retina. A similar distribution at a somewhat lower (about 10 times) level of test light illumination was obtained for the sensory threshold (*open symbols*) in the same experiments. Both sets of data generally agree with the number of rods reported by Østerberg (1935), indicated by a continuous line (*right hand ordinate*), as well as with the sensitivity profile obtained by pupillomotoric measurements (Alexandridis 1973).

Similar experiments performed under photopic conditions (steady exposure to blue light of 50 td, orange test flashes) yielded the results illustrated in the lower part of Fig. 6.9. The distribution of retinal thresholds as determined by the photopic VECP is generally in agreement with the earlier findings of Van Lith and Henkes (1968). The electrically determined thresholds are based on an implicit time of 190 ms (*filled triangles*) and indicate a steep rise of the threshold toward the retinal periphery, most of which covers the range of test fields between 0° and 10°. Again, Østerberg's

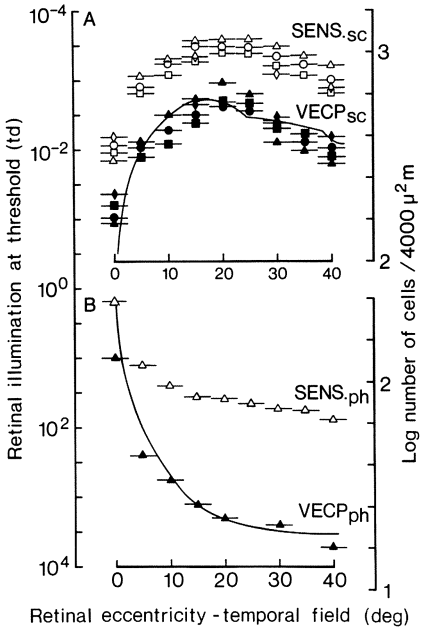

Fig. 6.9A, B. Local sensitivity distribution in the temporal retinal field as determined by measurement of retinal illumination necessary for sensory threshold (*open symbols*) and a constant implicit time criterion in the VECP (*filled symbols*) for test lights of 5° subtense. The data are compared with the distribution of rods (**A**) and cones (**B**) across the retina (*solid lines, right hand ordinate*), according to the data of Østerberg (1935). **A** Data obtained under scotopic (*sc*) conditions (40 min of dark adaptation, blue test light, BG 28, Schott). Implicit time criterion 340 ms. Four observers. **B** Data obtained under photopic (*ph*) conditions (steady exposure to blue light of 50 td, in order to suppress rod-activity; orange test light, OG 5, Schott). Implicit time criterion 190 ms. (Kojima and Zrenner 1980)

(1935) function for cones (as indicated by a *solid line, right hand ordinate*) closely agrees with the VECP data. Less agreement with Østerberg's function was obtained for the psychophysical thresholds (*open triangles*, one subject); apparently, the spatial summation occurring in the psychophysical measurements which involve higher cortical levels, is larger than that observed with the VECP in area 17 (and 18) alone.

The difference between the photopic, electrical and psychophysical threshold growing with retinal eccentricity might be caused by the increase of receptive and perceptive field size (see Ransom-Hogg and Spillmann 1980, Diehl and Zrenner 1980) toward the retinal periphery. A stimulus of a certain size might be recognized psychophysically in the retinal periphery when it stimulates the entire receptive field of only *one* ganglion cell, even though its electrical response is small. A stimulus of the same size, projected onto the foveal region, would necessarily cover the receptive fields of

many more ganglion cells and thereby produce a much larger electrical response; the psychophysical threshold might not have gained as much by area summation in foveal regions.

Moreover habituation, which is especially strong at the retinal periphery (as described by Frome et al. 1981), can decrease perceptual thresholds by more than 1 log unit, while the electrical thresholds at a lower level in the visual system do not become as strongly habituated.

As pointed out by Kojima and Zrenner (1977), the contribution of stray light to the electrical response is of major importance. In the present determination of scotopic VECP *thresholds*, the test flashes at the criterion level were about 1 log unit above the sensory threshold. According to Le Grand (1937) and de Mott and Boynton (1958), the amount of stray light decreases by two log units at 10° eccentricity from the retinal field illuminated, or by one log unit at 3°. Therefore, in the above measurements, stray light is effective only within 3° from the border of the stimulus field; in the photopic measurements, the stray light contribution is even smaller.

6.3 Fundamental Cone Functions

6.3.1 Trichromatic Observers

Selective Chromatic Adaptation. The spectral sensitivity function shown for photopic vision in Fig. 6.8 includes signals from all three cone mechanisms of a trichromatic human observer. In order to separate the signals from these cone mechanisms, the sensitivity of each can be depressed selectively by exposing the eye to visible radiation of appropriate wavelength; this method of selective chromatic adaptation was used in psychophysical experiments by Stiles (1949, 1959), and subsequently by Auerbach and Wald (1954), Wald (1964), Marré (1970) and many others, in the human VECP by Kellermann and Adachi-Usami (1972, 1973), Zrenner (1977a), Zrenner et al. (1977), Jankov (1978), Yokoyama and Yoshida (1978) and in cat by Schuurmans and Zrenner (1981a). For a survey of how chromatic adaptation has been studied see Wright (1981), for its limitations see Boynton and Whitten (1972).

Stiles' spectral sensitivity functions (see Stiles 1978) have for many years served as widely used estimates of the spectral sensitivity of individual cone mechanisms in man; he called the original blue-, green-, and red-sensitive mechanism π_1, π_4, and π_5 function. Stiles' measurements are based on the determination of the least amount of a given spectral light which must be added to a background of another spectral light for the increment to be

detected. Assuming the presence of more than one color vision mechanism, Stiles sought to isolate or reveal the individual color components by selectively reducing the sensitivitiy of the competing mechanisms (for a detailed discussion see Brindley 1970, Enoch 1972). The isolation of individual cone mechanisms was obtained by this psychophysical method to a rather large degree, as recent comparisons with absorption of pigments could demonstrate (Bowmaker and Dartnall 1980), although the isolation might be not complete with Stiles' technique (see Walraven 1981a,b). For a comparison with data on retinal ganglion cells, see Chap. 2.2.

In order to bleach the pigment of one or two cone types selectively with a monochromatic background, a retinal illumination of at least $10^{2.3}$ to $10^{3.7}$ td has to be applied in man, depending on the wavelengths used (Zrenner et al. 1977).

Detection of Cone Signals in the VECP. In order to obtain this high amount of retinal illumination, the so-called Maxwellian view is required, by which a condenser's light is projected directly onto the retina with the beam's focus positioned near the pupil's center (Westheimer 1966). The stimulus configuration used in the experiments described below is shown in Fig. 6.10 *upper left*. A flashed (10-400 ms, 1 Hz or c/s) test-field of 10° diameter (wavelength λ) was concentrically superimposed on an adapting field of 12°-18° diameter with a retinal illumination of 10,000 to 30,000 td (wavelength μ). VECP recordings (see method Chap. 6.1) were made for each of the 14 test wavelengths (in the range of 401 nm to 650 nm), first with pupillary radiant intensities (I_p) near the subjective threshold, then by increasing the intensity stepwise (by about 0.3 log units in Fig. 6.10, *left*). The amplitude of the VECP determined from the first negative trough N_1 (peak latency 55-85 ms) to the first positive peak P_1 (peak latency 95-125 ms) was plotted against the logarithm of I_p, as shown on the right of Fig. 6.10. The dynamic range of the response function was small, about 1.1-1.9 log units.

The wave shape did not vary systematically with stimulus wavelength. Color-specific features of VECP responses observed by Shipley et al. (1965), Cigánek and Ingvar (1969) and White et al. (1977) were not investigated in detail in this study. It was, however, regularly observed that peak latencies became longer as P_1 reached 160 ms, when stimuli of wavelengths shorter than 480 nm were applied; moreover, even on strong chromatic backgrounds, at some wavelengths, the slope of the V-log I function changed with higher stimulus intensities; therefore, a low amplitude criterion was chosen (3 to 4 μV), where the slope of the functions was parallel. It should be noted that on *white* background (situation in Fig. 6.10), the slope of the V-log I function is flatter for 575 nm, than for 602 nm. Below about 5 μV,

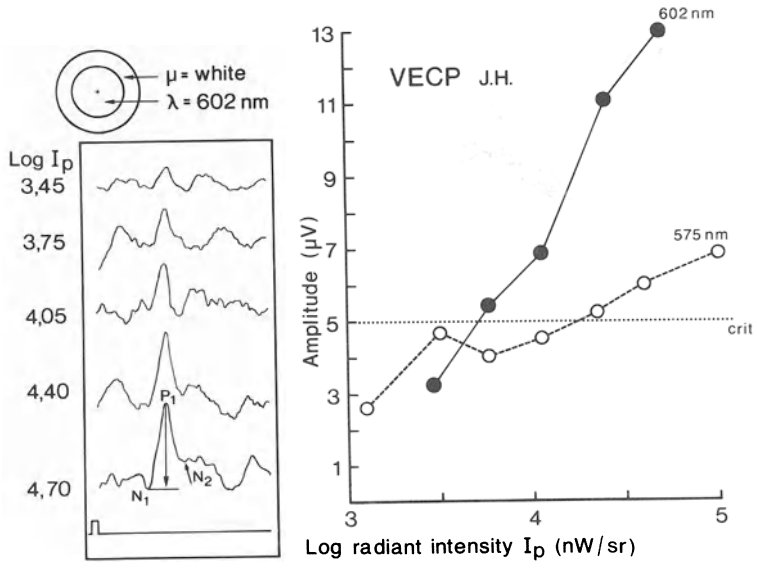

Fig. 6.10. *Left* Averaged VECP's (n = 128) of a normal trichromatic observer (foveal fixation) in response to circular test stimuli of 10° visual angle (radiant intensity I_p), superimposed on a steady background of 15° (30,000 td, 5500 K). Spectral composition of test pulse (λ) and adaptation light (μ) as indicated. A light pulse (*lowermost record*) of 20 ms duration with a repetition rate of 1 c/s was used. *Right* Plot of amplitudes N_1-P_2 (in the VECP) versus pupillary radiant intensity I_p for two wavelengths (602 nm and 575 nm). From these V-log I functions, the sensitivity was calculated by interpolating the radiant intensity I_p needed for a 5 μV amplitude criterion (*dotted line*)

the most effective wavelength is 575 nm, while above the intersection of the two functions, the 602 nm stimulus is more effective. A similar behavior of V-log I functions is reported also for the off-effect in the VECP by Jankov (1978). The flattening of the V-log functions indicates that *inhibitory* processes between the cone mechanisms are effective (see Naka and Rushton 1966b), especially noticeable when white backgrounds of higher intensities are used; this inhibitory interaction will be demonstrated in Fig. 6.17. These interactions lead to changes in VECP waveforms, noticeable in a break of the latency-vs-log I_p functions (see also Krauskopf 1973).

Spectral Sensitivity Functions. To determine an observer's spectral sensitivity, the reciprocal retinal radiant intensity I_p, necessary for a small criterion amplitude of 4.5 μV was interpolated from V-log I curves for each monochromatic stimulus and plotted against wavelength (Fig. 6.11).

Averaged spectral sensitivity curves of four normal trichromatic observers determined by a VECP amplitude criterion of 4.5 μV are depicted in Fig. 6.11. The R, G, and B function were obtained during exposure to

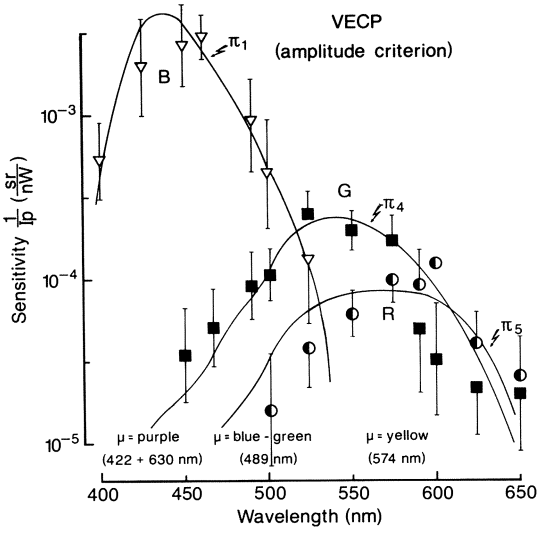

Fig. 6.11. Spectral sensitivity curves of 4 normal trichromatic observers (mean and S.D.) as determined by the reciprocal pupillary radiant intensity necessary to evoke a 4.5 μV amplitude criterion N_1-P_1 in the VECP. The R, G and B functions were obtained during exposure to a steady chromatic background μ (blue/green, purple or yellow, 30,000 td) of 15° visual angle, centered on the fovea. Remaining conditions as in Fig. 6.10. The corresponding Stiles' π-functions are represented by *solid lines*

strong monochromatic light of 30,000 td in order to diminish the sensitivity of two of the three assumed primary color mechanisms; a blue/green adaptation light (μ = 489 nm) was chosen for depressing the sensitivity of the B and G mechanism in order to reveal the R mechanism (*half-filled symbols* with peak sensitivity near 590 nm). A purple light (μ = 422 + 630 nm) depressed the B and R mechanism and yielded a function (*G*) with a peak sensitivity near 530 nm (*filled symbols*); yellow light depressed both the long-wavelength mechanisms' sensitivity and revealed a blue-sensitive mechanism (*B*) peaking near 450 nm (*open symbols*). Thus, these three functions represent the long-, middle- and short-wavelength-sensitive color vision mechanisms determined at the cortical level. The three functions represented by data points in Fig. 6.11 will be used below for the linear subtraction of the R and G functions in order to indicate the relative weight of the two mechanisms during white light adaptation, when several mechanisms are interacting antagonistically.

Comparison with the data on dichromats and monochromats (Figs. 6.13, 6.14, 6.16) will show that chromatic adaptation does not suppress parts of a mechanism but that it isolates individual mechanisms to a large degree (except at the spectral ends of each function, as pointed out below). For the problems involved in determining the spectral sensitivity function of single cone mechanisms see also Boynton et al. (1964a), Guth (1967), Regan (1968), Guth et al. (1969) and van Norren and Bouman (1976).

Comparisons with Sensory Measurements. Figure 6.12 represents spectral sensitivity functions obtained by measuring the *sensory* thresholds deter-

mined under similar conditions as in the VECP measurements. A modified staircase method (see Chap. 6.1), yielded functions similar to the electrically determined ones shown in Fig. 6.11. In presence of strong yellow adapting light (577 nm, *triangles*), the observer's spectral sensitivity is determined by that of the blue-sensitive cone mechanism; during purple adaptation (422 + 630 nm, *dots*), by that of the green sensitive cone mechanism; and during blue/green adaptation (487 nm, *squares*) by that of the red-sensitive cone mechanism. The three functions mainly resemble the Stiles' π_1, π_4 and π_5 functions. Under these conditions, the absolute sensitivity of the B mechanism was always higher than that of the R and G mechanism. This is in accordance with the data obtained in single cells with *chromatic* adaptation. Interestingly, when the determination of the spectral sensitivity of individual cone mechanisms is based upon the missing color ("Fehlfarbe") of

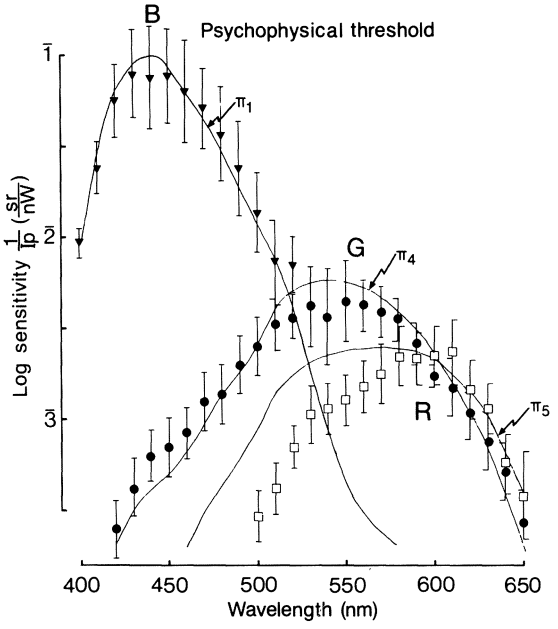

Fig. 6.12. Spectral sensitivity functions determined by psychophysical increment threshold measurements; mean and standard deviation in three normal trichromatic observers. A computerized staircase method (Little 1974; Chap. 6.1) was applied from which the mean value (frequency of seeing = 50%) and the standard deviation was calculated for four observers. The data of the blue-sensitive (*B*, *triangles*), the green-sensitive (*G*, *dots*) and the red-sensitive (*R*) system (*squares*) were obtained in presence of monochromatic yellow (577 nm), purple (422 + 630 nm) and blue/green (489 nm) adapting lights (16° in diameter, 80,000 td). The monochromatic test flashes (6° in diameter) were presented every 5-10 s for 400 ms. Stiles' π_1, π_4 and π_5 functions are represented by *solid lines*

dichromats (based on psychophysical color-matching experiments which do not suppress the activity of individual cone mechanisms as described by Vos and Walraven 1971, Paulus and Scheibner 1978), the sensitivity of the blue system has to be positioned very low, compared to that of the longer-wavelength-sensitive system. This is in close correspondence with the data obtained in blue-sensitive ganglion cells (Zrenner and Gouras 1981), which show low sensitivity in presence of neutral backgrounds, a high one however, in presence of yellow backgrounds. Apparently, in situations where both long-wavelength cones are active, the blue cones' action is suppressed to a certain degree, closely fitting the model given in Chapter 4.

Note that the sensitivity of the R function between 470 nm and 560 nm is about 0.2-0.4 log units lower than Stiles' (1959) π_5 mechanism, in both electrical and sensory measurements; in comparison with Stiles' mechanism, the G function shows a similar loss between 570 nm and 630 nm for VECP measurements only. This indicates that some weak antagonistic interaction between the R- and G-mechanism is still present, resulting in a narrowing of the functions (see also Foster 1980). The mechanism responsible for the narrowing of these functions was discussed in single color-opponent cells in Section 3.1 and will be subject of further discussion in Section 6.4 concerning opponent processes in the VECP.

Anomalous Trichromats. Anomalous trichromats are not included in these investigations. For recent papers on this issue based on colorimetry, see Wolf and Scheibner (1978, protanomaly) and Stöcker et al. (1979, deuteranomaly). It is of interest in this respect, that Alpern and Moeller (1977) have suggested from psychophysical data and Bowmaker (1981) from microspectrophotometric data that in normal human observers there are individual variations in the peak sensitivities of the red and green cone's pigment; they support the view that in anomalous trichromats both long-wave pigments are drawn from the same parent class, i.e., a deuteranomalous trichromat would have the two long-wave color channels originating from visual pigments drawn from two populations within the "red" class of cones. A similar theory was applied by Alpern (1981a,b) also to dichromatic vision, supported to a certain extent by psychophysical experiments (Kröger-Paulus 1980, Stöcker 1980). However, final proof for this hypothesis does not yet exist.

It should be noted that Yasuma et al. (1980) and Yasuma and Ichikawa (1981) reported a method of detecting also the non-affected *carriers* of congenital color vision defects by their lower ability to detect small flickering fields as compared to normals.

6.3.2 Dichromatic Observers

Incidence. In about 1.1%-9% of the male population and in about 0.3-1.04% of the female population, the function of one of the three fundamental cone mechanisms is defect or absent. The incidence reported varies with geographical location and ethnological factors (Waaler 1927, Garth 1933, François et al. 1957, Crone 1968, Jaeger 1972, Wagner 1974) In *deuteranopes* (1.4% of the European male population, according to the data collection of Wright 1946, p 303) the green-sensitive cone mechanism, in *protanopes* (1.2%) the red-sensitive mechanism and in *tritanopes* (0.0001% only) the blue-sensitive mechanism is deficient.

Due to the rareness of tritanopic observers, this type of dichromats could not yet be investigated in our laboratory. For literature on tritanopia see Wright (1952), Kalmus (1955), Sperling (1960), Walls (1964), Ohba and Tanino (1976), Alpern (1976), Padmos et al. (1978), for a new test van Norren and Went (1981). Their congenital character is questioned by Krill et al. (1970, 1971). There is another type of defect involving the blue-sensitive mechanism, the tetartan defect. Tetartanopia was postulated by Müller (1924) to allow for two types of blue-yellow defect parallel to the two types of red-green defect. In theory, tritanopia is considered a receptoral "blue" color defect and tetartanopia as a postreceptoral "blue/yellow" color defect (Judd 1943). For further references on the historical development of this differentiation see Linksz (1964); to date, there has been no documented case of *congenital* tetartanopia.

Since the very beginning of the investigation of color vision, the findings on subjects suffering from color vision defects played an important role in the development of theories of color vision. For reviews see among many others: Hillebrand (1889), von Kries (1897), Nagel (1898), Koellner (1929), Judd (1945), Müller (1924), Pitt (1935), Rosmanit (1914), Wright (1946), Graham and Hsia (1958), Kalmus (1965), Scheibner (1968), Hurvich (1972), Jaeger (1972), Heinsius (1973) and Walraven (1976).

Spectral Sensitivity in the VECP of Normals and Dichromats. Figure 6.13 shows spectral sensitivity functions obtained by Zrenner and Kojima (1976) with VECP criterion responses in normal, protanopic and deuteranopic observers; the data are compared with the CIE V_λ-function (*broken line*).

In normal subjects, steady exposure to purple light depresses the sensitivity at the long wavelength end of the spectrum resulting in a function with a maximum peak near 540 nm, essentially reflecting the spectral sensitivity of the G-cone mechanism; at 450 and 610 nm two rudimentary peaks are visible, indicating the remaining influence of the depressed B and R mechanisms, respectively. Exposure to blue/green light shifts the sensitivity maximum to 590 nm and leads to a sensitivity loss (hatched area) at shorter

wavelengths. The remaining function essentially reflects the spectral sensitivity of the R-cone mechanism.

Protanopes with an assumed deficiency of the red mechanism, when adapted to purple or blue/green light yielded very similar sensitivity functions. In contrast to the curves of normal individuals who, upon exposure

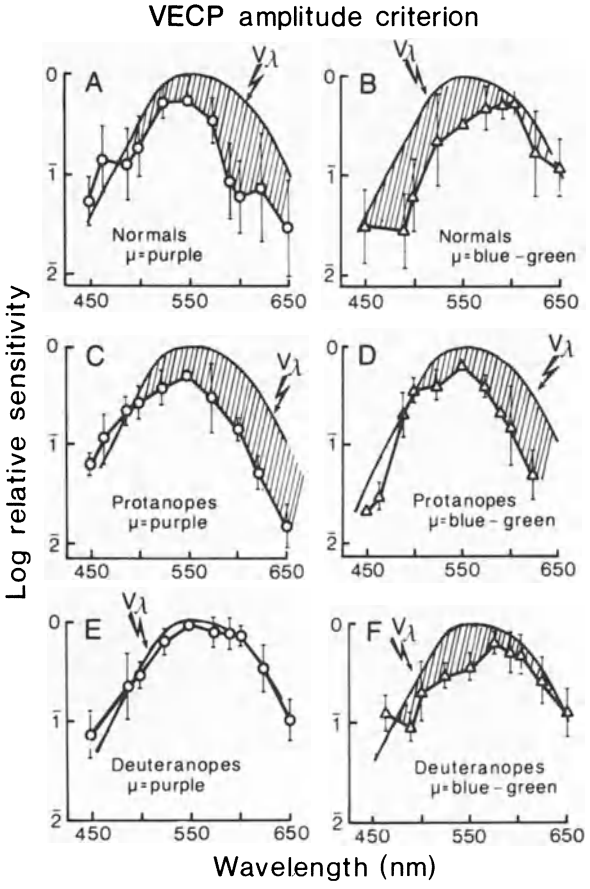

Fig. 6.13A-F. Relative spectral sensitivity functions (*thick lines*, mean ± S.D.) of three normals (**A**, **B**), three protanopes (**C**, **D**) and three deuteranopes (**E**, **F**), based on the measurement of a 4.0 μV *criterion amplitude of the VECP* in response to monochromatic light stimuli. Background illumination consisted of purple (μ = 422 + 630 nm; *circles*) and blue/green (μ = 489 nm, *triangles*) light of 80,000 td. The purple light was obtained by a additive mixture or two monochromatic lights. The interference filter used (Schott type PAL) had two transmission-bands (T), one with a maximum at 630 nm (bandwidth at $T_{max}/2$ = 50 nm), the other with a maximum at 422 nm (bandwidth at $T_{max}/2$ = 20 nm). The relation of the intensities of the two spectral bands was therefore fixed. The CIE photopic spectral luminosity curve (V_λ) is indicated by the *broken line*. The *hatched area* indicates the relative spectral loss of the spectral function compared to the V_λ-curve. Remaining conditions as in Fig. 6.10. (Modified from Zrenner and Kojima 1976)

to blue/green, exhibited a sensitivity loss at shorter wavelengths, those of the protanopes displayed a spectral sensitivity loss (*hatched area*) at longer wavelengths under *both* conditions of adaptation.

The spectral sensitivity functions of deuteranopes (with an assumed deficiency of the green mechanism) are quite different from those of protanopes when subjected to the same procedure. Exposure to purple light produced a spectral sensitivity curve that was essentially identical to the V_λ-function of a normal observer, whereas exposure to blue/green light produced a slight loss in the green part of the spectrum. These differences will be discussed in Section 6.6.

Comparison with Psychophysical Data. The corresponding psychophysical functions obtained by determing sensory increment thresholds are shown in Fig. 6.14; each data point represents the average value of three observers.

At wavelengths longer than 480 nm, the relation of each function to the V_λ-curve is qualitatively very similar to the data obtained by VECP measurements in Fig. 6.13. Thus, with chromatic adaptation and at low amplitude levels, a VECP threshold criterion shows good agreement with psychophysical data in normal and dichromatic observers. At wavelengths shorter than 480 nm and with blue/green adaptation (*triangles*), a second peak near 440 nm occurs in the psychophysical data, not seen in the VECP action spectra (Fig. 6.13). The blue-sensitive mechanism is apparently reflected differently in psychophysical and electrical data. This interesting discrepancy will be discussed in the next paragraph. Moreover, in presence of a purple background, protanopes do not show a peak near 440 nm as deuteranopes do under identical conditions; this clearly indicates a different interaction in the B/G (protanopes) and B/R (deuteranopes) system, as seen in Chapters 3 and 4 in single retinal ganglion cells.

6.3.3 The Peculiarities of the Blue-Sensitive Mechanism in the VECP

The blue-sensitive mechanism, when isolated by strong chromatic adaptation (Zrenner and Kojima 1976), shows some interesting characteristics. Results of experiments performed to investigate the blue mechanism are given in Fig. 6.15.

In normal individuals, purple adaptation of 80,000 td resulted in a predominantly green-sensitive function (*open symbols*) which closely corresponds to Stiles' π_4 function both in the sensory (**A**) and in the electrical measurements (**B**). The VECP threshold measurements are based on a 4 μV criterion amplitude which occurred after a latency of 95 to 125 ms. When the short wavelength transmission (422 nm) of the purple filter was cut off

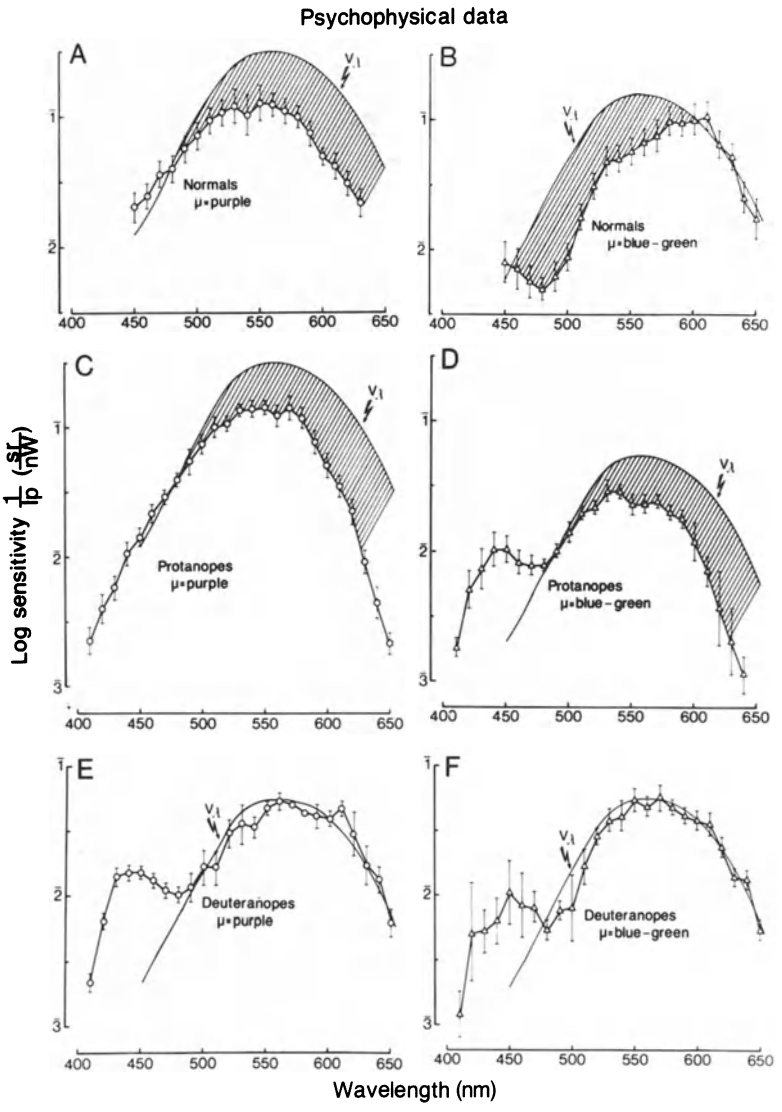

Fig. 6.14A-F. Spectral sensitivity curves determined by *psychophysical* increment threshold measurements; mean values and standard deviation of three normal individuals (**A**, **B**, derived from Fig. 6.12), three protanopes (**C**, **D**) and three deuteranopes (**E**, **F**). Background illumination (20,000 td) was either purple (422 + 630nm) or blue-green (489 nm). The CIE photopic spectral luminostiy curve (V_λ) is indicated by a *solid line*; it serves mainly for a comparison, to indicated the lacking mechanism (*hatched area*). Remaining conditions as in Fig. 6.12

by a Schott OG 5 absorption filter, the sensitivity at shorter wavelengths greatly increased in the subjective measurement of sensory thresholds and closely corresponded to Stiles' π_1 function (**A**, *filled symbols*).

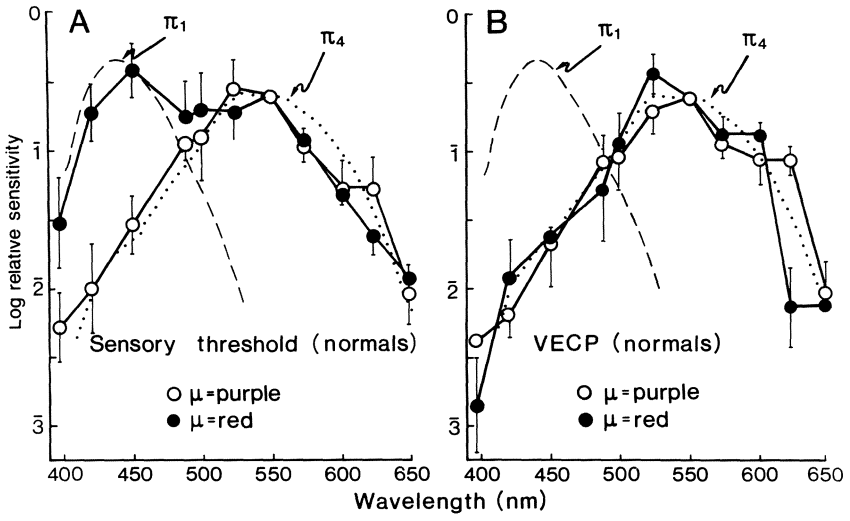

Fig. 6.15A, B. Relative spectral sensitivity curves of four normal observers (n = 6, mean ± S.D.) based on the measurement of sensory threshold (**A**) and on the measurement of a 4.0 μV criterion amplitude of the VECP in response to monochromatic light stimuli (**B**). Background illumination was purple light of 80,000 td (422 + 630 nm, *open circles*). For the description of the filter characteristics see Fig. 6.13. *Filled circles* indicate the change of sensitivity when the short wavelength transmission of the purple filter is cut off by an orange glass filter. Stiles' π_1 and π_4 mechanisms are indicated by *broken* and *dotted lines*, respectively. Remaining conditions as in Fig. 6.10. (Modified from Zrenner and Kojima 1976)

This is not seen in the electrical measurement of the VECP (**B**); exposure to the same blue-free adapting light exhibited a spectral sensitivity curve almost identical to that obtained during exposure to purple light. There was no sensitivity maximum in the short-wavelength part of the spectrum.

Obviously, the blue-sensitive mechanism is not revealed by the VECP criterion amplitude used under either condition of adaptation described above. Only when a smaller amplitude which occurs at longer latency (near 160 ms) is chosen as electrical criterion can the spectral sensitivity function of the blue-sensitive mechanism be measured during strong red or yellow adaptation (see Fig. 6.11). The short-wavelength mechanism therefore expresses itself in the VECP quite differently from the red- and the green-sensitive one, since it is marked by small amplitudes of long latency in the on-components (Zrenner et al. 1977) as well as in the off-components (Jankov 1978). This is in accordance with the findings of several other laboratories (see Walther et al. 1981).

The particular response properties of the blue cone mechanism, as seen in single retinal ganglion cells (Chap. 4), as well as in ERG recordings

(Zrenner and Gouras 1979a) and optic nerve potentials (Schuurmans and Zrenner 1981b), of cat clearly express themselves in cortical potentials as well.

6.3.4 Monochromatic Observers

Observers with only one receptor type (monochromats) are very rare, representing about 0.003% (Wright 1946) of the population. Nevertheless, over the years a considerable number of cases were reported (e.g., Hering 1891, König 1899, König and Dieterici 1893, von Kries 1897, Hess and Hering 1898, May 1907, Sloan 1954, Blackwell and Blackwell 1961, Alpern 1974). There are two general types, those who have only rods (rod monochromats or rod achromats) and those who have only one type of cones (cone monochromats). For observations on the various forms of monochromacy and its implications for the understanding of color vision, the interested reader is referred to Weale (1953), Walls and Heath (1954), Franceschetti et al. (1959), Alpern (1974), Lawwill (1978), Smith and Pokorny (1980), and Skottum et al. (1980). Interesting cases of *incomplete* or atypical forms of congenital achromatopsia were investigated by Jaeger (1950, 1951, 1958), Waardenburg (1963), van Lith (1973), Neuhann et al. (1978), Smith et al. (1978, 1979) and Hansen (1979). The recent study of Krastel et al. (1981) on several typical cases of achromatopsia showed that *large* stimulus areas (up to 120°) can often reveal remnants of a red receptor mechanism which appears even to interact with a shorter-wavelength-sensitive cone. *Strict complete* achromatopsia, diagnosed with this new criterion, can possibly be found only in every third "typical" congenital achromat (Krastel et al. 1982a) and practically in no case of acquired achromatopsia (Krastel and Jaeger 1982); all *three* cone mechanisms can even be present in cases of "achromatopsia" (Mollon et al. 1980).

A Case Report. In collaboration with the University Eye Clinic in Frankfurt/Main and with Dr. Teping (University Eye Clinic, Aachen) we were able to investigate a patient suffering from rod-monochromacy. The patient (E.L., female, age 56) reports that her father had tuberculosis and could not distinguish the colors green and blue; her brother suffers from convulsions, but has good vision; her daughter has normal vision. She is currently undergoing psychiatric treatment because of depressions; since age 3 she remembers having nystagmus, photophobia, and being color-blind.

Visual acuity (O.D. 0.07, O.S. 0.1) was constantly low over the years; the visual field showed normal limits; a central scotoma was present in both eyes; the lens was slightly opaque in both eyes; the anterior segment

and the optic disc (on both sides) appeared normal. Macula O.D. appeared to have a scar and to be slightly diffuse; macula O.S. seemed to be less pigmented; intraocular pressure was normal. The dark adaptation curve (Goldmann/Weekers adaptometer) was monophasic with normal thresholds in both eyes. The Farnsworth panel D-15 as well as the settings on the Nagel-anomaloscope clearly revealed an achromatic scotopic slope and position in both eyes, checked separately (see Fig. 6.2 and comments on the evaluation of such data in Jaeger and Grützner 1963, Verriest and Frey 1977). The Farnsworth-Munsell 100-Hue test yielded a high total error score (544, as shown in Fig. 6.1), with the maximal number of errors occurring near the blue/yellow and the scotopic axis. The electrooculogram was normal with a light/dark ratio of the standing potential of 2.14 O.D. and 1.88 O.S.; under scotopic conditions (see Zrenner et al. 1976) the electroretinogram revealed normal, under photopic conditions extremely subnormal V-log I functions; no oscillatory potentials were detectable. In the visually evoked cortical potentials no responses to small checkerboard stimuli (5-45 min of arc) could be found; responses to checkerboard stimuli larger than 45 min of arc (presented as single flashes in Ganzfeld mode) were subnormal. The patient could not detect flicker at frequencies beyond 18 c/s; this is in accordance with the electroretinographical data on critical flicker fusion frequencies in rod monochromacy of Schaternikoff (1902), Dodt and Wadensten (1954) and Dodt et al. (1967), with the evoked potential data of Van der Tweel and Spekreijse (1973) as well as with the early psychophysical measurements in monochromats of von Kries (1903) and Hessberg (1909).

The spectral sensitivity functions determined in our laboratory (Fig. 6.16, *below*), obtained with blue/green (487 nm, *squares*), yellow (577 nm, *triangles*) and white (*circles*) backgrounds after 40 min of dark adaptation were essentially identical, with a peak sensitivity near 515 nm. All data are very close to the CIE luminosity function for rod vision (V'_λ, *dotted line*) with the maximum slightly shifted to longer wavelengths. The small sensitivity elevation near 450 nm pointing to the influence of blue-sensitive cones and seen in the V'_λ curve as well as in normal trichromats (Fig. 6.16, *above*), is lacking in the monochromat. The dark-adapted, normal trichromats investigated under identical conditions show a slight elevation of spectral sensitivity also beyond 620 nm presumably caused by long-wavelength cones; the influence of cones in normal trichromats is possibly due to adaptational effects of repetitive stimulation (0.1-0.5 c/s).

While in normal observers different backgrounds yielded different sensitivity functions (Figs. 6.8 and 6.12), in this patient all backgrounds applied revealed only one type of sensitivity function; therefore, she most certainly has only one type of receptor. The similarity of the scotopic sensitivity

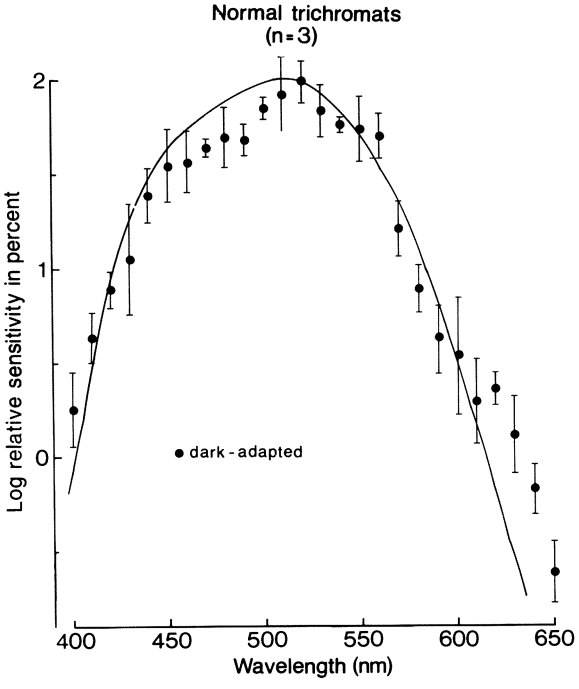

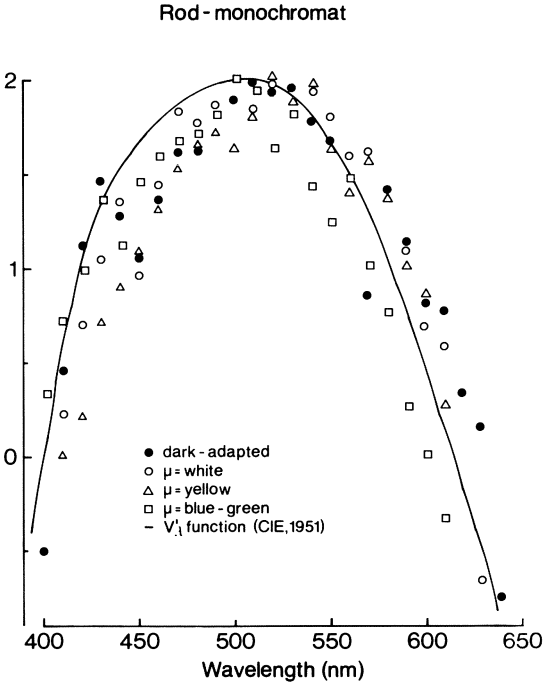

Fig. 6.16. Spectral sensitivity functions determined by sensory threshold measurements in normal trichromatic observers (*left*), mean and S.D. of six runs in three observers, and of a rod-monochromat (*below*). The data indicated by *dots* were obtained after 40 min dark adaptation, while the subject viewed a tiny red fixation mark (monochromatic light of 657 nm). Additionally, the rod monochromat's spectral sensitivity function was determined in presence of yellow (*triangles*) and blue/green (*squares*) adaptation light of about 10,000 td, as well as white adaptation light (*circles*) of about 100 td. The data obtained for normal observers under these light-adapted conditions can be found in Fig. 6.12 and 6.8. The scotopic luminosity function (V'_λ) is indicated by *solid lines*. Remaining conditions as in Fig. 6.12

function with spectral data obtained in light as well as in dark adaptation (Fig. 6.16, *below*) points clearly to rod monochromacy. The deviation from the short-wavelength branch of the V'_λ function and the slight shift of the maximum to longer wavelengths would disappear if the data points were corrected for absorption of the macular pigment (Wyszecki and Stiles 1967, p 219); this is valid, since the V'_λ refers to rod sensitivity undiminished by macular pigment. Typically, the patient shows low visual acuity and low critical flicker fusion frequency, a central scotoma and a single-branched, dark adaptation curve (which reached low threshold levels, resulting in a decrease of 5 log units during 25 min of dark adaptation). These data strongly support the diagnosis of congenital achromatopsia and thereby serve to demonstrate the function of a human visual system, which is based totally upon rod receptors. For the final diagnosis, the long-term course of this disease has to be considered, since also diffuse tapetoretinal degenerations can initially show symptoms that are very similar to those characteristic of rod monchromacy (Alexandridis and Jaeger 1978).

Visually evoked cortical potentials could not be utilized for recording spectral data, since the patient's willingness to cooperate declined after a few sessions. For electrophysiological data in rod monochromats, the interested reader is referred to Van der Tweel and Spekreijse (1973), Adachi-Usami et al. (1974a) and Klingaman (1977) for the VECP as well as to Alexandridis and Dodt (1967) for measurements of the pupillary light reflex, confirming the lack of a Purkinje-shift in rod monochromacy.

6.4 Color-Opponency in the VECP and in Psychophysical Measurements

6.4.1 Color-Opponency in Normal Color Vision

In color-opponent ganglion cells, antagonistic interactions between spectrally different cone systems take place which modify the spectral sensitivity function at the cell's output. The action spectra of the excitatory and inhibitory mechanism are narrowed and shifted apart, so that at the output of a color-opponent ganglion cell the spectral sensitivity function shows two narrow peaks, one for excitation, the other for inhibition (Chap. 3). Under conditions where the cone mechanisms are adapted to white background light in about equal proportions, enabling them to interact under daylight conditions, such spectral functions should also be detectable in higher visual centers. By determining such functions, psychophysical evidence of color-opponent processes was given by Sperling and Harwerth (1971), Harwerth and Sperling (1975) in macaque monkey and by King-

Smith (1975) and King-Smith and Carden (1976) in man. In colorimetry, certain problems can also be described best when color-opponent mechanisms are introduced (Valberg 1975, Richter 1979). Especially the analysis of color in terms of chrominance and luminance in a colorimetric system (Scheibner 1969) exhibits more the features of a color-opponent theory than of a trichromatic one, even though both are well compatible also in colorimetric terms (see Schrödinger 1925, Klauder and Scheibner 1980, Scheibner and Wolf 1982). Electrophysiological evidence was shown in graded potentials derived from the surface of monkey cortex by Padmos and van Norren (1975b). In man, only recent studies (Zrenner 1976, 1977a, 1982b, Jankov 1978) succeeded in revealing color-opponent processes in visually evoked cortical potentials.

Action Spectra. Figure 6.17 shows action spectra determined by electrical and psychophysical criteria indicating color-opponent processing in human observers. In contrast to the experiments described above, in which strong colored lights for selective chromatic adaptation were used (Fig. 6.11), in Fig. 6.17 increment spectral sensitivity functions during steady exposure to

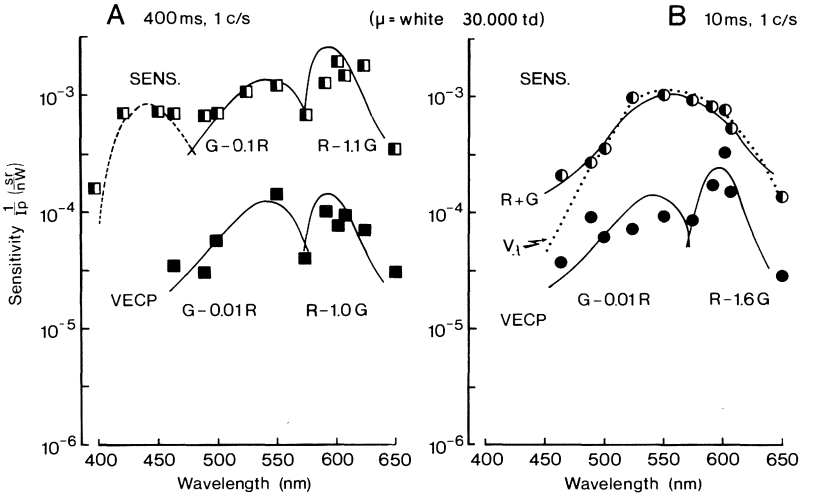

Fig. 6.17. Spectral sensitivity functions based on sensory thresholds (*half-filled symbols*) and VECP criterion thresholds (N_1-P_1 amplitude of 4.5 μV; *filled symbols*). Test light duration in part A is 400 ms (*squares*), in part B 10 ms (*circles*); repetition rate 1 c/s; test field size 10°. Each value represents the average of three experiments with observer J.H. during exposure to a white background of 15° visual angle (30,000 td). *Solid lines* were calculated by a linear subtraction of the functions $k_1 \cdot R$ and $k_2 \cdot G$ (Zrenner 1977a) as indicated under each branch of the functions. *Dotted line* is the CIE photopic luminous efficiency function (V_λ). *Broken line* represents the Stiles' π_1 function. (Zrenner 1977a, modified and corrected for loss in the ocular media)

a strong *white* background are shown. The results obtained with test flashes of long duration (400 ms) are given in part A. The sensitivity functions determined by means of the VECP as well as by sensory measurements exhibit broad, essentially two-peaked functions with sensitivity maxima near 610 nm and 525 nm, but with a trough near 575 nm. The shape of the curves can be described roughly by a linear subtraction similar to the model of Sperling and Harwerth (1971). The *solid lines* in Fig. 6.17 represent the values obtained by subtracting the weighted functions R and G from each other (see Zrenner 1977a); before the subtraction was performed, the logarithmic values were transformed back into a linear scale; the curve-fitting was performed by using the method of least squares with a DECLAB 11/40 system (see Chap. 6.1). The sensitivity curve in the middle wavelength range of the spectrum (*left branch of the solid lines*) is described by the expression $|G - k_1 \cdot R|$, the curve in the long wavelength section (right branch) by $|R - k_2 \cdot G|$. The values of k_1 and k_2 were computed to yield the best fit between the experimental data and the resulting function. Being relative values, k_1 and k_2 represent the relative participation of R and G for a given stimulus condition. The B mechanism was not considered in these calculations, even though in the sensory measurements (*half-filled symbols*) there is a clear elevation of sensitivity near 450 nm (*broken line*), which is lacking in the VECP data because of its peculiar response behavior described in Section 6.3. In both the sensory and the VECP measurements (Fig. 6.17A), k_1 is smaller than k_2, indicating that the participation of the G function in the subtractive process is stronger than that of the R function. These double-peaked, narrowed, and spectrally shifted functions with shapes typical of the spectral behavior of color-opponent ganglion cells clearly point to color-opponent processes originating in retinal neurons, being still active in the human visual cortex (Zrenner 1976, 1977a, 1982b).

Shortening the stimulus duration to 10 ms (Fig. 6.17B) causes the sensitivity trough at 574 nm to disappear; the spectral sensitivity function determined by subjective achromatic thresholds (*half-filled circles, above)* approaches the CIE photopic luminous efficiency function (V_λ, *dotted line*). The difference in sensitivity between the chromatic and the achromatic threshold, i.e., the photochromatic interval, becomes considerably smaller. Thus, the photochromatic interval not only depends on the state of adaptation (Spillmann and Conlon 1972) but also on stimulus duration.

The VECP-sensitivity function (*filled circles*) on the other hand retains the trough evidenced with short stimulus durations also with longer periods of stimulation. The peak in the red part of the spectrum is increased in accordance with the results of Krüger (1977), who in cortical cell populations of rhesus monkey found a predominance of red-sensitive cells apparently present already in the retina (see Section 3.4). While the psychophysically

determined sensitivity curves are best described by an addition of the R and the G function (*upper solid line*), the VECP sensitivity function obtained with flashes of short duration still requires subtraction of R and G functions (*lower solid line*).

Conclusion. Padmos and Graf (1974) and Padmos and van Norren (1975b) recorded locally from monkey visual cortex and found the bandwidth of the spectral sensitivity functions to be narrower than the action spectra of the individual cone mechanisms. Gouras and Padmos (1974) concluded from studies on the visual cortex of rhesus monkey that color-antagonistic interactions are also reflected in graded responses of the foveal striate cortex. The experiments carried out by Zrenner (1976, 1977a, 1982b) showed that similar mechanisms operate within the *human* visual cortex and that it is possible to describe these interactions by means of a linear subtraction procedure.

The effect of stimulus duration upon the spectral sensitivity in sensory measurements was explained by Ikeda and Boynton (1962) in terms of shifts in the threshold versus stimulus duration. Regan and Tyler (1971) found that the critical duration for the detection of a change in wavelength at the subjective threshold is longer than that for the detection of a change in luminance. By sensory threshold measurements, King-Smith (1975) and King-Smith and Carden (1976) found spectral sensitivity functions to be strongly dependent on stimulus duration as well as on frequency; they suggested that these differences might be caused by differences in the temporal and spatial integration properties of a luminance and a color-opponent system (for discussion of this model see Chap. 5). In contrast to common psychophysical methods, VECP thresholds permit the determination of spectral sensitivity functions in a range well above the sensory threshold. As shown here, suprathreshold measurements reveal color-opponent interactions under all conditions of stimulus duration and intensity. In the simultaneously determined sensory threshold, however, color-opponent interactions were seen only with *long* stimulus durations. These results can be explained if we assume that the maximum integration time of 10-20 ms for cones represents another type of threshold; barely visible flashes of longer duration than the maximal integration time would represent suprathreshold stimuli detected by the color-opponent system with its longer integration time. Considering the data shown in Fig. 6.17, the color-opponent system would be activated if a certain critical number of quanta above the threshold were exceeded, regardless of whether the suprathreshold condition is defined by the critical stimulus duration or by stimulus intensity. The electrophysiological basis of this phenomenon can be assumed to rest upon synchronization mechanisms similar to those shown in Sections 5.3 and 5.6;

when very short flashes are applied, cellular on- and off-responses occur almost simultaneously; the excitatory phases of both the inhibitory and the excitatory mechanism therefore can easily synchronize, so that color-opponency is lost (see also Fig. 5.8).

Sperling and Harwerth (1971) state that the strength of antagonistic interactions between the red and the green receptor responses increase as the fovea becomes adapted to higher intensity levels of white light. The VECP data presented show that this also occurs as the duration or intensity of *suprathreshold* stimulation is increased. Obviously, additive processes dominate near the sensory threshold, while at suprathreshold levels subtractive, (antagonistic, color-opponent) interactions predominate. Taking into consideration the dependence of action spectra and color-opponent processes on stimulus duration and intensity, as well as on the state of adaptation, it should become evident that the CIE photopic spectral luminosity (V_λ-) function does not at all describe human photopic spectral sensitivity in a constantly changing environment. On the other hand, Regan (1970) measured spectral sensitivity by means of the second harmonic of the VECP and found that it closely fitted the V_λ function. However these experiments employed a flicker method, which causes additive processing (Sections 5.3 and 5.6) between spectrally different cone mechanisms and cannot reveal antagonistic processes easily. This problem will be discussed further in Section 6.5, along with the relevant data.

6.4.2 Color-Opponency in Congenital Color Vision Deficiencies

Color-opponent processes, expressed in multipeaked, narrowband spectral sensitivity functions (of Fig. 6.17) were subsequently studied by psychophysical methods in dichromatic and monochromatic individuals including numerous control experiments in normal trichromats. As shown in Fig. 6.18, 26 wavelengths from 400 to 650 nm served as test lights in presence of *white* background (30,000 td); as described in Section 6.1, each wavelength was presented eight times in a computerized staircase-method; this "up-and-down method" for small samples, developed by Dixon (1965) and modified by Little (1974) improved the precision of threshold determination considerably, so that the standard deviation usually decreased to almost ± 0.1 log units. The curves of normal observers (n = 8, *squares* in Fig. 6.18) showed three very pronounced sensitivity peaks near 435, 530, and 610 nm, separated by dips near 489 and 570 nm; the latter wavelengths correspond well to the neutral points seen in B/L and R/G opponent ganglion cells (Fig. 3.4). Protanopes lack the peak near 610 nm, but still show opponency between the blue- and the green-sensitive mechanism since the

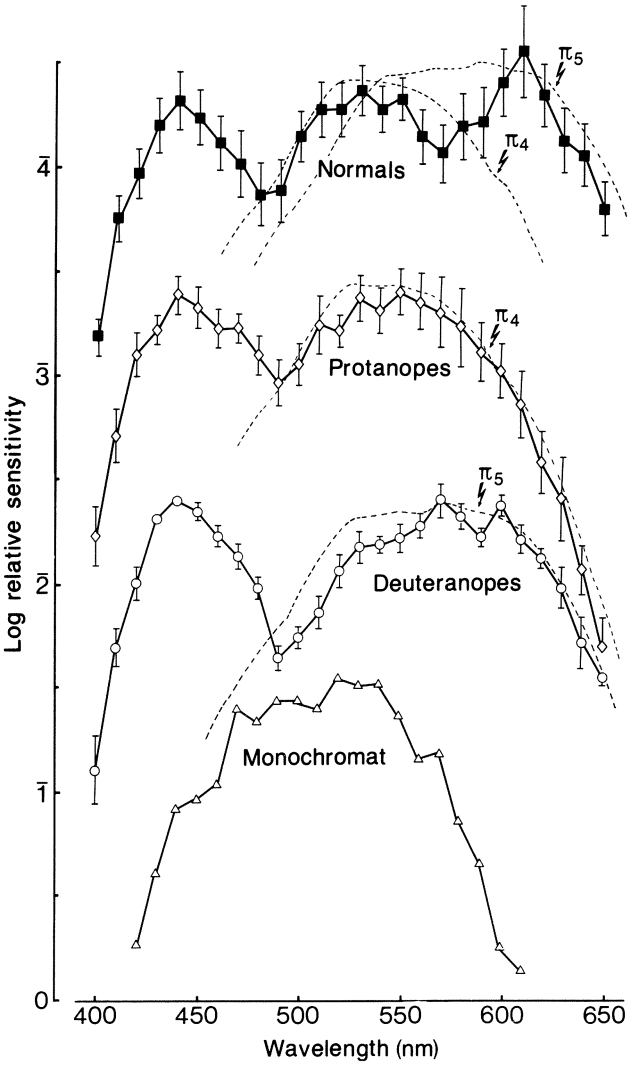

Fig. 6.18. Spectral sensitivity functions, based on psychophysical increment threshold measurements (sensory threshold, mean and ± S.D.) during light adaptation to a white background (5500 K) of 30,000 td in eight normal, two protanopic, two deuteranopic and one monochromatic observer. (Modified from Baier and Zrenner, in prep.). Other conditions as in Fig. 6.12. Curves were shifted along the Y-axis to prevent overlapping. Stiles' functions indicated by *broken lines*

action spectra are slightly narrower than the corresponding π-functions. Deuteranopes show sensitivity maxima near 580 and 435 nm with a very pronounced dip near 490 nm; their sensitivity in the blue/green region is considerably reduced, not seen with flickering stimuli (Fig. 6.27). The discussion in the literature, whether deuteranopes have a "luminosity loss" in

their spectral sensitivity function or not (see Heath 1960, Graham and Hsia 1960) might be based to a certain extent on specific methodical differences in determining sensory thresholds either with single flashes or with flickering lights.

Both types of dichromats report the sensation "white" near 490 nm, which represents the neutral point observed in ganglion cells of the B/L type (Fig. 3.4, *triangles*, sensitivity plotted upside down). Since the bandwidth of the individual peak in these functions is smaller than the fundamental cone functions (see Fig. 6.11), especially in the blue-sensitive part of the spectrum, color-opponent processing is still present in these types of congenital color vision defects at least to the same degree as in normals. In a monochromat, however (E.L., triangles in Fig. 6.18), only a single-peaked function with a maximum near 515 nm is seen under these conditions. This monochromatic patient's spectral function is not altered by light adaptation as pointed out in Fig. 6.16; any indication of color-opponent interaction is lacking in monochromats.

6.4.3 Acquired Color Vision Deficiencies

Visual defects caused by toxic agents often affect color vision as one of the first clinical symptoms. In acquired color vision deficiencies, the receptors and the other retinal neurons might be affected in very different ways. It therefore appears useful to apply psychophysical and electrophysiological tests for differentiating between defects in receptoral layers and the neuronal processing of chromatic signals at the more proximal retinal layers. The spectral sensitivity of the receptors themselves is mainly defined by pigment-absorption; yet spectral sensitivity functions of retinal neurons are changed considerably by color-opponency as demonstrated in the previous chapters. As shown above, typical *color-opponent spectra* recorded in single cells can also be demonstrated in human cortical processing, psychophysically as well as electrophysiologically in the visually evoked cortical potential (VECP). Thereby they provide a new tool for the investigation of acquired color vision deficiencies.

A detailed survey of acquired color vision deficiencies would lie beyond the scope of this book. The interested reader is referred to reviews by Wright (1946), François and Verriest (1957 a,b,c, 1961), Jaeger et al. (1961), Jaeger and Grützner (1963, 1966), Waardenburg (1963), Cruz-Coke (1970), Grützner (1972), Marré (1973), Lyle (1974a,b), Verriest (1974), Pinckers (1975), Marré and Marré (1978) and Pokorny et al. (1979b, see especially their Chap. 8, written by Birch et al.)

6.4.3.1 Acquired Red/Green Defects

A Drug-Induced Loss of Color-Opponency. Many of the pathophysiological alterations caused by toxic agents which influence color vision still remain unresolved. Therefore, it might be of interest to apply the methods described above to a subject with an acquired color vision deficiency. Together with Dr. C.J. Krüger from the University Eye Clinic in Hannover, the spectral sensitivity functions in patients suffering from damage caused by Ethambutol (Myambutol®, a tuberculostaticum) were determined by psychophysical and electrophysiological methods on various backgrounds. The experiments revealed that Ethambutol mainly affects opponent processing in red/green color-opponent neurons, while signals of the three spectrally different types of cones are still present in the visual cortex (Zrenner and Krüger 1981).

Case Report. A female patient (A.W., age 49) took a total of 200 g Ethambutol over a period of 8 months as treatment for tuberculosis of the urinary tract. Over a period of six weeks her visual acuity suddenly decreased to 0.3 (O.D.) and 0.2 (O.S.). Except for slightly pale optic disks, the fundus appeared normal. Visual fields determined by Goldmann perimetry were concentrically narrowed in both eyes. The Haitz campimeter revealed a small central scotoma for all colors. The Nagel anomaloscope settings were positioned along the deuteranopic line from 0 to 73 (cf. Fig. 6.1). Confusion in the Farnsworth-Munsell 100 Hue test (F.M. 100 Hue) occurred mainly along the deutan and protan axes with a a large total error score in both eyes (488 O.D. and 544 O.S.)[10]. The electro-ophthalmological investigations (see Zrenner et al. 1976) revealed a normal EOG with the light peak reaching a ratio of 254% of the basis value. The scotopic and photopic ERG were completely normal. In the VECP the peak latency was found to be delayed by about 20 ms when evoked by diffuse, flashed light stimuli. Stimulation with checkerboard patterns of various sizes in the central 5° of the retina showed pathological responses of reduced amplitude except when stimulated by squares of 36' visual angle; stimulation of peripheral retinal parts, with the foveal region blocked out, evoked normal responses.

The determination of spectral sensitivity functions on yellow, purple and blue-green backgrounds revealed that the same three fundamental cone mechanisms (B, G, and R) could be isolated, which are present in normal observers (Fig. 6.19a). However, as demonstrated in Fig. 6.19b, in presence

10 For the problems involved in the classification of acquired color vision defects with pseudo-isochromatic tables see Birch-Cox (1976). Interestingly, digitoxin has a similar effect on the confusion in the Farnsworth-Munsell 100 Hue test (Alken et al. 1980)

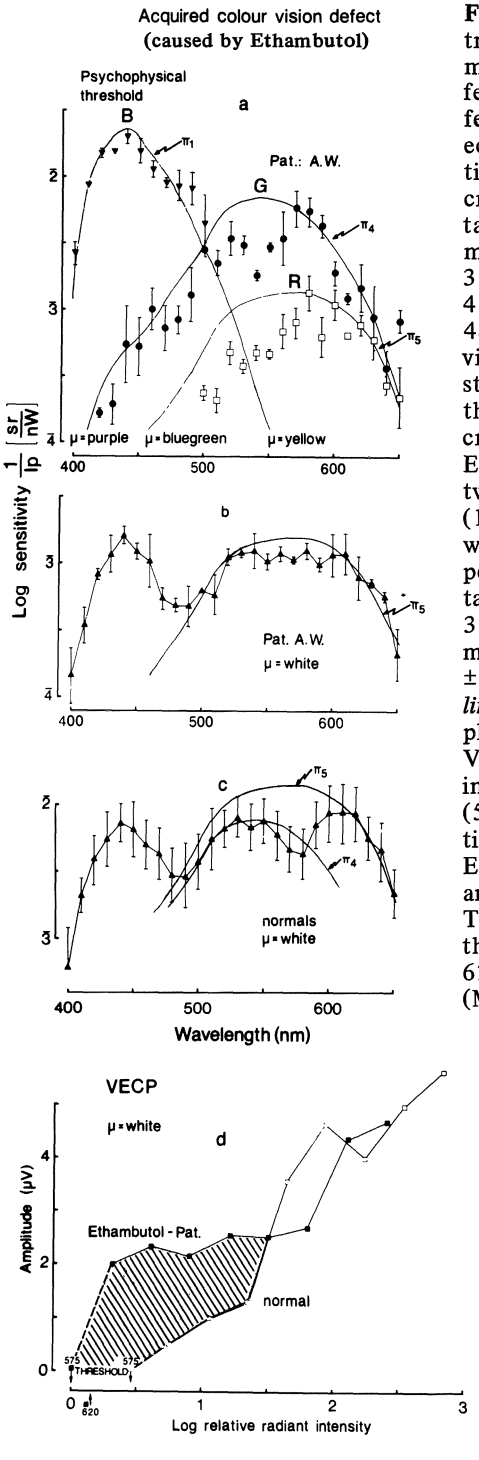

Fig. 6.19. a Chromatically separated spectral sensitivity functions of the three cone mechanisms (*B*, *G*, *R*) in patient A.W., suffering from an acquired color vision defect caused by Ethambutol. Data points fitted to corresponding Stiles (1959) π-functions (*solid lines*). The psychophysical increment threshold measurements were obtained during chromatic adaptation to monochromatic yellow (*triangles*; 574 nm, 3.3 log td), purple (*dots*; 422 + 630 nm, 4.1 log td) and blue/green light (*squares*; 487 nm, 3.9 log td). **b** The spectral sensitivity function determined in presence of strong *white* adapting light (3.7 log td) in the same patient, lacked the sensitivity decrease at 575 nm seen in normals (*below*). Each data point represents the mean of two measurements, matching the Stiles (1959) π-functions (*solid line*) in the long wavelength part of the spectrum. **c** Three-peaked spectral sensitivity functions, obtained during adaptation to white light of 3.7 log td and by psychophysical threshold measurements in 12 trichromats (mean and ± S.D.). Stiles' π_4 and π_5 functions (*solid lines*) are drawn in for comparison. **d** Amplitude of the first positive peak of the VECP, plotted against the pupillary radiant intensity of monchromatic test lights (575 nm, 400 ms duration) during adaptation to white light (4.2 log td) in the Ethambutol-patient A.W. (*filled squares*) and in a normal trichromat (*open squares*). The data are scaled on the X-axis, so that the psychophysical thresholds (*arrows*) at 620 nm are equal for both observers. (Modified from Zrenner and Krüger 1981)

of a white background the opponent interactions between the long and medium wavelength mechanism, as seen in normal (Fig. 6.19c), are lost in this patient. While in a normal trichromatic observer the spectral sensitivity follows a three-peaked function with peaks near 440, 530, and 610 nm, in this patient the dip near 570 nm is lost, so that a broad function emerges in the long-wavelength region. This part of the patient's spectral sensitivity function mainly resembles the Stiles π_5-function, or at least indicates a *synergistic* action between the red and green mechanism. Consequently, in these patients the *antagonistic* interactions between the green- and the red-sensitive mechanism seem to be lacking, while the receptors, including their individual pathways up to the visual cortex and perceptual areas, are not affected. Only when the dominant red- and blue-sensitive mechanism is considerably weakened or suppressed by strong purple light (Fig. 6.19a, *dots*) can the green-sensitive mechanism provide *some* opponent action on the red mechanism, as indicated by the dip at 550 nm. Apparently, even with purple adapting light, the green-sensitive mechanism is not dominant enough to determine the threshold throughout the entire spectrum, as seen in normals. Only the *absolute* sensitivity is reduced by 0.3-0.8 log units, an observation made already by Adachi-Usami et al. (1974b) in the VECP of Ethambutol patients.

While the psychophysical data serve more as indicators of the presence or absence of subtractive interaction at the visual threshold, the action of opponency in the *suprathreshold* range can easily be shown in the V-log I function of the VECP (Fig. 6.19d). As a routine clinical measurement, this was performed only for the critical wavelength of 575 nm, where the dip in the spectral sensitivity function is most pronounced in normals. On the X-axis, the data were scaled in such a manner that the radiant intensities required for producing a threshold sensation at 620 nm (where *only* the red mechanism is active) are equal for normals (*open squares*) and for patient A.W. (*filled squares*). Her threshold was about 0.2 log units *lower* at 575 nm than at 620 nm (*arrows* at the X-axis).

This is qualitatively the case for both wavelengths also in a Stiles π_5 function. The thresholds of normal observers, however, are about 0.3 log units *higher* at 575 nm than at 620 nm, due to the antagonistic interactions in normal observers (see threshold difference for both wavelengths in Fig. 6.19d, *bottom*). When the radiant intensity is increased, both V-log I functions initially rise over a range of about 0.5-0.7 log units (*hatched area*). Ultimately, however, the patient's V-log I function also shifts to the right by more than 1 log unit, indicating an increasing action of color-opponent processing between the two long-wavelength-sensitive cone mechanisms. At high test light intensities, the patient's data also match those of normals in which color-opponency was acting already from the psychophysical thresh-

old on. Consequently, color-opponent neurons are functioning despite the damage caused by Ethambutol, but only at distinctly suprathreshold levels. It is not surprising, then, that patient A.W., having stopped Ethambutol for half a year, performed perfectly on the normal Panel D-15, while on the desaturated version, large confusions still occurred along the red/green deficiency axis. In the period from Sept. 15, 1979 to May 9, 1980, she also improved on the matching range on the Nagel-anomaloscope, still showing deutan-like matches. The error score on the Farnsworth test decreased from 488 to 292 on the right eye, and from 544 to 328 on the left eye. In the psychophysical threshold measurements, few changes occurred, excepting a more pronounced peak at the red end of the spectrum; the visus also gradually increased to 0.6 OD and 0.45 OS. (for further details see Zrenner and Krüger 1981)

The Implications of a Functional Loss. In acquired color vision deficiencies caused by Ethambutol, the toxicity of this drug apparently does not manifest itself primarily at the receptoral level, since the ERG is normal and all three fundamental cone mechanisms remain unaltered up to the visual cortex. However, the signs of color-opponent interactions are lost in the spectral data on white backgrounds. It becomes very clear that Ethambutol mainly affects the function of those cells which provide the antagonistic interaction between red- and green-sensitive neurons on which *color-opponent* processing vitally depends (Zrenner and Krüger 1981).

Candidates for being affected by Ethambutol in the early stages of the afferent visual system would be the horizontal cells and/or the amacrine cells connecting the pathway of red- and green-sensitive cones (cf. Fig. 4.7), thereby providing color-opponent processing, which is revealed in retinal ganglion cells (see Gouras and Zrenner 1981b, Zrenner and Gouras 1981). It is very improbable that the patient's small central scotoma can have an effect, since in normal trichromats, color-opponent processes produce three-peaked spectra at least up to 7.5° retinal eccentricity, when eccentric fixation is employed. Still, the loss of color-opponent processing may have taken place at higher levels of the visual system as well. Very high dosages of Ethambutol (1300-1600 mg/kg/day) applied over 6 months in rhesus monkey (Schmidt 1966) caused demyelinization of the optic nerve. This would point to a loss of color-opponency due to pooling of information normally carried by individual, well-isolated fibers of the optic nerve. Such a high dosage was only applied experimentally, and lies far above the critical therapeutical level of 25 mg/kg/day (Leibold 1966) which still can cause damage of visual functions in about 0.5% to 1.5% of patients (Pau and Wahl

1974, Thaler et al. 1974). The pathological latency increase seen in the VECP indicates that at least in early stages of *cortical* processing of visual stimuli the defect manifests itself very clearly.

Interestingly, the action of the green-sensitive cone mechanism seems to be more strongly affected than that of the red-sensitive one, as judged from the spectral sensitivity functions and the performance on the Nagel anomaloscope. This is less surprising, since the green-sensitive cones functionally dominate in the fovea (see Chap. 3). Ethambutol probably affects the function of foveal elements to a higher degree than that of perifoveal ones; this becomes evident in the Haitz test, since scotoma for green stimuli appear earlier than for red ones (Stärk 1972), usually reversible after the intake is stopped. The fact that mainly the green-sensitive system's function is affected would also fit Köllner's (1912) rule, according to which those deutan-like defects should be caused by damage in the optic pathway. However, this rule is not unequivocally accepted, as exceptions commonly occur (Jaeger 1954, Jaeger et al. 1961, Marré 1970, 1973, Grützner 1972). According to Grützner (1966, 1972) and Verriest (1974), the position of the neutral band gives additional information about the site of the defect. Patient A.W.'s neutral bands were broad and positioned around 500 nm, while all colors longer than 520 nm were reported as more or less orange ("like fire" according to A.W.), while those shorter than 480 nm appeared bluish.

The damage is, with some exceptions, neither necessarily complete nor irreversible; strong chromatic stimuli show color-opponent processing also in these patients; color vision and visual acuity improved after stopping the intake of Ethambutol. The neutral bands, as revealed by a color-naming procedure (rather than by a matching experiment) therefore undergo considerable variations which are difficult to quantify.

Ethambutol apparently causes a retrobulbar neuropathy and consequently only secondarily a red/green color vision defect, as becomes evident from previous clinical reports (first by Carr and Henkind 1962, for a list of subsequent literature, see Verriest 1974, Pokorny et al. 1979b). The damage affecting particularly the function of color-opponent neurons might be a common feature of many types of retrobulbar neuritis, when combined with demyelinization and color vision defects. It is not necessarily the *loss* of color-opponent tonic *ganglion* cells itself which produces such action spectra (as suggested by King-Smith et al. 1980) but in cases like the one shown here, a loss of certain *functions* of these cells. Such damage must not necessarily be restricted to the color-opponent mechanisms, but can include damage of *receptor* mechanisms as well, as in a comparable case described by King-Smith et al. (1976). Defects in the color-opponent pro-

cessing can also be observed in cases of tobacco-amblyopia and some forms of retrobulbar neuritis (Zisman et al. 1978).

The hypothesis of Leber (1873) and Fick (1896), that a certain type of deuteranope can have three classes of visual photopigments but a "neural fusion" of signals of the red and green mechanism could also be reflected in this clinical case. A modified version of their theory would be that the loss of antagonistic interaction between the red- and green-sensitive cone mechanism apparently causes a deuteranopic confusion pattern, although all three cone mechanisms are present; the transition from antagonistic to synergistic processing of two of the three cone mechanisms would produce the Fick-Leber types of "fusion dichromats". On the other hand, there are certainly pathological cases where the defect in a specific cell system at a higher level of the visual system causes selective losses in color vision; such cases were reported, e.g., by Rovamo et al. (1982) and Ruddock (1980), usually involving disturbances in *cortical* processing. As shown by Zihl and von Cramon (1980) the underlying pathological mechanism of color vision disturbances can even be localized far beyond the visual cortex, such as in a disconnection from the language areas, resulting in a specific disturbance of color naming (see also review of Meadows 1974).

In Summary. The clinically applied electrophysiological and psychophysical tests described here permit the detection of signals of all three types of spectrally different cones up to the visual cortex; moreover, they allow to differentiate clearly between the *loss* of a receptor mechanism and a *defect* in the neuronal interaction between these cones in the human visual system. The method of investigation described here permits differentiation between toxic alterations affecting the cone receptor and their direct pathways to the visual cortex from those disturbing the action of color-antagonistic mechanisms, upon which chromatic as well as spatial coding strongly relies.

6.4.3.2 Acquired Blue/Yellow Defects

A Drug Affecting the Blue Cone Mechanism. In the course of an experimental series on the action of a new, non-glycoside, non-adrenergic, positive inotropic substance (AR-L 115 BS, Thomae, registered as VARDAX) on the visual system (see Kramer et al. 1981, 1982, Zrenner et al. 1982b), *spectral sensitivity functions* were measured in normal, trichromatic observers before, during, and after the action of this drug. Its chemical structure {2-[(2-methoxy-4-methylsulfinyl)phenyl]-1H-imidazo (4,5-b) pyridine} shows some similarity with methylxanthine derivatives and most possibly influences the cellular metabolism of calcium (Diederen and Weisen-

berger 1981) by inhibiting phosphodiesterase (details below); moreover, from a serum level of 900 ng/ml on, this drug causes significant errors in the Panel D-15 and Farnsworth-Munsell 100-Hue test along the tritan and tetartan axes (Zrenner et al. 1982b). Figure 6.20 shows action spectra of an experimental series, based on increment threshold measurements, determined by a computerized staircase method (Zrenner 1982a). In presence of a strong white background light, monochromatic test flashes were projected in Maxwellian view into the volunteer's eye. Before the injection of AR-L 115 BS, his spectral sensitivity followed a three-peaked function

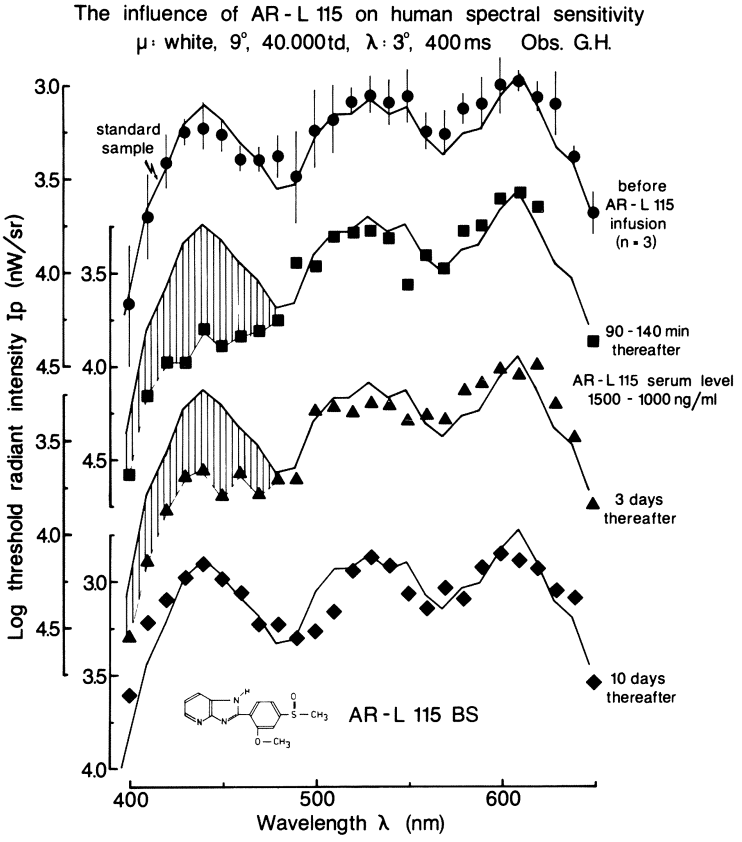

Fig. 6.20. Increment spectral sensitivity functions of observer G.H. (*filled symbols*) before (*bars* indicate ± S.D. of three trials) and several times after the infusion of AR-L 115 BS, a positive inotropic cardiotonicum. The psychophysical threshold for a monochromatic test flash (λ) of 400 ms duration and 3° visual angle was determined in presence of a steady white background light (μ) of 40,000 td and 9° in diameter. The serum level of AR-L 115 BS was continuously monitored; cardiotonic levels (above 900 ng/ml serum) were obtained only up to 3 hours after infusion. (Zrenner et al. 1982b). The patient's data are compared with those of our standard sample (*solid lines*) obtained in 6 normal trichromats. (Zrenner 1982a)

(*dots*) closely that of our standard sample (*solid lines*) determined in six observers. The action spectrum, measured between 90 and 140 min after the injection of 30 mg AR-L 115 BS (followed by an infusion of 4.2 mg/min for 40 min) shows a drastic change (*squares*), as reported by Zrenner (1982a); the peak sensitivity of the blue cone section (near 440 nm) decreases by 0.6 log units under the influence of AR-L 115 BS, while the rest of the action spectrum is unchanged. Even 3 days after the injection, when the serum level of AR-L 115 BS has long returned below the critical level of 900 ng/ml, the blue cone mechanism still has not yet recovered (*triangles*); only 10 days later does the B-cone's sensitivity approach its initial level (*diamonds*).

Transient Tritanopia Under AR-L 115 BS. To investigate this disturbance in the blue-sensitive mechanism further, experiments testing the transient tritanopia after the offset of yellow adapting light were undertaken, using a modified procedure developed by Mollon and Polden (1977b). For details on the particular method employed here see Zrenner (1982a,b), for a model of the underlying electrophysiological mechansims see Section 4.3. As shown in our standard sample in Fig. 6.21 (*upper left*), the threshold for a 440 nm test flash (determined by a modified staircase method) paradoxically rises by about 2 log units after the offset of a yellow adapting light (10,000 td). Since the blue cones were not affected by the yellow light, their sensitivity to the blue test light must have been controlled by a longer-wavelength-sensitive mechanism as described in Sections 4.3 and 4.4. The initial subsequent threshold decrease can be described by an exponential function (see *inset* of Fig. 6.21 for the formula). The deviation from this general time course is rather small among normal observers (curves are normalized at 300 ms) and it was never observed that any observer's threshold during the 2 s of the yellow light's interruption fell considerably below the value obtained during the yellow adaptation (*leftmost data points*). However, when these measurements were performed in observer G.H. under the influence of AR-L 115 BS (*upper right* of Fig. 6.21) a very pronounced threshold decrease was observed, especially at the lower end of his e-function, as described by Zrenner (1982a). Compared with his function before the AR-L 115 BS injection (*top center*), the threshold fell by about 2 log units. Only slowly, in the course of days (*lower row*), did the threshold rise to its initial values. Interestingly, the phenomenon of transient tritanopia itself, observed during the first 200 ms after the yellow light's offset, is not affected. The threshold for blue light also is not considerably affected in presence of yellow light (which leaves the blue cone dark-adapted); apparently, AR-L 115 BS influences mainly the blue cone's course of dark adaptation.

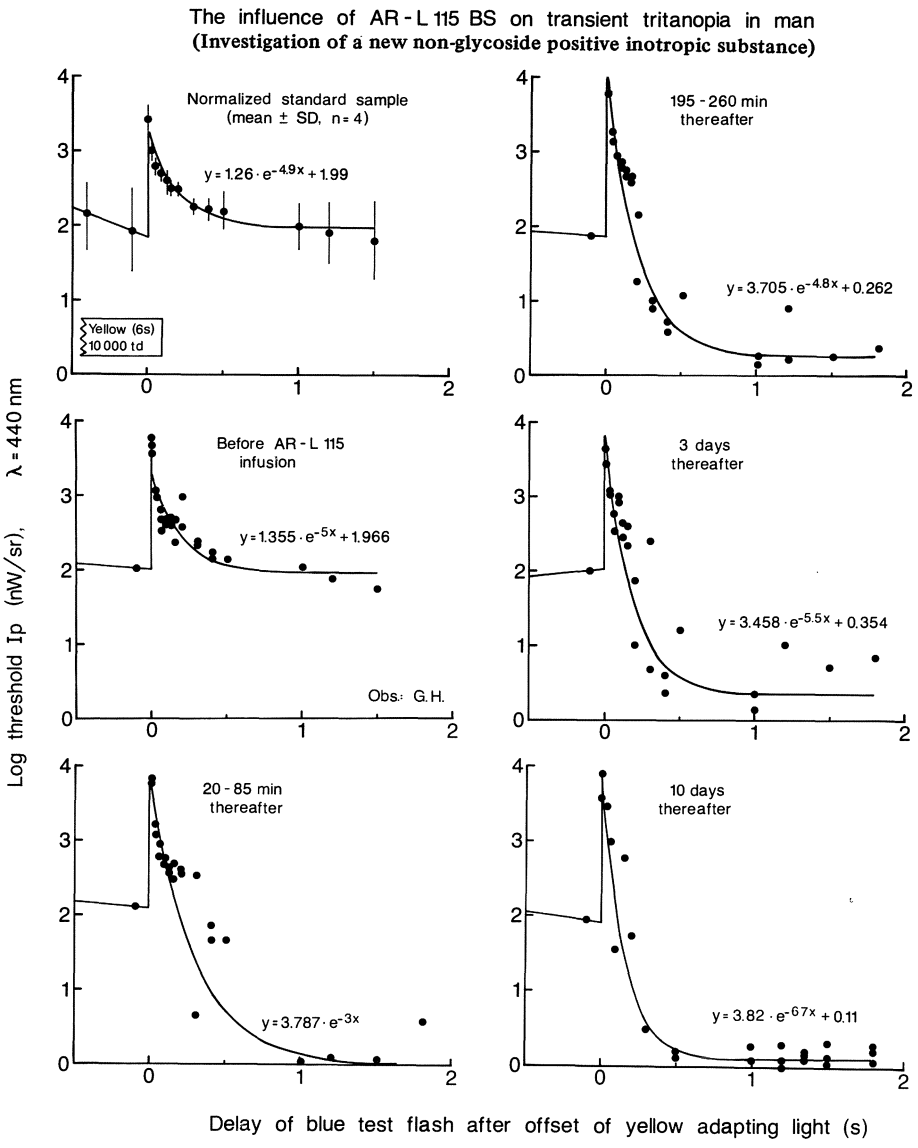

Fig. 6.21. The influence of AR-L 115 BS on transient tritanopia in man. In normal observers (*upper left*) the threshold for a blue test light (440 nm; 20 ms duration) rises by about 2 log units after offset of a yellow adapting light (bar, 10,000 td) and falls subsequently in the fashion of an e-function (formula as indicated). Observer G.H. (*upper middle*) behaves like a normal before AR-L 115 BS infusion; however, the threshold falls much faster (2 log units/first second) after infusion of AR-L 115 BS. The effect continues for several weeks. (Zrenner 1982a)

Standing Potentials Under AR-L 115 BS. Electro-oculographic measurements reflecting the standing potential generated by interaction between receptors (predominantly rods) and pigment epithelium revealed that the receptor layer is affected more than the post-receptoral cells. Before the administration of AR-L 115 BS, the standing potential of volunteer O.P. rose to a value of 160% of its dark value, 9 min after switching on a white test light of 320 cd/m^2 (following 40 min of dark adaptation), reaching a minimum of 70% during the 22nd min. AR-L 115 BS administered in the way described above caused his standing potential to rise considerably above 200% (maximum) and 85% (minimum), 40 min after the injection. The decrease in standing potential observed after 95 min is well correlated to the drug's serum level (Zrenner 1982a). The control measurements obtained after 10 weeks still show lowered thresholds. This indicates that AR-L 115 BS increase the metabolic processes in the receptor layer, to which the pigment epithelium responds passively after light stimulation; consequently, pathological changes observed with AR-L 115 BS are most probably located in the receptor layer.

The Possible Site of Action of AR-L 115 BS. AR-L 115 BS has a pronounced long-term effect on the blue-sensitive cone mechanism, while the red- and green-sensitive cones do not seem to be strongly affected. The rod system's responses are depressed as well, as could be demonstrated in electroretinographical recordings by Zrenner et al. (1982b). In the following, a hypothesis will be advanced which explains the receptor-specific reactions to AR-L 115 BS in terms of their different calcium metabolism. It seems appropriate first to discuss shortly the role of calcium in photoreceptors, and to explain to what extent AR-L 115 BS could influence this metabolism. Based on tests with noradrenaline and AR-L 115 BS, Diederen and Weisenberger (1981) provided strong evidence that AR-L 115 BS inhibits the phospho-diesterase (PDE in Fig. 6.22) which is necessary to metabolize cyclic AMP adenosine monophosphate; in cardiac muscle fibers this can produce an increased release of Ca^{2+} from the sarcoplasmatic reticulum and inhibit the re-uptake of calcium (Trube and Trautwein 1981). A corresponding mechanism was reported for cyclic-GMP guanosine monophosphate in vertebrate photoreceptors (Cavaggioni and Sorbi 1981). Since both cGMP and cAMP are present in outer segments of receptors (see Hagins 1979), the Ca^{2+} concentration in the receptor's cytoplasm can, initially, easily be raised by AR-L 115 BS until control mechanisms such as a phosphokinase-stimulated Ca^{2+}-pump can become active. On the other hand, any change which affects the cytoplasmic level of Ca^{2+} affects the flow of dark current in the receptors. As pointed out by Yoshikami and

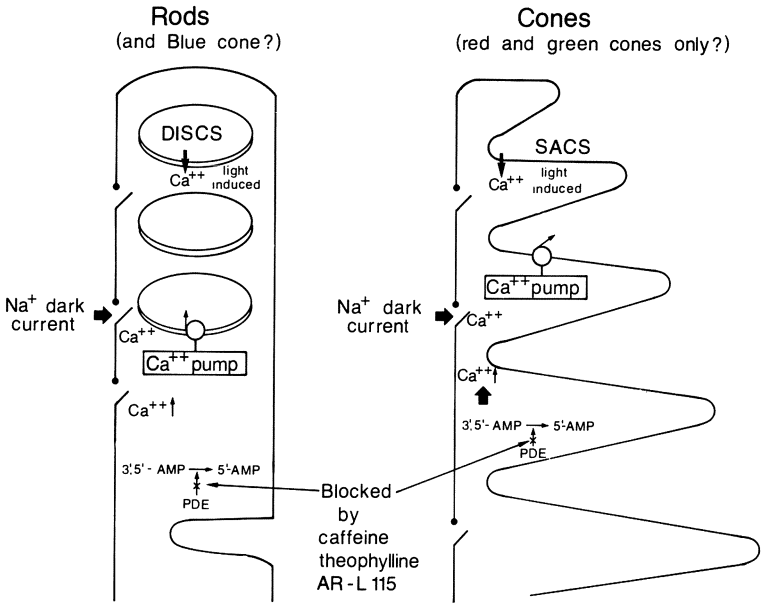

Fig. 6.22. Hypothesis to explain the differences between rods and blue-sensitive cones on the one side and red- and green-sensitive on the other. As deduced from experiments in cardiac muscle fibers (see text) AR-L 115 BS inhibits the phosphodiesterase (*PDE*); this increases the concentration of cyclic AMP (found also in receptors besides cyclic GMP) so that the cytoplasmic Ca^{2+} concentration increases. Red and green cones can pump the Ca^{2+} surplus into the extracellular space through their sac-like membranes. Rods and probably blue cones would lack an effective Ca^{2+} disposal system due to their disk structure, so that the increased Ca^{2+} level can cause the long term response suppression observed after intravenous injection of AR-L 115 BS in man. (Zrenner 1982a)

Hagins (1973), the receptor's dark current is lowered by an increased Ca^{2+} supply; the light-sensitive current is increased when the Ca^{2+} supply is reduced (Hodgkin et al. 1981). In short, the mechanism is as follows: according to the widely accepted model of Hagins (1972), Ca^{2+} acts as intracellular transmitter in receptor outer segments, modulating Na^{+} conductance. In the dark, the receptor membrane is kept depolarized by a constant inflow of Na^{+} (Tomita 1970). Absorption of an illuminating photon releases about 100 Ca^{2+} ions from one rhodopsin molecule and decreases the membrane's conductivity for Na^{+}, thereby hyperpolarizing the cell and producing a photoresponse. On the other hand, an increased cytoplasmic level of Ca^{2+} can close a large number of Na^{+} channels already in the dark, so that Ca^{2+} ions, released by light, could easily beome less effective. When the blue cone is light-adapted in a steady state, large additional amounts of Ca^{2+} ions are released and could totally block the sodium conductance, when the Ca^{2+} metabolism is changed by external influences such as AR-L 115 BS. If in

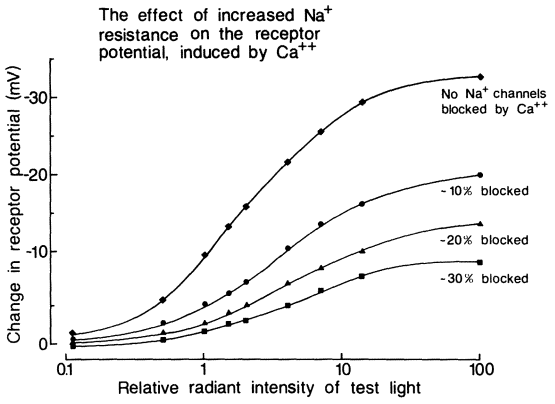

Fig. 6.23. Intensity/response functions as obtained by calculation of the membrane potential (in mV) in the electrical circuit shown in Fig. 4.10. The abscissa indicates the increments of $R_{Na\ blue}$ in relation to $R_{Na\ dark}$ (which was set at 1). Blockage of Na^+ channels, as simulated by adding a fixed resistance to $R_{Na\ dark}$ as well as to $R_{Na\ blue}$ compresses the intensity/response function, just as it was seen in the human ERG, after adding AR-L 115 BS. The more calcium channels are blocked, the more pronounced a compression is observed. (Zrenner 1982a)

the electrical model (Fig. 4.10) the influence of additional Ca^{2+} ions on the intensity/response function for blue test lights is calculated (Fig. 6.23), a compression of the functions indeed takes place, as was observed for the rod-ERG (see Zrenner et al. 1982b); consequently, an increase of calcium ions, induced by AR-L 115 BS, can explain the desensitization observed, on the basis of Hagin's (1972) model.

On the other hand, in the dark-adapted state, an increase of cytoplasmic calcium due to AR-L 115 BS can speed up the Ca^{2+} pumps, to ensure removal of Ca^{2+} surplus. This might be the reason for the higher speed of threshold decrease in the experiments on transient tritanopia during AR-L 115 BS (Fig. 6.21).

A Speculation Based on the Calcium Hypothesis. Can the effect of AR-L 115 BS on the Ca^{2+} metabolism be different in rods and cones? As Hagins (1972, 1979) pointed out in his model (on which Fig. 6.22 is based), in cones Ca^{2+} is pumped out from the cell since their *infolded* sac-like membranes can lose Ca^{2+} directly to the extra-cellular fluid. In rods, Ca^{2+} has to be stored mainly intracellularly since rod disks, which carry the photopigment molecules, are not extensively infolded (Cohen 1970); the decreased ability of rods to lower their intracellular Ca^{2+} level consequently reduces their light sensitivity when the Ca^{2+} level is raised by AR-L 115 BS. This could explain why the photoresponse, measured in the human ERG, is reduced, and the ERG V-log I functions are compressed, just as in Fig. 6.23

(see Zrenner et al. 1982b). In cones, however, calcium can be much more easily removed from the cytoplasm; consequently, since the dark current (Na^+-conductivity) is maintained, the action of the light-induced Ca^{2+} release is not inhibited. On the contrary, since an even greater amount of Ca^{2+} (acting as transmitter) would be present in the sacs of these cones, the photoresponse would be increased slightly in presence of AR-L 115 BS. This would explain why rods and cones respond quite differently to AR-L 115 BS.

Since AR-L 115 BS affected exclusively rods and *blue*-sensitive cones, but not red- and green-sensitive ones, the Ca^{2+} metabolism of blue-sensitive cones can be expected to be more similar to that of rods than of red- and green-sensitive cones. In addition to the many similarities between rods and blue cones listed above, they would share the handicap of not being able to remove Ca^{2+} quickly into the extracellular space. This leads to the speculation that the blue cones' *anatomical* structure of the outer segment might be less sac-like than that of the other cone types, and more disk-like, resembling rather membrane structures of rods.

6.5 The Influence of Flicker Frequency on Spectral Sensitivity

As shown in Chapter 5, color-opponent retinal ganglion cells lost their chromatic antagonism at higher flicker frequencies, so that their sensitivity changed from a double-peaked, opponent action spectrum to a single-peaked, non-opponent one (cf. Fig. 5.3); since this occurred in a single cell, it was emphasized in Chapter 5 that it is not necessary to postulate two functionally and anatomically different systems as being responsible for these two types of action spectra. The experiments described in Chapter 5 showed that synchronization processes between the center and surround mechanism take place, so that antagonism is turned into synergism.

Electrophysiological Recordings in Man

The experiments with flickering stimuli described above raise the question whether the change of chromatic information processing as indicated by the spectral sensitivity functions in Figs. 5.3 and 5.8 is only detectable in a single ganglion cell or whether it is also present in the electrical responses of a larger population of neurons in the visual system. The visually evoked cortical responses recorded from human scalp, shown in Fig. 6.24 and Fig. 6.25 will provide a clue toward answering this question.

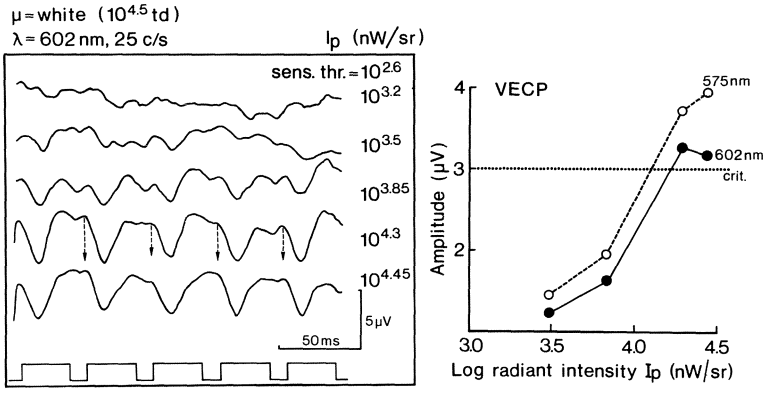

Fig. 6.24. *Left* Averaged VECP's (n = 128) of a normal trichromatic observer in response to circular test stimuli of 10° visual angle superimposed on a steady background of 15°. Spectral composition of test pulse (λ) and adaptation light (μ) as indicated. The radiant intensity of the test stimulus is indicated beside each record. The incidence of the light pulse is shown by upward deflection of the lowermost record. The repetition rate is 25 c/s. *Right* Plot of VECP-amplitudes averaged from 4 cycles (see *arrows* on the *left side*) versus pupillary radiant intensity I_p for two wavelengths (575 and 602 nm). From these V-log I functions the sensitivity was calculated by interpolating the inverted I_p necessary to evoke a 3 μV amplitude criterion in the VECP (*dotted line*). In contrast to the data obtained with low repetition rates (Fig. 6.10), the amplitude rises about equally for both wavelengths shown

Recordings obtained under the same conditions as in Fig. 6.10, but with the test stimulus frequency raised to 25 c/s are shown in Fig. 6.24 (*left*). About 0.5 to 1.0 log units above the sensory threshold (*thr.*) a small, uniformly modulated potential emerges which could be called steady-state potential (Regan 1972); at medium intensities of stimulation a double-peaked response predominates, while at $10^{4.45}$ nW/sr, the two peaks merge. The averaged amplitude of the second, usually more pronounced peak of each response (*arrows*) is plotted against test light radiant intensity on the right of this figure (*filled circles*). In contrast to the single flash condition (Fig. 6.10), a change from 602 nm to 575 nm (*open circle*) does not significantly alter the slope of the voltage versus intensity relation so that signs of two spectrally different antagonistic mechanisms are lacking in these functions.

Therefore, when the sensitivity of the observer to these and to eight other monochromatic lights is defined by an amplitude criterion of 3 μV and plotted against wavelength, a single-peaked, broadband sensitivity function results (Fig. 6.25, *triangles*); this action spectrum resembles to a large degree the V_λ-function, in contrast to its double-peaked shape observed at lower flicker frequencies (*squares*, plotted from Fig. 6.17, *left*) which could be matched (*solid lines*) only by subtractive procedures. Thus, as was seen

in single cells (Fig. 5.3), the loss of color-opponent processing between red- and green-sensitive cone mechanisms can be observed also in larger populations of cortical neurons at higher flicker frequencies (Zrenner 1977b). Since the results obtained in a single retinal cell are so similar to the results obtained in the VECP, there is probably no need to invoke separate cell systems in terms of luminance or chrominance channels to explain the alterations that occur in spectral sensitivity functions at low and high flicker frequencies. These data therefore support the hypothesis of Zrenner and Gouras (1978a,b) and Gouras and Zrenner (1979a) that at higher flicker frequencies the antagonistic interaction between spectrally different cone mechanisms is changed into a synergistic one. Phase shifts in the steady-state cortical potentials evoked by differently colored flickering lights (Regan 1973) might well be caused by such cellular mechanisms.

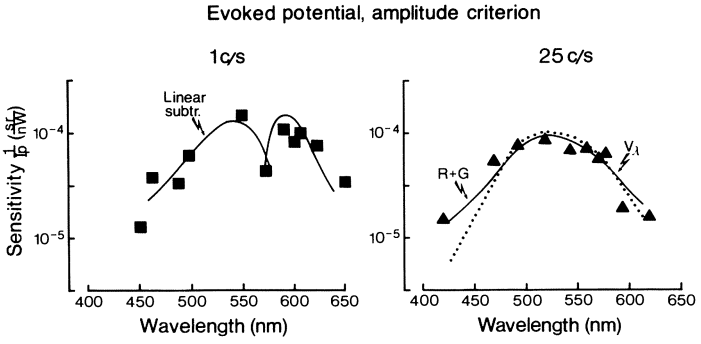

Fig. 6.25. Spectral sensitivity functions obtained in three normal trichromats (average value) by a VECP amplitude threshold criterion for low (1 c/s, *squares*) and high (25 c/s, *triangles*) repetition rates in presence of white background of 80,000 td. *Solid lines* on the *left* side represent a *subtraction* of the spectral R and G function (cf. Fig. 6.17), those on the *right* side a linear *addition* of the same functions. *Dotted line* indicates the CIE V_λ-function

Psychophysical Data

Considering these results, it is not surprising that psychophysical data on spectral sensitivity (Marks and Bornstein 1973, King-Smith 1975, Drum 1977) also show a marked dependence on flicker frequency. An example of the effect of flicker rate obtained with the computerized staircase-threshold method (see Chap. 6.1) is shown in Fig. 6.26.

At low frequencies of stimulation (Fig. 6.26, *left*), the spectral sensitivity function of a normal observer as determined with single test flashes of long duration does not at all resemble the V_λ-function, but clearly exhibits three peaks which are created by the interaction of the red-, green- and

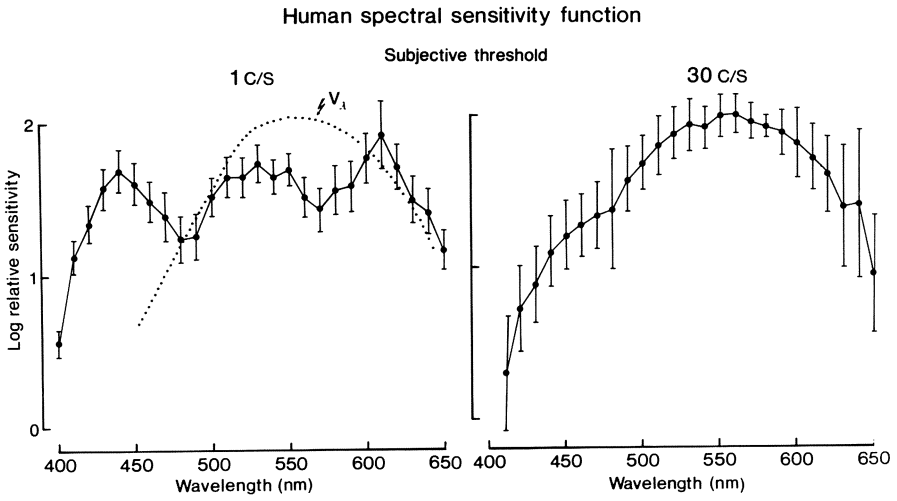

Fig. 6.26. Spectral sensitivity functions obtained by determination of the subjective threshold sensation for single flashes (*left* 1 c/s, 400 ms duration) and a flickering field (*right* 30 c/s, 33 ms duration) of 6° in diameter in presence of white background (20,000 td, 20° in diameter). Average values of 4 normal trichromatic observers (mean ± S.D.). *Dotted line* represents the CIE V_λ-function. (Modified from Zrenner 1982b)

blue-sensitive mechanism[11]. Only at high frequencies of stimulation (Fig. 6.26, *right*) does the curve resemble the V_λ-function, with the short wavelength part slightly enhanced, due probably to the large test field (see Stabell U. and Stabell B. 1980). Thus, the loss of opponent processing at higher frequencies of stimulation, seen in single ganglion cells of monkeys (Chap. 5), is also evident in psychophysical data of man. Consequently, when flickering test stimuli are applied, the presence or the loss of color-opponent processing (cf. Fig. 6.19) cannot be detected in increment threshold functions.

It should be emphasized that human spectral sensitivity for non-flickering stimuli of relatively large areas, as they are most often presented by our environment, clearly follows at threshold the *three-peaked* function of the type shown in Fig. 6.26 (*left*); since this function is determined by *achromatic* increment thresholds (i.e., by a colorless sensation), it is very difficult to assign the V_λ-function generally to a luminosity channel as is often done in psychophysical investigations (see Chap. 5 for references). The V_λ-function determined by heterochromatic flicker photometry (see Wyszecki and

11 In the VECP data of Fig. 6.25 the peak produced by the blue-sensitive cone was clearly less pronounced than in the psychophysical data for reasons explained in the discussion of Fig. 6.15

Stiles 1967) is obviously only valid in special cases, as in flickering stimuli or in minimally distinct border techniques (see Section 5.7.2). This is supported by sensitivity measurements of the pupillary reaction, which also follows the three-peaked sensitivity function when stimuli of long duration are employed (Krastel et al. 1982b, in prep.).

Flicker Studies in Normal Individuals as Compared with Flicker Responses in Protanopes and Deuteranopes

Fig. 6.27 represents the increment spectral sensitivity functions obtained in normal trichromats for the detection of flicker (*filled symbols*) and hue (*open symbols*) at five flicker rates obtained with a centrally fixated circular stimulus field superimposed on a steady white background. The flicker rate was varied by a motor which rotated a sectored disk with a 1-to-1 light to dark ratio. The test light's radiant intensity was increased stepwise and the subjects were asked to indicate the first appearance of flicker in the stimulus field, irrespective of an eventually appearing brightness or hue component; this threshold will be called flicker threshold in the following (*filled symbols*). In a second, similar trial, the subjects were asked to indicate the first appearance of a color in the stimulus field, again irrespectively of an eventually occurring flicker or brightness component; this threshold will be called hue threshold (*open symbols*). For control they were asked to choose a name for the color out of seven given terms. The final threshold was based on the mean value of four settings of the neutral density wedge for the appearance and disappearance of flicker and hue, respectively. From the position of both thresholds in the graphs it can easily be deducted whether the observer saw a non-flickering or a flickering color field, a colored or an colorless flickering field.

At 3 c/s, flicker threshold as well as hue threshold functions evidence three peaks with sensitivity maxima at 450, 530, and 610 nm[12]. As frequency increases, the flicker threshold function *gradually* approaches a one-peaked curve with a maximum near 550 nm. In contrast to the flicker threshold data, the hue threshold functions continue to be three-peaked at higher rates of stimulation and maintain a high sensitivity, particularly in the short-wavelength portion of the spectrum. Examination of the curves obtained with 30 c/s stimulation rate reveals a "cross-over" of the flicker and hue functions, so that below about 480 nm the subject sees hue before flicker, while above 480 nm the subject sees flicker before hue; this could

12 These data were presented at the Symposium of the International Research Group of Colour Vision Deficiencies in Brighton, U.K. 1979 (see also Klingaman et al. 1980)

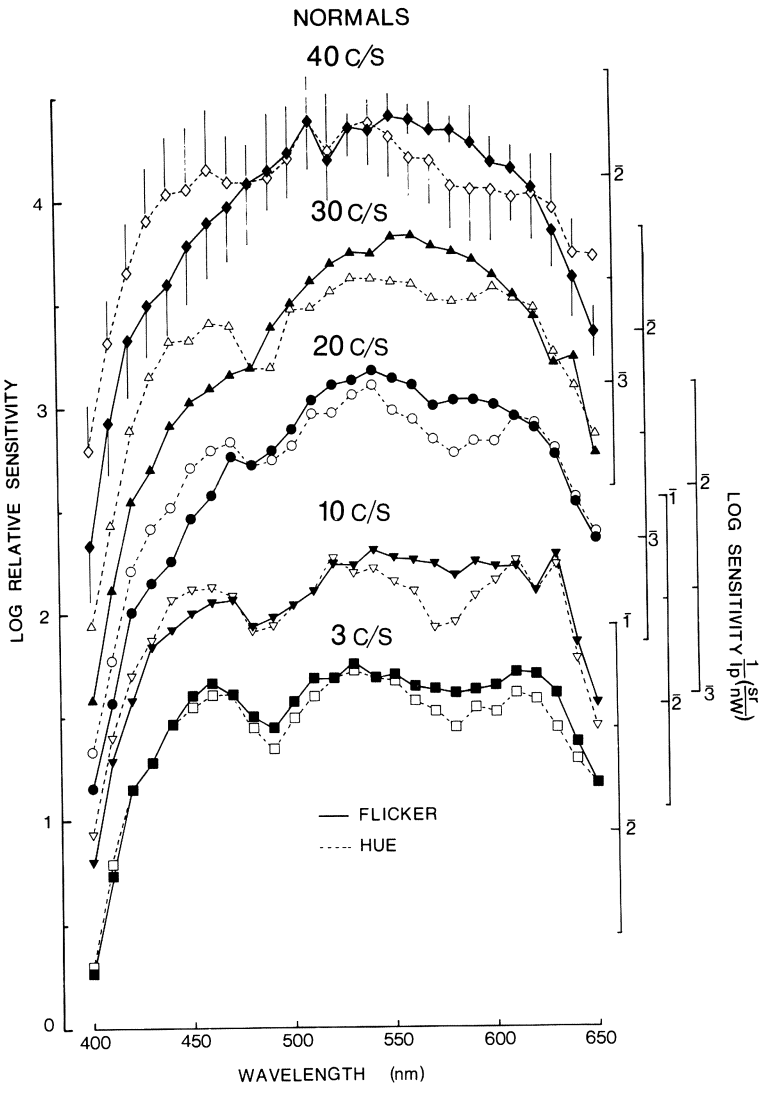

Fig. 6.27. Spectral sensitivity functions based on thresholds for the detection of flicker (*solid lines*) and hue (*broken lines*) for five different flicker rates (mean and S.D. of four normals). The monochromatic test lights subtend a visual angle of 6°, superimposed on a white (5500 K) background of 16° (20,000 td). For each stimulation frequency the flicker and hue curves have been displaced upward by 1 logarithmic unit to prevent overlapping. The right-hand ordinates indicate the absolute sensitivity values for each pair of curves. Thresholds were determined manually as described in Chap. 6.1. (Klingaman et al. 1980)

be correlated to the "photochromatic interval" (Monroe 1924, Graham and Hsia 1969) which is strongest near 575 nm. At 40 c/s an additional "cross-over" takes place near 620 nm.

Neurophysiologically, the "cross-over" indicates that a transition in detection takes place between color-opponent and non-opponent cells; at high frequencies of stimulation, color-opponent cells are more sensitive below 490 nm and above 620 nm than non-opponent cells. However, opponency as revealed by the three-peaked function is considerably weakened at higher frequencies (40 c/s), where the hue threshold functions become relatively broadband with a dominant maximum at 540 nm. In some of the opponent cells, depending on the temporal properties of their center and surround, the synchronization is optimal (see Chap. 5); these cells are the most

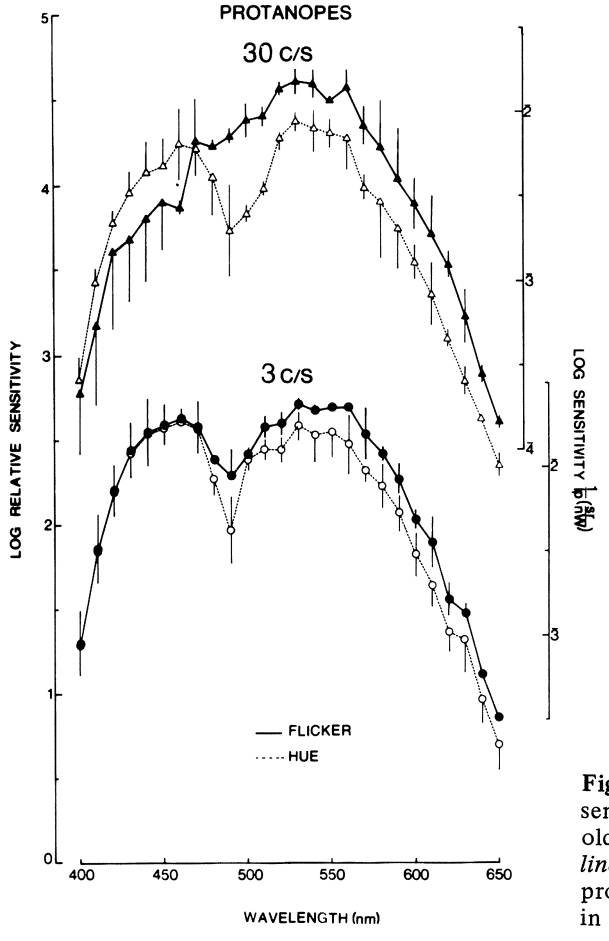

Fig. 6.28.A Increment spectral sensitivity curves based on thresholds for detection of flicker (*solid lines*) and hue (*broken lines*) in protanopes. Other conditions as in Fig. 6.28B

probable candidates for detecting flicker (*solid symbols*), however, they lose color-opponency due to the synergistic action of center and surround (see Chap. 5). Therefore the flicker threshold curve is broadband, possibly with some little deviations, due to beat-frequencies, i.e., resonance between center and surround excitations, occurring at some wavelengths (such as the consistent deviation at 530 nm in Fig. 6.27, 40 c/s). The blue cone system apparently does not contribute much to the detection of flicker at higher frequencies, whereas it is strongly involved in hue detection.

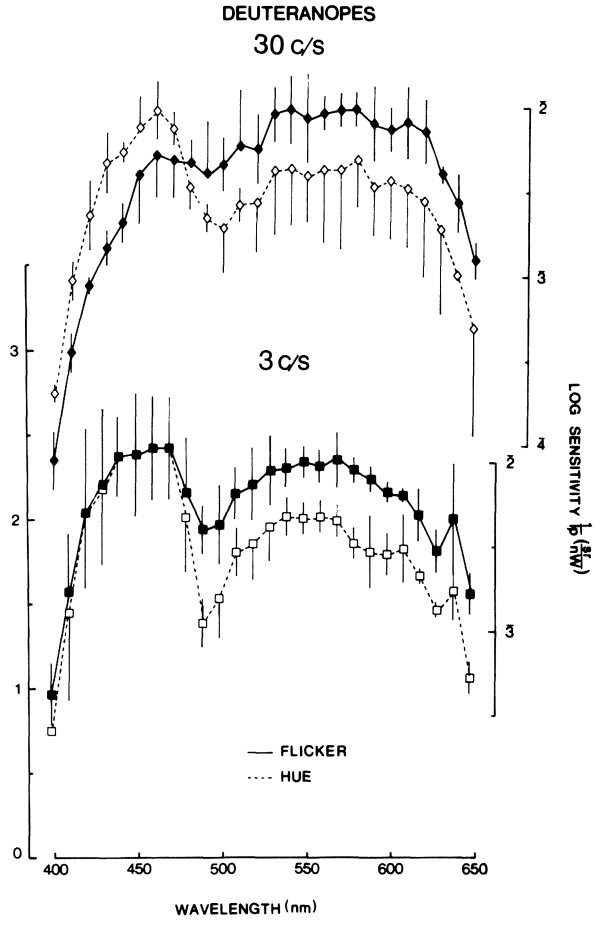

Fig. 6.28.B Increment spectral sensitivity curves based on thresholds for detection of flicker (*solid lines*) and hue (*broken lines*); flicker rates of 3 and 30 c/s. Each symbol represents the mean value for 4 experiments in two deuteranopes (mean ± S.D.). The curves obtained with 30 c/s have been raised by 1 logarithmic unit; the right-hand ordinates indicate the absolute sensitivity values of each curve. Other conditions as in Fig. 6.27

The flicker and hue spectral sensitivity functions of dichromats are displayed in Fig. 6.28, those of protanopes in Fig. 6.28A, and those of deuteranopes in Fig. 6.28B. Only flicker rates of 3 and 30 c/s are shown. At 3 c/s their sensitivity functions based on flicker as well as on hue detection manifest only two peaks with sensitivity maxima at 450 nm in both deuteranopes and protanopes; a second maximum was seen at 540 nm for protanopes and at 560 nm for deuteranopes. Both types of dichromats had a neutral point near 490 nm. Unlike the deuteranopes, the protanopes showed a rapid drop in their hue and flicker sensitivity in the long-wavelength region of the spectrum. At 30 c/s the dichromats also exhibited a "cross-over effect" near 475 nm between the hue and flicker curves; unlike normals, the hue-function's sensitivity (*open symbols*) remained substantially below the flicker curve, even at the extreme long-wavelength end of the spectrum (above 620 nm). In dichromats the flicker sensitivity of the long-wavelength mechanism is principally similar to the corresponding long-wavelength mechanism in normals (see also Cavonius and Estévez 1976). Interestingly, deuteranopes showed their highest sensitivity in the short-wavelength part of the spectrum, whereas normals and protanopes showed their highest sensitivity in the middle- and long-wavelength region. This may indicate that the interaction between the short- and the long-wavelength mechanism is different in deuteranopes from that in protanopes as noted by Zrenner and Kojima (1976). Electroretinographical studies on the spectral sensitivity of color-defective subjects employing high repetition rates – see Dodt et al. (1958) and Copenhaver and Gunkel (1959) – do not show a pronounced increase in sensitivity near 450 nm, due to the small contribution of blue-sensitive cones in the ERG.

To conclude: Considering the results obtained in single ganglion cells (Chap. 5), one could argue that in normals only one spectrally broadband mechanism is active at high flicker rates, due to the synergistic action of the red and green cone mechanism feeding red/green ganglion cells. Indeed, at higher flicker rates, *normals approach the spectral properties of dichromates,* since an individual tonic color-opponent ganglion cell, in which center and surround provide qualitatively identical signals at each point in time (synchronization, see Chap. 5), cannot differentiate between responses mediated by the red- and the green-sensitive cones; this becomes evident in Fig. 6.27, where the spectra obtained with low and high frequencies of stimulation are compared.

Nevertheless, the combined "long-wavelength" mechanism built up by the synergistic action of red- and green-sensitive cones is still able to interact in an opponent manner with the short-wavelength mechanism, as evidenced by the sensitivity dip (neutral point) near 480 nm. The fact that below 480 nm and at high flicker rates a steady blue light is reported as the first sensation

indicates that the neural systems which detect the short wavelength stimuli have reached their flicker *fusion* frequency, but are still able to code hue. Apparently, color-opponency is not affected as strongly in the short- as it is in the long-wavelength part of the spectrum.

In the middle-wavelength zone (above 480 nm), the first sensation reported is achromatic flicker. This is consistent with the finding that tonic ganglion cells lose their color-opponency at high flicker rates. However, with suprathreshold stimuli, color-opponency returns, as indicated by the neutral points in the hue threshold functions (cf. Figs. 6.27 and 6.28). Thus, the color-opponent mechanism is presumably activated under suprathreshold conditions, as concluded earlier from the data on human visually evoked cortical potentials (Zrenner 1977a).

6.6 Conclusion: To What Extent Can Visually Evoked Cortical Potentials Reveal the Function of Individual Receptor Mechanisms?

The recording of visually evoked electrical potentials and of psychophysical data is almost the only available means of studying the function of *intact* human visual systems (besides positron emission tomography). Knowledge about the underlying mechanisms becomes substantially broadened when data on primate single ganglion cells (Chap. 3-Chap. 5) are taken into consideration. Studies on individuals whose visual system is altered either by a congenital (such as the dichromats and monochromats discussed in this chapter) or by an acquired deficiency (Ethambutol, see Fig. 6.19), can provide additional insights. Since the connection to the relevant literature and the specific conclusions were given in each subchapter, the following discussion deals mainly with general aspects.

Rods and Cones

It could be demonstrated that with appropriate adaptive and test light conditions cortical responses originating from rods and cones can be differentiated; responses from both systems exhibit marked differences in their time course, spectral sensitivity and threshold distribution in the retinal periphery (Figs. 6.6 to 6.8), as well as in dark adaptation (Kojima and Zrenner 1977). Therefore it becomes crucial to choose the appropriate amplitude or implicit time criterion in these responses, especially when stimulating small areas of the retina which project onto different anatomical sites in the visual cortex (Holmes 1918). Any *amplitude* criterion will be influenced by the distance between the response-generating neurons and the recording electrode. The *implicit time* of a potential is less influenced by the

distance between the generators and the electrode than its amplitude; thus, it provides a more reliable criterion for comparing scotopic thresholds, especially when the stimulus is positioned at different retinal eccentricities, which project onto very differently distributed cortical areas. The amplitude needs only to be large enough (1.5-2.0 μV) for determining an implicit time (for details see Kojima and Zrenner 1980). In the determination of rod thresholds, the state of adaptation has to be carefully considered. According to previous experiments (Kojima and Zrenner 1977), weak stimuli (0.2-1.5 log units above the absolute sensory threshold) of 110 ms duration, presented at 2-s-intervals, do not interfere with the state of dark adaptation (see also Huber and Adachi-Usami 1972); 40 min have to elapse until a steady state of dark adaptation is reached. To avoid an influence of test light intensity on the state of adaptation, the temporal summation properties of the scotopic system (Barlow 1958) should be taken into account by using a test light duration of at least 0.1 s. Consequently, discharge-flash stimulation should be avoided in determining local scotopic thresholds by means of the VECP. By applying these experimental conditions, local scotopic VECP thresholds can be reliably measured up to 40° eccentricity; this reveals a close correlation between electrophysiological, psychophysical and anatomical data across the visual field (Fig. 6.9).

The Three Spectrally Different Cone Mechanisms

Appropriate chromatic backgrounds permit the isolation of the three fundamental cone mechanisms by electrical (Fig. 6.11) as well as by psychophysical threshold criteria (Fig. 6.12). Spectral sensitivity functions based on a constant threshold response of the blue- and green-sensitive cone mechanism match Dartnall's (1953) pigment nomograms for a 450 and a 535 nm cone, as well as Stiles' π_1- and π_4-function and the action spectra of blue and red/green-sensitive ganglion cells (Chaps. 3 and 4). This match does not extend to the red-sensitive cone mechanism; its spectral sensitivity function, when recorded electrophysiologically or psychophysically by the increment threshold technique, is slightly narrower than a Stiles' π_5-function, expecially in its short wavelength branch (e.g., Fig. 6.28); in turn, the Stiles π_5-function is smaller than a Dartnall (1953) nomogram for a 575 nm pigment. Remnants of color-opponent processing which are not suppressed by chromatic adaptation can be responsible for narrowing functions which are based on pigment absorption spectra; this applies especially to suprathreshold criteria, such as the VECP, which reveal color-opponent processing not present at threshold conditions (Fig. 6.17B).

Color-Opponency in Psychophysical and Electrical Data

The main concern in these studies was not so much the *isolation* of fundamental cone mechanisms in the VECP (which can be also obtained by a spectral compensation method, as shown by Estévez et al., 1975) as to study the *interaction* between these mechanisms. As pointed out in Chapters 3, 4, and 5, color-opponency is based on the functioning of a cone antagonistic retinal circuitry; these mechanisms, which express themselves in a narrowing of action spectra, are of major importance for good hue discrimination. It was demonstrated that the narrowing of action spectra can be determined by the human VECP (Fig. 6.17) and by psychophysical measurements; thus, a means of testing the function of color-opponent neurons in man became available (Zrenner 1976, 1977a). The strength of mutual antagonistic interactions can be estimated by matching a weighted subtraction of individual R and G functions with the data obtained (Fig. 6.17). By applying this technique of investigation in a case of acquired color vision deficiency, it was demonstrated that widely used drugs, such as Ethambutol, particularly affect the antagonistic function of red/green opponent neurons (Fig. 6.19), while the three spectrally different cone mechanisms can still be traced independently up to the visual cortex. Thereby it becomes possible to differentiate between toxic alterations affecting the cone receptors (and their direct pathway to the visual cortex) and those specifically disturbing the action of color antagonistic mechanisms, upon which chromatic as well as spatial coding strongly relies.

Congenital Color Vision Deficiencies

Protanopic and deuteranopic observers have color-opponent ganglion cells of only the B-L type (cf. Fig. 3.4) with a defect of either the red- (protanopes) or the green-sensitive pigment (deuteranopes). The various chromatic backgrounds applied in the VECP recordings (Fig. 6.13) did not alter the sensitivity function of protanopes; the constant shape of their sensitivity functions indicates that indeed only *one* mechanism with a maximum sensitivity at 540 nm operates in the long-wave region of the protanope's spectrum. Comparison of the VECP data of protanopes with Judd's (1945) spectral sensitivity curve, with Rushton's (1963) densitometric measurement of cone pigments, and with the electroretinographic luminosity curves in protanopes of Dodt et al. (1958) and Ui (1975) show close correspondence in the long-wavelength region.

The hypothesis that deuteranopia is also due to the loss of a green-sensitive mechanism is generally less accepted. Although the spectral functions of deuteranopes and protanopes can be described as a reduction form of trichromacy, (Vos and Walraven 1971, Kröger-Paulus and Scheibner 1978,

Scheibner and Paulus 1978, Klauder and Scheibner 1980), it was suggested by various authors on the basis of Fick's (1896) fusion hypothesis (for review see Alpern et al. 1968, Wagner 1971, Alpern 1974, and the comments in Section 6.3.2) that there might be two groups of deuteranopes, those whose chlorolabe is lacking (reduction-type, according to Rushton 1965), and those whose red and green cone signals are fused (fusion-type, Willmer 1949b).

Disagreement on this issue might be due to considerable variations in the action spectra of the long-wavelength mechanism among deuteranopes (Alpern and Pugh 1977, Alpern and Moeller 1977, Kröger-Paulus and Scheibner 1980 and Kröger-Paulus 1980, see also Chap. 6.3: anomalous trichromats), interpreted in terms of pigment shifts forming clusters of pigments; these, however, are questioned by Estévez (1979).

In the present experiments it is a striking fact that on purple background deuteranopes reveal a spectral luminosity function very close to the V_λ-function, *different* from that seen in normals on purple background (Fig. 6.13 and 6.14); moreover they show a marked change in the middle wavelength part of their spectral sensitivity function when the adaptation light changes from purple to blue-green (cf. Fig. 6.13 and Zrenner and Kojima 1976). In loss-type deuteranopes only an interaction between the blue- and the red-sensitive mechanism remains possible; if both adaptation lights used have comparable effects on the blue- and red-sensitive pigment in normals and deuteranopes, the differences in the action spectra (Fig. 6.13A versus E and B versus F) can only be explained by differences in the interaction of the two mechanisms which must be differently affected by purple and blue-green adaptation lights.

This can also be seen in the psychophysical measurements of Fig. 6.14 (E and F). When purple adaptation light is applied in deuteranopes, the blue-sensitive mechanism is readily apparent (Fig. 6.14E), while in normals (Fig. 6.14A) and protanopes (Fig. 6.14C) under identical conditions, it is suppressed. This supports the assumption that the interaction between the blue and the red mechanism in deuteranopes is different from that in normals and protanopes. If the pigments of blue- and red-sensitive cones are the same in both deuteranopes and normals (Rushton 1958b, 1975), the difference in the interaction between both mechanisms should be located in the *neural network* used by the cone signals. Considering the model of interaction between short and long wavelength sensitive cones in a dichromatic system (Fig. 4.8), in deuteranopes the R-mechanism suppresses the B-mechanism to a lesser extent (see Fig. 6.14E) than the green-sensitive one does in normals and protanopes (see Fig. 6.14A and C); therefore, the green-sensitive cone is the most probable candidate for being the long-wavelength-sensitive cone which provides the direct modulating signal onto B-cones

given in the model of Chapter 4 (Fig. 4.8). In addition, the interactions between the short- and long-wavelength-sensitive mechanism are more pronounced in deuteranopes than in protanopes (see Fig. 6.14C and E and 6.18).

The monochromatic observer's data are discussed in the text, along with Fig. 6.14; they show no signs of opponent interaction between cone mechanisms such as narrowed action spectra and shifts of the maxima characteristic of normal trichromats (Fig. 6.17 and 6.18).

Flicker

The data of experiments with flicker (Figs. 6.25 and 6.26) revealed that an increase in the rate of stimulation had the same effect in the human visual system as it had in single retinal ganglion cells of rhesus monkey (Figs. 5.3 and 5.4): at higher flicker frequencies, the signs of color-opponency are lost and the action spectra become broadband and single-peaked, resembling a linear addition of a G and R mechanism's action spectrum. It may be argued that a synchronization of the spectrally antagonistic center and surround mechanism of color-opponent neurons takes place in the human visual system as well; this synchronization was demonstrated in rhesus monkey ganglion cells (Fig. 5.5). It applies mainly to the interaction between red- and green-sensitive cones, particularly when the threshold for flicker detection is determined. When the threshold for hue detection is measured, opponent interactions are maintained up to relatively high flicker frequencies (Figs. 6.27 and 6.28).

Interestingly, the action spectrum of the 450 nm cone mechanism can still be detected at 30-40 c/s in these figures. Stabell U. and Stabell B. (1980) base their psychophysical measurements of pigment absorption on the assumption that at higher flicker rates the short wavelength cone is silent, causing tritanopia. This assumption does not hold entirely, since thresholds based on hue detection clearly revealed the blue-sensitive cone mechanism at these higher frequencies in single cell recordings (Fig. 5.1), as well as in the psychophysical measurements (Fig. 6.27 and 6.28).

In the long-wavelength region in normals, only one broadband, combined long-wavelength mechanism functions due to the synergism of the red and green cone activity feeding the red/green-opponent tonic ganglion cells. Therefore, spectral properties of normal individuals approach those of dichromats (cf. Figs. 6.27 and 6.28), since a tonic, red/green color-opponent cell, in which center and surround excitation is synchronized, cannot differentiate between responses mediated by the red- and green-sensitive cones. As a consequence, trichromats and dichromats show very similar spectral sensitivity functions when flicker photometry is employed (Grützner 1962). However, the comparison of retinal single-cell data on flicker with data obtained by psychophysical experiments is not without problems, since bin-

ocular interaction modifies flicker-perception (Cavonius 1979), indicating that a considerable amount of temporal processing is modulated by higher-order neurons.

Nevertheless, the combined "long-wavelength" mechanism of normal trichromats is still able to interact in an "opponent" manner with the short wavelength mechanism as evidenced by the dip (neutral point) in the action spectrum near 480 nm (Fig. 6.27, 30 c/s). The fact that a *continuous* blue light is reported as the *first* sensation below 480 nm and at 30 and 40 c/s indicates that the neural systems which detect the short wavelength stimuli have reached their flicker-fusion frequency; however, they are still able to code for hue, particularly in dichromats (Fig. 6.28) where the action spectrum of the 450-nm cone mechanism is very pronounced. Apparently color-opponency in the short-wavelength part of the spectrum is not affected as greatly as in the long-wavelength region. On the other hand, in the middle of the spectrum when the stimulus intensity is increased, achromatic flicker is the *first* sensation reported. This is consistent with the finding mentioned above that tonic ganglion cells lose their color-opponency at high flicker rates. However, at suprathreshold stimulation, color-opponency returns, as indicated by the dips in the hue threshold functions, causing narrowing of the fundamental cone sensitivity functions. Thus, the color-opponent mechanism is presumably re-activated under suprathreshold conditions, a conclusion which supports the findings obtained by recordings of human VECP (Fig. 6.17).

Epilogue

In the last century it was apparently still possible to be fully conversant with one or even several scientific disciplines. Anatomy and physiology, in most universities, were taught by one and the same professor; surgery most often included both ophthalmology and gynecology.

In contrast, our contemporary knowledge of the natural sciences is dependent on many disciplines and subdisciplines, each having its own independent life, often divided into several schools of thought; as a result, scientists working in different or even neighboring fields often are no longer able to understand each other, having developed their own language and their own system of metrics; indeed, it has become impossible for any single man and any single brain to have *complete* knowledge of the history and development of even a relatively circumscribed scientific area.

Therefore some readers might wonder that in the present book the author frequently dares to relate data from single cell physiology to perceptual phenomena, anatomical structures to physiological or ophthalmopathological processes and neurochemical observations to biocybernetical models. However, the visual system itself is constructed to analyze an object by utilizing various converging and diverging pathways and by carrying out comparisons between the information of neighboring neurons or by sending signals back and forth in recurrent circuits. Since the mechanisms of color perception are far from being completely understood, the trains of thought appearing in this publication might simply reflect the neuronal efforts required to analyze the object "color vision" by drawing upon all conceivable sources of information; by this manner of proceeding, one hopes that the fragments of information originating in many individual single cells may finally reach the one cortical neuron which really "*knows*" color. The attempt to discover in perceptual phenomena the mechanisms studied in single retinal cells seems justified, since these mechanisms beyond any doubt contribute to the generation of perceptual phenomena, although the direct neurophysiological link is lacking.

Carl Wilhelm Ludwig Bruch (1819-1884), the famous physiologist and anatomist who in 1844 discovered an extremely fine retinal layer of only 0.5 μ thickness, the electrophysiological importance of which has become

apparent only in recent years (see Brindley 1970, Rodieck 1973 on the R-membrane and C. Zrenner 1982a,b on the history of its discovery) describes to a certain extent the feelings I have in finishing this book. Bruch (1844) writes[13]:

> "Hypotheses will always be the guides of research; however, (dependable) knowledge is only the mathematically proven fact, or, in Heusinger's words: Science is *developing* knowledge, never a completed system. Might it be embarassing to publish unfinished work, it would be foolish to wait for its completion.
>
> If, on the one hand, I must deplore the fragmentary character of this investigation, on the other, I do not hope that much (of it) is too much. It happens only too often to a beginner, not mastering the literature, that at the end of a long investigation, somewhere in the publications of a leading scientist he finds a parenthetical note which at least renders the discussion unnecessary. I can assert that I have seen everything myself, where I did not expressly state the contrary; where I did not quote an earlier author, none was known to me. I believe, however, that in matters which have been so little investigated... and which have become controversial only in the very recent years..., even a simple confirmation of earlier observations is not without value. Of the conclusions I have drawn I can say that I did not seek but find them, if I made errors, I hope that it may not be to the detriment of the observations upon which the conclusions are based."

The original reads as follows:

> "Die Hypothese wird immer die Wegweiserin der Forschung sein; aber Wissen ist nur das mathematisch Erwiesene, oder, wie schon Heusinger sagte: Wissenschaft ist nur das werdende Wissen, nie vollendetes Sys-

13 Carl W. Bruch (1819-1884), a native of Mainz, studied medicine in Giessen and Berlin, graduating in 1842. In acknowledgement of his pioneering histological study *Untersuchungen zur Kenntniss des körnigen Pigments der Wirbelthiere in physiologischer und pathologischer Hinsicht* (Zürich 1844) which led to the discovery of an extremely fine retinal layer called "lamina elastica", "lamina vitrea", or: membrane of Bruch, he was appointed in 1845 lecturer in the Medical Faculty of the University of Heidelberg. From 1850 to 1855 he held the combined chair for Anatomy and Physiology at the University of Basel, a period in which he devoted his efforts mainly to comparative anatomy and zoology. In 1855 he was invited to succeed Th.L. Bischoff at the University of Giessen which enjoyed international fame due to the contributions of Justus von Liebig and the circle of his students. Bruch remained in Giessen until his retirement from active teaching in 1860; in 1859 and 1860 he was the editor of *Der Zoologische Garten*, to indicate the exceptionally wide range of his interests and scientific contributions. He died in 1884 in Heppenheim. (Personal communication obtained from Dr. Claudia Zrenner, Institute for History of Medicine, Justus-Liebig University of Giessen 1980)

tem. Mag es daher peinlich sein, eine unvollendete Arbeit zu veröffentlichen: es wäre thöricht, ihre Vollendung erwarten zu wollen.

Wenn ich auf der einen Seite das Fragmentarische dieser Untersuchungen anklagen muss, hoffe ich andrerseits nicht, dass Vieles – zu viel sei. Es begegnet einem Anfänger, der die Literatur nicht beherrscht, nur zu oft, dass er am Ende einer langen Untersuchung irgendwo bei einem Meister eine beiläufige Notiz findet, die wenigstens die Erörterung überflüssig macht. Ich kann versichern, das ich Alles, wo nicht ausdrücklich das Gegentheil bemerkt ist, selbst gesehen habe; wo kein früherer Beobachter citirt ist, war mir keiner bekannt; ich glaube aber, dass in Dingen, die verhältnismässig noch so wenig untersucht sind... und die erst in der jüngsten Zeit zur Controverse geworden..., selbst eine blosse Bestätigung früherer Beobachtungen nicht ohne Werth sei. Von den Schlüssen, die ich gezogen, kann ich sagen, dass ich sie nicht gesucht, sondern gefunden habe; wenn ich gleich wohl irre gegangen, so soll diess hoffentlich den Beobachtungen, worauf sie gestützt sind, nicht zum Nachteil gereichen."

Summary

The experiments described and discussed in this book were performed in order to elucidate basic mechanisms of color vision. This goal was approached in two ways: to get a better understanding of the manner in which chromatic stimuli are processed in the initial stages of the visual system, the neurophysiological functions of *single retinal neurons* were studied in a sample of 385 ganglion cells in rhesus monkey; and to show more clearly how the messages of these retinal neurons are processed in the *visual system as a whole* and how they are related to higher-order visual functions, corresponding experiments on the human visual cortex (i.e., recordings of visually evoked cortical potentials and of psychophysical data) were carried out.

The recordings from single cells revealed various mechanisms which *optimize* the ability of color-opponent ganglion cells to code differences in the spectral composition of light. After a brief introduction (Chap. 1), which also gives a short historical background and a description of methods of single cell recordings (Chap. 2), three major aspects of this optimizing capacity of the visual system are discussed in Chapters 3, 4, and 5.

First, *successive* color-contrast, even when minimal, can be strongly signalled. For almost any part of the visible spectrum a red/green-opponent cell can be found which is reversed in polarity by two successive stimuli even if their difference in spectral composition is very small (Chap. 3).

Second, the responsiveness to *chromatic* contrast can be enhanced by the blue sensitive system. The sensitivity of blue-sensitive ganglion cells seems to be controlled by long-wavelength-sensitive cones, probably by modulation of the conductances in the blue cone's ionic channels. A model is presented and tested, which accounts for several paradoxical phenomena occurring in the blue-sensitive system (Chap. 4).

Third, at high flicker rates, the chromatic antagonism changes to a synergism of center and surround responses in color-opponent ganglion cells. This considerably improves the detectability of high frequency luminance flicker. The impact of this mechanism on the processing of luminous and chromatic flicker as well as on the understanding of the Brücke-Bartley effect and flicker-induced colors (Fechner-Benham-illusion) is discussed (Chap. 5).

In all three chapters it was pointed out to what extent these retinal mechanisms can enhance the visual system's ability to detect objects of minimally different chromaticity and/or luminance.

Finally, the attempt was made to relate the data obtained in single-cell experiments from monkey to *human visual functions* at the cortical level; the experiments on the human visual system itself (Chap. 6) yielded additional aspects, particularly about the processing of color signals in congenital and acquired color vision deficiencies. Since the neurophysiological link between peripheral electrical events and perception is lacking, the main object was rather to discover the action of peripheral mechanisms in perceptual phenomena, than to explain the *generation* of these phenomena itself. With few exceptions, the data available on color coding in *single cortical* cells were considered as beyond the scope of this paper.

Nevertheless it was shown that visual information is often processed already in single retinal cells in the manner described by psychophysical investigations for the entire system; this is valid to a much larger extent than apparent in previous work. Apparently it is not so much the number or the specificity of separate visual channels which accounts for the primate visual system's outstanding performance, but its functional plasticity, present already in retinal neurons, which enables these cells to optimize their capabilities in carrying out the tasks required.

References

Abramov I (1972) Retinal mechanisms of colour vision. In: Fuortes MGF (ed) Handbook of sensory physiology of photoreceptor organs. VII/2. Springer, Berlin Heidelberg New York, pp 567–607

Abramov I, Gordon J (1977) Color vision in the peripheral retina. I. Spectral sensitivity. J Opt Soc Am 67:195–202

Adachi-Usami E, Heck J, Gavriysky V, Kellermann F-J (1974a) Spectral sensitivity function determined by the visually evoked cortical potential in several classes of colour deficiency (cone monochromatism, rod monochromatism, protanopia, deuteranopia). Ophthalmol Res 6:273–290

Adachi-Usami E, Kellermann F-J, Makabe R (1974b) Visuell evozierte Antworten bei Patienten mit Ethambutol-Schäden. Ber Dtsch Ophtalmol Ges 72:181–185

Adamczak W (1981) The amacrine cells as an important processing site of pattern-induced flicker colors. Vision Res 21:1639–1642

Adams EQ (1923) A theory of color vision. Psychol Rev 30:56–76

Adams WL, Arden GB, Behrmann J (1969) Responses of human visual cortex following excitation of peripheral rods. Br J Ophthalmol 53: 439–452

Aguilar M, Stiles WS(1954) Saturation of the rod mechanism of the retina at high levels of stimulation. Optica Acta 1:59–65

Alexandridis E, Dodt E (1967) Pupillenlichtreflexe und Pupillenweite einer Stäbchenmonochromatin. Albrecht von Graefes Arch Ophthalmol 173: 153–161

Alexandridis E, Jaeger W (1978) Fehldiagnose „Achromatopsie" bei einem Kind, welches später an tapetoretinaler Degeneration erblindete. In: Straub W, Remler O (Hrsg) Buech Augenarzt 73:133–138

Alken RG, Miller A, Semjan R, Rietbrock N (1980) Colour vision deficiencies detected by Farnworth's 100 hue test in patients under long-term treatment with digitalis. In: Verriest G (ed) Colour vision deficiencies, vol V. Adam Hilger, Bristol, pp 320–326

Alpern M (1974) What is it that confines in a world without color? Invest Ophthalmol 13:648–674

Alpern M (1976) Tritanopia. Am J Optom Physiol Opt 53:340–349

Alpern M (1981a) Color blind color vision. Trends Neurosci 4:131–135

Alpern M (1981b) The color vision of the color blind. Jpn J Ophthalmol 25:1–17

Alpern M, Moeller J (1977) The red and green cone visual pigments of deuteranomalous trichromacy. J Physiol 266:647–675

Alpern M, Pugh EN Jr (1977) Variation in the action spectrum of erythrolabe among deuteranopes. J Physiol 266:613–646

Alpern M, Mindel J, Torii S (1968) Are there two types of deuteranopes? J Physiol 199:443–456

Arden GB (1976) The retina – Neurophysiology. In: Davson H (ed) The Eye, vol 2A. Academic Press, London New York, pp 330–356

Armington JC (1974) The electroretinogram. Academic Press, San Francisco London New York

Auerbach E, Wald G (1954) Identification of a violet receptor in human color vision. Science 120:401–405

Augenstein EJ, Pugh EN Jr (1977) The dynamics of the Π_1 colour mechanism: Further evidence for two sites of adaptation. J Physiol 272:247–281
Baier M, Zrenner E (in prep.) Rechnergestützte Verfahren zur Klassifizierung von angeborenen und erworbenen Farbensinnstörungen
Balaraman S (1962) Color vision research and the trichromatic theory: A historical review. Psychol Bull 59:434–448
Barber C (1980)Evoked potentials. MTP-Press. Lancaster
Balen van ATM, Henkes HE (1960) Recording of the occipital lobe response in man after light stimulation. Brit J Ophthal 44:449–460
Barber C (1980) Evoked potentials. MTP-Press, Lancaster
Barlow HB, Fitzhugh R, Kuffler SW (1957) Change of organization in the receptive fields of the cat's retina during dark adaptation. J Physiol 137:338–354
Barlow HB (1958) Temporal and spatial summation in human vision at different background intensities. J Physiol 141:337–350
Barlow HB (1979a) Three theories of cortical function. In: Freeman RD (ed) Development neurobiology of vision. Plenum Press, New York London, pp 1–16
Barlow HB (1979b) Reconstructing the visual image in space and time. Nature (London) 279:189–190
Baron WS (1980) Cone difference signal in foveal local electroretinogram of primate. Invest Ophthalmol Vis Sci 19:1442–1448
Baron WS, Boynton RM, Hammon RW (1979) Component analysis of the foveal local electroretinogram elicited with sinusoidal flicker. Vision Res 19:479–490
Baumann Ch (1965) Receptorpotentiale der Wirbeltiernetzhaut. Pflügers Arch Gesamte Physiol Menschen Tiere 282:92–101
Baumann Ch (1968) Neuere Ergebnisse der Physiologie des Farbensehens. Hippokrates 39:477–483
Baumann Ch (1972) The regeneration and renewal of visual pigment in vertebrates. In: Dartnall HJA (ed) Handbook of Sensory Physiology, vol VII/1. Springer, Berlin Heidelberg New York, pp 395–416
Baumann Ch (1977) Boll's phenomenon. Vision Res 17:1325–1327
Baumann Ch (1978) Visual pigments. Methodicum Chimicum, vol 11/3. Thieme, Stuttgart, pp 200–205
Baumgartner G, Hakas P (1962) Die Neurophysiologie des simultanen Helligkeitskontrastes. Reziproke Reaktionen antagonistischer Neuronengruppen des visuellen Systems. Pflügers Arch 274:489–510
Baumgartner G, Bornschein H, Hanitzsch R, Jung K, Kornhuber HH, Rentschler I, Schober H, Thoden U (1978) Sehen. Sinnesphysiologie, vol III. In: Gauer OH, Kramer K, Jung R (Hrsg) Physiologie des Menschen, vol 13. Urban und Schwarzenberg, München Wien Baltimore
Baylor DA (1974) Lateral interaction between vertebrate photoreceptors. Fed Proc 33:1074–1077
Baylor DA, Fuortes MGF (1970) Electrical responses of single cones in the retina of the turtle. J Physiol 207:77–92
Baylor DA, Hodgkin AL (1974) Changes in time scale and sensitivity in turtle photoreceptors. J Physiol 242:729–758
Baylor DA, Fuortes MGF, O'Bryan PM (1971) Receptive fields of cones in the retina of the retina of the turtle. J Physiol 214:265–294
Baylor DA, Hodgkin AL, Lamb TD (1974) The electrical response of turtle cones to flashes and steps of light. J Physiol 242:685–727
Békésy G (1968) Mach- and Hering-type lateral inhibition in vision. Vision Res 8: 1483–1499
Benham CE (1895) Letter. Nature (London) 51:371
Birch-Cox J (1976) Design of diagnostic tests for congenital and acquired colour vision defects. Mod Probl Ophthalmol 17:196–201

Blackwell HR, Blackwell OM (1961) Rod and cone receptor mechanisms in typical and atypical congenital achromatopsia. Vision Res 1:62–107
Boll F (1877) Zur Anatomie und Physiologie der Retina. Arch Anat Physiol (Physiol Abt) 4–36. Quoted after Baumann Ch (1977) Vision Res 17:1325–1327
Bonaventure N, Wioland N, Roussel G (1980) Effects of some amino acids (GABA, glycine, taurine) and of their antagonists (picrotoxin, strychnine) on spatial and temporal features of frog retinal ganglion cell responses. Pflügers Arch 385: 51–64
Bortoff A (1964) Localization of slow potential responses in the necturus retina. Vision Res 4:627–635
Bowen RW, Markell KA (1980) Temporal brightness enhancement studied with a large sample of observers: evidence for individual differences in brightness perception. Perception and Psychophysics 27:465–476
Bowen RW, Nissen MJ (1979) Luminance, not brightness, determines temporal brightness enhancement with chromatic stimuli. J Opt Soc Am 69:581–584
Bowling DB, Michael CR (1980) Projection patterns of single physiologically characterized optic tract fibres in cat. Nature (London) 286:899–902
Bowmaker JK (1981) Visual pigments and colour vision in man and monkeys. J Soc Med 74:348–356
Bowmaker JK, Dartnall HJA (1980) Visual pigments of rods and cones in a human retina. J Physiol 298:501–511
Bowmaker JK, Dartnall HJA, Mollon JD (1980) Microspectrophotometric demonstration of four classes of photoreceptors in an old world primate, macacca fascicularis. J Physiol 298:131–143
Boycott BB, Dowling JE (1969) Organization of the primate retina. Light microscopy. Philos Trans Soc London Ser B 255:109–184
Boycott BB, Kolb H (1973) The horizontal cells of the rhesus monkey retina. J Comp Neurol 148:115–139
Boycott BB, Wässle H (1974) The morphological types of ganglion cells of the domestic cat's retina. J Physiol 240:397–419
Boycott BB, Dowling JE, Fisher SK, Kolb H, Laties AM (1975) Interplexiform cells of the mammalian retina and their comparison with catecholamine-containing retinal cells. Proc R Soc Lond B 191:353–368
Boynton RM (1960) Theory of color vision. J Opt Soc Am 50:929–944
Boynton RM (1978) Discriminations that depend upon blue cones. In: Cool SJ, Smith EL (eds) Frontiers in visual science, vol III. Springer, Berlin Heidelberg New York, pp 154–164
Boynton RM (1979) Human color vision. Holt, Rinehart and Winston, New York Chicago San Francisco Dallas Montreal Toronto London Sidney
Boynton RM, Whitten DN (1972) Selective chromatic adaptation in primate photoreceptors. Vision Res 12:855–874
Boynton RM, Ikeda M, Stiles WS (1964a) Interactions among chromatic mechanisms as inferred from positive and negative increment thresholds. Vision Res 4:87–117
Boynton RM, Schafer W, Neun MA (1964b) Hue-wavelength relation measured by color naming method for three retinal locations. Science 146:666–668
Braitenberg V (1979) Skizze einer Theorie der Großhirnrinde. Verh Dtsch Zool Ges. Fischer, Stuttgart, pp 201–206
Breitmeyer B, Levi DM, Harwerth RS (1981) Flicker masking in spatial vision. Vision Res 21:1377–1385
Breton ME (1977) Hue substitution. Wavelength latency effects. Vision Res 17: 435–443
Brigdges CDB (1972) The rhodopsin-porphyropsin visual system. In: Dartnall HJA (ed) Handbook of sensory physiology, vol VII/1, Photochemistry of vision. Springer, Berlin Heidelberg New York, pp 417–480

Brindley GS (1954) The summation areas of human colour-receptive mechanisms at increment threshold. J Physiol 124:400–408
Brindley GS (1970) Physiology of the retina and visual pathway. Monogr Physiol Soc 6 2nd ed. Edward Arnold Publ. London
Brindley GS, Du Croz JJ, Rushton WAH (1966) The flicker fusion frequency of the blue sensitive mechanism of colour vision. J Physiol 183:497–500
Brown KT, Murakami M (1968) Rapid effects of light and dark adaptation upon the receptive field organization of S-potentials and late receptor potentials. Vision Res 8:1145–1171
Brown PK, Wald G (1964) Visual pigments in single rods and cones of the human retina. Science 144:45–52
Brown WRJ (1952) The effect of field size and chromatic surroundings on color discrimination. J Opt Soc Am 42:837–844
Bruch C (1844) Untersuchungen zur Kenntniss des körnigen Pigments der Wirbelthiere in physiologischer und pathologischer Hinsicht. Meyer und Zeller, Zürich
Brücke E (1864) Über den Nutzeffect intermittirender Netzhautreizungen. Sizungsber. (Österr.) Akad Wiss Math Naturwiss KI 49 Abt 2
Buck SL, Makous W (1981) Rod-cone interaction on large and small backgrounds. Vision Res 21:1181–1187
Büttner C, Büttner U, Grüsser O-J (1971) Interaction of excitation and direct inhibition in the receptive field center of retinal neurons. Plügers Arch 322:1–21
Bunt AH, Hendrickson AE, Lund RD, Lund JS, Fuchs AF (1975) Monkey retinal ganglion cells: Morphometric analysis and tracing of axonal projections, with a consideration of the peroxidase technique. J Comp Neurol 164:265–286
Burbeck CA, Kelly DH (1980) Spatiotemporal characteristics of visual mechanisms: excitatory-inhibitory model. J Opt Soc Am 70:1121–1126
Byzov AL (1979) Origin of non-linearity of voltage-current relationships of turtle cones. Vision Res 19:469–477
Byzov AL, Golubtzov KV, Trifonov YuA (1977) The model of mechanism of feedback between horizontal cells and photoreceptors in vertebrate retina. In: Barlow HB, Fatt P (eds) Vertebrate photoreception. Academic Press, London New York San Francisco
Cajal SR (1933) Die Retina der Wirbelthiere. Bergmann Wiesbaden, Transl by Thorpe SA, Glickstein M (1972) The structure of the retina. (first ed in 1894) Thomas, Springfield
Campenhausen C von (1968a) Über die Farben der Benhamschen Scheibe. Z Vergl Physiol 60:351–374
Campenhausen C von (1968b) Über den Ursprungsort von musterinduzierten Flickerfarben im visuellen System. Z Vergl Physiol 61:355–360
Carr RE, Henkind P (1962) Ocular manifestation of Ethambutol. Toxic amblyopia after administration of an experimental antituberculotic drug. Arch Ophthalmol 67:566–571
Cavaggioni A, Sorbi RT (1981) Cyclic GMP releases calcium from disk membranes of vertebrate photoreceptor. Proc Natl Acad Sci USA 78:3964–3968
Cavonius CR (1964) Color sensitive responses in the human flicker ERG. Doc Ophthalmol 18:103–113
Cavonius CR (1965) Evoked response of the human visual cortex: Spectral sensitivity. Psychon Sci 2:185–186
Cavonius CR (1979) Binocular interactions in flicker. Q J Exp Psychol 31:273–280
Cavonius CR, Estévez O (1975) Sensitivity of human color mechanisms to gratings and flicker. J Opt Soc Am 65:966–968
Cavonius CR, Estévez O (1976) Flicker sensitivity of the long-wavelength mechanisms of normal and dichromatic observers. Mod Probl Ophthal 17: 36–40
Cavonius H, Schumacher AW (1966) Human visual acuity measured with colored test objects. Science 152:1276–1277
Cicerone CM, Krantz DH, Larimer J (1975) Opponent-process additivity – III. Effect of moderate chromatic adaption. Vision Res 15:1125–1135

CIE: (1970) International Lighting Vocabulary, 3 rd edn. CIE publ Nr 17. Paris
Ciganek L, Ingvar DH (1969) Colour specific features of visual cortical responses in man evoked by monochromatic flashes. Acta Physiol Scand 76:82–92
Cleland BG, Dubin MW, Levick WR (1971) Sustained and transient neurones in the cat's retina and lateral geniculate nucleus. J Physiol 217:473–496
Cleland BG, Levick WR, Wässle H (1975) Physiological identification of a morphological class of cat retinal ganglion cells. J Physiol 248:151–171
Cohen AI (1970) Further studies on the question of the patency of saccules in outer segments of vertebrate photoreceptors. Vision Res 10:445–453
Connors MM, Kinney JAS (1962) Relative red-green sensitivity as a function of retinal position. J Opt Soc Am 52:81–84
Copenhaver RM, Gunkel RD (1959) The spectral sensitivity of color-defective subjects determined by electroretinography. Arch Ophthalmol 62:55–68
Cornsweet TN (1970) Visual perception. Academic Press, London New York
Creutzfeldt O (1979) Repräsentation der visuellen Umwelt im Gehirn. Verh Dtsch Zool Ges. Fischer, Stuttgart, pp 5–18
Creutzfeldt OD, Kuhnt U (1964) The visual evoked potential: Physiological, developmental and clinical aspects. Electroencephalogr Clin Neurophysiol Suppl 26:29–41
Creutzfeldt OD, Lee BB (1978) Chromatic and spatial receptive field properties of cells in the lateral geniculate body of macaques. J Physiol 284:116
Creutzfeldt OD, Nothdurft HC (1978) Representation of complex visual stimuli in the brain. Naturwissenschaften 65:307–318
Creutzfeldt O, Sakmann B (1969) Neurophysiology of vision. Ann Rev Physiol 31:499–544
Creutzfeldt OD, Lee BB, Elepfandt A (1979) A quantitative study of chromatic organization and receptive fields of cells in the lateral geniculate body of the rhesus monkey. Exp Brain Res 35:527–545
Crone RA (1968) Incidence of known and unknown colour vision defects. A study of secondary school pupils in Amsterdam. Ophthalmologica 155:37–55
Cruz-Coke R (1970) Color blindness. An evolutionary approach. In Kugelmass IN (ed) American lecture series, publ Nr 786. Thomas, Springfield, pp 112–148
Dartnall HJA (1953) The interpretation of spectral sensitivity curves. Br Med Bull 9:24–30
Dartnall HJA (1972) Photosensitivity. In: Dartnall HJA (ed) Handbook of sensory physiology, vol VII/1, Photochemistry of vision. Springer, Berlin Heidelberg New York, pp 122–145
Dartnall HJA, Lythgoe JN (1965) The spectral clustering of visual pigments. Vision Res 5:81–100
Das SR (1964) Foveal increment thresholds in dark adaptation. J Opt Soc Am 54: 541–546
Davidson N (1976) Neurotransmitter amino acids. Academic Press, London New York San Francisco
Davson H (ed) (1976) The eye. 2nd edn vol IIA. Visual function in man. Academic Press, London New York
Davson H, Graham LT Jr (eds) (1974) The eye. Comparative Physiology, vol VI. Academic Press, London New York
Daw NW (1968) Colour-coded ganglion cells in the goldfish retina: Extension of their receptive fields by means of new stimuli. J Physiol 197:567–592
Daw NW (1972) Colour-coded cells in goldfish, cat and rhesus monkey. Invest Ophthalmol 11:411–417
Daw NW (1973) Neurophysiology of color vision. Physiol Rev 53:571–611
Desmedt JE (ed) (1977) Visual evoked potentials in man: New developments. Clarendon Press, Oxford
Diederen W, Weisenberger H (1981) Studies on the mechanism of the positive-inotropic action of AR–L 115 BS, a new cardiotonic drug. Arzneim Forsch/Drug Res 31 (I) Nr 1a:177–182

Diehl R, Zrenner E (1980) Multispot stimuli reveal spatial organization in the human electroretinogram (ERG). Doc Ophthalmol Proc Ser 23:209–216, ed by Schmöger E, Kelsey JH, Dr. Junk Publ: The Hague

Dixon WJ (1965) The up-and-down method for small samples. J Am Stat Assoc 60: 967–978

Djamgoz MBA, Ruddock KH (1980) Evidence for a GAGA-ergic feedback loop in the outer plexiform layer of the vertebrate retina. In: Verriest G (ed) Colour vision deficiencies, vol V. Hilger Ltd, Bristol, pp 45–50

Dodt E (1964) Erregung und Hemmung retinaler Neurone bei intermittierender Belichtung. Doc Ophthalmol 18:259–274

Dodt E, (1979) Lichtsinn. In: Keidel WD (Hrsg) Kurzgefaßtes Lehrbuch der Physiologie, 5 Aufl. Thieme, Stuttgart

Dodt E (1979) Lichtsinn. In: Keidel WD (ed) Kurzgefaßtes Lehrbuch der Physiologie, 5th edn. Thieme, Stuttgart

Dodt E, Copenhaver RM, Gunkel RD (1958) Photopischer Dominator und Farbkomponenten im menschlichen Elektroretinogramm. Pflügers Arch Gesamte Physiol Menschen Tiere 267:497–507

Dodt E, Elenius V (1956) Spektrale Sensitivität einzelner Elemente der Kaninchennetzhaut. Pflügers Archiv Ges Physiol Menschen Tiere 262:301–306

Dodt E, Enroth Chr (1954) Retinal flicker response in cat. Acta Physiol Scand 30: 375–390

Dodt E, Wadensten L (1954) The use of flicker electroretinography in the human eye. Observations in some normal and pathological retinae. Acta Ophthalmologica 32: 165–180

Dodt E, Copenhaver RM, Gunkel RD (1958) Photopischer Dominator und Farbkomponenten im menschlichen Elektroretinogramm. Pflügers Archiv Gesamte Physiol Menschen Tiere 267:497–507

Dodt E, Lith van GH, Schmidt B (1967) Electroretinographic evaluation of the photopic malfunction in a totally colour blind. Vision Res 7:231–241

Dowling JE (1979) Information processing by local circuits. The vertebrate retina as a model system. In: Schmitt FO, Worden FG (eds) The neurosciences, Fourth study program. MIT Press, Cambridge, Mass, pp 163–181

Dowling JE, Ripps H (1971) S-potentials in the skate retina. Intracellular recordings during light and dark adaptation. J Gen Physiol 58:163–189

Dowling JE, Werblin FS (1971) Synaptic organization of the vertebrate retina. Vision Res Suppl 3:1–15

Dreher B, Fukada Y, Rodieck R (1976) Identification, classification and anatomical segregation of cells with X-like and Y-like properties in the lateral geniculate nucleus of old-world primates. J Physiol 258:433–452

Drum BA (1977) Cone interactions at high flicker frequencies: Evidence for cone latency differences? J Opt Soc Am 67:1601–1603

Dubin MW (1970) The inner plexiform layer of the vertebrate retina: A quantitative and comparative electron microscopic analysis. J Comp Neurol 140:479–506

Ehinger B (1976) Biogenic monoamines and amino acids as transmitters in the retina. In: Bonting SL (ed) Transmitters in the visual process. Pergamon Press, Oxford

Ehinger B, Falck B (1971) Autoradiography of some suspected neurotransmitter substances: GABA, glycine, glutamic acid, histamine, dopamine and L-Dopa. Brain Res 33:157–172

Eisner A, MacLeod DIA (1981) Flicker photometric study of chromatic adaptation: selective suppression of cone inputs by colored backgrounds. J Opt Soc Am 71: 705–718

Enoch JM (1972) The two-color threshold technique of Stiles and derived component color mechanisms. In: Jameson D, Hurrich LM (eds) Handbook of Sensory Physiology vol 7/IV. Springer, Berlin Heidelberg New York, pp 537–567

Enroth Chr (1952) The mechanism of flicker and fusion studied on single retinal elements in the dark-adapted eye of the cat. Acta Physiol Scand 27, Suppl 100: 1–67

Enroth-Cugell Chr, Lennie P (1975) The control of retinal ganglion cell discharge by receptive field surrounds. J Physiol 247:551–578

Enroth-Cugell Ch, Pinto LH (1972a) Properties of the surround response mechanism of cat retinal ganglion cells and centre-surround interaction. J Physiol 220:403–439

Enroth-Cugell Ch, Pinto LH (1972b) Pure central responses from off-centre cells and pure surround responses from on-centre cells. J Physiol 220:441–464

Enroth-Cugell Ch, Robson JG (1966) The contrast sensitivity of retinal ganglion cells of the cat. J Physiol 187:517–552

Enroth-Cugell Ch, Lennie P and Shapley RM (1975) Surround contribution to light adaptation in cat retinal ganglion cells. J Physiol 247:579–588

Essen van DC (1979) Visual areas of the mammalian cerebral cortex. Ann Rev Neurosci 2:227–263

Estévez O (1979) On the fundamental data-base of normal and dichromatic color vision. Diss Univ Amsterdam (1979)

Estévez E, Cavonius CR (1975) Flicker sensitivity of the human red and green color mechanisms. Vision Res 15:879–881

Estévez O, Spekreijse H (1974) A spectral compensation method for determining the flicker characteristics of the human colour mechanisms. Vision Res 14:823–830

Estévez O, Spekreijse H, Berg van den TJTP, Cavonius CR (1975) The spectral sensitivities of isolated human color mechanisms determined from contrast evoked potential measurements. Vision Res 15:1205–1212

Exner F (1902) Über die Grundempfindungen im Young-Helmholtz'schen Farbensystem. Sitzungsber. der mathem.-naturwiss. Classe der Öst Akad Wiss Wien 111 Abt 2a pp 857–877

Eysel UTh, Grüsser O-J (1971) Neurophysiological basis of pattern recognition in the cat's visual system. In: Grüsser O-J, Klinke R (eds) Zeichenerkennung durch biologische und technische Systeme. Springer, Berlin Heidelberg New York, pp 60–80

Eysel UTh, Grüsser O-J (1974) Simultaneous recording of pre- and post-synaptic potentials during the degeneration of the optic tract fiber input to the lateral geniculate nucleus of cats. Brain Res 81:552–557

Famiglietti EV (1981) Functional architecture of cone bipolar cells in mammalian retina. Vision Res 21:1559–1563

Famiglietti EV, Kolb H (1976) Structural basis for on- and off-center responses in retinal ganglion cells. Science 194:193–195

Famiglietti EV, Kaneko A, Tachibana M (1977) Neuronal architecture of on and off pathways to ganglion cells in carp retina. Science 198:1267–1271

Farnsworth D (1943) The Farnsworth-Munsell 100-Hue and dichotomous tests for color vision. J Opt Soc Am 33:568–578

Farnsworth D (1947) The Farnsworth dichotomous test for color blindness, panel D-15. Psychol Corp, New York

Farnsworth D (1957) The Farnsworth-Munsell 100-Hue test for the examination of color discrimination. (Revised 1957) Munsell Color Company, Baltimore, Md

Fatt P (1981) Proteins of vertebrate rod outer segments: a possible role for multiple forms of rhodopsin. Exp Eye Res 33:31–46

Fechner GT (1838) Über eine Scheibe zur Erzeugung subjektiver Farben. Ann Phy Chem 45:227–332

Festinger L, Allyn MR, White ChW (1971) The perception of color with achromatic stimulation. Vision Res 11:591–612

Fick A (1896) Zur Theorie der Farbenblindheit. Pflügers Arch gesamte Physiol Menschen Tiere 64:313–320

Fisher SK, Boykott BB (1974) Synaptic connections made by horizontal cells within the outer plexiform layer of the cat and the rabbit. Proc R Soc Lond B 186: 317–331
Foerster MH, Grind van de WA, Grüsser O-J (1977a) Frequency transfer properties of three distinct types of cat horizontal cells. Exp Brain Res 29:347–366
Foerster MH, Grind van de WA, Grüsser O-J (1977b) The response of cat horizontal cells to flicker stimuli of different area, intensity and frequency. Exp Brain Res 29:367–385
Foster DH (1980) Opponency of red- and green-sensitive cone mechanisms in field spectral sensitivity measurements. J Physiol 298:21
Foster DH (1981) Changes in field spectral sensitivities of red-, green- and blue-sensitive colour mechanisms obtained on small background fields. Vision Res 21: 1433–1455
Franceschetti A, Jaeger W, Klein D, Ohrt V, Rickli H (1959) Etude pathophysiologique et génétique de la grande famille d'achromates de l'île de Fur. Acta XVIII Concil Ophthalmol Bruxelles 2:1582–1588
François J, Verriest G (1957a) Les dyschromatopsies acquises (1). Ann Ocul 190: 713–729
François J, Verriest G (1957b) Les dyschromatopsies acquises (2). Ann Ocul 190: 812–859
François J, Verriest G (1957c) Les dyschromatopsies acquises (3). Ann Ocul 190: 893–943
François J, Verriest G (1961) On acquired deficiency of colour vision, with special reference to its detection and classification by means of the tests of Farnworth. Vision Res 1:201–219
François J, Verriest G, Montier V, Vanderdonck R (1957) De la fréquence des dyschromatopsies congénitales chez l'homme. Ann Ocul 190:5–16
Frome FS, MacLeod DIA, Buck S, Williams DR (1981) Large loss of visual sensitivity of flashed peripheral targets. Vision Res 21:1323–1328
Fuortes MGF (ed) (1972) Handbook of sensory physiology, vol VII/2. Springer, Berlin Heidelberg New York
Fuortes MGF, Simon EJ (1974) Interactions leading to horizontal cell responses in the turtle retina. J Physiol 240:177–198
Gallego A (1971) Horizontal and amacrine cells in the mammal's retina. Vision Res Suppl. 3:33–50
Garth T (1933) The incidence of color-blindness among races. Science 77:333–334
Gerschenfeld HM, Piccolino M (1979) Pharmacology of the connections of cones and L-horizontal cells in the vertebrate retina. In: Schmitt FO, Worden FG (eds) The neurosciences, fourth study program. MIT Press, Cambridge, Mass
Gerschenfeld HM, Piccolino M (1980) Sustained feedback effects of L-horizontal cells on turtle cones. Proc R Soc London Ser B 206:465–480
Gielen CCAM (1980) Spatio-temporal and chromatic properties of visual neurones in the rhesus monkey geniculate nucleus. Dissertation Katholieke Univ Nijmwegen
Gordon J, Abramov I (1977) Color vision in the peripheral retina. II. Hue and saturation. J Opt Soc Am 67:202–207
Gouras P (1967) The effects of light-adaptation on rod and cone receptive field organization of monkey ganglion cells. J Physiol 192:747–760
Gouras P (1968) Identification of cone mechanisms in monkey ganglion cells. J Physiol 199:533–547
Gouras P (1969) Antidromic responses of orthodromically identified ganglion cells in monkey retina. J Physiol 204:407–419
Gouras P (1970) Electroretinography: Some basic principles. Invest Ophthalmol 9:557–569
Gouras P (1971) The function of the midget cell system in primate color vision. Vision Res 3:397–410

Gouras P (1972) S-Potentials. In: Fuortes MGF (ed) Handbook of sensory physiology, vol VII/2, Physiology of Photoreceptor Organs. Springer, Berlin Heidelberg New York, pp 513–529
Gouras P (1974) Opponent-colour cells in different layers of foveal striate cortex. J Physiol 238:583–602
Gouras P, Krüger J (1979) Responses of cells in foveal visual cortex of the monkey to pure color contrast. J Neurophysiol 42:850–860
Gouras P, Link K (1966) Rod and cone interaction in dark-adapted monkey ganglion cells. J Physiol 184:499–510
Gouras P, Padmos P (1974) Identification of cone mechanisms in graded responses of foveal striate cortex. J Physiol 238:569–581
Gouras P, Zrenner E (1979a) Enhancement of luminance flicker by color-opponent mechanisms. Science 205:587–589
Gouras P, Zrenner E (1979b) The blue sensitive cone system. Excerpta Medica, Int Cong Ser 450/1:379–384
Gouras P, Zrenner E (1981a) Color coding in the primate retina. Vision Res 21: 1591–1598
Gouras P, Zrenner E (1981b) Color vision: A review from a neurophysiological perspective. In: Autrum H, Ottoson D, Perl ER, Schmidt RF (eds) Progress in sensory physiology, vol I. Springer, Berlin Heidelberg New York, pp 139–179
Graham CH (ed) (1965) Vision and Visual Perception. John Wiley, New York
Graham CH, Hsia Y (1958) Color defect and color theory. Studies of normal and color-blind persons, including a subject color-blind in one eye but not in the other. Science 127:675–682
Graham CH, Hsia Y (1960) Luminosity losses in deuteranopes. Science 131:417–418
Graham CH, Hsia Y (1969) Saturation and the foveal achromatic interval. J Opt Soc Am 59:993–997
Grand Le Y (1937) Recherches sur la diffusion de la lumière dans l'oeil humain. Rev Opt 16:241
Grand Le Y (1968) Light, colour and vision. Approved transl by Hunt RWG, Walsh JWT, Hunt FRW 2nd edn. Chapman and Hall Ltd, London
Granit R (1941) Isolation of colour-sensitive elements in a mammalian retina. Acta Physiol Scand 2:93–109
Granit R (1945) The electrophysiological analysis of the fundamental problem of colour reception. Proc Phys Soc London 57:447–463
Granit R (1947) Sensory mechanisms of the retina. Univ Press Oxford
Granit R (1949) The effect of two wave-lengths of light upon the same retinal element. Acta Physiol Scand 18:281–294
Granit R (1955) Receptors and sensory perception. Yale Univ Press, New Haven Conn
Granit R (1975) Adaptability of the nervous system in relation to chance, purposiveness, and causality. Proc Am Philos Soc 119:262–266
Granit R, Harper P (1930) Comparative studies on the peripheral and central retina. Am J Physiol 95:211–228
Granit R, Tansley K (1948) Rods, cones and the localization of pre-excitatory inhibition in the mammalian retina. J Physiol 107:54–66
Grassmann H (1853) Zur Theorie der Farbenmischung. Ann Phys Leipzig 89:69–84
Green DG (1968) The contrast sensitivity of the colour mechanisms of the human eye. J Physiol 196:415–429
Green DG (1969) Sinusoidal flicker characteristics of the color-sensitive mechanisms of the eye. Vision Res 591–601
Green DG (1972) Visual acuity in the blue cone monochromat. J Physiol 222:419–426
Green M (1981) Psychophysical relationships among mechanisms sensitive to pattern, motion and flicker. Vision Res 21:971–983
Grind van de W, Grüsser O-J (1981) Frequency transfer properties of cat retina horizontal cells. Vision Res 21:1565–1572

Grind van de W, Grüsser O-J, Lunkenheimer H-U (1973) Temporal transfer properties of the afferent visual system. Psychophysical, neurophysiological and theoretical investigations. In: Jung R (ed) Handbook of sensory physiology, vol VII/3. Central visual information A. Springer, Berlin Heidelberg New York

Grüsser O-J (1971) A quantitative analysis of spatial summation of excitation and inhibition within the receptive field of retinal ganglion cells of cats. Vision Res Suppl 3:103–127

Grüsser O-J (1979) Cat ganglion-cell receptive fields and the role of horizontal cells in their generation. In: Schmitt FO, Worden FG (eds) The Neurosciences, fourth study program. MIT Press, Cambridge, Mass, pp 247–273

Grüsser O-J, Creutzfeld O (1957) Eine neurophysiologische Grundlage des Brücke-Bartley-Effektes: Maxima der Impulsfrequenz retinaler und corticaler Neurone bei Flimmerlicht mittlerer Frequenzen. Pflügers Arch 263:668-681

Grüsser O-J, Reidemeister Ch (1959) Flimmerlichtuntersuchungen an der Katzenretina. II. Off-Neurone und Besprechung der Ergebnisse. Z Biol 111:254–270

Grützner P (1962) Beitrag zur Frage der spektralen Hellempfindlichkeit bei angeborenen Farbensinnstörungen. Albrecht von Graefes Arch Ophthalmol 164:411–420

Grützner P (1966) Über erworbene Farbensinnstörungen bei Sehnerverkrankungen. Albrecht von Graefes Arch Ophthalmol 169:366–384

Grützner P (1972) Acquired color vision defects. In: Jameson D, Hurvich LM (eds) Handbook of sensory physiology, vol VII/4, visual psychophysics. Springer, Berlin Heidelberg New York, pp 643–659

Guild J (1931) The colorimetric properties of the spectrum. Philos Trans R Soc London Ser A 230:149–187

Guth SL (1967) Nonadditivity and inhibition among chromatic luminances at threshold. Vision Res 7:319–328

Guth SL, Donley NJ, Marrocco RT (1969) On luminance additivity and related topics. Vision Res 9:537–575

Hagins WA (1972) The visual process: Excitatory mechanisms in the primary receptor cells. Annu Rev Biophys Bioeng 1:131–158

Hagins WA (1979) Excitation in vertebrate photoreceptors. In: Schmitt FO, Worden FG (eds) The neurosciences. Fourth study program. MIT Press, Cambridge Mass, pp 183–191

Hajos A (1968) Psychophysiologische Probleme bei „Farbkonturen" und „Konturfarben". Stud Psychol Bratislava 10:254–266

Hansen E (1979) Typical and atypical monochromacy studied by specific quantitative perimetry. Acta Ophthalmol 57:211–224

Hansen E, Seim T, Olsen BT (1978) Transient tritanopia experiment in blue cone monochromacy. Nature (London) 276:390–391

Hartline HK (1938) The response of single optic nerve fibers of the vertebrate eye to illumination of the retina. Am J Physiol 121:400–415

Hartline HK (1949) Inhibition of activity of visual receptors by illuminating nearby retinal areas in the limulus eye. Fed Proc 8:69

Harwerth RS, Sperling HG (1975) Effects of intense visible radiation on the increment threshold spectral sensitivity of the rhesus monkey eye. Vision Res 15: 1193–1204

Hashimoto Y, Inokuchi M (1981) Characteristics of second order neurons in the dace retina: physiological and morphological studies. Vision Res 21:1541–1550

Hassenstein B (1968) Modellrechnung zur Datenverarbeitung beim Farbensehen des Menschen. Kybernetik 4:209–223

Hassler R (1965) Die zentralen Systeme des Sehens. Ber Dtsch Ophthalmol Ges 66: 229–251

Heath GG (1960) Luminosity losses in deuteranopes. Science 131:417–418

Hecht S (1931) The interrelation of various aspects of color vision. J Opt Soc Am 21:615–639

Hecht S, Shlaer S (1936) The color vision of dichromats. I. Wavelength discrimination, brightness distribution, and color mixture. J Gen Physiol 20: 57–93

Heinsius E (1973) Farbsinnstörungen und ihre Prüfung in der Praxis. Enke, Stuttgart
Helmholtz von HLF (1860) Handbuch der physiologischen Optik, vol II, 1st edn. Voss, Leipzig
Helmholtz von HLF (1911) Handbuch der physiologischen Optik, vol II, 3rd edn. Gullstrand A, Kries von J, Nagel W (Hrsg) Voss, Hamburg Leipzig
Hemminger H, Mahler P (1980) Psychophysical saturation scales and the spectral sensitivity in human vision. Psychol Res 42:207–212
Herbolzheimer WG (1976) The effect of area and retinal position on the luminance required to discrimate flicker. Dissertation med Giessen
Hering E (1878) Zur Lehre vom Lichtsinne. Gerold's Sohn, Wien, pp 107–141 (See also Hering E (1920) Grundzüge der Lehre vom Lichtsinn. Springer, Berlin)
Hering E (1891) Untersuchung eines total Farbenblinden. Pflügers Arch 49:563–608
Hess C, Hering E (1898) Untersuchungen an total Farbenblinden. Pflügers Arch gesamt Physiol Menschen Tiere 71:105–127
Hessberg R (1909) Ein Beitrag zur angeborenen totalen Farbenblindheit. Klin Monatsbl Augenheilkd 47:129–138
Hillebrand F (1889) Über die specifische Helligkeit der Farben. Beiträge zur Psychologie der Gesichtsempfindungen. Sitzungsber Kais Akad Wiss Wien, Math Nat Cl 98:70–120
Hochstein S, Shapley RM (1976) Quantitative analysis of retinal ganglion cell classifications. J Physiol 262:237–264
Hodgkin AL (1974) The conduction of the nervous impulse. Liverpool Univ Press, Liverpool
Hodgkin AL, McNaughton PA, Yau K-W (1981) Effect of ions on the light-sensitive currents generated by the rod outer segments of Bufo marinus. J Physiol 317:71P–72P
Hoffmann K-P, Stone J, Sherman SM (1972) Relay of receptive-field properties in dorsal lateral geniculate nucleus of the cat. J Neurophysiol 35:518–531
Holmes G (1918) Disturbances of vision by cerebral lesions. Br J Ophthalmol 2: 353–384
Honig B, Dinur U, Nakanishi K, Balogh-Nair V, Gawinowicz MA, Arnaboldi M, Motto MG (1979) An external point-charge model for wavelength regulation in visual pigments. J Am Chem Soc 101:7084–7086
Horst van der GJC (1969) Chromatic flicker. J Opt Soc Am 59:1213–1217
Horst van der GJC, De Weert CMM, Bouman MA (1967) Transfer of spatial chromaticity-contrast at threshold in the human eye. J Opt Soc Am 57:1260–1266
Horst van der GJC, De Weert CMM, Bouman MA (1967) Transfer of spatial chromaticity-contrast at threshold in the human eye. J Opt Soc Am 57:1260–1266
Hubbard JI, Llinás R, Quastel DMJ (1969) Electrophysiological analysis of synaptic transmission. Arnold Ltd, London
Hubbel WL, Bownds MD (1979) Visual transduction in vertebrate photoreceptors. Annu Rev Neurosci 2:17–34
Hubel DH, Wiesel TN (1960) Receptive fields of optic nerve fibres in the spider monkey. J Physiol 154:572–580
Hubel DH, Wiesel TN (1968) Receptive fields and functional architecture of monkey striate cortex. J Physiol 195:215–243
Hubel DH, Wiesel TN (1977) Functional architecture of macaque monkey visual cortex. Proc R Soc London B 198:1–59
Huber C, Adachi-Usami E (1972) Scotopic visibility curve in man obtained by the VER. In: Arden GB (ed) The visual system: Neurophysiology, biophysics, and their clinical application. Plenum Publ Corp, New York, pp 189–198
Hughes A (1979) A rose by any other name... On "naming of neurones" by Rowe and Stone. Brain Behav Evol 16:52–64
Hurvich LM (1972) Color vision deficiencies. In: Jameson D, Hurvich L (eds) Handbook of sensory physiology, vol VII/4, Visual psychophysics. Springer, Berlin Heidelberg New York, pp 381–412

Hurvich LM (1977) Two decades of opponent processes. In: Colour 77. Proc Int Colour Asso. Hilger, London, pp 33–61
Hurvich LM (1981a) Colour vision and its deficiencies. Impact Sci Soc 31:151–164
Hurvich LM (1981b) Colour vision. Sinauer Assoc, Sunderland, Mass
Hurvich LM, Jameson D (1955) Some quantitative aspects of an opponent-colors theory. II. Brightness, saturation, and hue in normal and dichromatic vision. J Opt Soc Am 45:602–616
Hurvich LM, Jameson D (1957) An opponent-process theory of color vision. Psychol Rev 64:384–403
Hurvich LM, Jameson D (1964) Outlines of a theory of the light sense. Harvard Univ Press, Cambridge Mass
Hylkema BS (1942) Examination of the visual field by determining the fusion frequency. Acta Ophthalmol 20, 181–193
Ikeda M, Boynton RM (1962) Effect of test flash duration upon the spectral sensitivity of the eye. J Opt Soc Am 52:697–699
Ikeda H, Wright MJ (1972) Receptive field organization of "sustained" and "transient" retinal ganglion cells which subserve different functional roles. J Physiol 227:769–800
Ingling CR Jr (1977) The spectral sensitivity of the opponent-color channels. Vision Res 17:1083–1089
Ingling CR Jr (1978) Luminance and opponent color contributions to visual detection and to temporal and spatial integration. Comment. J Opt Soc Am 68:1143–1147
Ingling CR Jr, Drum BA (1973) Retinal receptive fields: Correlations between psychophysics and electrophysiology. Vision Res 13:1151–1163
Ingling CR Jr, Martinez E (1981) Opponent theory: revision to include the X-cell achromatic channel. Abstr S5, Proc 4th Congr Int Color Assoc Berlin
Ingling CR Jr, Scheibner HMO, Boynton RM (1970) Color naming of small foveal fields. Vision Res 10:501–511
Ingling CR Jr, Burns S, Drum BA (1977) Desaturating blue increases only chromatic brightness. Vision Res 17:501–503
Ingling CR Jr, Russel PW, Rea MS, Tsou BH-P (1978) Red-green opponent spectral sensitivity. Disparity between cancellation and direct matching methods. Science 201:1221–1223
Ishihara S (1964) Test for colour-blindness. Kanehara Shuppan, Tokyo
Jacobs GH (1974) Spectral sensitivity of the short wavelength mechanism in the squirrel monkey visual system. Vision Res 14:1271–1273
Jaeger W (1950) Systematische Untersuchungen über „inkomplette" angeborene totale Farbenblindheit. Albrecht von Graefes Arch Ophthalmol 150:509–528
Jaeger W (1951) Angeborene totale Farbenblindheit mit Resten von Farbempfindung. Klin Monatsbl Augenheilkd 118:282–288
Jaeger W (1954) Dominant vererbte Opticusatrophie. (Unter besonderer Berücksichtigung der dabei vorhandenen Farbensinnstörung) Albrecht von Graefes Arch Ophthalmol 155:457–484
Jaeger W (1958) Diagnose und Differentialdiagnose der angeborenen totalen Farbenblindheit in der augenärztlichen Praxis. Klin Monatsbl Augenheilkd 133:586
Jaeger W (1972) Genetics of congenital colour deficiencies. In: Jameson D, Hurvich LM (eds) Handbook of sensory physiology, vol VII/4, Visual Psychophysics. Springer, Berlin Heidelberg New York, pp 625–642
Jaeger W (1979) Goethes Untersuchungen an Farbenblinden. Heidelberger Jahrbücher 23:27–38. Springer, Berlin Heidelberg New York
Jaeger W, Grützner P (1963) Erworbene Farbensinnstörungen. In: Sautter H (ed) Entwicklung und Fortschritt in der Augenheilkunde. Enke, Stuttgart, pp 591–614
Jaeger W, Grützner P (1966) Le alterazioni del senso cromatico nelle degenerazioni famigliari maculari e nelle atrofie ereditarie. Boll Ocul 45:Fasc 11, 783–810
810

Jaeger W, Lauer HJ (1976) Non-allelic compounds of protan and deutan deficiencies. Mod Probl Ophthalmol 17:121–130

Jaeger W, Lux P, Grützner P, Jessen KH (1961) Subjektive und objektive spektrale Helligkeitsverteilung bei angeborenen und erworbenen Farbsinnstörungen. In: Jung R, Kornhuber H (eds) Neurophysiologie und Psychophysik des visuellen Systems, Symposium Freiburg/Br 1960. Springer, Berlin Heidelberg New York, pp 199–209

Jankov E (1978) Spektralsensitivität der off-Antwort im menschlichen VECP bei verschiedenfarbiger Adaptation. Albrecht von Graefes Arch klin Exp Ophthalmol 206: 121–133

Judd DB (1943) Facts of color-blindness. J Opt Soc Am 33:294–307

Judd DB (1945) Standard response functions for protanopic and deuteranopic vision. J Opt Soc Am 35:199–221

Judd DB (1952) Color in business, science and industry, see p. 171. Wiley and Sons, New York

Judd DB (1966) Fundamental studies of color vision from 1860 to 1960 Proc Natl Acad Sci USA 55:1313–1330

Jung R (1965) Neuronale Grundlagen des Hell-Dunkelsehens und der Farbwahrnehmung. Ber Dtsch Ophthalmol Ges 66:69–111

Jung R (1973) Visual perception and neurophysiology. In: Jung R (ed) Handbook of sensory physiology, vol VII/3. Central processing of visual information, Part A. Springer, Berlin Heidelberg New York, pp 1–152

Jung R (1978) Einführung in die Sehphysiologie. In: Gauer OH, Kramer K, Jung R (eds) Physiologie des Menschen, vol 13, Sehen. Sinnesphysiologie III. Urban und Schwarzenberg, München Wien Baltimore, pp 1–140

Kaiser PK, Blick DW Jr, Brown JL (1977) Flicker fusion of opponent and non-opponent LGN cells in macaque. J Opt Soc Am 67:1379

Kalmus H (1955) The familiar distribution of congenital tritanopia with some remarks on some similar conditions. Ann Hum Genet 20:39–56

Kalmus (1965) Diagnosis and genetics of defective colour vision. Pergamon Press, New York

Kaneko A (1970) Physiological and morphological identification of horizontal, bipolar and amacrine cells in goldfish retina. J Physiol 207:623–633

Kaneko, A (1971) Physiological studies of single retinal cells and their morphological identification. Vision Res Suppl 3:17–26

Kaneko A (1973) Receptive field organization of bipolar and amacrine cells in the goldfish retina. J Physiol 235:133–153

Kaneko A (1979) Physiology of the retina. Annu Rev Neurosci 2:169–191

Kaneko A, Shimazaki H (1975) Synaptic transmission from photoreceptors to bipolar and horizontal cells in carp retina. Cold Spring Harbor Symp Quant Biol 40:537–546

Kaneko A, Tachibana M (1981) Retinal bipolar cells with double colour-opponent receptive fields. Nature (London) 293:220–222

Kaneko A, Nishimura Y, Tachibana M, Tauchi M, Shimai K (1981) Physiological and morphological studies of signal pathways in the carp retina. Vision Res 21:1519–1526

Kato S, Negishi K (1979) Rod- and cone-bipolar cell-responses in the carp retina. Exp Eye Res 28:159–166

Katz B (1966) Nerv, Muskel und Synapse. (transl. by Bentrup F-W, Hengstenberg R. Nerve, muscle and synapse. McGraw-Hill Book Company, New York

Kellermann F-J, Adachi-Usami E (1972/73) Spectral sensitivities of colour mechanisms isolated by the human visual evoked response. Ophthalmol Res 4:199–210

Kelly DH (1973) Lateral inhibition in human colour mechanisms. J Physiol 228: 55–72

Kelly DH (1974) Spatio-temporal frequency characteristics of color-vision mechanisms. J Opt Soc Am 64:983–990

Kelly DH (1975) Luminous and chromatic flickering patterns have opposite effects. Science 188:371–372
Kelly DH (1978) Sine-wave contrast, flicker, and motion sensitivity with stabilized retinal images. Invest Ophthalmol Visual Sci (ARVO-Suppl) 17:222
Kelly DH (1981) Disappearance of stabilized chromatic gratings. Science 214:1257–1258
Kelly DH, Norren van D (1977) Two-band model of heterochromatic flicker. J Opt Soc Am 67:1081–1091
King-Smith PE (1975) Visual detection analyzed in terms of luminance and chromatic signals. Nature London 255:69–70
King-Smith PE, Carden D (1976) Luminance and opponent-color contributions to visual detection and adaptation and to temporal and spatial integration. J Opt Soc Am 66:709–718
King-Smith PE, Carden D (1978) Luminance and opponent color contributions to visual detection and to temporal and spatial integration: Author's reply to comments. J Opt Soc Am 68:1146–1147
King-Smith PE, Kranda K, Wood ICJ (1976) An acquired color defect of the opponent-color system. Invest Ophthalmol 15:584–587
King-Smith PE, Rosten JG, Alvarez S, Bhargava SK (1980) Human vision without tonic cells? In: Verriest G (ed) Colour vision deficiencies, vol V. Hilger, Bristol, pp 99–105
Kirby AW, Enroth-Cugell C (1976) The involvement of gamma-aminobutyric acid in the organization of cat retinal ganglion cell receptive fields. J Gen Physiol 68: 465–484
Klauder A, Scheibner H (1980) Dichromatisches Gegenfarbensehen. In: Farbe und Design 15/16:65–70
Klingaman RL (1977) A comparison of psychophysical and VECP increment threshold functions of a rod monochromat. Invest Ophthalmol Visual Sci 16:870–873
Klingaman RL, Zrenner E, Baier M (1980) Increment flicker and hue spectral sensitivity functions in normals and dichromats: The effect of flicker rate. In: Verriest G (ed) Colour vision deficiencies, vol V. Hilger, Bristol, pp 240–243
Köllner H (1912) Die Störungen des Farbensinnes. Karger, Berlin
Köllner H (1929) Die Abweichungen des Farbensinnes (mit Nachträgen ab 1924 von E. Engelking). In: Bethe A, Embden G, Bergmann von G, Ellinger A (eds) Handbuch der normalen und pathologischen Physiologie. Mit Berücksichtigung der experimentellen Pharmakologie, vol 12, Receptionsorgane II (1), Photoreceptoren. Springer, Berlin Heidelberg New York
König A (1891) Über den Helligkeitswert der Spektralfarben bei verschiedener absoluter Intensität. Beitr Psychol Physiol Sinnesorg (Helmholtz-Festschrift) Voss, Hamburg, pp 309–388 Abdruck in: König A (1903) Gesammelte Abhandlungen zur Physiologischen Optik. Barth, Leipzig
König A (1899) Bemerkungen über angeborene totale Farbenblindheit. Z Psychol Physiol Sinnesorg 20:425–434 Abgedruckt in: König A (1903) Gesammelte Abhandlungen zur Physiologischen Optik. Barth, Leipzig
König A (1903) Über Blaublindheit. Sitzungsber Akad Wiss Berlin 8. Juli 1897, pp 718–731. Abgedruckt in: König A. Gesammelte Abhandlungen zur Physiologischen Optik. Barth, Leipzig
König A, Dieterici C (1893) Die Grundempfindungen in normalen und anomalen Farbensystemen und ihre Intensitätsverteilung im Spektrum. Z Psychol Physiol Sinnesorg 4:241–347
Kojima M, Zrenner E (1977) Local and spatial distribution of photopic and scotopic responses in the visual field as reflected in the visually evoked cortical potential (VECP). Doc Ophthalmol Proc Ser 13:31–40, Dr. Junk Publ: The Hague
Kojima M, Zrenner E (1980) Determination of local thresholds in the visual field by recording the scotopic visually evoked cortical potential in man. Ophthalmic Res 12:1–8

Kolb H (1970) The organization of the outer plexiform layer of the primate retina: Electron microscopy of Golgi-impregnated cells. Philos Trans R Soc London Ser B 258:261–283

Kolb H (1974) The connections between horizontal cells and photoreceptors in the retina of the cat: Electron microscopy of Golgi preparations. J Comp Neurol 155:1–14

Kolb H (1977) The organization of the outer plexiform layer in the retina of the cat: electron microscopic observations. J Neurocytol 6:155–170

Kolb H (1979) The inner plexiform layer in the retina of the cat: electron microscopic observations. J Neurocytol 8:295–329

Kolb H, Famiglietti EV Jr (1976) Rod and cone pathways in the retina of the cat. Invest Ophthalmol 15:935–946

Kolb H, Boycott BB, Dowling JE (1969) A second type of midget bipolar cell in the primate retina. Appendix to Boycott and Dowling (1969). Philos Trans R Soc London Ser B 255:177–184

Kolb H, Famiglietti EV, Nelson R (1976) Neural connections in the inner plexiform layer of the cat's retina. Repr from: Yamada E, Mishima S (eds) Structure of the eye, vol III. Jpn J Ophthalmol, pp 319–332

Kolb H, Mariani A, Gallego A (1980) A second type of horizontal cell in the monkey retina. J Comp Neurol 189:31–44

Kolb H, Nelson R, Mariani A (1981) Amacrine cells, bipolar cells and ganglion cells of the cat retina: A Golgi study. Vision Res 21:1081–1114

Kramer W, Thormann J, Schlepper N, Bittner Ch, Zrenner E (1981) Aktivitätsprofil von AR-L 115 BS bei therapierefraktärer kongestiver Kardiomyopathie (CC) und Herzgesunden (HG): Wirkungsverlust durch Ca^{++} Antagonisten. Verh Dtsch Ges Inn Med 87:446–450

Kramer W, Schlepper M, Thormann J, Bittner Ch (1982) Pharmacodynamics and pharmacokinetics of AR-L 115 BS, a new positive inotropic substance, and their alterations by Verapamil in healthy volunteers. Eur Heart J (in press)

Kranda K, King-Smith PE (1979) Detection of coloured stimuli by independent linear systems. Vision Res 19:733–745

Krastel H, Jaeger W (1982) Large field spectral sensitivity in congenital and acquired achromatopsia. Doc Ophthalmol Proc Ser 33:329–332, ed by Verriest G: Dr Junk Publ: The Hague

Krastel H, Jaeger W, Blankenagel A (1981) Nachweis von Resten eines „Rot-Rezeptors" unter chromatischer Adaptation bei Patienten mit zunächst typisch erscheinender angeborener totaler Farbenblinheit. Ber Dtsch Opthalmol Ges 78:717–726

Krastel H, Jaeger W, Blankenagel A (1982a) Zapfenrestaktivitäten bei verschiedenen Typen angeborener totaler Farbenblindheit und das Konzept der inkompletten Achromatopsie. Ber Dtsch Ophthalmol Ges (in press)

Krastel H, Alexandridis E, Gertz J (1982b) Pupil thresholds are influenced by colour opponent mechanisms (in prep)

Krauskopf J (1973) Contributions of the primary chromatic mechanisms to the generation of visual evoked potentials. Vision Res 13:2289–2298

Kries von J (1882) Die Gesichtsempfindungen und ihre Analyse. Leipzig

Kries von J (1897) Über Farbensysteme. Z Psychol Physiol Sinnesorg 13:241–324

Kries von J (1903) Über die Wahrnehmung des Flimmerns durch normale und durch total farbblinde Personen. Z Psychol 32:113–117

Kries von J (1904) Die Gesichtsempfindungen. In: Nagel W (ed) Handbuch der Physiologie des Menschen, vol III. Vieweg, Braunschweig, pp 109–282

Krill AE, Smith VC, Pokorny J (1970) Similarities between congenital tritan defects and dominant optic-nerve atrophy: Coincidence or identity? J Opt Soc Am 60: 1132–1139

Krill AE, Smith VC, Porkorny J (1971) Further studies supporting the identity of congenital tritanopia and hereditary dominant optic atrophy. Invest Ophthalmol 10:457–465

Krnjević K (1974) Chemical nature of synaptic transmission in vertebrates. Physiol Rev 54:418–540
Kröger-Paulus A (1980) Reduktion der Deuteranopie aus der normalen Trichromasie. Farbe 28:73–116
Kröger-Paulus A, Scheibner H (1978) Reduktion der Deuteranopie aus der Trichromasie. Ber Dtsch Ophthalmol Ges 75:515–517
Kröger-Paulus, Scheibner H (1980) Variation of deuteranopic blind fundamentals and the visual cone pigment erythrolabe. Ophthalmic Res 12:183
Krüger J (1977) Stimulus dependent colour specificity of monkey lateral geniculate neurones. Exp Brain Res 30:297–311
Krüger J (1981) The difference between X- and Y-type responses in ganglion cells of the cat's retina. Vision Res 21:1685–1687
Krüger J, Fischer B (1973) Strong periphery effect in cat retinal ganglion cells. Excitatory responses in on- and off-center neurones to single grid displacements. Exp Brain Res 18:316–318
Krüger J, Gouras P (1980) Spectral selectivity of cells and its dependence on slit length in monkey visual cortex. J Neurophysiol 43:1055–1069
Ksinsik R (1967) Adaptive Parameter der Blauverschiebung der Spektralsensitivität des Kaninchenauges. Albrecht von Graefes Arch Ophthalmol 172:112–124
Kühne W (1879) Chemische Vorgänge in der Netzhaut. In: Hermann L, Vogel FCW (eds) Handbuch der Physiologie der Sinnesorgane, vol III, part 3. Leipzig. Translation by Hubbard R, Wald G in: Vision Res 17:1269–1316
Kuffler SW (1953) Discharge patterns and functional organization of mammalian retina. J Neurophysiol 16:37–68
Kuffler SW, Fitzhugh R, Barlow HB (1957) Maintained activity in the cat's retina in light and darkness. J Gen Physiol 40:683–702
Kupfermann I (1979) Modulatory actions of neurotransmitters. Ann Rev Neurosci 2:447–465
Lam DMK (1975) Synaptic chemistry of identified cells in the vertebrate retina. Cold Spring Harbor Symp Quant Biol 40:571–579
Lam DMK, Lasater EM, Naka KI (1978) γ-aminobutyric acid: A neurotransmitter candidate for cone horizontal cells of catfish retina. Proc Natl Acad Sci USA 75: 6310–6313
Landis C (1954) Determinants of the critical flicker-fusion threshold. Physiol Rev 34:259–286
Lange Dzn de H (1958) Research into the dynamic nature of the human fovea → cortex systems with intermittent and modulated light. I. Attenuation characteristics with white and colored light. J Opt Soc Am 48: 784–789
Langer H (ed) (1973) Biochemistry and physiology of visual pigments. Springer, Berlin Heidelberg New York
Langhof HJ (1977) Gegensätzliche Wirkungen farbiger Adaptation auf den on- und off-Effekt im photopischen Elektroretinogramm. Albrecht von Graefes Arch klin exp Ophthalmol 204:265–274
Langhof HJ, Zrenner E (1977) Wirkung chromatischer Adaptation auf a-Welle und off-Effekt im menschlichen Elektroretinogramm. Klin Monatsbl Augenheilkd 171:160
Lasansky A (1981) Synaptic action mediating cone responses to annular illumination in the retina of the larval tiger salamander. J Physiol 310:205–214
Lasansky A, Marchiafava PL (1974) Light-induced resistance changes in retinal rods and cones of the tiger salamander. J Physiol 236:171–191
Lasansky A, Vallerga S (1975) Horizontal cell responses in the retina of the larval tiger salamander. J Physiol 236:171–191
Lawwill T (1978) Congenital achromatopsia and macular hypoplasia. Perspectives in Ophthalmology 2:5–12
Leber T (1873) Über die Theorie der Farbenblindheit und über die Art und Weise, wie gewisse, der Untersuchung von Farbenblinden entnommene Einwände gegen die Young-Helmholtz'sche Theorie sich mit derselben vereinigen lassen. Klin Monatsbl Augenheilkd 11:467–473

Lee BB, Creutzfeldt OD, Elepfandt A (1979) The responses of magno- and parvocellular cells of the monkey's lateral geniculate body to moving stimuli. Exp Brain Res 35: 547–557
Legge GE (1978) Sustained and transient mechanisms in human vision. Temporal and spatial properties. Vision Res 18:69–81
Lehmann D, Callaway E (eds) (1979) Human evoked potentials. Plenum Press, New York
Leibold JE (1966) The ocular toxicity of Ethambutol and its relation to dose. Ann NY Acad Sci 135:904–908
Lennie P (1980) Parallel visual pathways: A review. Vision Res 20:561–594
Leventhal AG, Rodieck RW, Dreher B (1981) Retinal ganglion cell classes in the Old World monkey: Morphology and central projections. Science 213:1139–1142
Liebman PA (1972) Microspectrophotometry of photoreceptors. In: Dartnall HJA (ed) Handbook of sensory physiology, vol VII/1. Photochemistry of vision. Springer, Berlin Heidelberg New York, pp 481–528
Linksz A (1964) An essay on color vision and clinical color-vision tests. Grune and Stratton, New York
Lith van GHM (1973) General cone dysfunction without achromatopsia. Doc Ophthalmol Proc Series 2:175–180, ed by Pearlman JT: Dr Junk Publ: The Hague
Lith van GHM, Henkes E (1968) The local electric response of the central retinal area. 6th ISCERG Symp Erfurt 1967. VEB Georg Thieme, Leipzig, pp 163–170
Little RE (1974) A mean square error comparison of certain median response estimates for the up-and-down method with small samples. J Am Statist Assoc 69:202–206
Lomonosov MV (1757) Lecture on the origin of light, presenting a new theory of colours (In Russian) St Petersburg, Academy of Sciences (Quoted from Brindley 1970)
Lüddeke H, Aulhorn E (1974) Verschmelzungsfrequenz bei schwellenbezogener Reizlichtdichte. Ber Dtsch Ophthalmol Ges 72:275–279
Lyle WM (1974a) Drugs and conditions which may affect color vision. Part I — Drugs and chemicals. J Am Optometric Assoc 45:47–61
Lyle WM (1974b) Drugs and conditions which may affect color vision. Part II — Diseases and conditions. J Am Optometric Ass 45:173–182
Mach E (1865) Über die Wirkung der räumlichen Verteilung des Lichtreizes auf der Netzhaut. Sitzungsber Akad Wiss 52
Mach E (1918) Die Analyse der Empfindungen und das Verhältnis des Physischen zum Psychischen, 7th edn. Gustav Fischer, Jena. 1st publ 1885
MacLeod DIA (1978) Visual sensitivity. Ann Rev Psychol 29:613–645
MacNichol EF Jr (1964) Retinal mechanisms of color vision. Vision Res 4:119–133
MacNichol EF Jr, Feinberg R, Hárosi FI (1973) Colour discrimination processes in the retina. In: Colour 73. Adam Hilger, London, pp 191–251
Maffei L (1968) Inhibitory and facilitatory spatial interactions in retinal receptive fields. Vision Res 8:1187–1194
Maffei L, Cervetto L, Fiorentini A (1970) Transfer characteristics of excitation and inhibition in cat retinal ganglion cells. J Neurophysiol 33:276–284
Magnussen S, Bjørklund RA, Krüger J (1979) The perception of flicker: Theoretical note on the relation between brightness and darkness enhancement. Scand J Psychol 20:257–258
Malpeli JG, Schiller PH (1978) Lack of blue off-center cells in the visual system of the monkey. Brain Res 141:385–389
Marc RE, Sperling HG (1977) Chromatic organization of primate cones. Science 196: 454–456
Marc RE, Stell WK, Bok D, Lam DMK (1978) GABA-ergic pathways in the goldfish retina. J Comp Neurol 182:221–246
Marchiafava PL, Weiler R (1980) Intracellular analysis and structural correlates of the organization of inputs to ganglion cells in the retina of the turtle. Proc R Soc Lond 208:103–113

Mariani AP (1981) A diffuse, invaginating cone bipolar cell in primate retina. J Comp Neurol 197:661–671
Mariani A (1982a) Newly identified bipolar cells in monkey retina. Invest Ophthalmol Vis Sci (ARVO-Suppl) 22:247
Mariani A (1982b) Biplexiform cells. Ganglion cells of the primate retina that contact photo-receptors. Science 216:1134–1136
Marks LE, Bornstein MH (1973) Spectral sensitivity by constant CFF: Effect of chromatic adaptation. J Opt Soc Am 63:220–226
Marks WB, Dobelle WH, MacNichol EF (1964) Visual pigments of single primate cones. Science 143:1181–1183
Marr D (1974) The computation of brightness by the primate retina. Vision Res 14: 1377–1388
Marré M (1970) Die Darstellung von drei Farbseh-Mechanismen bei erworbenen Farbensehstörungen. In: Richter M (ed) Color 69, vol I. Muster-Schmidt, Göttingen Zürich Frankfurt, pp 97–106
Marré M (1973) The investigation of acquired colour vision deficiencies. In: Colour 73. Adam Hilger, London, pp 99–135
Marré M, Marré E (1978) Different types of acquired colour vision deficiencies on the base of CVM patterns in dependence upon the fixation mode of the diseased eye. Mod Probl Ophthalmol 19:248–252
Marrocco RT (1976) Sustained and transient cells in monkey lateral geniculate nucleus: Conduction velocities and response properties. J Neurophysiol 39:340–353
Matthaei R (1971) Goethes Farbenlehre. Ausgewählt und erläutert von R. Matthaei. Otto Maier, Ravensburg
Maxwell JC (1857) Experiments on colour, as perceived by the eye, with remarks on colour-blindness. Trans. R Soc Edinburgh 21:275–298
May B (1907) Ein Fall totaler Farbenblindheit. Z Sinnesphysiol 42:69–82
McKee SP, Westheimer G (1970) Specificity of cone mechanisms in lateral interaction. J Physiol 206:117–128
Meadows JC (1974) Disturbed perception of colours associated with localized cerebral lesions. Brain 97:615–632
Mehaffey L, Berson EL (1974) Cone mechanisms in the electroretinogram of the cynomolgus monkey. Invest Ophthalmol 13:266–273
Michael CR (1966) Receptive fields of opponent color units in the optic nerve of the ground squirrel. Science 152:1095–1097
Michael CR (1978a) Color vision mechanisms in monkey striate cortex: Simple cells with dual opponent-color receptive fields. J Neurophysiol 41:1233–1249
Michael CR (1978b) Color-sensitive complex cells in monkey striate cortex. J Neurophysiol 41:1250–1266
Miller RF (1979) The neuronal basis of ganglion-cell receptive field organization and the physiology of amacrine cells. In: Schmitt FO, Worden FG (eds) The neurosciences, 4th Stud Prog. MIT Press, Cambridge, pp 227–246
Miller RF, Dacheux RF (1976) On and off channels in mudpuppy retina. I. J Gen Physiol 67:639–659
Mitzdorf U, Singer W (1978) Prominent excitatory pathways in the cat visual cortex (A 17 and A 18): a current source density analysis of electrically evoked potentials. Exp Brain Res 33:371–394
Mollon JD (1982a) A taxonomy of tritanopias. Doc Ophthalmol Proc Ser 33:87–101, ed by Verriest G. Dr Junk Publ:The Hague
Mollon JD (1982b) Color Vision. Ann Rev Psychol 33:41–85
Mollon JD, Polden PG (1975) Some properties of the blue cone mechanism of the eye. J Physiol 254:1-2
Mollon JD, Polden DG (1977a) Saturation of a retinal cone mechanism. Nature 265:243–246

Mollon JD, Polden PG (1977b) An anomaly in the response of the eye to light of short wavelengths. Phil Trans R Soc Lond B 278:207–240
Mollon JD, Polden PG (1979) Post-receptoral adaptation. Vision Res 19:435–440
Mollon JD, Polden PG (1980) A curiosity of light adaptation. Nature (London) 286:59–62
Mollon JD, Newcombe F, Polden PG, Ratcliff G (1980) On the presence of three cone mechanisms in a case of total achromatopsia. In: Verriest G (ed) Colour vision deficiencies, vol V. A Hilger Ltd, Bristol, pp 130–135
Monasterio de FM (1978a) Properties of concentrically organized X and Y ganglion cells of macaque retina. J Neurophysiol 41:1394–1417
Monasterio de FM (1978b) Center and surround mechanisms of opponent-color X and Y ganglion cells of retina of macaques. J Neurophysiol 41:1418–1434
Monasterio de FM (1979a) Signals from blue cones in „red-green" opponent-colour ganglion cells of the macaque retina. Vision Res 19:441–449
Monasterio de FM (1979b) Asymmetry of on- and off-pathways of blue-sensitive cones in the retina of macaques. Brain Res 166:39–48
Monasterio de FM, Gouras P (1975) Functional properties of ganglion cells of the rhesus monkey retina. J Physiol 251:167–195
Monasterio FM, Gouras P (1977) Responses of macaque ganglion cells to far violet lights. Vision Res 17:1147–1156
Monasterio FM, Gouras P, Tolhurst DJ (1975a) Trichromatic colour opponency in ganglion cells of the rhesus monkey retina. J Physiol 251:197–216
Monasterio de FM, Gouras P, Tolhurst DJ (1975b) Concealed colour opponency in ganglion cells of the rhesus monkey retina. J Physiol 251:217–229
Monasterio FM, Schein SJ, McCrane EP (1981) Staining of blue-sensitive cones of the macaque retina by a fluorescent dye. Science 213:1278–1281
Monroe MM (1924) The energy value of the minimum visible chromatic and achromatic for different wave-lengths of the spectrum. Psychol Rev Public 34. Psychol Monographs No 158
Motokawa K (1970) Physiology of color and pattern vision. Igaku Shoin Ltd, Tokyo and Springer, Berlin Heidelberg New York
Motokawa K, Yamashita E, Ogawa T (1960) Studies on receptive fields of single units with colored lights. Tohoku J Exp Med 71:261–272
Mott De DW, Boynton RM (1958) Retinal distribution of entopic stray light. J Opt Soc Am 48:13–22
Müller G, Korth M, Rix R, Weimer E (1980) Information coding in the visual system: A new hypothesis. Albrecht von Graefes Arch Ophthalmol 214:1–7
Müller GE (1924) Darstellung und Erklärung der verschiedenen Typen der Farbenblindheit. Vandenhoek und Ruprecht, Göttingen
Müller GE (1930a) Über die Farben-Empfindungen, vol I. Z Psychol Physiol Sinnesorg Erg Bd 17:1-430
Müller GE (1930b) Über die Farben-Empfindungen, vol II. Z Psychol Physiol Sinnesorg Erg Bd 18:435–648
Müller-Limmroth HW (1956) Die Theorien des Farbensehens. Die Naturwissenschaften 43:337–346, 364–370
Müller-Limmroth HW (1959) Elektrophysiologie des Gesichtssinns. Theorie und Praxis der Elektroretinographie. Springer, Berlin Göttingen Heidelberg
Murakami M, Ohtsu K, Ohtsuka T (1972) Effects of chemicals on receptors and horizontal cells in the retina. J Physiol 227:899–913
Nagel WA (1898) Beiträge zur Diagnostik, Symptomatologie und Statistik der angeborenen Farbenblindheit. Arch Augenheilk 38:31–66
Nagel WA (1907) Zwei Apparate für die augenärztliche Funktionsprüfung. Adaptameter und kleines Spektralphotometer (Anomaloskop) Z Augenheilk 17:201–222
Naka KI, Rushton WAH (1966a) S-potentials from colour units in the retina of fish (cyprinidae) J Physiol 185:536–555

Naka KI, Rushton WAH (1966b) An attempt to analyze colour reception by electrophysiology. J Physiol 185:556–586
Nelson R (1973) A comparison of electrical properties of neurons in necturus retina. J Neurophysiol 36:519–535
Nelson R (1977) Cat cones have rod input: A comparison of the response properties of cones and horizontal cell bodies in the retina of the cat. J Comp Neurol 172: 109–136
Nelson R, Lützow von A, Kolb H, Gouras P (1975) Horizontal cells in cat retina with independent dendritic systems. Science 189:137–139
Nelson R, Kolb H, Famiglietti EV Jr, Gouras P (1976) Neural responses in the rod and cone system of the cat retina: Intracellular records and procion stains. Invest Ophthalmol 15:946–953
Nelson R, Famiglietti EV Jr, Kolb H (1978) Intracellular staining reveals different levels of stratification for on- and off-center ganglion cells in cat retina. J Neurophysiol 41:472–483
Nelson R, Zrenner E, Gouras P (1978) Patterned stimuli reveal spatial organization in the electroretinogram. Proc 16th ISCEV-Symposium, Morioka, ed by Tazawa Y. Jap J Ophthalmol Suppl, pp 161–169
Nelson R, Kolb H, Robinson MM, Mariani AP (1981) Neural circuitry of the cat retina: cone pathways to ganglion cells. Vision Res 21:1527–1536
Nelson R (1982) AII amacrine cells quicken the time course of rod signals in the cat retina. J Neurophysiol 47:928–947
Nelson R, Kolb H (1982) Synaptic patterns and response properties of bipolar and ganglion cells in the cat retina. Invest Ophthalmol Vis Sci (ARVO-Suppl) 22:175
Neuhann T, Krastel H, Jaeger W (1978) Differential diagnosis of typical and atypical congenital achromatopsia. Albrecht von Graefes Arch Ophthal 209:19–28
Newton I (1672) Letter to the Royal Society, London (Quoted after J. Bronowski: The ascent of man. Little Brown & Co, Boston Toronto, p 227, 236)
Neyton J, Piccolino M, Gerschenfeld HM (1981a) Involvement of small-field horizontal cells in feedback effects on green cones of turtle retina. Proc Nat Acad Sci USA 78: 4616–4619
Neyton J, Piccolino M, Gerschenfeld HM (1981b) Involvement of small field horizontal cells in the feedback effects on green cones. Vision Res 21:1599
Nicoll RA, Alger BE (1979) Presynaptic inhibition: Transmitter and ionic mechanisms. International Rev of Neurobiol 21:217–258
Niemeyer G, Gouras P (1973) Rod and cone signals in S-potentials of the isolated perfused cat eye. Vision Res 13:1603–1612
Normann RA, Perlman I (1979) Signal transmission from red cones to horizontal cells in the turtle retina. J Physiol 286:509–524
Norren van D, Baron WS (1977) Increment spectral sensitivities of the primate late receptor potential and b-wave. Vision Res 17:807–810
Norren van D, Bouman MA (1976) Is it possible to isolate fundamental cone mechanisms with Wald's method of chromatic adaptation? Mod Probl Ophthal 17:27–32. Karger, Basel
Norren van D, Padmos P (1973) Human and macaque blue cones studied with electroretinography. Vision Res 13:1241–1254
Norren van D, Went LN (1981) New test for the detection of tritan defects evaluated in two surveys. Vision Res 21:1303–1306
O'Bryan PM (1973) Properties of the depolarizing synaptic potential evoked by peripheral illumination in cones of the turtle retina. J Physiol 235:207–223
Oehler R, Spillmann L (1981) Sensory colour changes in coloured Hermann grids varying only in hue. Vision Res 21:527–541
Østerberg G (1935) Topography of the layer of rods and cones in the human retina. Acta Ophthalmol Kbh Suppl 6:1–102
Ohba N, Tanino T (1976) Unilateral colour vision defect resembling tritanopia. Mod Probl Ophthalmol 17:331–335

Ohta Y, Kato H (1976) Colour perception changes with age. Mod Probl Ophthalmol 17:345–352

Padmos P, Graf V (1974) Colour vision in rhesus monkey, studied with subdurally implanted cortical electrodes. Doc Ophthalmol Proc Series 4:307–314, ed by Dodt E, Pearlman JT, Dr Junk Publ: The Hague

Padmos P, Norren van D (1971) Cone spectral sensitivity and chromatic adaptation as revealed by human flicker-electroretinography. Vision Res 11:27–42

Padmos P, Norren van D (1975a) Cone systems interaction in single neurons of the lateral geniculate nucleus of the macaque. Vision Res 15:617–619

Padmos P, Norren van D (1975b) Increment spectral sensitivity and colour discrimination in the primate studied by means of graded potentials from the striate cortex. Vision Res 15:1103–1113

Padmos P, Norren van D, Faijer JW (1978) Blue cone function in a family with an inherited tritan defect, tested with electroretinography and psychophysics. Invest Ophthalmol Visual Sci 17·436–441

Pastore N (1971) Selective history of theories of visual perception. Oxford Univ Press, London, pp 1650–1950

Pau H, Wahl M (1974) Myambutol-Schädigung des Auges. Ber Dtsch Ophthalmol Ges 72:176–181

Paulus W, Scheibner H (1978) Fehlfarben und Univarianz. Ber Dtsch Ophthol Ges 75:518–521

Paulus W, Scheibner H (1980) A model of the color vision network. Vision Research (in press)

Peichl L, Wässle H (1979) Size, scatter and coverage of ganglion cell receptive field centres in the cat retina. J Physiol 291:117–141

Peichl L, Wässle H (1981) Morphological identification of on- and off-centre brisk transient (Y) cells in the cat retina. Proc R Soc London Ser B 212:139–156

Perry VH, Cowey A (1981) The morphological correlates of X- and Y-like retinal ganglion cells in the retina of monkeys. Exp Brain Res 43:226–228

Piccolino M, Gerschenfeld HM (1978) Activation of a regenerative calcium conductance in turtle cones by peripheral stimulation. Proc R Soc Lond B 201:309–315

Piccolino M, Neyton J, Gerschenfeld H (1981) Center-surround antagonistic organization in small-field luminosity horizontal cells of turtle retina. J Neurophysiol 45: 363–375

Piéron H (1931) La sensation chromatique. Donnée sur la latence propre et l'établissement des sensations de couleur. Année Psychol 32:1–29

Pinckers A (1975) Dyschromatopsies acquises d'axe bleu-jaune. Ann d'Oculist (Paris) 208:659–666

Pitt FHG (1935) Characteristics of dichromatic vision. Med Res Council Rep Comm Physiol Vision XIV. Special Report Series 200, London

Pitt FHG (1944) The nature of normal trichromatic and dichromatic vision. Proc R Soc Lond B 132:101–117

Pokorny J, Bowen RW, Lindsey DT, Smith VC (1979a) Duration thresholds for chromatic stimuli. J Opt Soc Am 69:103–106

Pokorny J, Smith I, Verriest G, Pinckers AJL (eds) (1979b) Congenital and acquired color vision defects. Grune and Stratton, New York London Toronto Sydney San Francisco

Polden PG, Mollon JD (1980) Reversed effect of adapting stimuli on visual sensitivity. Proc R Soc Lond B 210:235–272

Polyak SL (1941) The retina. The anatomy and the histology of the retina in man, ape and monkey. Including the consideration of visual functions, the history of physiological optics and the histological laboratory technique. Univ Chicago Press, Chicago Ill, pp 309–337

Polyak S (1957) Structure of the vertebrate retina. In: Klüver H (ed) The vertebrate visual system. Univ Chicago Press, Chicago, pp 207–287

Potts AM, Marriot FHL (1965) Studies on the visual evoked response. I. The use of a 0.06 degree red target for evaluation of foveal function. Invest Ophthalmol 4:303–309
Pourcho RG (1980) Localization of GABA receptors in the cat retina using ^{3}H-Muscimol. Invest Ophthalmol Visual Sci (ARVO-Suppl) 19:71–72
Pugh EN Jr, Mollon JD (1979) A theory of the Π_1 and Π_3 color mechanisms of Stiles. Vision Res 19:293–312
Rackensperger W, Grüsser O-J (1966) Sinuslichtreizung der rezeptiven Felder einzelner Retinaneurone. Experientia 22:192–193
Ransom-Hogg A, Spillmann L (1980) Perceptive field size in fovea and periphery of the light and dark adapted retina. Vision Res 20:221–228
Ratliff F, Knight BW, Toyoda J, Hartline HK (1967) Enhancement of flicker by lateral inhibition. Science 158:392–393
Ratliff F, Knight BW, Graham N (1969) On tuning and amplification by lateral inhibition. Proc Natl Acad Sci 62:733–740
Rauschecker PJ, Campbell FW, Atkinson J (1973) Colour opponent neurones in the human visual system. Nature 245:42–43
Reeves A (1980) Transient tritanopia after flicker adaptation. Vision Res 21:657–664
Reeves A (1981a) Transient tritanopia: its abolition at high intensites. Vision Res 21: 665–672
Reeves A (1981b) Transient desensitization of a red-green opponent site. Vision Res 21:1267–1277
Regan D (1968) Chromatic adaptation and steady-state evoked potentials. Vision Res 8:149–158
Regan D (1970) Objective method of measuring the relative spectral-luminosity curve in man. J Opt Soc Am 60:856–859
Regan D (1972) Evoked potentials in psychology, sensory physiology and clinical medicine. Chapman and Hall Ltd, London
Regan D (1973) An evoked potential correlate of colour. Evoked potential findings and single cell speculations. Vision Res 13:1933–1941
Regan D (1977) Evoked potential indications of the processing of pattern, colour and depth information. In: Desmedt JE (ed) Visual evoked potentials in man: New developments. Clarendon Press, Oxford, pp 234–249
Regan D, Spekreijse H (1974) Evoked potential indications of colour blindness. Vision Res 14:89–95
Regan D, Tyler CW (1971) Temporal summation and its limit for wavelength change: An analog of Bloch's law for color vision. J Opt Soc Am 61:1414–1421
Reidemeister Ch, Grüsser O-J (1959) Flimmerlichtuntersuchungen an der Katzenretina. I. On-Neurone und Off-Neurone. Z Biol 111:241–253
Richter K (1979) Beschreibung von Problemen der höheren Farbmetrik mit Hilfe des Gegenfarbensystems. Forschungsbericht 61, Bundesanstalt für Materialprüfung (BAM), Berlin
Richter M (1951) Über einige neuere Theorien des Farbensehens. Klin Monatsbl Augenheilkd 118:240–259
Riggs LA, Wooten BR (1972) Electrical measures and psychophysical data on human vision. In: Jameson D, Hurvich LM (eds) Handbook of sensory physiology, vol VII/4. Visual psychophysics. Springer, Berlin Heidelberg New York, pp 690–731
Ripps H, Weale RA (1963) Cone pigments in the normal human fovea. Vision Res 3: 531–543
Ripps H, Weale RA (1969) Color vision. Ann Rev Psychol 20:193–216
Robinson DN (1966) Disinhibition of visually masked stimuli. Science 154:157–158
Robinson DN (1968) Visual disinhibition with binocular and interocular presentations. J Opt Soc Am 58:254–257
Robinson DN (1970) Critical flicker-fusion of solid and annular stimuli. Science 167:207–208

Robinson DN (1976) An intellectual history of psychology. MacMillan, New York London
Robinson DN (1980) The enlightened machine. An analytical introduction to neuropsychology. Columbia Univ Press, New York
Rodieck RW (1973) The vertebrate retina. Principles of structure and function. WH Freeman and Co, San Francisco
Rodieck RW (1979) Visual pathways. Ann Rev Neurosci 2:193–225
Rosenblum K, Anderson ML, Purple RL (1981) Normal and color defective perception of Fechner-Benham colors: implications for color vision theory. Vision Res 21:1483–1490
Rosmanit J (1914) Anleitung zur Feststellung der Farbentüchtigkeit, vol I, II. Franz Deuticke, Leipzig Wien
Rovamo J, Hyvärinen L, Hari R (1982) Human vision without luminance-contrast system: selective recovery of the red-green colour-contrast system from acquired blindness. Doc Ophthalmol Proc Ser 33:457–466, ed by Verriest G, Dr Junk Publ: The Hague
Ruddock KH (1980) Psychophysical evidence concerning independent processing of visual stimulus parameters. In: Verriest G (ed) Colour vision deficiencies, vol V. A Hilger Ltd, Bristol, pp 115–121
Rushton WAH (1958a) Kinetics of cone pigments measured objectively on the living human fovea. Ann New York Acad Sci 74:291–304
Rushton WAH (1958b) Visual pigments in the colour blind. Nature 182:690–692
Rushton WAH (1963) A cone pigment in the protanope. J Physiol 168:345–359
Rushton WAH (1965) A foveal pigment in the deuteranope. J Physiol 176:24–37
Rushton WAH (1972a) Review lecture, pigments and signals in colour vision. J Physiol 220:1P–31P
Rushton WAH (1972b) Visual pigments in man. In: Dartnall HJA (ed) Handbook of sensory physiology, vol VII/1. Photochemistry of vision. Springer, Berlin Heidelberg New York, pp 364–394
Rushton WAH (1975) Visual pigments and colour blindness. Sci Am 232:64, 65, 68–74
Saito T, Kondo H (1978) Ionic mechanisms underlying the center and surround responses of on-center bipolar cells in the carp retina. Sensory Processes 2:350–358
Saito T, Kondo H, Toyoda J-I (1979) Ionic mechanisms of two types of on-center bipolar cells in the carp retina. J Gen Physiol 73:73–90
Schaternikoff M (1902) Über den Einfluß der Adaptation auf die Erscheinung des Flimmerns. Z Psychol Physiol Sinnesorg 29:241–254
Scheibner H (1968) Trichromasie, Dichromasie, Monochromasie. Optica Acta 15: 329–338
Scheibner H (1969) Über die Begriffe Farbvalenz, Farbart und Chrominanz in der Farbmetrik. Die Farbe 18: 221–232 (1969)
Scheibner H (1976a) Die physiologischen Vorstellungen über das Farbensehen in unserer Zeit. Die Farbe 25:48–62
Scheibner H (1976b) Prüfung von Farbsinnstörungen. Med Klin 71:1452–1459
Scheibner H (1976c) Missing colours (Fehlfarben) of deuteranopes and extreme deuteranomalous observes. Mod Probl Ophthalmol 17:21–26
Scheibner H, Paulus W (1978) An analysis of protanopic colour vision. Mod Probl Ophthalmol 19:206–211
Scheibner H, Schmidt B (1969) Zum Begriff der spektralen visuellen Empfindlichkeit mit elektroretinographischen Ergebnissen am Hund. Albrecht von Graefes Arch Ophthalmol 177:124–135
Scheibner H, Thranberend C (1974) Colour vision in a case of neuritis retrobulbaris. Mod Probl Ophthalmol 13:339–344
Scheibner H, Wolf E (1982) Direkte Zerlegungen, isomorphe und homomorphe Abbildungen in der linearen Farbentheorie. 4 AIC Kongreß COLOR 81 Berlin (in press)

Schellart NAM (1973) Dynamics and statistics of photopic ganglion cell responses in isolated goldfish retina. Diss Univ Amsterdam
Schellart NAM, Spekreijse H (1972) Dynamic characteristics of retinal ganglion cell responses in goldfish. J Gen Physiol 59:1–11
Schellart NAM, Riemslag FCC, Spekreijse H (1979) Center-surround organization and interaction in receptive fields of goldfish tectal units. Vision Res 19:459–467
Schiller PH, Malpeli JG (1977) Properties and tectal projections of monkey retinal ganglion cells. J Neurophysiol 40:428–445
Schiller PH, Malpeli JG (1978) Functional specificity of lateral geniculate nucleus laminae of the rhesus monkey. J Neurophysiol 41:788–797
Schmidt IG (1966) Central nervous system effects of Ethambutol in monkeys. Ann New York Acad Sci 135:759–774
Schober H (1964) Das Sehen, vol II, 3rd edn. VEB Fachbuchverlag, Leipzig
Scholes HJ (1975) Colour receptors and their synaptic connections in the retina of a cyprinid fish. Phil Trans R Soc Lond 270:61–118
Schrödinger E (1920) Grundlinien einer Theorie der Farbmetrik im Tagessehen. Ann Physik (IV) 63:397–456, 481–520
Schrödinger E (1925) Über das Verhältnis der Dreifarben zur Vierfarbentheorie. Sitzungsber Akad Wiss Wien, IIa 134:471–490
Schuurmans RP (1981) Colour vision in cat. Thesis Univ of Amsterdam, Giessen
Schuurmans RP, Zrenner E (1979) The short and long wavelength sensitive cone mechanisms in the cat's visual system. ERG, optic nerve and VECP recordings. Pflügers Arch 382, Suppl. R 47
Schuurmans RP, Zrenner E (1981a) Chromatic signals in the visual pathway of the domestic cat. Doc Ophthalmol Proc Ser 27:27–40, ed by Spekreijse H, Apkarian PA, Dr Junk Publ: The Hague
Schuurmans RP, Zrenner E (1981b) Responses of the blue sensitive cone system from the visual cortex and the arterially perfused eye in cat and monkey. Vision Res 21:1611–1615
Schuurmans RP, Zrenner E (1982) Color vision: Methods of pharmacology (in press)
Schuurmans RP, Zrenner E (1983) The Westheimer paradigm, applied for the blue cone mechanism (in prep)
Schuurmans RP, Baier M, Zrenner E (1981) Westheimer's paradigm for the blue sensitive cone mechanism. Pflügers Arch 391 Suppl R 43
Schwartz EA (1982) Calcium-independent release of GABA from isolated horizontal cells in the toad retina. J Physiol 323:196–211
Semm P (1977) Retinofugale Fasern der Kaninchenretina. Reaktionen retinaler Ganglienzellen auf die Lichtreizprogramme der Benham-Scheibe. Dissertation Johannes Gutenberg-Univ, Mainz
Serra A (1981) An annotated bibliography on MDB technique and related topics. Fondazione "Giorgio Ronchi", Firenze
Sheppard JJ (1968) Human color perception. A critical study of the experimental foundation. American Elsevier Publ Co, New York
Sherman PD (1981) Colour vision in the nineteenth century. The Young-Helmholtz-Maxwell theory. Adam Hilger, Bristol
Sherman SM, Wilson JR, Kaas JH, Webb SV (1976) X- and Y-cells in the dorsal lateral geniculate nucleus of the owl monkey (aotus trivirgatus) Science 192:475–476
Shipley T, Jones RW, Fry A (1965) Evoked visual potentials and human color vision. Science 150:1162–1164
Sickel W (1966) The isolated retina maintained in a circulating medium; combined optical and electrical investigations of metabolic aspects of generation of the electroretinogram. In: Burian HM, Jacobson JH (eds) Clinical electroretinography. Pergamon Press, Oxford, pp 115–124

Siegfried JB (1971) Spectral sensitivity of human visual evoked cortical potentials: A new method and a comparison with psychophysical data. Vision Res 11:404–417

Singer W, Creutzfeldt OD (1970) Reciprocal lateral inhibition of on- and off-center neurones in the lateral geniculate body of the cat. Exp Brain Res 10:311–330

Skottun BC, Nordby K, Magnussen S (1980) Rod monochromat sensitivity to sine wave flicker at luminances saturating the rods. Invest Ophthalmol Visual Sci 19:108–111

Sloan LL (1954) Congenital achromatopsia: A report of 19 cases. J Opt Soc Am 44:117–128

Smith VC, Pokorny J (1975) Spectral sensitivity of the foveal cone photopigments between 400 and 500 nm. Vision Res 15:161–171

Smith VC, Pokorny J (1980) Cone dysfunction syndromes defined by colour vision. In: Verriest G (ed) Color vision deficiencies vol V. A Hilger, Bristol, pp 69–82

Smith VC, Pokorny J, Newell FW (1978) Autosomal recessive incomplete achromatopsia with protan luminosity function. Ophthalmologia 177:197–207

Smith VC, Pokorny J, Newell FW (1979) Autosomal recessive imcomplete achromatopsia with deutan luminosity. Am J Ophthalmol 87:393–402

Spekreijse H, Norton AL (1970) The dynamic characteristics of color-coded S-potentials. J Gen Physiol 56:1–5

Spekreijse H, Norren van D, Berg van den TJTP (1971) Flicker responses in monkey lateral geniculate nucleus and human perception of flicker. Proc Natl Acad Sci 68:2082–2085

Spekreijse H, Estévez O, Reits D (1977) Visually evoked potentials and the physiological analysis of visual processes in man. In: Desmedt J (ed) Visual evoked potentials in man: New developments. Clarendon Press, Oxford, pp 16–89

Sperling G (1970) Model of visual adaptation and contrast detection. Perception and Psychophysics 8:143–157

Sperling HG (1960) Case of congenital tritanopia with implications for a trichromatic model of color reception. J Opt Soc Am 50:156–163

Sperling HG, Harwerth RS (1971) Red-green cone interactions in the increment-threshold spectral sensitivity of primates. Science 172:180–184

Spillmann L (1981) Illusions of contrast, brightness, color and motion and their neurophysiological interpretation. In: Hirnforschung, Grundlagen und Klinik 74:73–77

Spillmann L, Conlon JE (1972) Photochromatic interval during dark adaptation and as a function of background luminance. J Opt Soc Am 62:182–185

Spillman L, Redies C (1980) Illusory perception of brightness, color and movement. (Poster presented at the Satellite Symp of the XXVIIIth Int Congr of Physiol Sci, Braunlage)

Stabell B, Stabell U (1980) Spectral sensitivity in the far peripheral retina. J Opt Soc Am 70:959–963

Stabell B, Stabell U (1981) Absolute spectral sensitivity at different eccentricities. J Opt Soc Am 71:836–840

Stabell U, Stabell B (1979) Bezold-Brücke phenomenon of the extrafoveal retina. J Opt Am 69:1648–1652

Stabell U, Stabell B (1980) Variation of macular pigmentation and in short-wave cone sensitivity with eccentricity. J Opt Soc Am 70:706–711

Stärk N (1972) Toxische Sehnervschädigung durch Myambutol. Med Klin 67:913–916

Steinberg RH (1969a) Rod and cone contributions to S-potentials from the cat retina. Vision Res 9:1319–1929

Steinberg RH (1969b) Rod-cone interaction in S-potentials from cat retina. Vision Res 9:1331–1344

Steinberg RH (1969c) The rod after-effect in S-potentials from the cat retina. Vision Res 9:1345–1355
Stell WK (1972) The morphological organization of the vertebrate retina. In: Fuortes MGF (ed) Handbook of sensory physiology vol VII/2. Physiology of photoreceptor organs. Springer, Berlin Heidelberg New York, pp 111–213
Stell WK (1976) Functional polarization of horizontal cell dendrites in goldfish retina. Invest Ophthalmol 15:895–908
Stell WK (1978) Inputs to bipolar cell dendrites in goldfish retina. Sensory Processes 2:339–349
Stell WK, Lightfoot DO (1975) Color-specific interconnections of cones and horizontal cells in the retina of the goldfish. J Comp Neur 159:473–502
Stell WK, Lightfoot DO, Wheeler TG, Leeper HF (1975) Goldfish retina: Functional polarization of horizontal cell dendrites and synapses. Science 190:989–990
Stell WK, Ishida AT, Lightfoot DO (1977) Structural basis for on- and off-center responses in retinal bipolar cells. Science 198:1269–1271
Sternheim CE, Stromeyer CF, Spillmann L (1978) Increment thresholds: Sensitization produced by hue differences. In: Armington JC, Krauskopf J, Wooten BR (eds) Visual psychophysics and physiology. Academic Press, New York London, pp 209–220
Sternheim CE, Stromeyer CF, Khoo MCK (1979) Visibility of chromatic flicker upon spectrally mixed adapting fields. Vision Res 19:175–183
Stiles WS (1939) The directional sensitivity of the retina and the spectral sensitivities of the rods and cones. Proc R Soc Lond Ser B 127:64–105
Stiles WS (1949) Increment thresholds and the mechanisms of colour vision. Doc Ophthalmol 3:138–163
Stiles WS (1959) Color vision: The approach through increment-threshold sensitivity. Proc Nat Acad Sci 45:100–114
Stiles WS (1978) Mechanisms of colour vision. Selected papers of WS Stiles, with a new introductory essay. Academic Press, London New York
Stöcker H (1980) Psychophysische Untersuchungen zur Charakterisierung der Deuteranomalie durch die beiden langwelligen Zapfenpigmente. Thesis, Univ Düsseldorf
Stöcker H, Wolf E, Scheibner H (1979) Erythrolab und Deuteranomalie. Ber Dtsch Ophthalmol Ges 76:409–414
Stöhr M, Dichgans J, Diener HC, Buettner UW (1982) Evozierte Potentiale. SEP-VEP-AEP. Springer, Berlin Heidelberg New York
Stone SL, Chappell RL (1981) Synaptic feedback onto photoreceptors in the ocellar retina. Brain Res 271:374–381
Straub W (1961) Das Elektroretinogramm. Experimentelle und Beobachtungen. In: Thiel R (ed) Bücherei des Augenarztes, Heft 36. Enke Verlag, Stuttgart
Stromeyer CF III, Khoo MCK, Muggeridge D, Young RA (1978a) Detection of red and green flashes: Evidence for cancellation and facilitation. Sensory Processes 2: 248–271
Stromeyer CF III, Kronauer RE, Madsen JC (1978b) Apparent saturation of blue-sensitive cones occurs at a color-opponent stage. Science 202:217–219
Stromeyer CF III, Zeevi YY, Klein S (1979) Response of visual mechanisms to stimulus onsets and offsets. J Opt Soc Am 69:1350–1353
Svaetichin G (1953) The cone action potential. Acta Physiol Scand 29: (Suppl 106) 565–600
Svaetichin G (1956) II. Spectral response curves from single cones. Acta Physiol Scand 39, Suppl 134:19–46
Svaetichin G, MacNichol Jr EF (1958) Retinal mechanisms for chromatic and achromatic vision. Ann New York Acad Sci 74:385–404
Thaler A, Heilig P, Heiss W-D, Lessel MR (1974) Toxische Schädigung des nervus opticus durch Ethambutol. Klin Monatsbl Augenheilkd 165:660–664
Thoma W, Scheibner H (1980) Die spektrale tritanopische Sättigungsfunktion beschreibt die spektrale Distinktibilität. Farbe und Design 17:49–52

Thoma W, Scheibner H (1982) Tritanopic saturation and borderline distinctivity. Doc Ophthalmol Proc Series 33:19–28, ed by Verriest G: Dr Junk Publ: The Hague
Tomita T (1965) Electrophysiological study of the mechanisms subserving color coding in the fish retina. Cold Spring Harbor Symp Quant Biol 30:559–566
Tomita T (1970) Electrical activity of vertebrate photoreceptors. Quart Rev Biophysics 3, 2 , pp 179–222
Tomita T (1972) Light-induced potential and resistance changes in vertebrate photoreceptors. In: Fuortes MGF (ed) Handbook of sensory physiology vol. VII/2. Physiology of photoreceptor organs. Springer, Berlin Heidelberg New York, pp 483–511
Tomita T (1973) Electrophysiology of the receptors and postsynaptic neurons in the vertebrate retina. Nova Acta Leopoldina 37/2:13–30
Tomita T (1978) ERG waves and retinal cell function. Sensory Processes 2:276–284
Toyoda J, Tonosaki K (1978) Studies on the mechanisms underlying horizontal-bipolar interaction in the carp retina. Sensory Processes 2:359–365
Toyoda J-I, Nosaki H, Tomita T (1969) Light-induced resistance changes in single photoreceptors of necturus and gekko. Vision Res 9:453–463
Trendelenburg W (1961) Der Gesichtssinn. Gründzüge der physiologischen Optik, vol II, bearbeitet von Monjé M, Schmidt I, Schütz E. Springer, Berlin Göttingen Heidelberg
Trezona PW (1970) Rod particicipation in the blue mechanism and its effect on colour matching. Vision Res 10:317–332
Trezona PW (1976) Aspects of peripheral colour vision. Mod Probl Ophthalmol 17: 52–70. Karger, Basel
Trifonov Yu A (1968) Study of synaptic transmission between the photoreceptor and the horizontal cell using electrical stimulation of the retina. Biophysics (Oxford) 13:948–957 (From: Biofizika 13: No 5, 809–817)
Trifonov Yu A, Byzov AL, Chailahian LM (1974) Electrical properties of subsynaptic membranes of horizontal cells in fish retina. Vision Res 14:229–241
Trube G, Trautwein W (1981) Experiments with AR–L 115 BS on skinned cardiac fibres. Arzneim Forsch/Drug Res 31(I) Nr 1a:185–188
Tschermak-Seysenegg A von (1947) Einführung in die physiologische Optik, vol II, 2nd edn. Springer, Wien
Tujil HFJM van (1975) A new illusion: neonlike color spreading and complementary color induction between subjective contours. Acta Psychol 39:441–445
Tweel van der LH, Spekreijse H (1973) Psychophysics and electrophysiology of a rod achromat. Doc Ophthalmol Proc Series 2:163–173, ed by Pearlman JT: Dr Junk: The Hague
Ui K (1975) Photopic electroretinogram. Jp J Ophthalmol 19:57–68
Valberg A (1975) Color induction, a study of lateral interactions in human vision. Dissertation Inst Phys Univ Oslo
Valberg A (1981) Advantages of an opponent-colour metrics and the opponent purity concept. Die Farbe 29:127–144
Valeton JM, Norren van D (1979a) Transient tritanopia at the level of the ERG b-wave. Vision Res 19:689–693
Valeton JM, Norren van D (1979b) Retinal site of transient tritanopia. Nature 280: 488–490
in the retina of the larval tiger salamander. Vision Res 21:1307–1318
Valois De RL (1965) Analysis and coding of color vision in the primate visual system. Cold Spring Harbor Symp Quant Biol 30:567–579
Valois De RL (1972) Processing intensity and wavelength information. Invest Ophthalmol 11:417–427
Valois De RL, Abramov I (1966) Color Vision. Ann Rev Psychol 17:337–362
Valois De RL, Valois De KK (1975) Neural coding of color. In: Carterette E, Freedman MP (eds) Handbook of perception, vol V, Seeing. Academic Press, London New York, pp 117–166

Valois De RL, Abramov I, Jacobs GH (1966) Analysis of response patterns of LGN cells. J Opt Soc Am 56:966–977
Valois De RL, Smith CJ, Karoly AJ, Kitai ST (1958) Electrical responses of primate visual system, I. Different layers of macaque lateral geniculate nucleus. J Comp Physiol Psychol 51:662–668
Valois De RL, Snodderly DM, Yund EW, Hepler NK (1977) Responses of macaque lateral geniculate cells to luminance and color figures. Sensory Processes 1:244–259
Varjú D (1965) Über nichtlineare Analogschaltungen zur Simulierung biologischer Adaptationsvorgänge. In: Wiener N, Schadé JP (eds) Prog Brain Res, vol 17, Cybernetics of the nervous system. Elsevier, Amsterdam, pp 74–101
Vaughan HG Jr (1964) The perceptual and physiological significance of visual evoked responses recorded from the scalp in man. In: Burian HH, Jacobson JH (eds) Clinical Electroretinography. Vision Res Suppl, pp 203–223
Verriest G (1974) Recent advances in the study of the acquired deficiencies of colour vision. Fondazione "Giorgio Ronchi" XXIV. Baccini & Chiappi, Florence
Verriest G, Frey RG (1977) Normales Farbensehen. In: François J, Hollwich F (eds) Augenheilkunde in Klinik und Praxis, vol I. Georg Thieme, Stuttgart, pp 5.1–5.45
Voaden MJ (1970) Gamma-aminobutyric acid and glycine as retinal transmitters. In: Bonting SL (ed) Transmitters in the visual process. Pergamon Press, Oxford New York, pp 108–125
Voaden MJ, Marshall J, Murani N (1974) The uptake of (^{3}H)γ-aminobutyric acid and (^{3}H) glycine by the isolated retina of the frog. Brain Res 67:115–132
Voe de RG, Ripps H, Vaughan HG Jr (1968) Cortical responses to stimulation of the human fovea. Vision Res 8:135–147
Vos JJ, Walraven PL (1971) On the derivation of the foveal receptor primaries. Vision Res 11:799–818
Waaler GHM (1927) Über die Erblichkeitsverhältnisse der verschiedenen Arten von angeborener Rotgrünblindheit. Z f induktive Abstammungs- Vererbungslehre 45: 279–333
Waardenburg PJ (1963) Genetics and ophthalmology, vol II (neuroophthalmological part). Royal van Gorcum, Assen (Netherlands)
Wässle H, Levick WR, Cleland BG (1975) The distribution of the alpha type of ganglion cells in the cat's retina. J Comp Neurol 159:419–437
Wässle H, Illing B, Peichl L (1979) Morphologische Klassen und zentrale Projektion von Ganglienzellen in der Retina der Katze. Verh Dtsch Zool Ges, Gustav Fischer, Stuttgart, pp 180–193
Wässle H, Boycott BB, Illing R-B (1981a) Morphology and mosaic of on- and off-beta cells in the cat retina and some functional considerations. Proc R Soc Lond Ser B 212:177–195
Wässle H, Peichl L, Boycott BB (1981b) Morphology and topography of on- and off-alpha cells in the cat retina. Proc R Soc Lond Ser B 212:157–175
Wässle H, Peichl L, Boycott BB (1981c) Dendritic territories of cat retinal ganglion cells. Nature 292:344–345
Wagner HG (1971) Deuteranopie: Fusions- oder Ausfall-Dichromasie? Farbe 20:317–326
Wagner G (ed) (1974) Sehvermögen-Farbtüchtigkeit-Augeninnendruck. Methodik und Ergebnisse einer Voruntersuchung in einem chemischen Großbetrieb. FK Schattauer, Stuttgart New York
Wagner G, Boynton RM (1972) Comparison of four methods of heterochromatic photometry. J Opt Soc Am 1508–1515
Wagner HG, MacNichol EF Jr, Wolbarsht ML (1960a) The response properties of single ganglion cells in the goldfish retina. J Gen Physiol 43 (Suppl 2):45–62
Wagner HG, MacNichol EF Jr, Wolbarsht ML (1960b) Opponent color responses in retinal ganglion cells. Science 131:1314

Wagner HG, MacNichol EF Jr, Wolbarsht ML (1963) Functional basis for "on"-center and "off"-center receptive fields in the retina. J Opt Soc Am 53:66–70
Wald G (1945) Human vision and the spectrum. Science 101:653–658
Wald G (1964) The receptors of human color vision. Action spectra of three visual pigments in human cones account for normal color vision and color-blindness. Science 145:1007–1017
Wald G (1967) Blue-blindness in the normal fovea. J Opt Soc Am 57:1289–1301
Walls GL (1964) Notes on four tritanopes. Vision Res 4:3–16
Walls GL, Heath GG (1954) Typical total color blindness reinterpreted. Acta Ophthalmol 32:253–297
Walls GL, Heath GG (1956) Neutral points in 138 protanopes and deuteranopes. J Opt Soc Am 46:640–649
Walls GL (1956) The Palmer Story. J Hist Med Allied Sci XI:66–96
Walraven PL (1972) Color vision. Annu Rev Psychol 23:347–374
Walraven PL (1976) Basic mechanisms of defective colour vision. Mod Probl Ophthalmol 17:2–16. Karger, Basel
Walraven J (1977) Colour signals from incremental and decremental light stimuli. Vision Res 17:71–76
Walraven J (1981a) Perceived colour under conditions of chromatic adaptation: evidence for gain control by II mechanisms. Vision Res 21:611–620
Walraven J (1981b) Chromatic induction. Psychophysical studies on signal processing in human colour vision. Thesis, Univ Utrecht
Walther A, Marré E, Mierdel P (1981) Peakzeit- und Amplitudenparameter des VECP der isolierten Farbsehmechanismen beim Menschen. Folia Ophthalmol 6:206–211
Wasserman GS (1978) Color vision: An historical introduction. In: MacCorquodale K (ed) Wiley series in behavior. Wiley and Sons, New York Chichester Brisbane Toronto
Weale RA (1951) Hue-discrimination in para-central parts of the human retina measured at different luminance levels. J Physiol 113:115–122
Weale RA (1953) Cone-monochromatism. J Physiol 121:548–569
Weiler R, Marchiafava PL (1981) Physiological and morphological study of the inner plexiform layer in the turtle retina. Vision Res 21:1635–1638
Werblin FS (1974) Control of retinal sensitivity. II. Lateral interactions at the outer plexiform layer. J Gen Physiol 63:62–87
Werblin FS, Copenhagen DR (1974) Control of retinal sensitivity III. Lateral interactions at the inner plexiform layer. J Gen Physiol 63:88–110
Werblin FS, Dowling JE (1969) Organization of the retina of the mudpuppy, necturus maculosus. II. Intracellular recording. J Neurophysiol 32:339–355
Werner JS, Wooten BR (1979) Opponent chromatic mechanisms: Relation to photopigments and hue naming. J Opt Soc Am 69:422–434
Westheimer G (1965) Spatial interaction in the human retina during scotopic vision. J Physiol 181:881–894
Westheimer G (1966) The Maxwellian view. Vision Res 6:669–682
White CT, Kataoka RW, Martin J (1977) Colour-evoked potentials: Development of a methodology for the analysis of the processes involved in colour vision. In: Desmedt JE (ed) Visual evoked potentials in man: New developments. Clarendon Press, Oxford
Wienrich M, Zrenner E (1981) Chromatic signals in retinal ganglion cells: cat versus monkey. Pflügers Arch 389 Suppl R 29 (full paper in prep)
Wiesel TN, Hubel DH (1966) Spatial and chromatic interactions in the lateral geniculate body of the rhesus monkey. J Neurophysiol 29:1115–1156
Williams DR, MacLeod DIA, Hayhoe MM (1981) Punctate sensitivity of the blue-sensitive mechanism. Vision Res 21:1357–1375
Willmer EN (1949a) Colour vision in the central fovea. Doc Ophthalmol 3:194–213

Willmer EN (1949b) Further observations on the properties of the central fovea in colour-blind and normal subjects. J Physiol 110:422–446 (vol 110 publ partly 1950)
Willmer EN (1961) Human colour vision and the perception of blue. J Theoret Biol 2:141–179
Witkovsky P (1965) The spectral sensitivity of retinal ganglion cells in the carp. Vision Res 5:603–614
Witkovsky P, Burkhardt DA, Nagy AR (1979) Synaptic connections linking cones and horizontal cells in the retina of the pikeperch (stizostedion vitreum) J Comp Neur 186:541–560
Wolf E, Scheibner H (1978) One versus two altered cone pigments in protanomalous colour vision. Pflügers Arch 373, Suppl R 79
Wooten BR (1972) Photopic and scotopic contributions to the human visually evoked cortical potential. Vision Res 12:1647–1660
Wooten BR, Wald G (1973) Color-vision mechanisms in the peripheral retinas of normal and dichromatic observers. J Gen Physiol 61:125–145
Wooten BR, Werner JS (1979) Short-wave cone input to the red-green opponent channel. Vision Res 19:1053–1054
Wooten BR, Fuld K, Spillmann L (1975) Photopic spectral sensitivity of the peripheral retina. J Opt Soc Am 65:334–342
Wright WD (1946) Researches on normal and defective colour vision. Henry Kimpton, London
Wright WD (1952) The characteristics of tritanopia. J Opt Soc Am 42:509–521
Wright WD (1969) The measurement of colour. Adam Hilger Ltd, London
Wright WD (1981) Why and how chromatic adaptation has been studied. Color Res Applic 6:147–152
Wyszecki G, Stiles WS (1967) Color science: Concepts and methods, quantitative data and formulas. John Wiley and Sons Inc, New York
Yasuma T, Ichikawa H (1981) Characteristics of genetic carriers of congenital color vision defects: spatial summation function of flicker-detecting properties. Jap J Ophthalmol 25:194–201
Yasuma T, Ichikawa H, Tanabe S (1980) Characteristics of genetic carriers of congenital colour vision defects: deutero-carriers. Colour Vision Deficiencies 5:273–277
Yazulla S (1976) Cone input to horizontal cells in the turtle retina. Vision Res 16:727–735
Yazulla S (1981) GABAergic synapses in the goldfish retina: An autoradiographic study of ^{3}H-muscimol and ^{3}H-GABA binding. J Comp Neurol 200:83–93
Yokoyama M, Yoshida T (1978) Spectral response of the human eye as displayed by time-locked scanning method. Excerpta Medica International Congress Series 442:191
Yoshikami S, Hagins WA (1973) Control of the dark current in vertebrate rods and cones. Biochemistry and physiology of visual pigments. Springer, Berlin Heidelberg New York, pp 245–255
Yoshikami S, George JS, Hagins WA (1980) Light-induced calcium fluxes from outer segment layer of vertebrate retinas. Nature 286:395–398
Young T (1802) On the theory of light and colours. Philos Trans R Soc 92:12–48
Young Th (1807) Lectures on natural philosophy and the mechanical arts, vol 2, London, p 345
Zeki S (1980) The representation of colours in the cerebral cortex. Nature 284:412–418
Zihl J, Cramon von D (1980) Colour anomia restricted to the left visual hemifield after splenial disconnexion. J Neurol Neurosurg Psychiatry 43:719–724
Zisman F, King-Smith PE, Bhargava SK (1978) Spectral sensitivities of acquired color defects analyzed in terms of color opponent theory. Mod Probl Ophthalmol 19: 254–257
Zrenner C (1982a) CWL Bruch: Leben und Werk. Pflügers Arch Suppl 392:R 51

Zrenner C (1982b) The discovery of the Lamina basalis choroidea by CWL Bruch (1819–1884): His life and work. Historia ophthalmologica internationalis (in press)

Zrenner E (1976) Evidence of colour opponency as detected by the visually evoked cortical potential (VECP). Pflügers Arch 365: Suppl R 48

Zrenner E (1977a) Influence of stimulus duration and area on the spectral luminosity function as determined by sensory and VECP measurements. Doc Ophthalmol Proc Series 13:21–30: ed by Lawwill Th: Dr Junk Publ: The Hague

Zrenner E (1977b) Antagonistische Farbsinnmechanismen im visuell evozierten kortikalen Potential (VECP) des Menschen. Klin Monatsbl Augenheilkd 171:162–163

Zrenner E (1977c) Color opponency in visually evoked cortical potentials (VECP) Invest Ophtalmol Visual Sci (ARVO-Suppl) 16:157

Zrenner E (1979) Die Verarbeitung von farbigen Reizen in der Primatenretina. Klin Monatsbl Augenheilkd 174:654–656

Zrenner E (1982a) Electrophysiological characteristics of the blue sensitive mechanism: Test of a model of cone interaction under physiological and pathological conditions. Doc Ophthal Proc Series 33:103–125, ed by Verriest G: Dr Junk Publ: The Hague

Zrenner E (1982b) Interactions between spectrally different cone mechanisms: On the clinical applicability of psychophysical and electrophysiological tests. Doc Ophthal Proc Series 31:287–295, ed by Niemeyer G, Huber C: Dr Junk Publ: The Hague

Zrenner E (1983) Neurophysiological aspects of colour vision mechanisms in the primate retina. In preparation for the Proceedings of the Nato-meeting, ed by Mollon JD, Cambridge 1982

Zrenner E, Baier M (1978) Einsatz eines Prozeßrechners für on-line Untersuchungen der lichtinduzierten elektrischen Antwort des menschlichen Auges. EDV in Medizin und Biologie 9:41–46

Zrenner E, Baier M (1978) Baier M (1978) Einsatz eines Prozeßrechners for on-line Untersuchungen der lichtindzierten electrischen Antwort des menschlichen Auges. EDV in Medizin und Biologie 9:41–46

Zrenner E, Gouras P (1977) Spectral opponency and asymmetry between cone mechanisms in the cat electroretinogram (ERG). Soc Neurosci Abstr 3:583

Zrenner E, Gouras P (1978a) Retinal ganglion cells lose color opponency at high flicker rates. Invest Ophthalmol Visual Sci (ARVO-Suppl) 17:130

Zrenner E, Gouras P (1978b) Luminous and chromatic flicker functions are based on the phase relation between center and surround responses of color opponent ganglion cells. Pflügers Arch 377, Suppl R 48

Zrenner E, Gouras P (1979a) Blue-sensitive cones of the cat produce a rodlike electroretinogram. Invest Ophthalmol Visual Sci 18:1076–1081

Zrenner E, Gouras P (1979b) Cone opponency in tonic ganglion cells and its variation with eccentricity in rhesus monkey retina. Invest Ophthalmol Visual Sci (ARVO-Suppl) 18:77

Zrenner E, Gouras P (1979c) Modulation of blue cone signals by long-wavelength sensitive cones in primate retina. Pflügers Arch 382 Suppl R 47

Zrenner E, Gouras P (1980) The blue sensitive mechanism in ganglion cells of macaque retina. Invest Ophthalmol Visual Sci (ARVO Suppl) 19:7

Zrenner E, Gouras P (1981) Characteristics of the blue sensitive cone mechanism in primate retinal ganglion cells. Vision Res 21:1605–1609

Zrenner E, Gouras P (1983) Cone opponency in tonic ganglion cells and its variation with eccentricity in rhesus monkey retina. Proceedings of the Nato-meeting, Cambridge 1982, ed by Mollon JD, Academic Press (in prep)

Zrenner E, Kojima M (1976) Visually evoked cortical potential (VECP) in dichromats. Mod Probl Ophthalmol 17:241–246

Zrenner E, Kojima M (1977) Colour vision mechanisms isolated by selective adaptation in normals and dichromats as detected by the visually evoked cortical potential (VECP) Doc Ophthalmol Proc Series 11:115–121, ed by Lawwill Th: Dr Junk Publ: The Hague

Zrenner E, Krüger C-J (1981) Ethambutol mainly affects the function of red-green-opponent neurons. Doc Ophthalmol Proc Series 27:13–25, ed by Spekreijse H, Apkarian PA: Dr Junk Publ: The Hague, Boston London

Zrenner E, Langhof H-J, Welt R, Kojima M (1976) Elektro-ophthalmologische Beobachtungen zum Verlauf einseitiger tapetoretinaler Dystrophie. Klin Monatsbl Augenheilkd 169:331–337

Zrenner E, Kojima M, Jankov E (1977) Untersuchung des Farbsinns mit der Methode der visuell evozierten corticalen Potentiale (VECP). Ber Dtsch Ophthalmol Ges 74:727–732

Zrenner E, Nelson R, Mariani H (1982a) Intracellular recordings from a biplexiform ganglion cell in macaque retina, stained with horseradish peroxidase. Brain Res (in press)

Zrenner E, Kramer W, Bittner Ch, Bopp M, Schlepper M (1982b) Rapid effects on colour vision, following intravenous injection of a new, non glycoside positive inotropic substance (AR-L 115 BS) Doc Ophthal Proc Series 33:507–521, ed by Verriest G: Dr Junk Publ: The Hague, Boston London

Subject Index

Handbook of Sensory Physiology

Volume 7, Part 6

Comparative Physiology and Evolution of Vision in Invertebrates

A: Invertebrate Photoreceptors

By H. Autrum, M. F. Bennet, B. Diehn, K. Hamdorf, M. Heisenberg, M. Järvilehto, P. Kunze, R. Menzel, W. H. Miller, A. W. Snyder, D. G. Stavenga, M. Yoshida

Editor: **H. Autrum**

1979. 314 figures, 17 tables. XI, 729 pages
ISBN 3-540-08837-7

B: Invertebrate Visual Centers and Behavior I

By M. F. Land, S. B. Laughlin, D. R. Nässel, N. J. Strausfeld, T. H. Waterman

Editor: **H. Autrum**

1981. 319 figures, 10 tables. X, 635 pages
ISBN 3-540-08703-6

C: Invertebrate Visual Centers and Behavior II

By H. Autrum, L. J. Goodman, J. B. Messenger, R. Wehner

Editor: **H. Autrum**

1981. 216 figures. IX, 665 pages. ISBN 3-540-10422-4

Springer-Verlag
Berlin
Heidelberg
New York